



**This electronic thesis or dissertation has been
downloaded from Explore Bristol Research,
<http://research-information.bristol.ac.uk>**

Author:

Harper, Matt

Title:

Redox Gold Catalysis

General rights

Access to the thesis is subject to the Creative Commons Attribution - NonCommercial-No Derivatives 4.0 International Public License. A copy of this may be found at <https://creativecommons.org/licenses/by-nc-nd/4.0/legalcode>. This license sets out your rights and the restrictions that apply to your access to the thesis so it is important you read this before proceeding.

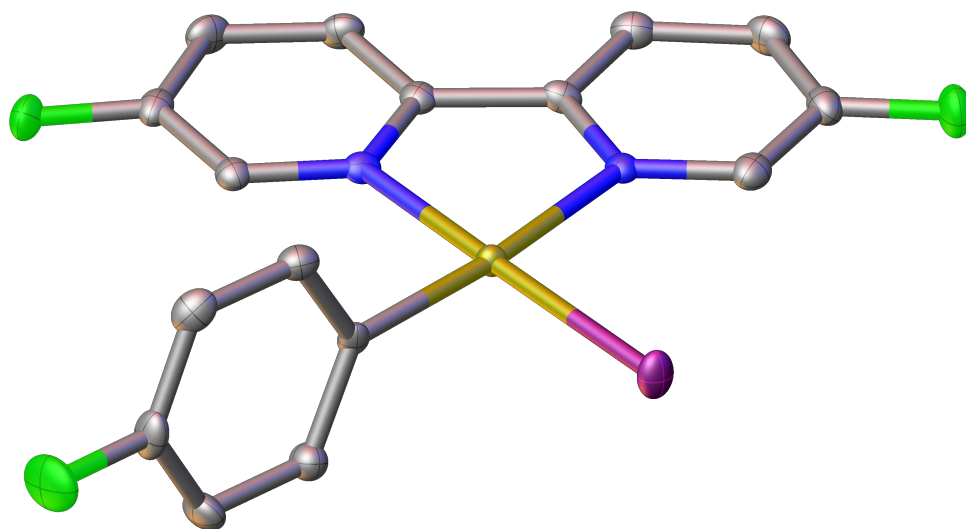
Take down policy

Some pages of this thesis may have been removed for copyright restrictions prior to having it been deposited in Explore Bristol Research. However, if you have discovered material within the thesis that you consider to be unlawful e.g. breaches of copyright (either yours or that of a third party) or any other law, including but not limited to those relating to patent, trademark, confidentiality, data protection, obscenity, defamation, libel, then please contact collections-metadata@bristol.ac.uk and include the following information in your message:

- Your contact details
- Bibliographic details for the item, including a URL
- An outline nature of the complaint

Your claim will be investigated and, where appropriate, the item in question will be removed from public view as soon as possible.

Redox Gold Catalysis



Matthew James Harper

A thesis submitted to the University of Bristol in accordance with the requirements for award of the degree of Doctor of Philosophy in the Faculty of Science

School of Chemistry

November 2018

Word count: 67,945

Abstract

This thesis explores *redox gold catalysis*: catalysis by gold whereby the gold centre alternates between the +1 and +3 oxidation states throughout the catalytic cycle. Results herein describe the development of redox gold catalysis both with and without the use of external oxidants.

Following a brief general introduction, the second chapter describes the gold-catalysed oxyarylation of ethylene as a modular route to homobenzylic ethers. Using catalytic Ph_3PAuCl , a variety of arylsilanes and alcohols undergo 1,2-addition to ethylene in the presence of an iodine(III) oxidant. Optimisation studies led to the identification of an iodine(III) oxidant new to gold catalysis, 1-trifluoromethanesulfonyl-1,2-benziodoxol-(1*H*)-one (IBA-OTf), which allowed efficient oxyarylation under neutral conditions. A substrate scope demonstrated the compatibility of a variety of arylsilanes and alcohols in the protocol. Mechanistic investigations implicated the involvement of the ancillary phosphine throughout the catalytic cycle, in contrast to previous reports. Additionally, stoichiometric experiments suggest transmetalation of the arylsilane moiety occurs onto a gold(III) centre, prior to activation of ethylene towards alcohol attack and subsequent product forming reductive elimination.

The third chapter investigates the influence of the 2,2'-bipyridine (bipy) ligand on the chemistry of gold, with an emphasis on the activation of gold(I) towards oxidative addition with aryl iodides. $[(\kappa^2\text{-bipy})\text{Au}(\eta^2\text{-C}_2\text{H}_4)][\text{NTf}_2]$ complexes were found to undergo reversible oxidative addition of a range of aryl iodides under mild conditions. The rate of oxidative addition with respect to the electronic properties of the aryl iodide was found to follow the inverse order to that observed with, for example, palladium; faster oxidative addition was observed for electron rich aryl iodides. The resulting gold(III) complexes

$[(\kappa^2\text{-bipy})\text{Au}(\text{aryl})\text{I}][\text{NTf}_2]$ were found to undergo transmetalation with arylzinc chlorides and subsequent reductive elimination to give biaryl products. The overall process represents the first gold-mediated Negishi cross-coupling, albeit in a stoichiometric manner.

The fourth chapter builds upon the results of Chapter 3 and explores the possibility of redox gold catalysis in the absence of an external oxidant. With the hypothesis that a phosphine ligand will better stabilise a gold centre throughout the catalytic cycle, a range of small bite-angle P,N-ligands were synthesised and coordinated to gold(I). Complexes supported by 8-quinolyl phosphine (8-QP) ligands were found to catalyse the Suzuki cross-coupling between 4-fluoroiodobenzene and 4-tolylboronic acid. Optimum activity was achieved using an electron-withdrawing 8-QP ligand, furnishing the target biaryl in 28% yield. Of particular note is that the reaction proceeds in the absence of an external base, in contrast to standard palladium-catalysed Suzuki conditions. The results described herein represent progress towards the development of a gold-catalysed Suzuki cross-coupling, however, further optimisation is required to achieve an attractive methodology.

Many of the results presented this thesis have been communicated:

Harper, M. J.; Emmett, E. J.; Bower, J. F.; Russell, C. A. *J. Am. Chem. Soc.* **2017**, *139*, 12386.

Harper, M. J.; Arthur, C. J.; Crosby, J.; Emmett, E. J.; Falconer, R. L.; Fensham-Smith, A. J.; Gates, P. J.; Leman, T.; McGrady, J. E.; Bower, J. F.; Russell, C. A. *J. Am. Chem. Soc.* **2018**, *140*, 4440.

Acknowledgements

I would like to begin by extending my gratitude to my academic supervisors, Chris Russell and John Bower. I'm particularly grateful to Chris for giving me the research freedom to satisfy my ever-changing chemical interests. I thank John for his drive and enthusiasm that often kept me going when chemistry wasn't playing ball. And I thank both of you for being all-round great mentors over four thoroughly enjoyable years. And obviously none of this work would have been possible without the gold group project meetings.

Thanks to everyone in the Russell group for being great company, in roughly chronological order: Andy Stonor, Sam Timson, Kelly Butterfield, Andy Fensham-Smith, Ignacio Navarette, Rosie Falconer, Paulina Genzels, Jamie Cadge and Sam Scott. I am also grateful to Liam Ball, a Russell group alumnus whose work initiated the research presented in Chapter 2. Additionally, I give credit to Andy Fensham-Smith for synthesising the original bipy gold(I) ethylene complex, which was crucial for the work described in Chapter 3.

In addition to the Russell group, I was fortunate enough to share lab space with the great people of the Bedford and Manners groups; thanks for making the lab such a fun place to work in! I would also like to thank the members of the Bower group, past and present, and my industrial supervisor at Syngenta, Ed Emmett.

Thanks also go to the NMR, MS, and technical staff: Tom Leman, Paul Laurence, Paul Gates, Chris Arthur, and Tony Rogers. I'm particularly grateful to Tom Leman, who allowed me the unfettered access to MS that was so crucial to the project. Thanks for the patience of Hazel Sparkes and Natalie Pridmore in the X-ray department for teaching me X-ray crystallography and putting up with my excessive questions. Thanks to everyone

in the Bristol Chemical Synthesis CDT: Emma Rose, Kevin Booker-Milburn, Mar Ruiz, Laura Chavda, and the whole of the 2014 CDT cohort.

Perhaps the biggest thanks goes to all my friends in Bristol and beyond, thanks for being awesome!

Finally, I thank my parents for their support, and Bristol for being Bristol.

Author's Declaration

I declare that the work in this dissertation was carried out in accordance with the requirements of the University's Regulations and Code of Practice for Research Degree Programmes and that it has not been submitted for any other academic award. Except where indicated by specific reference in the text, the work is the candidate's own work. Work done in collaboration with, or with the assistance of, others, is indicated as such. Any views expressed in the dissertation are those of the author.

SIGNED: DATE:.....

Abbreviations

1,2-DCB	1,2-dichlorobenzene
8-QP	8-quinolyl phosphine
acac	acetylacetonate
Ad	adamantyl
bipy	2,2'-bipyridine
cod	1,5-Cyclooctadiene
CSA	camphorsulfonic acid
DFT	density functional theory
DMA	dimethylacetamide
DMSO	dimethylsulfoxide
dppm	bis(diphenylphosphino)methane
ESI	electrospray ionisation
F ₂ -bipy	5,5'-difluoro-2,2'-bipyridine
GC-MS	gas chromatography–mass spectrometry
HOMO	highest occupied molecular orbital
HRMS	high-resolution mass spectrometry
HSAB	hard and soft acid base theory
IBA	1-hydroxy-3-oxobenziodoxole

IBA-OTf	1-trifluoromethanesulfonyl-1,2-benziodoxol-(1 <i>H</i>)-one
IBDA	PhI(OAc) ₂
IPr	1,3-Bis(2,6-diisopropylphenyl)imidazol-2-ylidene
LDA	lithium diisopropylamide
LED	light-emitting diode
LUMO	lowest unoccupied molecular orbital
Ms	methanesulfonyl
Nf	nonafluorobutanesulfonate
Phth	phthalimido
Piv	trimethylacetyl
<i>p</i> -TSA	<i>p</i> -toluenesulfonic acid
r.t.	room temperature
<i>R_F</i>	retention factor
Tf	trifluoromethanesulfonyl
TfOH	trifluoromethane sulfonic acid
tht	tetrahydrothiophene

Contents

1	Introduction	1
1.1	Thesis Structure	2
1.2	A Brief History of Gold	2
1.3	The Chemistry of Gold	4
1.4	Gold Catalysis	9
1.4.1	Isohypsic Gold Catalysis	9
1.4.2	Redox Gold Catalysis	11
1.5	Research Objectives	16
2	Oxyarylation of Ethylene	19
2.1	Ethylene in Synthesis	20
2.2	Oxyarylation: Literature Precedent	22
2.3	Objectives	27
2.4	Initial Results and Optimisation	28
2.5	Substrate Scope for the IBA/TfOH System	31
2.6	Development of the IBA-OTf Oxidant System	34
2.7	Substrate Scope for the IBA-OTf System	36
2.8	Reaction Limitations	39
2.9	Mechanism	40
2.9.1	Previous Mechanistic Hypotheses	40
2.9.2	Stoichiometric Studies	43
2.9.3	Oxidant Speciation	50
2.9.4	Role of the Phosphine	52
2.9.5	Mechanistic Hypothesis	54

2.10	Conclusion	56
2.11	Future Work	56
3	Organometallic Steps with Gold	61
3.1	Introduction	63
3.1.1	Oxidative Addition to Gold(I)	65
3.1.2	Objectives	76
3.2	Synthesis of $[(\kappa^2\text{-bipy})\text{Au}(\text{C}_2\text{H}_4)][\text{NTf}_2]$	77
3.3	Oxidative Addition: Initial Results	81
3.4	Oxidative Addition: Aryl Iodide Scope	85
3.5	Oxidative Addition: 2,2'-Bipyridine System	89
3.6	$[(\kappa^2\text{-bipy})\text{Au}(\eta^2\text{-norbornene})][\text{NTf}_2]$	90
3.7	Oxidative Addition: Mechanism	92
3.8	Transmetalation	96
3.9	Negishi Coupling Mechanism	98
3.10	Transmetalation of a $\text{C}(\text{sp}^3)$ Reagent	102
3.11	Investigations Toward Catalysis	103
3.12	Conclusion	105
3.13	Future Work	106
3.13.1	Catalysis	106
3.13.2	Oxidative Addition Scope	107
3.13.3	Bipy Gold(I) Carbonyl	107
4	P,N-Ligands for Gold Catalysis	109
4.1	Suzuki Coupling	110
4.2	Suzuki Coupling Catalysed by Gold	110
4.3	Objectives	114
4.4	λ^3 -phosphinines	114

4.5	Pyridyl Phosphines	117
4.5.1	Pyridyl Phosphines: Synthesis	117
4.5.2	Pyridyl Phosphine Complexes: Reactivity	119
4.6	Quinolyl Phosphines	121
4.6.1	Initial Observations with (8-(Diphenylphosphino)quinoline)AuCl	123
4.6.2	Catalysis with (8-(Diphenylphosphino)quinoline)AuCl	125
4.6.3	Synthesis of New 8-Quinolyl Phosphine Ligands	129
4.6.4	Evaluation of 8-QP Complexes in Catalysis	136
4.7	Conclusion	137
4.8	Future Work	138
5	Experimental	141
5.1	General Considerations	141
5.2	Experimental Procedures Relevant to Chapter 2	142
5.2.1	Gold Complexes	142
5.2.2	Arylsilanes	147
5.2.3	Iodine(III) Compounds	160
5.2.4	Oxyarylation General Procedures	162
5.2.5	Oxyarylation Products	163
5.2.6	Optimisation Procedure	180
5.2.7	Mechanistic Experiments	181
5.3	Experimental Procedures Relevant to Chapter 3	182
5.3.1	Organic Compounds	182
5.3.2	Gold Complexes	185
5.3.3	Reaction Profiles	197
5.3.4	Transmetalation: Low Temperature ¹⁹ F NMR Studies	199
5.3.5	Mass Spectrometry	200

5.4	Experimental Procedures Relevant to Chapter 4	202
5.4.1	General Procedure for Suzuki Biaryl Coupling	202
5.4.2	Ligands	202
5.4.3	Gold Complexes	216
5.5	Crystallographic Data	225
	References	247

Chapter 1

Introduction

Abstract

This chapter will give a briefing on the chemistry of gold. The discussion will include fundamental aspects about the chemistry of gold, from available oxidation states, structure, and reactivity, to the relativistic effects that are crucial to understanding the special properties of gold. Homogeneous isohypsic and redox gold catalysis will be introduced, with an emphasis placed upon the redox gold(I)/(III) manifold. Heterogeneous gold catalysis is of less relevance to this thesis and will only be discussed briefly.

1.1 Thesis Structure

Multiple aspects of the field of gold chemistry are covered within this thesis: Chapter 2 describes redox gold catalysis facilitated by an external iodine(III) oxidant; Chapter 3 explores the use of the 2,2'-bipyridyl ligand to unlock fundamental organometallic chemistry with gold; and Chapter 4 returns to redox gold catalysis but in the absence of an external oxidant. Due to the variety of topics discussed, this general introduction serves only to provide a brief overview on the chemistry of gold; a more detailed introductory discussion precedes each chapter.

1.2 A Brief History of Gold

Gold has historically been prized for its inertness and characteristic shiny lustre. For these reasons, its primary use has always been, and still is, for jewellery.¹ In fact, archaeologists have found intact gold jewellery in Egypt from as long ago as 5000 years.² One reason that ancient civilisations used gold is that it is a native metal, meaning that it is one of the few metals found in a pure, metallic state in nature.³ Surprisingly large pieces of metallic gold have been found; the largest gold nugget was found in 1869 in the town of Moliagul in central Victoria, Australia.² Known as the "Welcome Stranger", the nugget weighed 66 kg, measured approximately 60×30 cm, and would have been worth around £3 million today (Figure 1.1).⁴



Figure 1.1: A replica of the "Welcome Stranger" golden nugget, measuring approximately 60×30 cm and found in the town of Moliagul in central Victoria, Australia, in 1869.⁴

China is the largest miner of gold, followed by Australia and then Russia.¹ In 2017, the worldwide mine production of gold was 3,305 tonnes, with another 1,268 tonnes produced from recycling.¹ Of this total, 53% is used for jewellery, 39% is sold for investment and banking, and only 8% goes towards technological applications. Most of the technologically used gold is used for dentistry and electronics (85% combined); the remaining 15% is used for "other industrial" applications according to the The World Gold Council. It is from this category (1.2% of global gold demand) that the gold used for chemistry comes from.

A common misconception is that the consumption of gold for chemistry is prohibitively expensive, however, a price comparison with other commonly used precious metals reveals comparable prices (Table 1.1).⁵ Rhodium and iridium are both more expensive, whereas palladium and platinum are only slightly cheaper. In fact, the widespread use of gold for investment and currency has led to a fairly stable price, contrasting to the often large price fluctuations observed with ruthenium and rhodium.

Table 1.1: Precious metal prices as of 29th August 2018.⁵

Entry	Metal	Price (USD/troy ounce) ^a
1	gold	1202
2	silver	15
3	platinum	791
4	palladium	939
5	ruthenium	255
6	rhodium	2380
7	iridium	1430

^aOne troy ounce is equal to 31.1 grams.

1.3 The Chemistry of Gold

Perhaps surprisingly for what is known as the noblest metal,⁶ gold can adopt the oxidation states -1, 0, +1, +2, +3, and +5. Examples of gold(-I) include tetramethylammonium auride (Me_4NAu)⁷ and the alkali metal salts RbAu and CsAu .⁸ Complexes of gold in the +2 oxidation state are usually dimeric, however, a recent example of a mononuclear gold(II) porphyrin complex was reported by Heinze *et al.*⁹ Accessing the +5 oxidation state requires forcing conditions, however, Seppelt and Hwang succeeded in isolating and characterising the dimeric gold(V) species $(\text{AuF}_5)_2$.¹⁰ Very recently, Ma and Yang have predicted approaches to synthesise AuF_4 and AuF_6 using high pressure methods, however, no experimental evidence was provided.¹¹ Even so, the chemistry of gold is undeniably dominated by the +1 and +3 oxidation states, and these will be discussed in further detail below.

Gold(I)

Gold(I) has the electronic configuration $[\text{Xe}]4f^{14}5d^{10}$, and primarily forms colourless, 2-coordinate, 14-electron complexes with linear geometries. Common examples include phosphine-supported gold(I) chlorides such as Ph_3PAuCl (Figure 1.2). Higher coordina-

tion numbers such as 3ⁱ (trigonal planar) and 4 (tetrahedral) are also found but are less common.^{12,13}

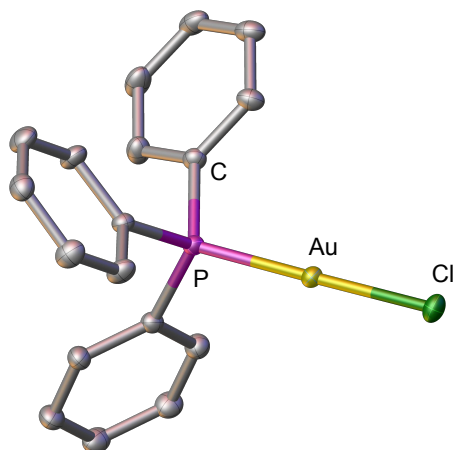


Figure 1.2: Molecular structure of Ph_3PAuCl , taken from ref. 14. Thermal ellipsoids are shown at the 50% probability level, hydrogen atoms have been omitted for clarity. Selected bond lengths (Å) and angles ($^\circ$): Au-P 2.2314(4), 2.2903(4), P-Au-Cl 179.239(14).

In terms of hard and soft acid base theory (HSAB),⁶ gold(I) is a soft metal and preferentially binds soft donor atoms such as phosphorus or sulfur. Tetrachloroauric acid ($\text{HAuCl}_4 \cdot x\text{H}_2\text{O}$) is the most common source of soluble gold, and treatment with excess Ph_3P or Me_2S in ethanol provides a convenient route to Ph_3PAuCl or Me_2SAuCl , respectively. Me_2SAuCl (or the tetrahydrothiophene analogue) serves as a convenient, bench stable precursor to R_3PAuCl compounds *via* substitution with the free phosphines in CH_2Cl_2 .

Gold(III)

Gold(III) has the electronic configuration $[\text{Xe}]4f^{14}5d^8$, and preferentially forms 4-coordinate, 16 electron complexes which are often characteristically yellow. As is common for d^8 metals, a square planar geometry is strongly preferred, such as in $\text{Cy}_3\text{PAuCl}_3$ (Figure 1.3).¹⁵ Gold(III) complexes with coordination numbers other than 4 are extremely

ⁱSee Chapter 3 for 3-coordinate gold(I) complexes.

rare; a 5-coordinate example is $(\text{Me}_3\text{P})_2\text{AuI}_3$ which adopts a trigonal bipyramidal geometry.^{16,17} Additionally, a 3-coordinate Y-shaped complex of gold(III) was reported by Bourissou *et al.*, although the structure was not characterised crystallographically.¹⁸

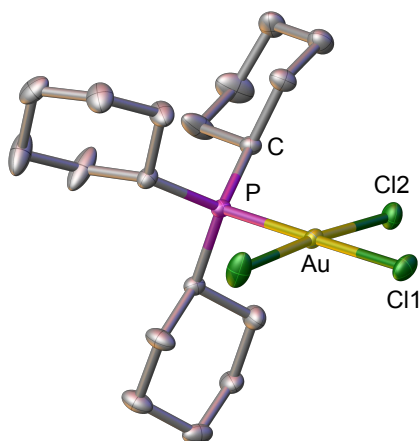
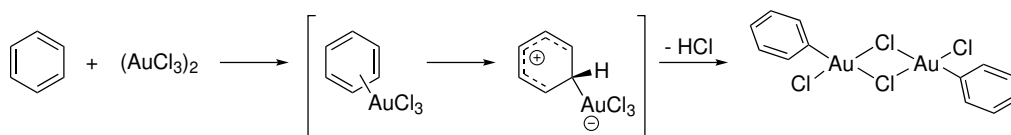


Figure 1.3: Molecular structure of $\text{Cy}_3\text{PAuCl}_3$, taken from ref. 15. Thermal ellipsoids are shown at the 50% probability level, hydrogen atoms have been omitted for clarity. Selected bond lengths (\AA) and angles ($^\circ$): Au-P 2.3452(10), Au-Cl1 2.3501(11), P-Au-Cl1 179.06(4), Cl1-Au-Cl2 88.50(5), P-Au-Cl2 92.14(4).

With respect to HSAB theory, gold(III) possesses intermediate hard character and prefers hard donors such as nitrogen, oxygen, and fluorine.¹⁹ Gold(III) is highly electrophilic and readily activates arene C–H bonds *via* an $\text{S}_{\text{E}}\text{Ar}$ mechanism. This is exemplified by the facile auration of benzene by $(\text{AuCl}_3)_2$, first reported by Kharasch *et al.* in 1931 (Scheme 1.1).^{20,21}



Scheme 1.1: Auration of benzene by $(\text{AuCl}_3)_2$.^{20,21}

Relativistic Effects

When discussing the chemistry of gold, one must take into account Einstein's theory of special relativity, and specifically, Dirac's inclusion of relativity into the Schrödinger equation.^{22,23} The theory of special relativity states that as the velocity of an object approaches the speed of light (c), the mass of that object increases. Given that the radial velocity of an electron increases with atomic number (Z), and for gold $Z = 79$, an electron in the $1s$ orbital of gold has a velocity of approximately $0.58c$. This results in a mass increase of that electron by a factor of approximately 1.23.¹³ Now given that the Bohr radius of an atomic orbital is inversely proportional to the mass of an electron, a consequence is the contraction of the s and p orbitals of gold; the *relativistic contraction*.²² As the calculated relativistic vs. non-relativistic radii of the $6s$ orbitals show (Figure 1.4), this effect reaches a maximum at gold.

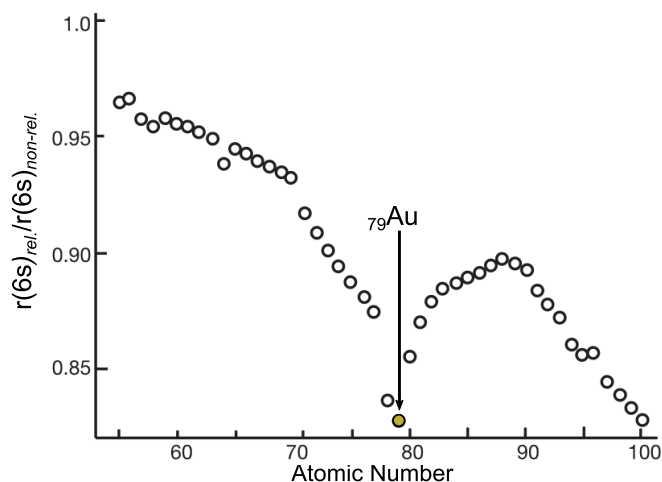


Figure 1.4: Calculated relativistic contraction of the $6s$ orbital, taken with permission from ref. 22.

The relativistic contraction results in the s and p orbitals being held closer to the nucleus. This results in increased shielding of, and subsequent expansion of the d and f orbitals. Energetically, the $6s$ orbital is lowered in energy, whereas the $5d$ orbitals are increased in

energy. The practical consequences of this are as follows:

Colour: The small energy gap between the $5d$ and $6s$ orbitals of gold brings the absorbance of electromagnetic radiation down from the ultraviolet (as in for *colourless* silver) into the visible region (starting at around 521 nm). This corresponds to absorption of green light and the characteristic yellow colour of gold.²⁴

Oxidative stability: A consequence of the diffuse d and f orbitals is that electrons in the $5d$ orbitals of gold experience reduced electron-electron repulsion. This manifests as decreased nucleophilicity and stability towards oxidation. An example of this is the reluctance of gold(I) to undergo oxidative addition. Additionally, the resistance towards oxidation renders the majority of gold-catalysed processes tolerant to air and moisture, a significant operational advantage.

Aurophilicity: Au...Au aurophilicity is the tendency of gold(I) atoms to attract each other, with energies comparable to that of hydrogen bonding. As gold(I) has a closed d^{10} shell, there should be no orbitals available for bonding. Due to the relativistic energetic convergence of gold's $5d$ and $6s$ orbitals, the $5d$ orbital becomes a better donor and the $6s$ orbital becomes a better acceptor. This gives gold mixed donor-acceptor characteristics leading to Au...Au aurophilic interactions.¹³ This effect was illustrated in 1988 by Schmidbaur *et al.* in the isolation of the hexaauriomethane dication $[(\text{Ph}_3\text{PAu})_6\text{C}]^{2+}$, which was stabilised by aurophilic interactions.²⁵

Electronegativity: The relativistic contraction results in an increased ionization energy (IE) and electron affinity (EA) for gold. This results in a Pauling electronegativity (EN) that is approximately 0.45 times higher than expected. The EN for gold is 2.54, which is comparable to that of carbon (EN = 2.55).^{26,27}

Lewis Acidity: The contracted s and p orbitals of gold result in a low-lying LUMO, rendering gold a strong Lewis acid.²² Gold acts as a soft Lewis acid and preferentially

activates soft species such as carbon-carbon multiple bonds.

1.4 Gold Catalysis

The field of gold catalysis has undergone exponential growth in the last quarter century. What was once termed both "*catalytically dead*"²⁸ and "*a lethargic and overweight version of catalytically interesting copper*",²⁹ gold catalysis is now a rich and diverse field. A natural division arises arranging gold catalysis into two distinct categories, homogeneous and heterogeneous. The latter uses surface supported and nanoparticulate gold to catalyse processes such as CO oxidation, acetylene hydrochlorination, hydrogenation of N–O bonds, and oxidation of alcohols.^{30–32} However, this thesis will focus only on homogeneous gold catalysis; heterogeneous gold catalysis will not be discussed further.

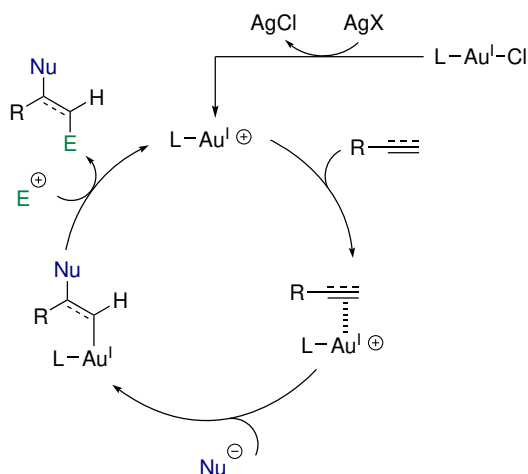
Within homogeneous gold catalysis, a further subdivision can be drawn differentiating the process based on whether or not the oxidation state of gold changes. For *isohypsic* gold catalysis, the gold centre remains in the same oxidation state (usually +1) throughout the catalytic cycle. *Redox* gold catalysis involves a change in the oxidation state of gold throughout the catalytic cycle; this is predominantly between the +1 and +3 oxidation states.

1.4.1 Isohypsic Gold Catalysis

In the majority of isohypsic gold catalysis, a generalised mode of action is that gold(I) (or less commonly, gold(III)) serves as a soft Lewis acid activating π -systems towards attack from nucleophiles. A generic mechanism is depicted in Scheme 1.2 and consists of:

1. Coordination of gold to the π -system.
2. *Anti* nucleophilic attack onto the gold-activated π -system.³²

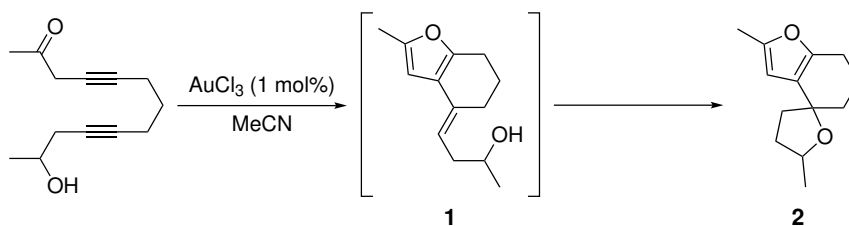
3. Trapping of the resulting organogold complex with an electrophile, releasing the new organic product and reforming the gold catalyst.



Scheme 1.2: A simplified catalytic cycle for a gold(I) catalyzed process.

The most commonly encountered precatalysts for isohypsic gold catalysis are gold(I) complexes of the type LAuCl , where the ligand L is an N -heterocyclic carbene (NHC) or phosphine (R_3P). Cationic gold species $[\text{LAu}]^+$ are usually required for the activation of π -systems; these can be generated *in situ* by addition of a silver salt such as AgSbF_6 , AgNTf_2 , or AgOTf to the LAuCl precatalyst.

An early example of isohypsic gold catalysis was a combined C–C and C–O bond forming spirocyclization reaction reported by Hashmi *et al.* in 2000 (Scheme 1.3).^{32,33} In this reaction, an initial cyclization occurs involving both C–C and C–O bond formation to give the intermediate homoallylic alcohol **1**, which then undergoes a spirocyclization to furnish the product **2**. This reaction serves as a good general illustration to the reactivity available in isohypsic gold catalysis, involving the activation of both alkynes and alkenes towards attack from carbonyl groups, π -systems, and alcohols.

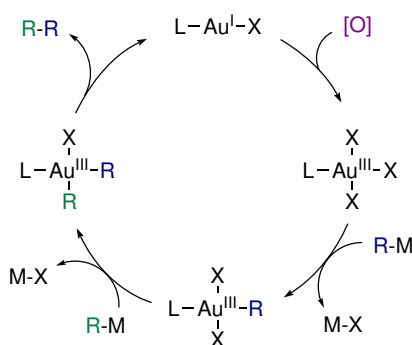


Scheme 1.3: Gold(III) catalysed spirocyclization by Hashmi *et al.*³³

More recently, isohypsic gold catalysis has been used extensively to introduce molecular complexity, including enantioselective protocols. The field has been extensively reviewed; for further detail the reader is directed to these publications.^{32,34–47}

1.4.2 Redox Gold Catalysis

A generalised mechanism for a redox gold catalysed coupling process is outlined in Scheme 1.4. Oxidation of gold(I) to gold(III) is followed by two subsequent transmetalation type events, then reductive elimination forms the new product and reforms the gold(I) catalyst.



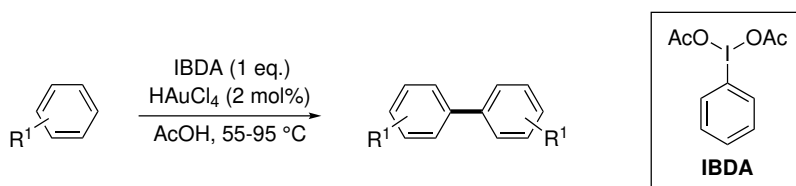
Scheme 1.4: A simplified redox gold catalytic cycle. X represents an anionic ligand, [O] represents an oxidant.

For traditional transition-metal-catalysed coupling reactions, oxidation of the metal is achieved *via* an oxidative addition process (for example, with aryl halides), a fundamental

organometallic step that gold(I) is highly reluctant to undergo.ⁱ To overcome this inherent property of gold, two main strategies have been identified to give access to the gold(I)/(III) manifold: the use of external oxidants, and the use of highly electrophilic (and *oxidative*) reagents such as diazonium salts.

Redox Gold Catalysis with External Oxidants

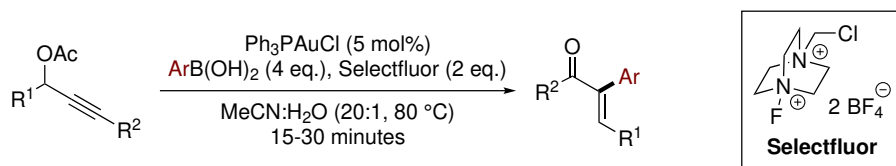
The first oxidants to be used for redox gold catalysis were iodine(III) reagents. Tse *et al.* reported the gold-catalysed homo- and heterocoupling of arenes mediated by iodobenzene diacetate (IBDA) as the oxidant (Scheme 1.5).^{48,49} The reaction involves a double C–H activation and the coupling of two formal nucleophiles, hence the requirement for an oxidant.



Scheme 1.5: Gold-catalysed iodine(III)-mediated homocoupling of arenes, reported by Tse *et al.*^{48,49}

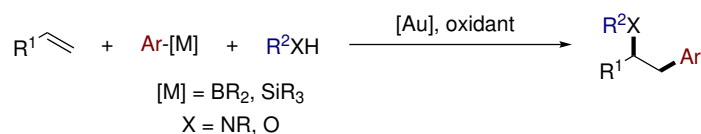
Zhang *et al.* then introduced Selectfluor as a suitable oxidant for redox gold catalysis within the context of the oxidative cross-coupling of propargylic acetates with arylboronic acids (Scheme 1.6).⁵⁰ Zhang *et al.* further demonstrated the potential of the Selectfluor-mediated gold(I)/(III) catalytic cycle with a C–O bond-forming reaction involving intramolecular acyl migration of propargylic benzoates.⁵¹

ⁱSee Chapter 3 for a more detailed discussion on the reluctance of gold(I) to undergo oxidative addition.



Scheme 1.6: Gold-catalysed oxidative cross-coupling of propargylic acetates and arylboronic acids, reported by Zhang *et al.*⁵⁰

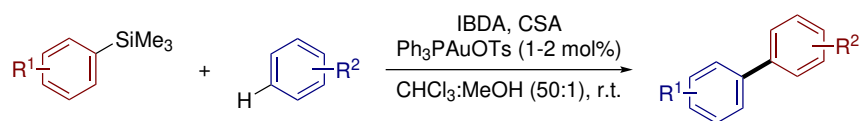
In 2010, Zhang *et al.* reported the first gold-catalysed oxidative heteroarylation of alkenes.⁵² The report described the addition of O- or N-nucleophiles and arylboronic acids across an alkene (Scheme 1.7). The versatility and modularity of the reaction prompted further development by the groups of Toste^{53,54} and Russell,^{55,56} for a more detailed discussion see Chapter 2, Section 2.2.



Scheme 1.7: General scheme for gold-catalysed heteroarylation of alkenes.

In addition to alkene heteroarylation, further modes of oxidative gold catalysis developed during the following few years include: alkynylation of arenes⁵⁷ and arylboronic acids;⁵⁸ acyloxylation of arenes;⁵⁹ and the homo- and cross-coupling of alkynes.^{60–62}

In 2012, Russell *et al.* reported a new avenue in oxidative gold catalysis; gold-catalysed direct C–H arylation of aryltrimethylsilanes.^{63,64} The reaction was facilitated by IBDA as oxidant, and provided a method for the efficient construction of biaryls under mild conditions (Scheme 1.8). The reaction has since been further developed by Lloyd-Jones *et al.* for the construction of medium-sized rings and towards the total synthesis of the natural product (\pm)-alcolchicine.^{65–68}



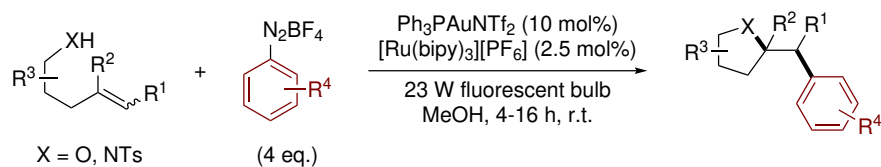
Scheme 1.8: Gold-catalysed direct arylation.^{63,64}

The gold-catalysed activation of C–H bonds under oxidative conditions has since been exploited by a number of groups, examples include: direct arylation of heterocycles,⁶⁹ birayl synthesis *via* double C–H activation,⁷⁰ amination of C–H bonds,^{71,72} oxidative cyclisation,⁷³ and C–H arylation with arylboron reagents.⁷⁴

Oxidant-Free Redox Gold Catalysis

Redox gold catalysis in the absence of external oxidants is dominated by the use of aryldiazonium salts (Ar-N₂X) as the coupling partner; the topic has recently been reviewed by Patil *et al.*⁷⁵ Aryldiazonium salts are highly electrophilic species that react with concurrent loss of dinitrogen (N₂), a strongly energetically favoured process due to the thermodynamic stability of dinitrogen.

The first example of combined photoredox and gold catalysis using aryldiazonium salts was by Glorius *et al.* in 2013.⁷⁶ Using the combined catalytic system of Ph₃PAuNTf₂ and [Ru(bipy)₃][PF₆] with visible light irradiation, two-component heteroarylation was achieved using aryldiazonium tetrafluoroborates (Ar-N₂BF₄) as the internal oxidant (Scheme 1.9). The three-component, intermolecular variant was reported by Glorius *et al.* a year later.⁷⁷ The reactions were proposed to proceed *via* a gold(I)/(II)/(III) redox cycle facilitated by single electron transfers, see Scheme 2.17 (page 43) for further details. Proof that aryldiazonium salts oxidise gold(I) was obtained *via* stoichiometric oxidations of gold(I) to gold(III) by the groups of Hashmi⁷⁸ and Glorius.⁷⁹

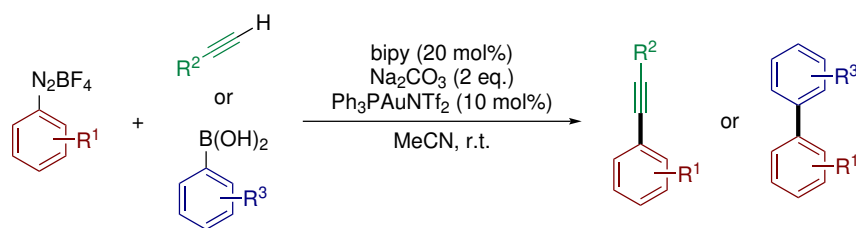


Scheme 1.9: Heteroarylation of alkenes with aryldiazonium salts *via* combined photoredox gold catalysis.⁷⁶

Following these initial reports, a plethora of reactions were reported exploiting dual gold and photoredox catalysis,⁷⁵ including: Sonogashira-type couplings between alkynes and aryldiazonium salts;^{80,81} alkyne difunctionalisation;^{82–84} arylative ring expansion;⁸⁵ C–P bond formation *via* cross-coupling of aryldiazonium salts with diethyl phosphite;⁸⁶ arylative cyclisations of alkynes;^{87–89} and allylation of aryldiazonium salts.⁹⁰

In addition, and of relevance to the work presented within this thesis (See Chapter 4), the groups of Lee⁹¹ and Fouquet⁹² reported the Suzuki-type coupling of aryldiazonium salts with arylboronic acids, catalysed by gold in the presence of photosensitizers. Patil *et al.* expanded the scope of these reactions to employ aryltrimethylsilanes as coupling partners,⁹³ and Lee *et al.* reported a direct C–H arylation of aryldiazonium salts.

Activation of aryldiazonium salts in the absence of photosensitizers was reported by Shi *et al.* in 2015.⁹⁴ Gold-catalysed cross-coupling of alkynes and arylboronic acids with aryldiazonium salts was achieved in the presence of 20 mol% bipy as an additive (Scheme 1.10). It was proposed that the bipy additive served to aid nitrogen extrusion in the absence of photochemical excitation.



Scheme 1.10: Bipy-assisted gold-catalysed cross-coupling of alkynes and arylboronic acids with aryldiazonium salts.⁹⁴

A year later, Hashmi *et al.* reported the gold-catalysed difunctionalisation of internal alkynes with aryldiazonium salts using blue LEDs, also in the absence of photosensitizers.⁹⁵ Hashmi *et al.* then expanded the protocol to the photosensitizer-free Suzuki-type coupling of arylboronic acids and aryldiazonium salts.⁹⁶

The stability of aryldiazonium salts is often dictated by the corresponding anion (X⁻); for example chlorides and acetates tend to be unstable above 0 °C, whereas tosylates and tetrafluoroborates are stable at room temperature.⁹⁷ However, due to the energetic nature of aryldiazonium salts, their reactivity cannot always be predicted and they must be treated with caution, especially on scale.⁹⁷ An alternative to the use of aryldiazonium salts is to access redox gold catalysis *via* the oxidative addition of gold. See Chapters 3 and 4 for a more detailed discussion on the inherent challenges this presents, and strategies to accomplish this aim.

1.5 Research Objectives

The first part of this thesis will exploit redox gold catalysis in combination with an iodine(III) oxidant. The work will build upon previous methodology developed in the Russell group^{55,56} and will apply gold-catalysed oxyarylation to affect the functionalisation of the abundant feedstock chemical, ethylene.

The second part of the thesis will pursue alternative entries into the gold(I)/(III) catalytic manifold. Specifically, the well known reluctance of gold(I) to undergo oxidative addition will be addressed using cheap and readily available 2,2'-bipyridyl ligands.

The final part of the thesis will explore gold catalysis facilitated by P,N-ligands, with the goal of achieving redox gold catalysis using aryl iodides as the internal oxidant. Through ligand design, a gold-catalysed Suzuki biaryl coupling will be demonstrated. The results represent progress towards a gold-catalysed Suzuki cross-coupling, however, further optimisation will be required to achieve an attractive methodology.

Chapter 2

Oxyarylation of Ethylene

Abstract

This chapter describes the gold-catalysed oxidative oxyarylation of ethylene. A variety of arylsilanes and alcohols were found to undergo 1,2-addition addition to ethylene using catalytic gold(I) and the iodine(III) oxidant 1-trifluoromethanesulfonyl-1,2-benziodoxol-(1*H*)-one (IBA-OTf). This process provides a modular and efficient route to homobenzylic ethers from ethylene, an abundant feedstock chemical.

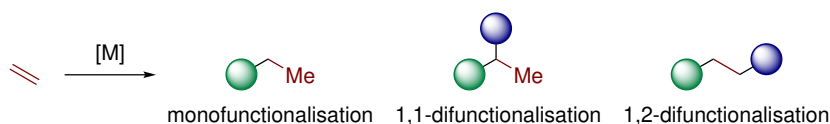
The contents of this chapter have been communicated:⁹⁸ Harper, M. J.; Emmett, E. J.; Bower, J. F.; Russell, C. A. *J. Am. Chem. Soc.* **2017**, *139*, 12386. Parts of this chapter have been reproduced from the aforementioned publication. Author contributions for the publication are as followed: M.J.H performed all experimental work. The manuscript was drafted by M.J.H then refined and edited by M.J.H, J.F.B and C.A.R. E.J.E was the industrial supervisor. X-ray diffraction analysis was performed by Dr. Hazel Sparkes and Dr. Natalie Pridmore with the University of Bristol X-ray crystallographic service.

2.1 Ethylene in Synthesis

Global ethylene production is in excess of 140 million tonnes per year; it is the most abundantly synthesized organic molecule in the world.^{99–101} The majority is used in the large scale synthesis of commodity chemicals such as polyethylene, ethylene oxide, acetaldehyde and vinyl chloride.¹⁰² Despite underpinning a wide range of industrial processes, the direct conversion of ethylene into fine chemical products is uncommon, such that this abundant feedstock is rarely exploited as a reactant in organic synthesis.

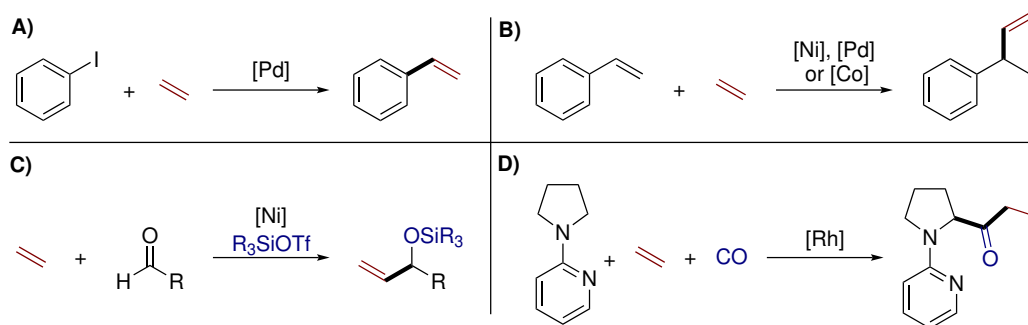
Although there are various well established industrial processes that utilise ethylene, such processes will not be discussed in this thesis. Herein the focus will be directed upon catalytic reactions involving ethylene.¹⁰¹

Given the simplicity of ethylene, its limited functionalisation modes can be divided into three categories: monofunctionalisation, 1,1-difunctionalisation and 1,2-difunctionalisation (Scheme 2.1).



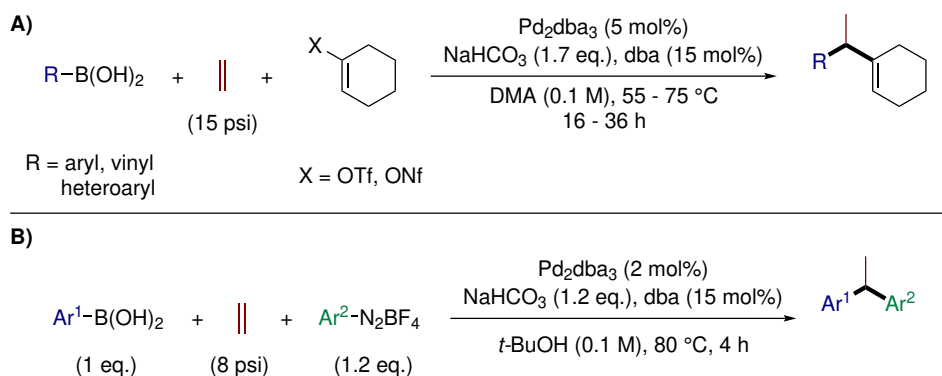
Scheme 2.1: Target products for the metal-catalysed functionalisation of ethylene. [M] = metal catalyst.

Examples of catalytic ethylene monofunctionalisation are rare, however, examples include Heck-like reactions (Scheme 2.2, A),^{103–108} alkene hydrovinylation (Scheme 2.2, B),^{109–117} processes where ethylene functions as a vinylmetal surrogate (Scheme 2.2, C),^{118–120} and Rh-catalysed hydroacylations (Scheme 2.2, D),^{121,122}



Scheme 2.2: Examples of catalytic monofunctionalisation of ethylene: Heck-like reaction (A); hydrovinylation (B); ethylene acting as a vinylmetal surrogate (C); hydroacylation (D).

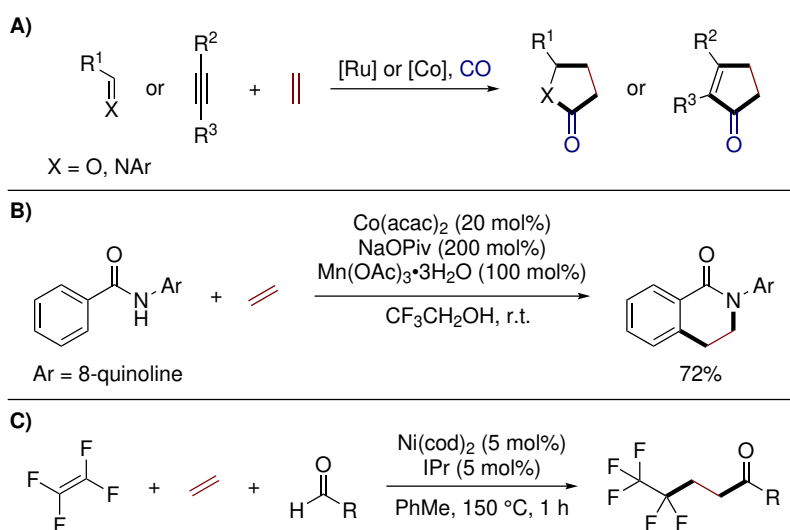
Rarer still is the catalytic 1,1-difunctionalisation of ethylene; in 2012, Sigman *et al.* reported that under Pd-catalysis, sp^2 transmetalating reagents and vinyl-sulfonate electrophiles undergo 1,1-addition to ethylene (Scheme 2.3, A).¹²³ The scope was expanded the following year to allow the 1,1-diarylation of terminal alkenes, including ethylene (Scheme 2.3, B).¹²⁴ The use of either an arylboronic acid or an aryldiazonium salt allows differentiation between the two added aryl groups.



Scheme 2.3: Pd-catalysed 1,1-difunctionalisation (A) and 1,1-diarylation (B) of ethylene.^{123,124}

With respect to catalytic ethylene 1,2-difunctionalisation, with the exception of metathesis-type reactions,^{101,125} only a handful of examples exist (Scheme 2.4). The 1,2-carbo-

functionalisation of ethylene has been demonstrated in the three-component carbonylative cyclocoupling with CO and alkenes or alkynes (Scheme 2.4, A).^{126–128} Daugulis *et al.* described an aminoquinoline-directed C-H carboamination of alkenes, giving one example with ethylene (Scheme 2.4, B),¹²⁹ and Ogoshi *et al.* developed a nickel-catalysed selective cross-trimerisation to couple tetrafluoroethylene and ethylene with a range of aldehydes (Scheme 2.4, C).¹³⁰

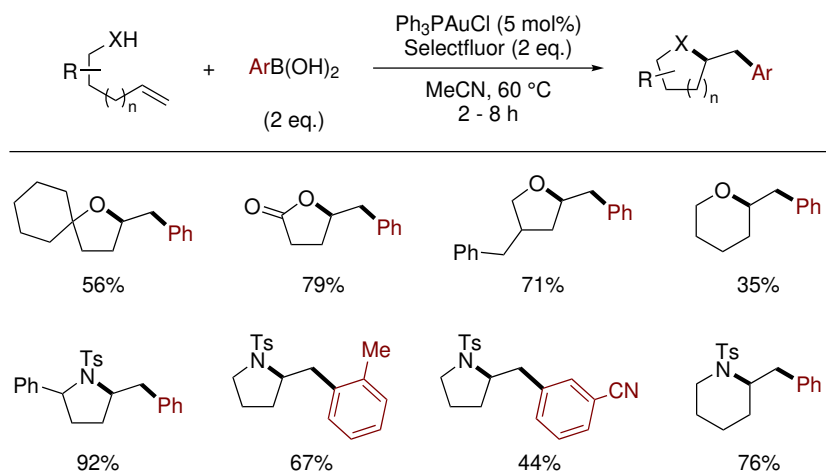


Scheme 2.4: 1,2-Difunctionalisation of ethylene: carbonylative cyclocoupling (A);^{126–128} cobalt-catalysed 1,2-carboamination *via* C-H activation (B);¹²⁹ and nickel-catalysed cross-trimerisation (C).¹³⁰

2.2 Oxyarylation: Literature Precedent

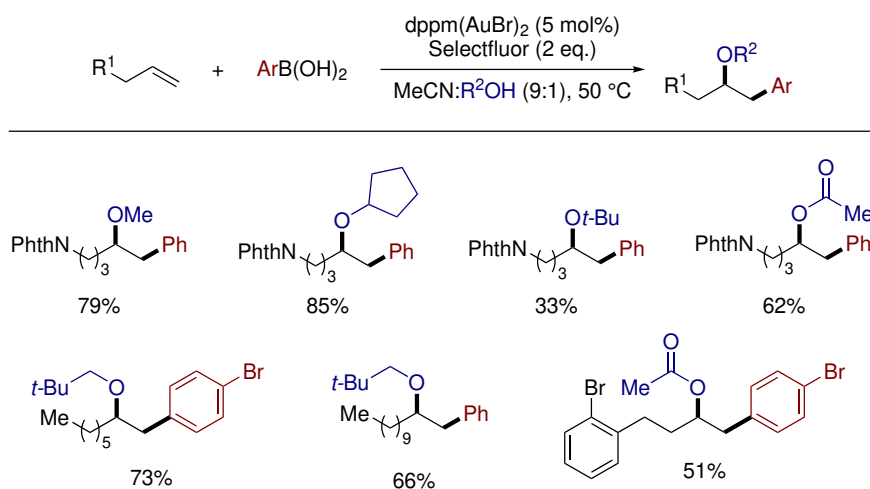
Gold-catalysed alkene heteroarylation was first reported in 2010 by Zhang *et al.*⁵² The process involved intramolecular addition of *N*- or *O*-nucleophiles and arylboronic acids across a double bond with the heteroatom component exhibiting Markovnikov selectivity (Scheme 2.5). Primary and secondary alcohols, carboxylic acids, and tosyl protected amines were compatible to afford 5- and 6-membered heterocycles in moderate to excellent yields using 5 mol% Ph_3PAuCl . The protocol effects the addition of two for-

mally nucleophilic species to a double bond, therefore an oxidant is required (in this case Selectfluor). Toste *et al.* reported, also in 2010, an almost identical intramolecular gold-catalysed aminoarylation methodology using 3 mol% $\text{dppm}(\text{AuBr})_2$ instead of Ph_3PAuCl .¹³¹



Scheme 2.5: Gold-catalysed oxidative 1,2-heteroarylation of alkenes, facilitated by Selectfluor as oxidant.⁵²

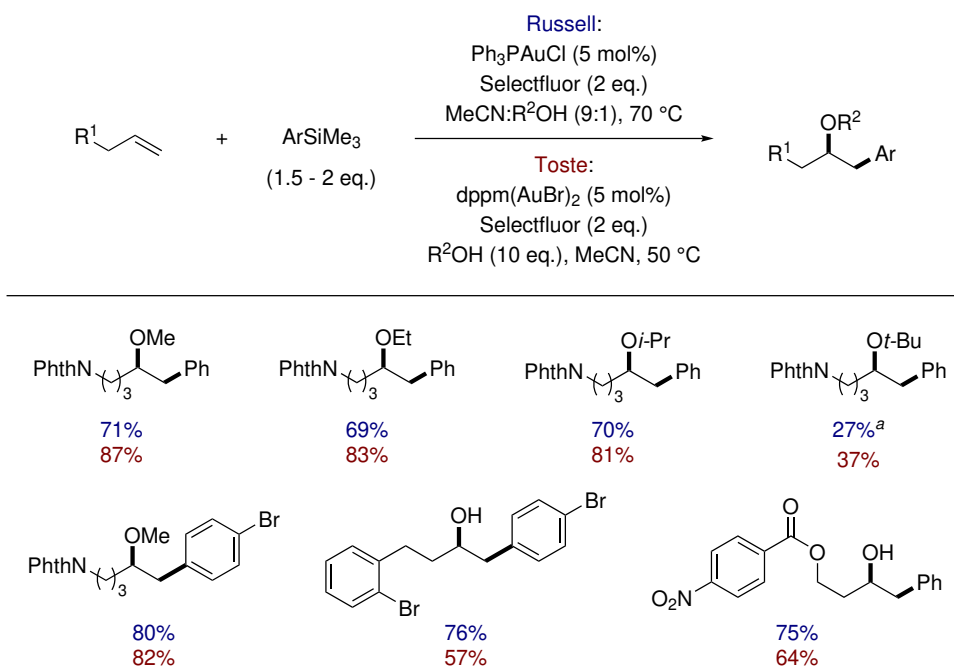
The modularity of Gold-catalysed oxyarylation was expanded by Toste *et al.* to a three-component, intermolecular reaction (Scheme 2.6).⁵⁴ A range of simple carboxylic acids and alcohols, including the bulky *t*-BuOH, underwent oxyarylation with various alkenes and arylboronic acids. Due to the requirement that the alcohol be present in large excess (as co-solvent), extension of the protocol to complex alcohols was precluded. Another significant drawback was that a large total gold loading of 10 mol% was needed, and both the catalyst and boronic acid required portionwise addition throughout the reaction.



Scheme 2.6: Three-component, intermolecular gold-catalysed oxyarylation of alkenes.⁵⁴

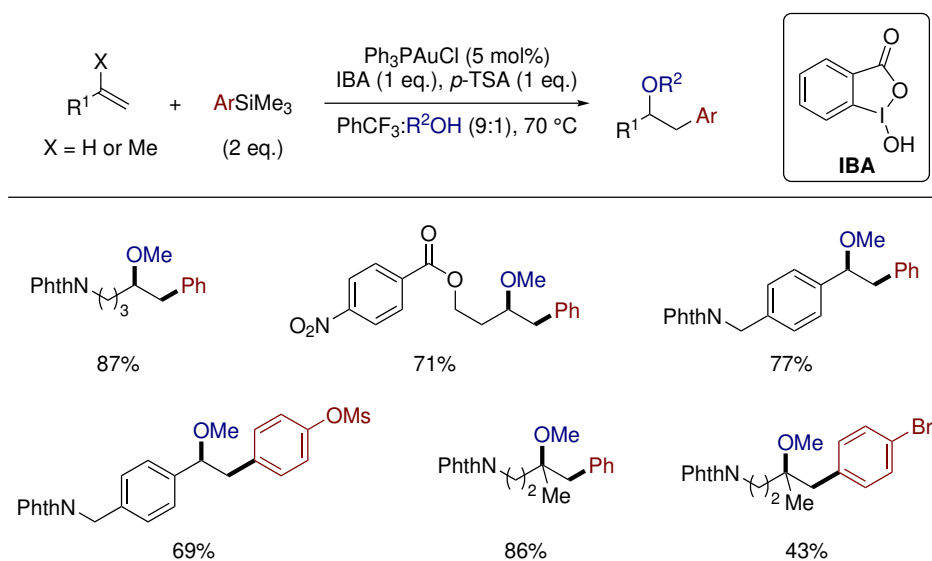
The proposed mechanism (see Section 2.9.1 for a more detailed discussion) for Selectfluor-mediated gold-catalysed heteroarylation involves a putative gold(III) fluoride intermediate.^{52,54,131} It was hypothesised by Russell *et al.* that such a gold(III) fluoride might facilitate activation of an arylsilane moiety, akin to the palladium-catalysed Hiyama reaction.^{56,132} This hypothesis was proved accurate by the groups of Russell and Toste in two simultaneous reports of gold-catalysed oxyarylation utilising arylsilanes as the aryl source (Scheme 2.7).^{53,56} Comparable yields were obtained by both groups, however, notable differences include the requirement for portionwise catalyst addition and a higher total gold loading (10 mol% *vs* 5 mol%) for the procedure reported by Toste *et al.* An important advantage of arylsilanes over arylboronic acids is that the formation of biaryl side-products, a result of oxidative homocoupling, is attenuated.

2.2. Oxyarylation: Literature Precedent



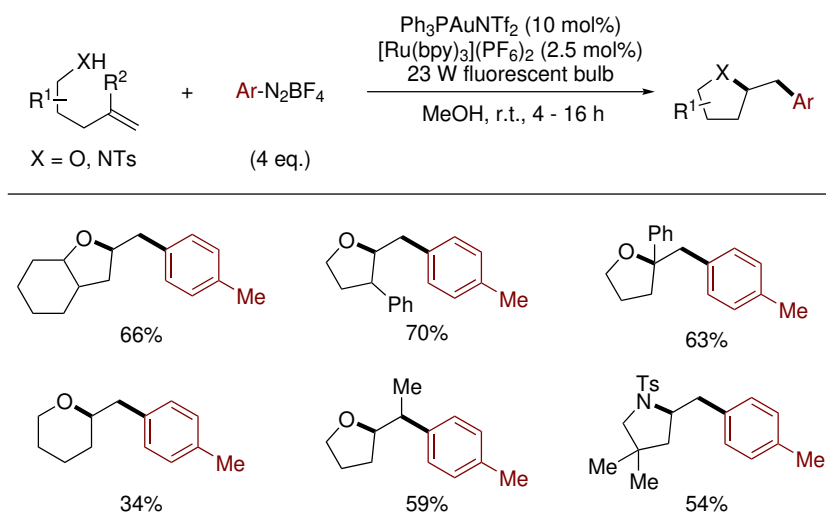
Scheme 2.7: Application of arylsilanes to gold-catalysed oxyarylation by Russell⁵⁶ (yields in blue) and Toste⁵³ (yields in red). ^aProduct not isolated, *in situ* yield determined by ¹H NMR spectroscopy.

The use of Selectfluor, a potent oxidant and fluorinating reagent, presents substrate compatibility issues; direct fluorination of electron-rich substrates, such as styrenes and *gem*-disubstituted alkenes, was found to be an undesired competing process.^{55,56} Addressing this issue, Russell *et al.* reported that the replacement of Selectfluor with the combination of the iodine(III) oxidant 1-hydroxy-1,2-benziodoxol-3(1*H*)-one (IBA) and *p*-toluenesulfonic acid (*p*-TSA) facilitated the oxyarylation of both styrenes and *gem*-disubstituted alkenes (Scheme 2.8).⁵⁵ Changing the solvent from MeCN to PhCF₃ suppressed arylsilane homocoupling, however, the protocol was largely restricted to the use of MeOH as the *O*-nucleophile.



Scheme 2.8: Iodine(III)-mediated gold-catalysed oxyarylation of styrenes and *gem*-disubstituted alkenes.⁵⁵

More recently, the use of aryldiazonium salts (ArN_2^+X^-) as both oxidant and coupling partner under photoredox conditions was established by Glorius *et al.* using 10 mol% Ph_3PAuCl with 2.5 mol% $[\text{Ru}(\text{bpy})_3][\text{PF}_6]_2$ (Scheme 2.9).⁷⁶ The reaction proved highly selective towards the intramolecular process; competing methoxyarylation from the solvent was not observed. However, the following year Glorius *et al.* expanded the scope of the reaction to operate in an intermolecular three-component fashion.⁷⁷ Furthermore, in 2017 Shi *et al.* reported that in the absence photoredox conditions, base-initiated activation of aryldiazonium salts occurs to effect gold-catalysed intramolecular heteroarylation.¹³³ Although the aforementioned heteroarylation reactions are attractive in that no external oxidant is required, the use of diazonium salts is undesirable due to their unpredictable and hazardous nature.⁹⁷



Scheme 2.9: Gold-catalysed oxyarylation of alkenes with aryldiazonium salts under photoredox conditions.⁷⁶

2.3 Objectives

As discussed in Section 2.1, general methods to effect the catalytic 1,2-difunctionalisation of ethylene remain elusive. Such a process would allow for the generation of molecular complexity in a highly modular manner, using ethylene as an abundant and cheap feedstock chemical. The research contained in this chapter will aim to apply the gold-catalysed heteroarylation methodology to ethylene, which raises a number of questions:

- Gaseous ethylene might be present in low concentrations compared to other reaction partners; will competing oxidation pathways predominate?
- Will Au(III) provide sufficient π -activation of ethylene to allow addition of the heteroatom nucleophile?^{134–138}
- Are the stabilising substituents (e.g. alkyl, aryl vs H in the case of ethylene) that have been present on the alkene in previous 1,2-heteroarylations required?

2.4 Initial Results and Optimisation

Homobenzylic ether **4a** was chosen as the target compound to assess the feasibility of the gold-catalysed 1,2-oxyarylation of ethylene (Table 2.1). After evaluating a range of conditions, it was found that **4a** could be generated in 21% yield using a combination of PhSiMe₃ **3a** as nucleophile, Selectfluor as oxidant, and 5 mol% Ph₃PAuCl as precatalyst in MeCN:MeOH (9:1) at 70 °C (Table 2.1, entry 3). The formation of biphenyl **5**, the undesired consequence of oxidative homocoupling, was also detected in 5% yield. Under analogous conditions, other oxidants previously employed in gold-catalysed 1,2-oxyarylation, such as IBA and IBDA (Figure 2.1), were completely ineffective (Table 2.1, entries 1 and 2). Although the result in entry 3 was promising, further optimisation with Selectfluor did not lead to any improvement. The combination of one equivalent of both IBA and *p*-TSA, an oxidant system previously used for gold-catalysed oxyarylation (see Section 2.2),⁵⁵ generated **4a** in an improved 35% yield (Table 2.1, entry 4). Replacement of Ph₃PAuCl with 5 mol% of the digold species dppm(AuCl)₂ resulted in a slightly improved yield of 42%, although this marginal improvement does not justify doubling of the total gold loading.

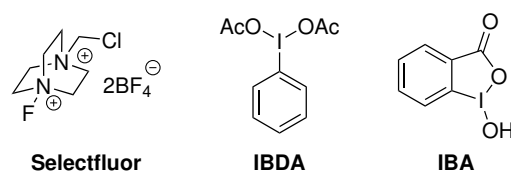


Figure 2.1: Oxidants commonly used for oxidative gold catalysis.

It was shown by Russell *et al.* that for the gold-catalysed direct arylation of arylsilanes, the first step in the catalytic cycle is the oxidation of PPh₃ to Ph₃P=O, thus releasing a phosphine-free active catalyst.⁶³ However, use of both Au(I) and Au(III) phosphine-free catalysts tthAuCl and tthAuBr₃ did not lead to any improvement in efficiency, giving yields of 35% and 12%, respectively (Table 2.1, entries 5 and 6).

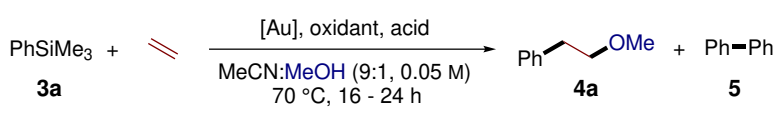
Increasing the loading of *p*-TSA to two equivalents increased the yield markedly to 68% (Table 2.1, entry 8), however, similar improvements were not observed upon increasing the loading of IBA (Table 2.1, entries 10 and 11). The reaction proved sensitive to increases in temperature; an increase to 80 °C saw homocoupling predominate giving an 11% yield of **5** and only 7% of **4a** (Table 2.1, entry 12). A range of alternative iodine(III) oxidants were screened, however, all gave yields of **4a** below 10% (Table 2.1, entries 13-17).

A screen of alternative sulfonic acids revealed that substitution of *p*-TSA with TfOH improved the yield of **4a** to 81% (Table 2.1, entry 20). A decrease in temperature to 50 °C and further refinement of the conditions to 1.1 equivalents IBA and 1.5 equivalents TfOH resulted in an excellent 92% yield of **4a** with only 1% of the undesired **5** (Table 2.1, entry 22).

Although chemistsⁱ often shy away from the use of gaseous reagents, the protocol is simple and can be conducted with conventional experimental apparatus using either a balloon of ethylene or a sealed reaction flask blanketed with the gas at 1 atm. Furthermore, as typical for oxidative gold catalysis, the procedure appears insensitive to air (Table 2.1, compare entries 8 and 9), thus operationally simplifying the process.

ⁱThis statement refers primarily to chemists in an academic environment; the use of gaseous reagents in industry is commonplace (and often desirable).

Table 2.1: Selected optimisation results for the 1,2-oxyarylation of ethylene.^a



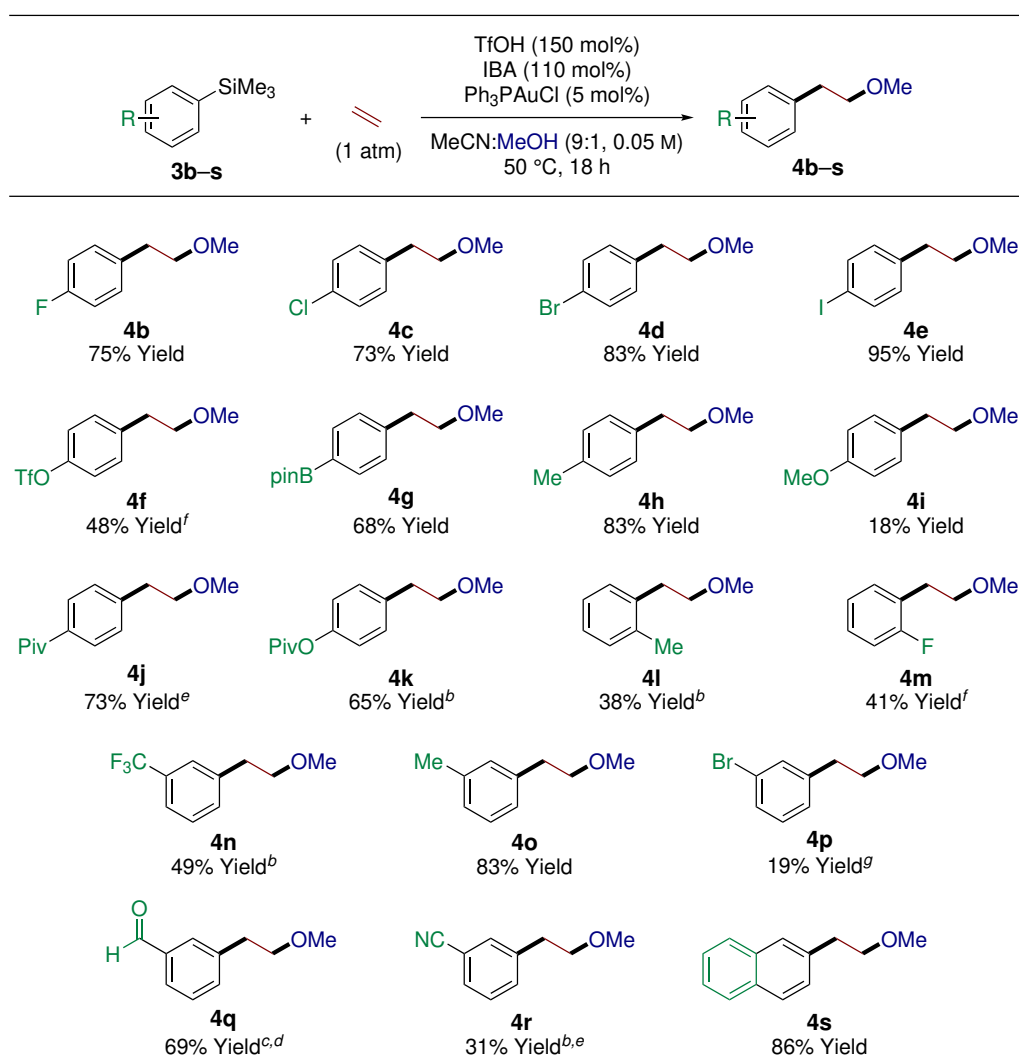
PhSiMe₃ + C_2H_4 $\xrightarrow[\text{70 } ^\circ\text{C, 16 - 24 h}]{\text{[Au], oxidant, acid, MeCN:MeOH (9:1, 0.05 M)}}$ Ph-CH₂-CH₂-OMe (4a) + Ph-Ph (5)

Entry	Catalyst (mol%)	Oxidant (eq.)	Acid (eq.)	4a	5
1	Ph ₃ PAuCl (5)	IBDA (2)	-	0	0
2	Ph ₃ PAuCl (5)	IBA (2)	-	0	0
3	Ph ₃ PAuCl (5)	Selectfluor (1)	-	21	5
4	Ph ₃ PAuCl (5)	IBA (1)	<i>p</i> -TSA (1)	35	3
5	thtAuCl (5)	IBA (1)	<i>p</i> -TSA (1)	35	2
6	thtAuBr ₃ (5)	IBA (1)	<i>p</i> -TSA (1)	12	2
7	dppm(AuCl) ₂ (5)	IBA (1)	<i>p</i> -TSA (1)	42	2
8	Ph ₃ PAuCl (5)	IBA (1)	<i>p</i> -TSA (2)	68	5
9 ^b	Ph ₃ PAuCl (5)	IBA (1)	<i>p</i> -TSA (2)	66	7
10	Ph ₃ PAuCl (5)	IBA (2)	<i>p</i> -TSA (2)	54	2
11	Ph ₃ PAuCl (5)	IBA (1.5)	<i>p</i> -TSA (2)	60	2
12 ^c	Ph ₃ PAuCl (5)	IBA (1)	<i>p</i> -TSA (2)	7	11
13	Ph ₃ PAuCl (5)	IBDA (1)	<i>p</i> -TSA (2)	9	0
14	Ph ₃ PAuCl (5)	PhI(OH)(OTs) (1)	<i>p</i> -TSA (2)	8	0
15	Ph ₃ PAuCl (5)	PhI(CO ₂ C <i>t</i> -Bu) ₂ (1)	<i>p</i> -TSA (2)	8	0
16	Ph ₃ PAuCl (5)	PhI(CO ₂ CF ₃) ₂ (1)	<i>p</i> -TSA (2)	9	1
17	Ph ₃ PAuCl (5)	C ₆ F ₅ I(CO ₂ CF ₃) ₂ (1)	<i>p</i> -TSA (2)	8	0
18	Ph ₃ PAuCl (5)	IBA (1)	MsOH (2)	65	5
19	Ph ₃ PAuCl (5)	IBA (1)	CSA (2)	52	7
20	Ph ₃ PAuCl (5)	IBA (1)	TfOH (2)	81	5
21	Ph ₃ PAuCl (5)	IBA (1)	TfOH (3)	79	4
22 ^d	Ph ₃ PAuCl (5)	IBA (1.1)	TfOH (1.5)	92	1
23 ^d	-	IBA (1.1)	TfOH (1.5)	0	0
24 ^d	Ph ₃ PAuCl (5)	-	TfOH (1.5)	0	0

^a1 atm ethylene. Yields determined by GC-FID analysis using dodecane as internal standard. ^bAir:ethylene atmosphere (approximately 1:1). ^c80 °C. ^d50 °C.

2.5 Substrate Scope for the IBA/TfOH System

In Section 2.4 an optimised set of conditions was identified to effect the 1,2-methoxyphenylation of ethylene (Table 2.1, entry 22). With this in hand, the scope and generality of the reaction was examined, first with respect to the arylsilane component (Table 2.2). A range of differentially substituted arylsilanes were prepared by reaction of either the aryl-Grignard or -lithium reagent prepared from the corresponding aryl halides (see Chapter 5, Section 5.2 for more details).

Table 2.2: Substrate scope for the arylsilane component.^a

^aIsolated yields are quoted. ^b70 °C. ^c40 °C. ^d24 h reaction time. ^e36 h reaction time. ^f48 h reaction time. ^g6 day reaction time.

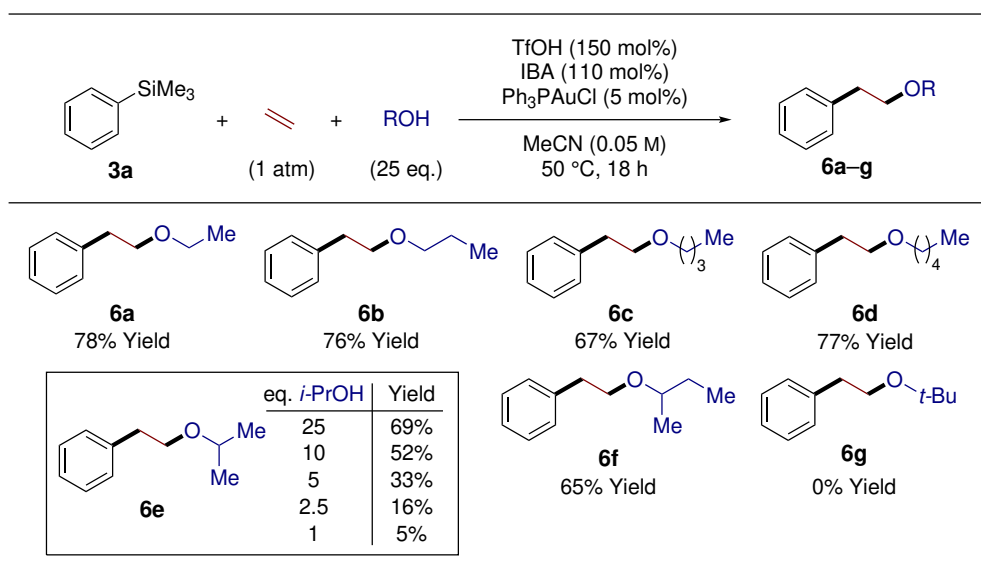
Arylsilanes bearing halides in the *para* position were all well tolerated (**4b–e**), in addition to *para*-substituted -OTf (**4u**) and -Bpin (**4g**) functionality. Although **4f** was obtained in a modest 48% yield, the above results highlight the compatibility of both electrophilic and nucleophilic coupling partners commonly employed in palladium-catalysed coupling reactions.

The ability to access the oxidatively sensitive Bpin (**4g**) and aldehyde (**4q**) systems highlights the mild nature of the oxidative process. A limitation of the conditions is that very electron rich arylsilanes perform poorly; use of the *p*-methoxy substituted **3i** resulted in only an 18% yield of **4i**. This is likely due to consumption of the arylsilane *via* competing protodesilylation,^{139,140} a process accelerated by the presence of strongly acidic TfOH (pK_a in water = -14.7 ± 2.0).¹⁴¹

Arylsilanes bearing electron withdrawing *meta* substituents such as trifluoromethyl (**3n**), nitrile (**3r**) or bromo (**3p**) derivatives resulted in low conversion to the desired products, likely due to electronic deactivation of the arylsilane. Furthermore, it appears that substituents in the sterically demanding *ortho* position result in lower yields, such as for *o*-Me (**4l**, 38% yield) and *o*-F (**4m**, 41% yield) systems.

The reaction scope with respect to the alcohol component was explored next (Table 2.3). Attempts to lower the loading of alcohol resulted in significantly reduced yields (see Table 2.3, **6e**); 25 equivalents of *i*-PrOH gave a 69% yield of **6e**, reducing this to 10 equivalents lowered the yield to 52%, and using a single equivalent produced only 5% of **6e**. Consequently, only simple alcohols were examined.

The primary alcohols ethanol, *n*-propanol, *n*-butanol, and *n*-pentanol all reacted smoothly to furnish compounds **6a–d** in 67% to 78% yield. The secondary alcohol, *s*-butanol was also compatible to give **6f** in 65% yield. However, increasing the steric bulk to *t*-BuOH proved unsuccessful with no conversion to **6g** being detected.

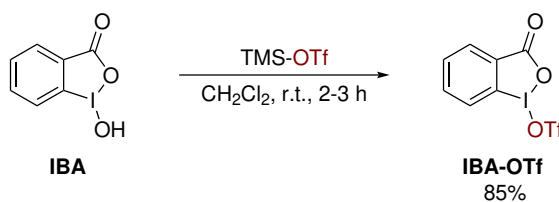
Table 2.3: Substrate scope for the alcohol component.^a^aIsolated yields are quoted.

2.6 Development of the IBA-OTf Oxidant System

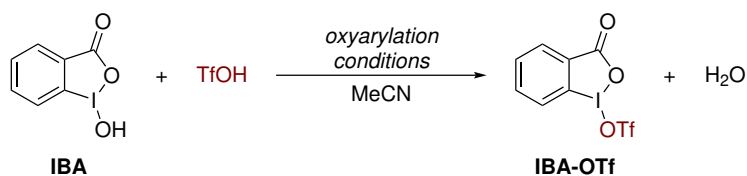
In Section 2.5 the gold-catalysed oxyarylation of ethylene was demonstrated using IBA in the presence of TfOH as the oxidant system. Although the aforementioned conditions allow a fairly wide substrate scope, the use of TfOH is not ideal. TfOH is strongly acidic, extremely corrosive, and requires precautions for safe handling. For example, the use of standard disposable plastic syringes is not possible as rapid (<5 seconds) and hazardous corrosion of the syringe body occurs. Additionally, the functional group tolerance of the protocol is limited by the acidic conditions imparted by TfOH.

Although the preclusion of acid from the reaction would be desirable, initial optimisation studies showed that an acid is essential for oxyarylation to occur. However, given the known lability of ligands at iodine(III),¹⁴² and that IBA reacts with TMS-OTf to give IBA-OTf (Scheme Scheme 2.10),¹⁴³ it was postulated that the combination of IBA and TfOH in the oxyarylation conditions was producing IBA-OTf *in situ* as the active oxidant

(Scheme 2.11).

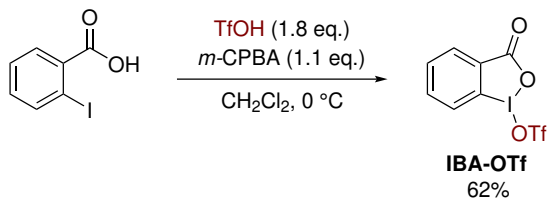


Scheme 2.10: Synthesis of IBA-OTf from *via* treatment of IBA with TMS-OTf by Zh-dankin *et al.*¹⁴³



Scheme 2.11: *In situ* formation of IBA-OTf from IBA and TfOH under oxyarylation conditions.

If, as shown in Scheme 2.11, IBA-OTf is indeed the active oxidant, then replacement of IBA/TfOH with IBA-OTf should negate the requirement for TfOH. An authentic sample of IBA-OTf was prepared in 62% yield according to the procedure reported by Olofsson and Merritt *via* treatment of 2-iodobenzoic acid with *m*-CPBA and TfOH in CH₂Cl₂ (Scheme 2.12).¹⁴⁴



Scheme 2.12: Synthesis of IBA-OTf *via* *m*CPBA oxidation of 2-iodobenzoic acid in the presence of TfOH.¹⁴⁴

With IBA-OTf to hand, its efficacy as oxidant in the oxyarylation protocol was evaluated (Table 2.4). Substitution of IBA with IBA-OTf maintained the efficiency of oxyarylation (compare Table 2.4, entries 1 and 2). Satisfyingly, using IBA-OTf in the absence of TfOH resulted in an improved 98% yield of **4a** alongside only 2% homocoupling product (Table 2.4, entry 3). As expected, a control experiment using IBA-OTf in the absence of gold resulted in no conversion to either **4a** or **5** (Table 2.4, entry 4).

Table 2.4: IBA-OTf as oxidant for the 1,2-oxyarylation of ethylene.^a

Entry	Catalyst (mol%)	Oxidant (eq.)	Acid (eq.)	4a	5
1	Ph ₃ PAuCl (5)	IBA (1.1)	TfOH (1.5)	92	1
2	Ph ₃ PAuCl (5)	IBA-OTf (1.1)	TfOH (1.5)	91	1
3	Ph ₃ PAuCl (5)	IBA-OTf (1.1)	-	98	2
4	-	IBA-OTf (1.1)	-	0	0

^a1 atm ethylene. Yields determined by GC-FID analysis using dodecane as internal standard.

2.7 Substrate Scope for the IBA-OTf System

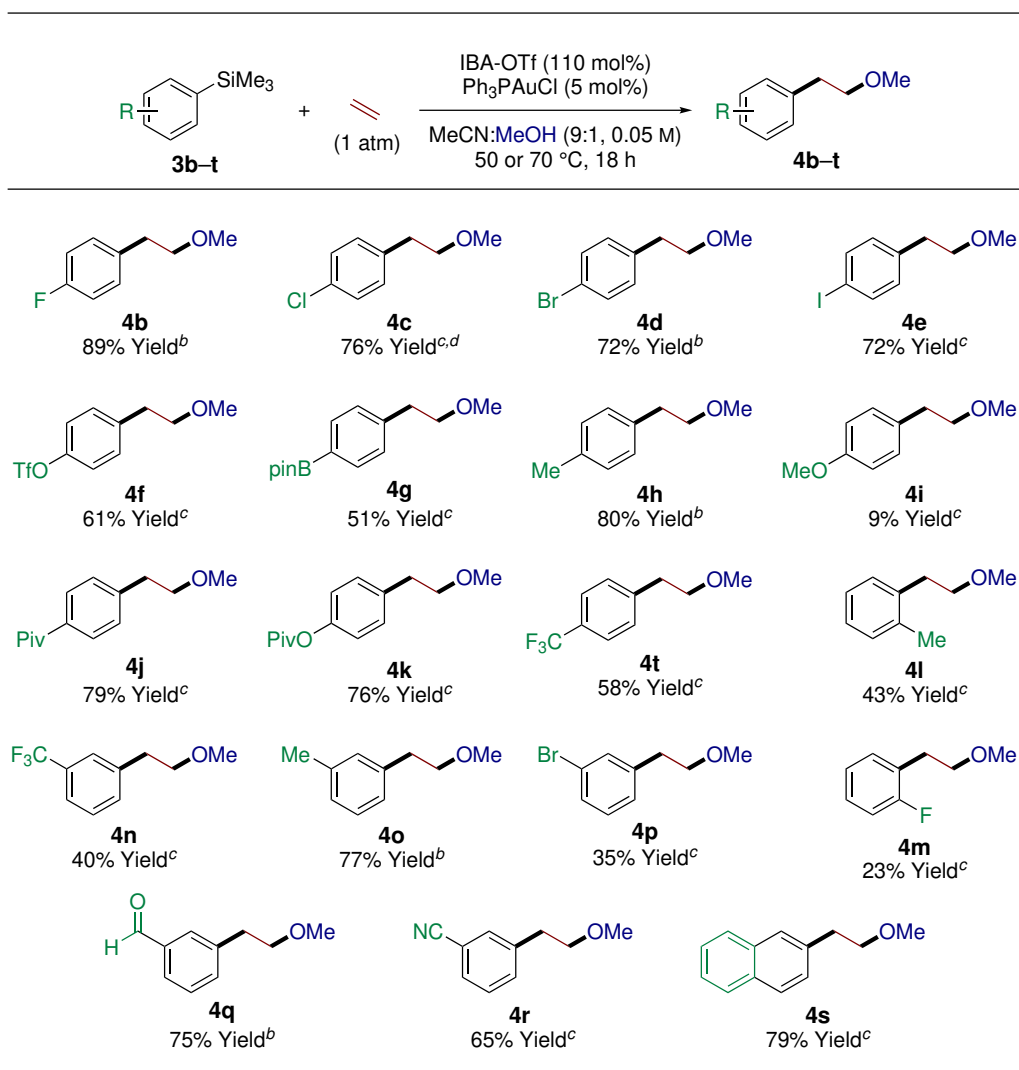
With optimised conditions to hand using IBA-OTf as oxidant, the substrate scope with respect to the arylsilane component was repeated (Table 2.5). In general, when compared to the IBA/TfOH system (Table 2.5), the new IBA-OTf oxidant gave similar results. However, increased yields were obtained for substrates bearing particularly sensitive substituents, such as **4f**, **4q**, and **4r**. In particular, nitrile **4r** was only obtained in 31% yield using IBA/TfOH, whereas this was increased to 65% using IBA-OTf. Overall, although IBA-OTf gave similar yields of **4b–t**, the use of a single substrate oxidant, as opposed to

2.7. Substrate Scope for the IBA-OTf System

a binary system where TfOH is one of the components, presents significant operational advantages.

A further point to note is that in most cases, trace amounts (approximately <1-5% by uncalibrated GC-MS) of biphenyl byproducts were also observed. These undesired byproducts were not quantified or fully characterised.

Table 2.5: Arylsilane substrate scope using IBA-OTf as oxidant.^a

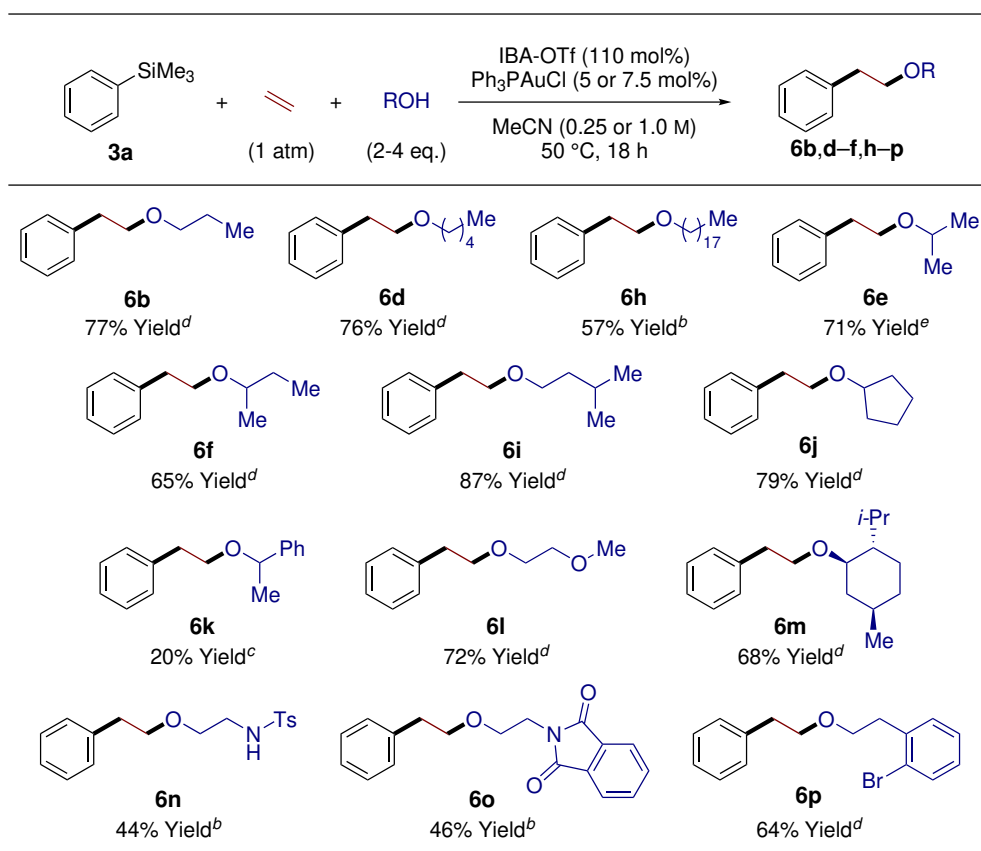


^aIsolated yields are quoted. ^b50 °C. ^c70 °C. ^d24 h reaction time.

In Section 2.5 using IBA/TfOH, a limited alcohol scoping study was conducted using

simple primary and secondary alcohols (Table 2.3). Analogous to previously reported gold-catalysed oxyarylations,^{53–56} a significant drawback was the requirement for a large excess of alcohol in order to maintain acceptable yields (see Table 2.3, **6e**). In order to extend the process to higher-value alcohols, the 1,2-oxyarylation protocol required optimisation to lower the alcohol loading. Gratifyingly, it was found that by increasing the concentration to 0.25–1.0 M, efficient conversions were obtained using only 2–4 equivalents of alcohol (Table 2.6). However, an increase in gold loading from 5 mol% to 7.5 mol% was required in certain cases.

Under these new conditions, a diverse range of primary and secondary alcohols engage in ethylene oxyarylation, providing compounds **6b,d–f,h–p** in moderate to excellent yields. Of the secondary alcohols examined, benzylic systems proved the most challenging, with **6k** formed in only 20% yield. This was accompanied by dehydrative dimerisation of the alcohol to the corresponding dibenzyl ether. Structurally complex alcohols (**6m**), aryl halides (**6p**), and alcohols containing protected heteroatoms (**6l**, **6n**, and **6o**) participated smoothly to generate the targets in moderate to very good yields. Of particular note is the formation of **6n**, containing a free -NH group. This highlights that oxyarylation outcompetes potential aminoarylation *via* the NH-sulfonamide moiety. Attempts to extend the process to the bulky *t*-BuOH and electron poor CF₃CH₂OH were unsuccessful.

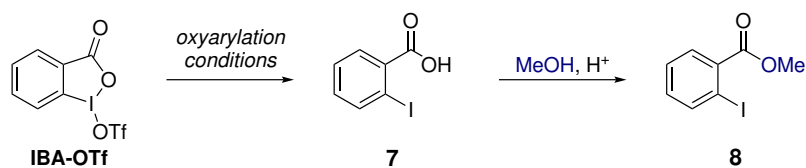
Table 2.6: Alcohol substrate scope using IBA-OTf as oxidant.^a

^aIsolated yields are quoted. ^b2 eq. ROH, 7.5 mol% Ph₃PAuCl, 1.0 M. ^c3 eq. ROH, 5 mol% Ph₃PAuCl, 1.0 M. ^d4 eq. ROH, 7.5 mol% Ph₃PAuCl, 0.25 M. ^e4 eq. ROH, 5 mol% Ph₃PAuCl, 0.25 M.

2.8 Reaction Limitations

Under oxyarylation conditions, IBA-OTf reacts, presumably *via* 2-iodobenzoic acid **7**, to form the corresponding methyl ester **8** as a by-product (Scheme 2.13). It was found that **8** had a very similar retention factor (R_F) to many of the oxyarylation products, which complicated purification *via* flash column chromatography. To circumvent this issue, a simple *in situ* hydrolysis protocolⁱ was applied to convert ester **8** to acid **7**, allowing separation of **7** *via* simple aqueous work-up.

ⁱSee Chapter 5, Section 5.2 for full details.



Scheme 2.13: Production of **8** from IBA-OTf under oxyarylation conditions.

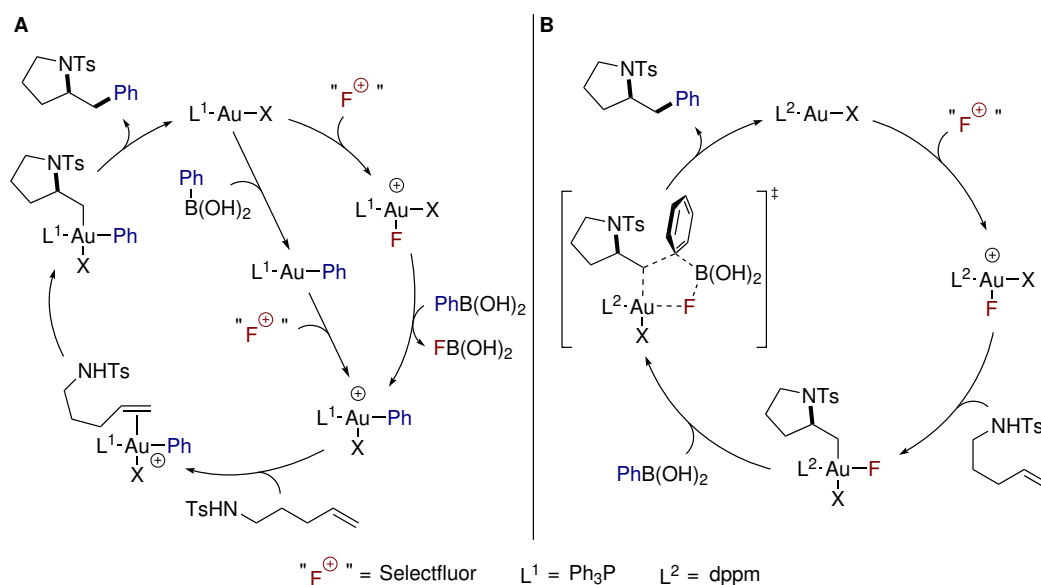
2.9 Mechanism

2.9.1 Previous Mechanistic Hypotheses

For Selectfluor mediated gold-catalysed heteroarylation, Zhang⁵² (Scheme 2.14, A) and Toste^{54,131} (Scheme 2.14, B) proposed two similar mechanisms involving a gold(I)/(III) redox cycle. The primary difference between the two concerns ordering of the transmetalation and alkene activation steps.

Zhang suggests transmetalation occurs before alkene coordination, although oxidation of gold(I) by Selectfluor was proposed to occur either prior to or after transmetalation. Alkene coordination to the aryl gold(III) intermediate then induces a *5-exo-trig* cyclisation, followed by C(sp²)-C(sp³) reductive elimination to generate the product and reform the gold(I) catalyst (Scheme 2.14, A).

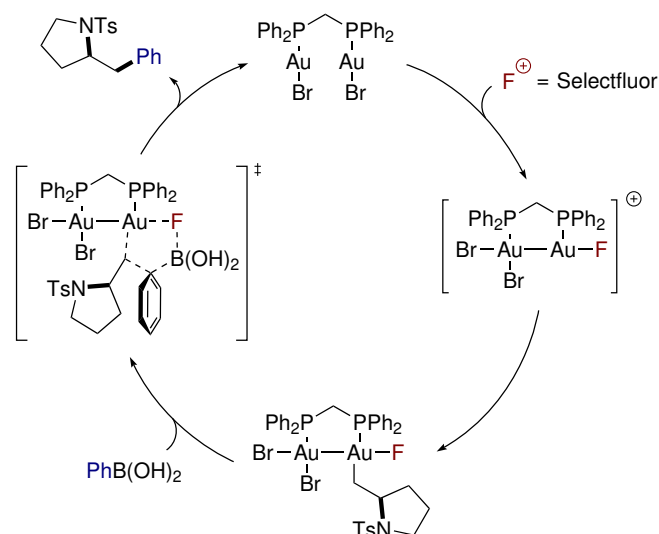
Toste, however, suggests that initial oxidation to give a gold(III) fluoride is followed by alkene coordination and *5-exo-trig* cyclisation to give an alkyl gold(III) fluoride. Instead of undergoing a formal transmetalation to gold, it is proposed that C(sp²)-C(sp³) bond formation occurs *via* a 5-centred transition state (Scheme 2.14, B) to yield the product and regenerate the gold(I) catalyst. Toste proposes that the same mechanism is in operation when an arylsilane replaces the boronic acid.⁵³



Scheme 2.14: Proposed mechanisms by Zhang⁵² (A) and Toste^{53,54,131} (B) for the gold-catalysed 1,2-oxyarylation of alkenes.

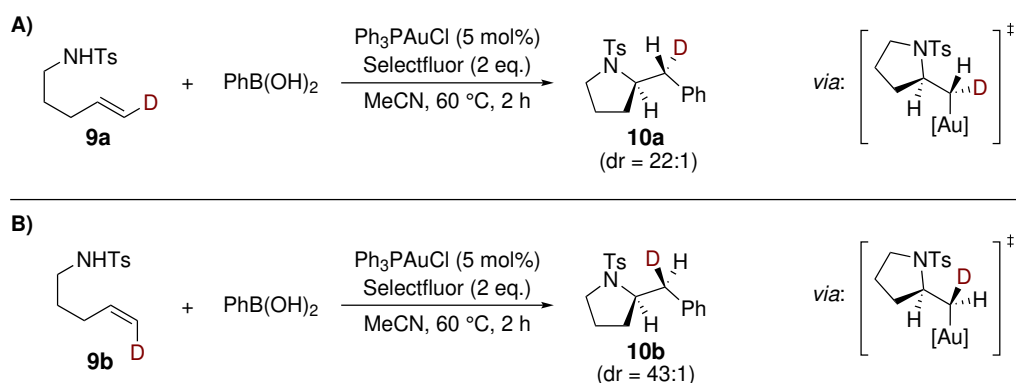
The mechanism of gold-catalysed heteroarylation was examined further in a study by Goddard and Toste combining experimental results and DFT calculations.¹⁴⁵ In contrast to prior reports, a gold(I)/(II) redox cycle was proposed whereby oxidation of the binuclear $\text{dppm}(\text{AuBr})_2$ forms a gold(II) fluoride intermediate (Scheme 2.15). It was proposed that formation of this somewhat unusualⁱ gold(II) intermediate is driven by Au(II)-Au(II) σ -bond formation. This cationic gold(II) fluoride then facilitates the 5-*exo-trig* cyclisation giving a neutral alkylgold(II) species. A bimolecular concerted reductive elimination then occurs without formal transmetalation to yield the product with regeneration of the $\text{dppm}(\text{AuBr})_2$.

ⁱAlthough gold(II) complexes are rare when compared to gold(I) and gold(III), several examples of binuclear gold(II) complexes have been reported, usually when the two gold centres are held in close proximity by the ancillary ligand.¹⁴⁶



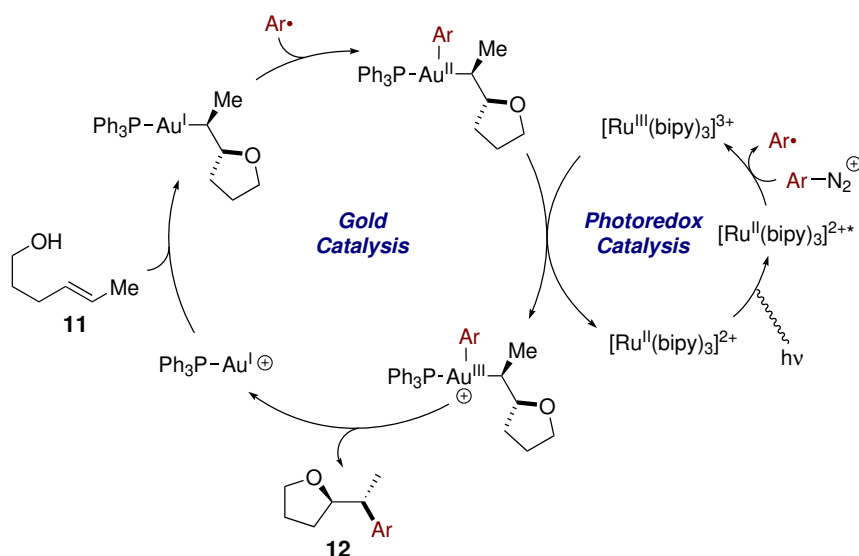
Scheme 2.15: Revised gold(I)/(II) cycle for the gold-catalysed 1,2-oxyarylation of alkenes, as proposed by Toste and Goddard.¹⁴⁵

Zhang *et al.* probed the nature of nucleophilic attack on the gold-activated alkene with a deuterium-labelling study (Scheme 2.16).⁵² Aminoarylation of *trans*-deutero-alkene **9a** resulted in the formation of **10a** with high stereoselectivity (Scheme 2.16, A). Conversely, aminoarylation of *cis*-deutero-alkene **9b** resulted in formation of the other diastereomer **10b** (Scheme 2.16, B). The above results suggest that aminoarylation occurs in an *anti* fashion, followed by C-C reductive elimination with retention of configuration.



Scheme 2.16: Deuterium-labelling evidence supporting the *anti* nature of gold-catalysed aminoarylation of alkenes.⁵²

The *anti* nature of the heteroarylation was further confirmed by Glorius *et al.* in the study of their dual gold/ruthenium photoredox-catalysed heteroarylation. In this reaction, aryldiazonium salts act as both oxidant and arylating agent in a mechanism proposed to involve sequential single-electron oxidations *via* a gold(I)/(II)/(III) redox cycle (Scheme 2.17). The *trans*-alkene **11** reacted stereoselectively to give the *anti* oxyarylated product **12**.



Scheme 2.17: Proposed mechanism for the dual gold/ruthenium photoredox catalysed heteroarylation of alkenes with aryldiazonium salts.⁷⁶

2.9.2 Stoichiometric Studies

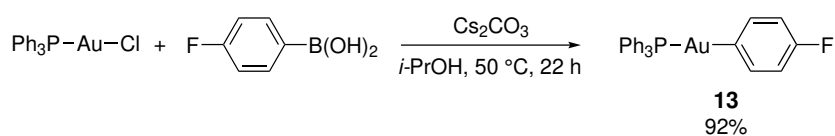
Although the mechanisms discussed in Section 2.9.1 are largely complementary, they differ in terms of the specific ordering of certain steps. For example, Zhang *et al.* propose the order of gold-oxidation→transmetalation→alkene activation (Scheme 2.14, A), whereas Toste *et al.* propose gold-oxidation→alkene activation→arylation (Scheme 2.14, B and Scheme 2.15). Furthermore, Glorius *et al.* propose a more complex photoredox mechanism involving single electron oxidation whereby the reaction goes alkene activation→radical aryl addition→single-electron oxidation (Scheme 2.17). Due to the inherent dif-

ferences between our 1,2-oxyarylation and the system of Glorius *et al.*, mechanisms of this type will not be discussed further.

In order to gain some insight into the ordering of steps in the gold-catalysed 1,2-oxyarylation of ethylene, model gold(I) and gold(III) aryl complexes were synthesised and their reactivity towards oxyarylation conditions was examined.

Synthesis and Reactivity of a Gold(I) Aryl Complex

The gold(I) aryl complex **13**, bearing Ph₃P and *p*-fluorophenyl ligands, was synthesised in 92% yield from Ph₃PAuCl *via* transmetalation with 4-fluorophenylboronic acid, according to the procedure reported by Hashmi *et al.* (Scheme 2.18).¹⁴⁷ The 4-fluorophenyl group was chosen as it would allow convenient monitoring of subsequent reactions *via* ¹⁹F NMR spectroscopy. Single crystals of **13** were grown from MeCN:MeOH (9:1) and its solid-state structure was determined *via* X-ray crystallographic analysis (Figure 2.2). Complex **13** exhibits approximately linear geometry with a 177° bond angle around the gold centre, as expected for gold(I).



Scheme 2.18: Synthesis of Ph₃PAu(4-F-C₆H₄) **13**.¹⁴⁷

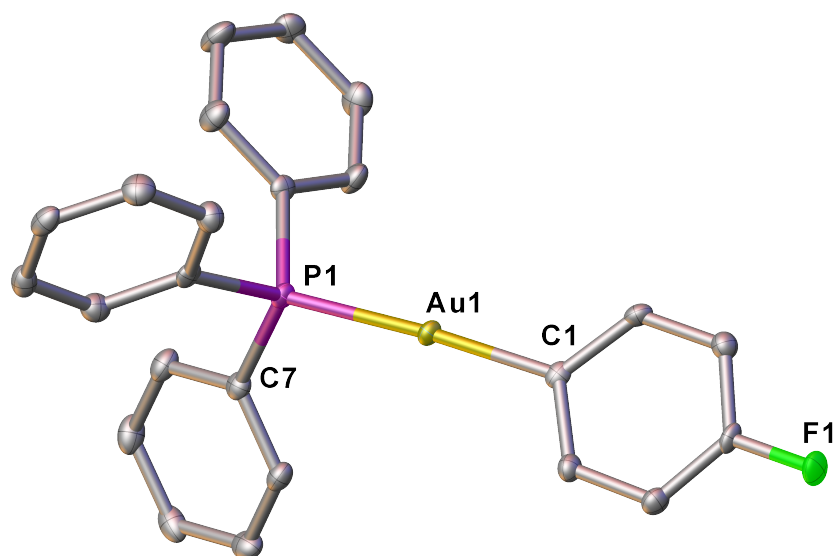
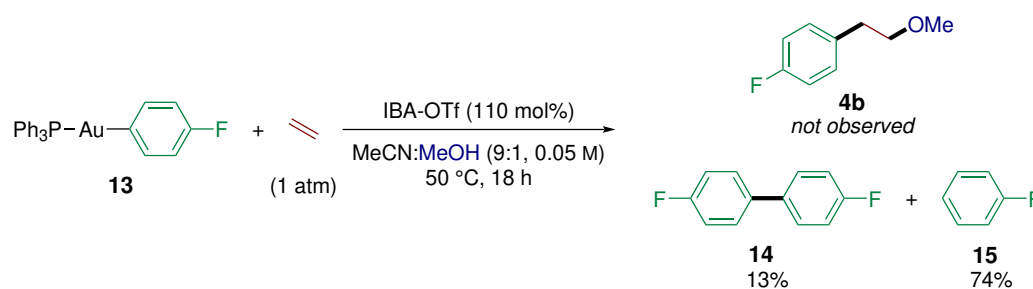


Figure 2.2: Molecular structure of **13**, thermal ellipsoids are shown at the 50% probability level. Hydrogen atoms have been omitted for clarity. Selected bond lengths (Å) and angles (°): Au1-P1 2.2906(7), Au1-C1 2.043(3), P1-C7 1.818(3), C1-Au1-P1 176.51(8), C7-P1-Au1 113.09(9). See Section 5.5, Table 5.1 for full crystallographic details.

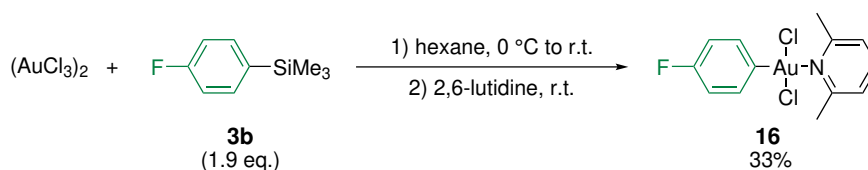
Exposure of **13** to the optimised oxyarylation conditions (in the absence of arylsilane) did not afford any of the expected 1,2-oxyarylation product **4b** (Scheme 2.19). Instead, the homocoupling product **14** and proto-deauration product **15** were obtained as the sole products in 13% and 74% yields, respectively. This result suggests that for the mechanism of oxyarylation: a) oxidation of gold occurs prior to transmetalation, and b) that if transmetalation does occur onto a gold(I) centre, only unproductive proto-deauration or homocoupling occurs. However, the absence of protodeauration products coupled with presence of homocoupling products in catalytic reactions suggests it is unlikely that aryl-gold(I) species of the type **13** are intermediates in the catalytic cycle.



Scheme 2.19: Submission of arylgold(I) **13** to oxyarylation conditions.

Synthesis and Reactivity of a Gold(III) Aryl Complex

The gold(III) aryl complex *trans*-Au(4-F-C₆H₄)(2,6-lutidine)Cl₂ **16** was synthesised according to a modified procedure reported by Russell *et al.*^{63,148} Reaction of anhydrous gold(III) chloride ((AuCl₃)₂) with 4-fluorophenyltrimethylsilane **3b** in hexane results in *ipso*-auration of the arylsilane. Trapping of the resultant dimeric (AuCl₂(4-F-C₆H₄))₂ with 2,6-lutidine gives the air-stable arylgold(III) complex **16** after chromatographic purification. Complex **16** proved challenging to synthesise; it was found that freshly prepared anhydrous (AuCl₃)₂ (a bright red powder) was required;¹⁴⁹ use of commercially available (AuCl₃)₂ (usually a brown/black solid) was either unsuccessful or gave very low yields of **16**.



Scheme 2.20: Synthesis of gold(III) aryl *trans*-Au(4-F-C₆H₄)(2,6-lutidine)Cl₂ **16**.⁶³

Single crystals of **16** were grown from a CH₂Cl₂ solution layered with hexane, X-ray crystallographic analysis was performed and the molecular structure is shown in Figure 2.3. **16** adopts the *trans* configuration in a slightly distorted square-planar geometry,

as expected for a four-coordinate d^8 complex.

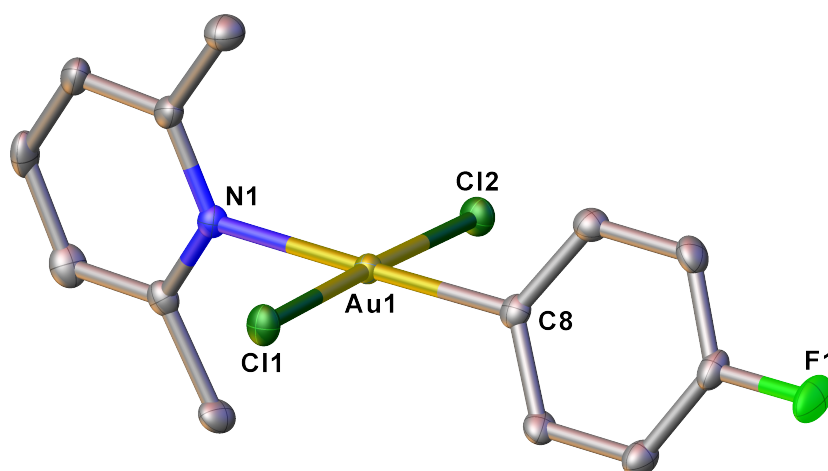
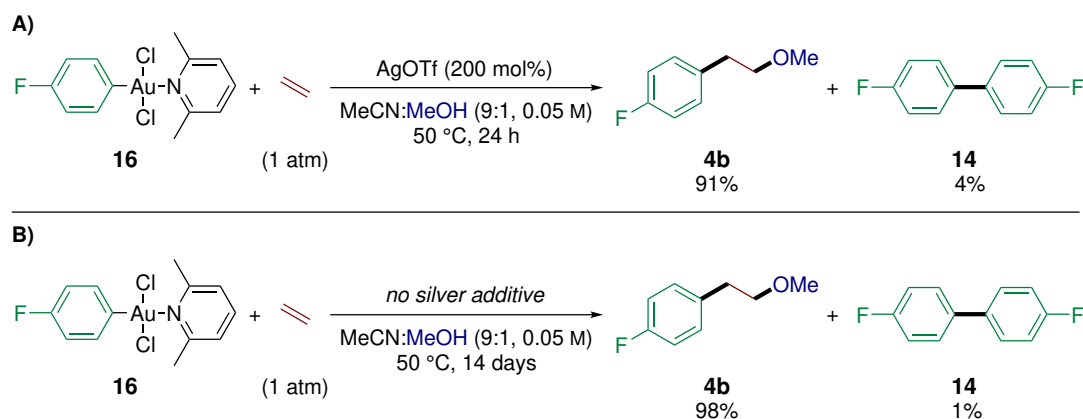


Figure 2.3: Molecular structure of **16**, thermal ellipsoids are shown at the 50% probability level. Hydrogen atoms have been omitted for clarity. Selected bond lengths (Å) and angles (°): Au1-Cl1 2.2810(9), Au1-Cl2 2.2762(9), Au1-N1 2.150(3), Au1-C8 2.017(4), Cl2-Au1-Cl1 178.06(3), C8-Au1-N1 179.01(13), N1-Au1-Cl1 91.75(8), C8-Au1-Cl2 89.07(10). See Section 5.5, Table 5.2 for full crystallographic details.

Exposure of **16** to oxyarylation conditions in the presence of AgOTf resulted in formation of the 1,2-oxyarylation product **4b** in 91% yield alongside 4% of **14** (Scheme 2.21, A). The addition of AgOTf serves to increase the rate of reaction, presumably through abstraction of a chloride to render a more reactive gold(III) centre. Importantly, exposure of **16** to analogous conditions in the absence of silver still resulted in a 98% yield of **4b** after 14 days at 50 °C (Scheme 2.21, A).

That a gold(III) aryl complex reacts with MeOH and ethylene to give the oxyarylation product **4b** supports the previous hypothesis (see Page 45) that oxidation of gold(I) occurs prior to transmetalation, and that arylsilane transmetalation occurs at a gold(III) centre. Furthermore, it supports a mechanism whereby transmetalation occurs prior to alkene coordination/activation, which is in contrast to the mechanism proposed by Toste *et al.*^{53,54,131} (Scheme 2.14, B) but in agreement with that proposed by Zhang *et al.*⁵²

(Scheme 2.14, A). Additionally, successful conversion of **16** to **4b** in the absence of IBA-OTf suggests that the role of the oxidant in gold-catalysed oxyarylation is limited to oxidation of gold.



Scheme 2.21: Submission of arylgold(III) **16** to oxyarylation conditions with AgOTf (A) and without AgOTf (B).

To gain further insight into the conversion of **16** to **4b**, the reaction was monitored by ^{19}F NMR spectroscopy (Figure 2.4). This revealed the formation of an intermediate (shown in green in the reaction profile) which had a maximum coinciding with complete consumption of **16**, and then decreased at a rate approximately equal to the formation of **4b**. Although the intermediate was not fully characterised, it is tentatively assigned (*vide infra*) to a gold(III) complex bearing aryl and methoxyethyl ligands such as **17**, prior to formation of **4b** *via* reductive elimination.

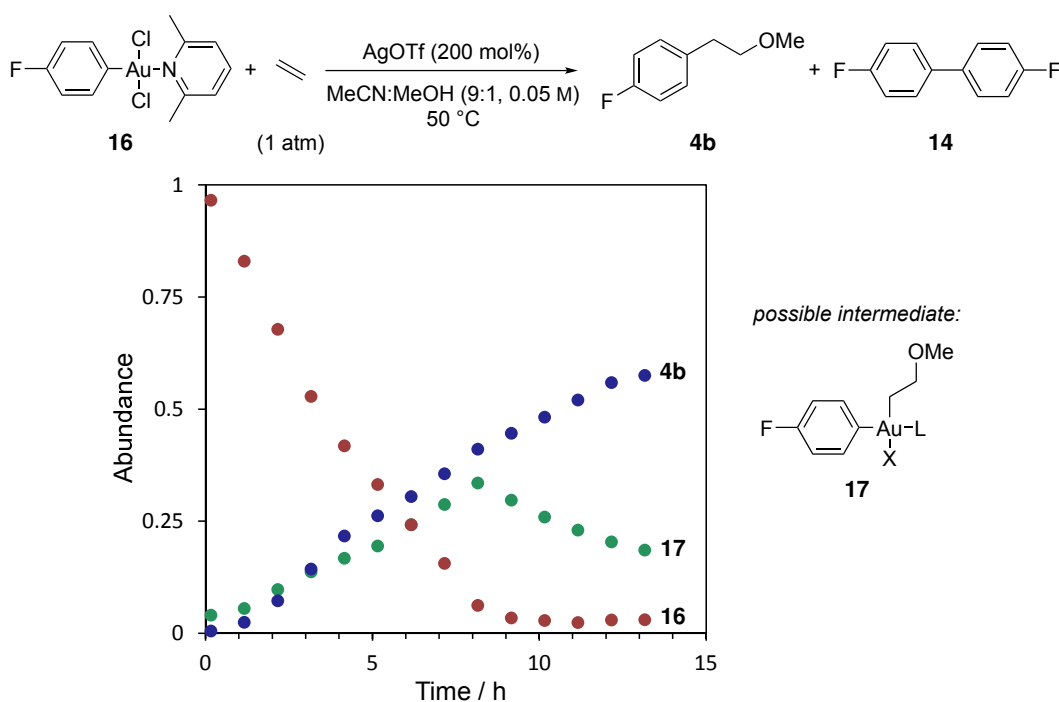


Figure 2.4: Reaction profile obtained from submission of **16** to oxyarylation conditions in the presence of AgOTf. Reaction monitored by ^{19}F NMR spectroscopy using hexafluorobenzene as internal standard.

In support of the presence of a complex of type **17**, monitoring the reaction by ^1H NMR spectroscopy (Figure 2.5) revealed a triplet ($\delta = 3.42$) and multiplet ($\delta = 2.31$) in a 1:1 ratio which is tentatively assigned to the methoxyethyl ligand of **17**. These ^1H NMR signals are also broadly consistent with the similar gold(III) complexes **18**,¹³⁶ **19**,¹⁵⁰ and **20**¹³⁷ reported in the literature (Figure 2.6).

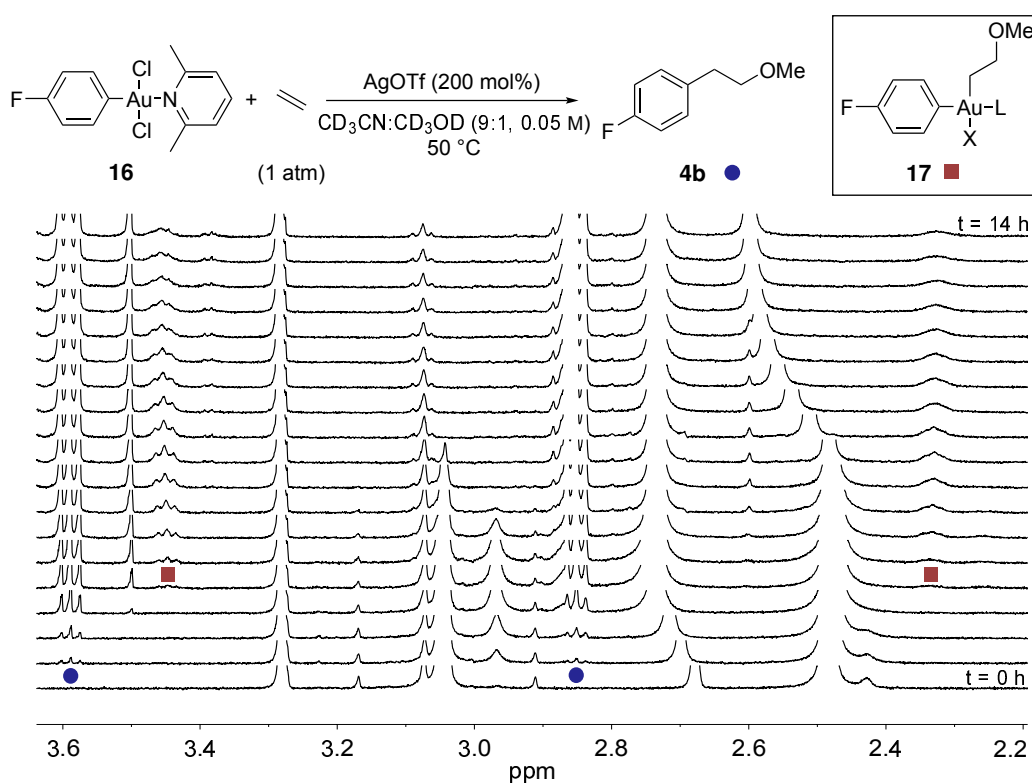


Figure 2.5: Monitoring the conversion of **16** to **4b** by ^1H NMR spectroscopy.

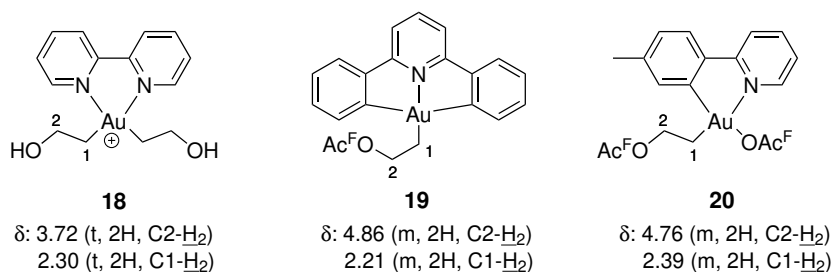
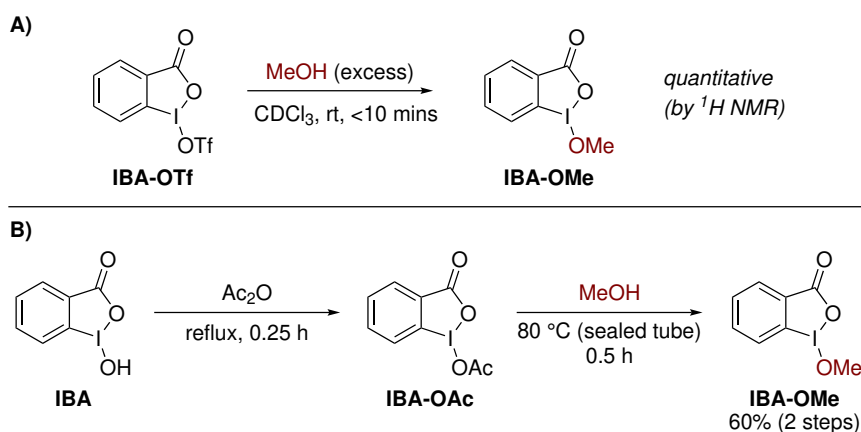


Figure 2.6: Characteristic ^1H NMR chemical shifts of ethyl ligated gold(III) complexes **18**,¹³⁶ **19**,¹⁵⁰ and **20**.¹³⁷ OAc^{F} = trifluoroacetyl.

2.9.3 Oxidant Speciation

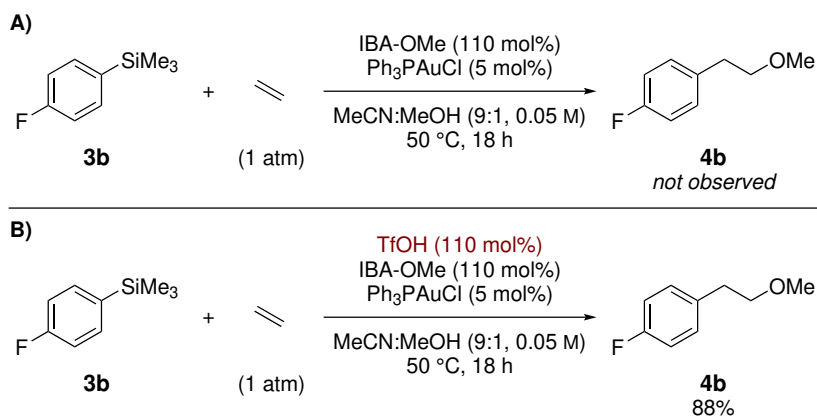
As discussed in Section 2.6, the identification of IBA-OTf as an effective oxidant stemmed from the observation that a combination of IBA and a Brønsted acid can also promote the 1,2-oxyarylation process, albeit with decreased efficiency. One drawback of

IBA-OTf is its low solubility in common solvents; with the exception of DMSO, only alcoholic solvents such as MeOH and EtOH can solubilise it. During a brief solvent screen to assess solubility, it was observed that dissolution of IBA-OTf (a beige amorphous solid) in MeOH led to the precipitation of a colourless crystalline solid after approximately 1 hour. To investigate further, IBA-OTf was mixed with MeOH in CDCl₃ in an NMR tube, which resulted in quantitative conversion to IBA-OMe in under 10 minutes (Scheme 2.22, A). The identity of IBA-OMe was confirmed by comparison to an authentic sample, prepared by the route reported by Togni *et al.* (Scheme 2.22, B).¹⁵¹



Scheme 2.22: Reaction of IBA-OTf with MeOH to give IBA-OMe (A), and preparation of an authentic sample of IBA-OMe *via* the reported procedure (B).¹⁵¹

Given that IBA-OTf reacts rapidly and quantitatively with MeOH to form IBA-OMe, it was proposed that under oxyarylation conditions IBA-OTf reacts with the alcohol (ROH) to form the corresponding IBA-OR as the active oxidant. Surprisingly, submission of arylsilane **3b** to oxyarylation conditions using IBA-OMe as oxidant resulted in no detectable formation of **4b** (Scheme 2.23, A). However, catalytic activity was recovered by repeating the reaction in the presence of 110 mol% TfOH (Scheme 2.23, B). Thus, for efficient 1,2-oxyarylation, it appears that mildly acidic conditions are required to activate *in situ* generated IBA-OMe (or IBA-OR).



Scheme 2.23: Submission of **3b** to oxyarylation conditions using IBA-OMe as oxidant (A), and with added TfOH (B).

2.9.4 Role of the Phosphine

Previously proposed gold-catalysed oxyarylation mechanisms have suggested that a phosphine is ligated to gold throughout the catalytic cycle (see Section 2.9.1). However, a detailed mechanistic study by Russell *et al.* on a related gold-catalysed oxidative process highlighted the requirement for initial oxidative removal of the phosphine from the precatalyst. Thus, the first step in the cycle was found to be oxidation of Ph₃P to Ph₃P=O. To gain further insight into this, the oxyarylation of **3b** was monitored by ¹⁹F NMR spectroscopy using different gold precatalysts.

Figure 2.7 compares the difference in initial rate when the electronic properties of (4-**R**-C₆H₄)₃PAuCl was varied. Electron rich phosphine ligands resulted in an increased rate of reaction with the initial rate order for (4-**R**-C₆H₄)₃PAuCl going **R** = OMe > H > F > CF₃ (Figure 2.7).

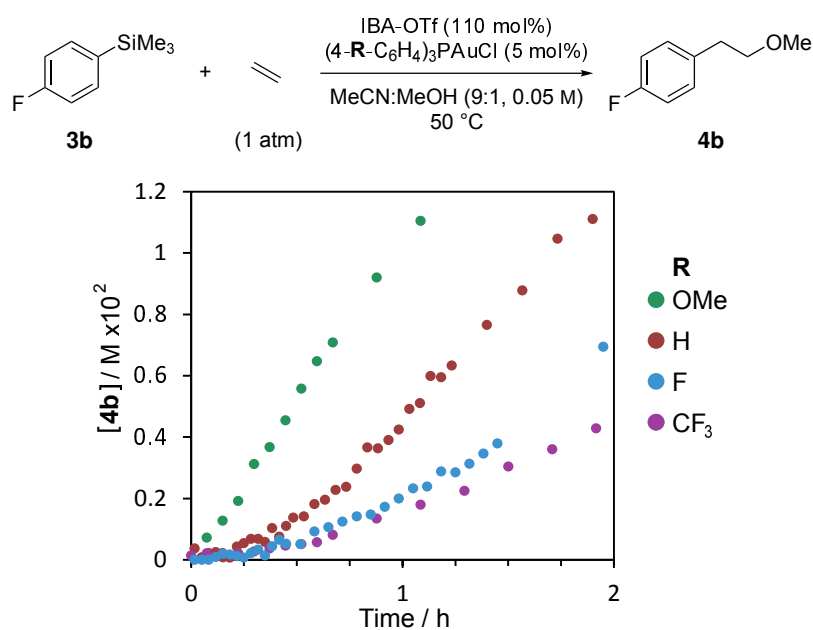


Figure 2.7: Effect of varying the electronic properties of the phosphine on the relative rates of oxyarylation of **3b**. Reactions monitored by ¹⁹F NMR spectroscopy.

In addition to precatalysts of the type (4-R-C₆H₄)₃PAuCl, thtAuBr₃ and IPrAuCl (IPr = 1,3-Bis(2,6-diisopropylphenyl)imidazol-2-ylidene) were evaluated. The phosphine-free system of thtAuBr₃ was not an efficient precatalyst, effecting only 20% conversion after 12 hours (Figure 2.8, grey), and IPrAuCl did not effect oxyarylation at all (Figure 2.8, yellow).

Although (4-MeO-C₆H₄)₃PAuCl provides the highest initial rate, catalytic activity was attenuated after approximately two hours (at 30% conversion) (Figure 2.8, green). Using an additional 10 mol% (4-MeO-C₆H₄)₃P resulted in lengthened catalytic activity and an increased conversion of 70% (Figure 2.8, dark blue). Analysis of a completed reaction mixture with (4-MeO-C₆H₄)₃PAuCl as precatalyst exhibited two signals in the ³¹P NMR spectrum at $\delta = 64.5$ and 45.6, which were found to correspond to [(4-MeO-C₆H₄)₃POMe][OTf] and (4-MeO-C₆H₄)₃P=O, respectively, as confirmed by comparison to authentic samples.^{152,153} The above data suggests that competing oxidation of the phos-

phine may be halting the reaction. This process would be most facile for electron-rich phosphines, such that Ph_3PAuCl offers better overall efficiency even though $(4\text{-MeO-C}_6\text{H}_4)_3\text{PAuCl}$ provides the best initial turnover frequency.

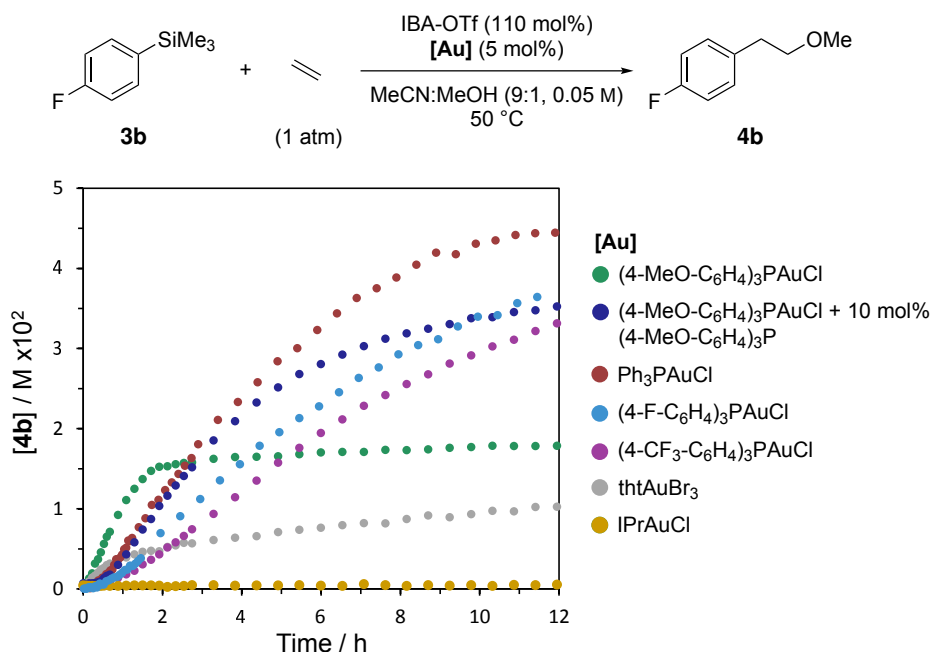


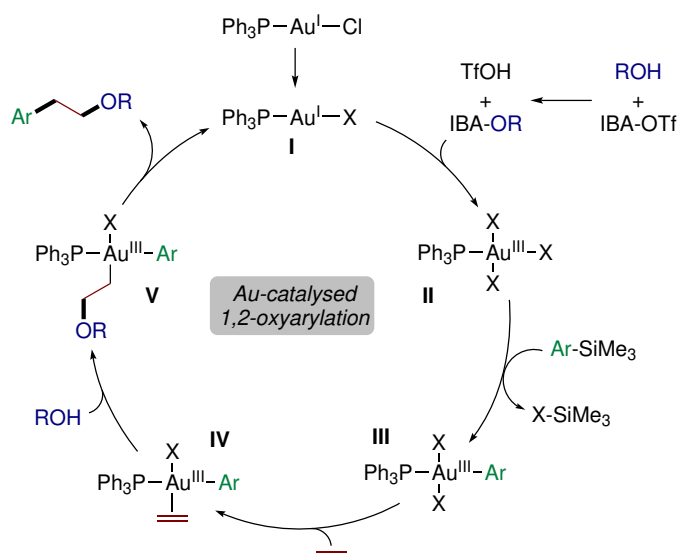
Figure 2.8: Reaction profiles for the oxyarylation of **3b** for varying gold catalysts. Reactions monitored by ^{19}F NMR spectroscopy.

The data discussed in this section suggest an involved and beneficial role of the phosphine ligand in gold-catalysed 1,2-oxyarylation. However, one cannot determine from these preliminary mechanistic analysis whether the phosphine is ligated to gold during catalysis, or serves primarily to stabilise off-cycle species.

2.9.5 Mechanistic Hypothesis

Given the evidence discussed in this section, and taking into account previously proposed mechanisms,^{52–54,131,145} outlined in Scheme 2.24 is our working mechanistic hypothesis. The induction period observed in Figure 2.7 and Figure 2.8 suggests that Ph_3PAuCl is not a catalytic intermediate. Following generation of the active gold(I) species **I** oxidation

occurs to gold(III) intermediate **II**. As discussed in Section 2.9.3, IBA-OTf likely reacts with the alcohol to form IBA-OR in solution. Activation of this species is promoted by the *in situ* generated TfOH. Complex **II** then undergoes transmetalation with the arylsilane to afford the gold(III) aryl complex **III**. That this step occurs at a gold(III) centre, and also prior to alkene activation, is supported by the data presented in Section 2.9.2. Alkene activation then occurs, likely *via* a gold(III) π -complex of type **IV**, to give gold(III) complex **V**, bearing both alkyl and aryl ligands (evidence for which is presented in Section 2.9.2). From **V**, product forming C(sp²)-C(sp³) reductive elimination occurs to close the catalytic cycle.



Scheme 2.24: Proposed mechanism for the gold-catalysed 1,2-oxyarylation of ethylene. X corresponds to an unidentified anionic ligand.

In order to fully elucidate each step of the mechanism of gold-catalysed 1,2-oxyarylation, a thorough mechanistic study including kinetic analysis and DFT calculations is required. Therefore, one cannot discount the possibility that alternative pathways may be operative. For example, some of the transformations may be facilitated by iodine(III) or the Brønsted acid.

2.10 Conclusion

In summary, this chapter discussed the gold-catalysed oxidative 1,2-oxyarylation of ethylene using arylsilanes as aryl source, IBA-OTf as oxidant, and Ph₃PAuCl as precatalyst. This provides a method to add an alcohol and aryl group across ethylene, enabling a mild and modular entry to homobenzylic ethers. Of note is the mild conditions required, and significant molecular complexity built in a single step from the simple feedstock chemical, ethylene.

The substrate scope was explored with respect to both the arylsilane and alcohol component, which revealed a broad scope. Of particular interest is that both nucleophilic and electrophilic coupling partners commonly used in palladium-catalysed cross-coupling were compatible, as well as sensitive functionality such as aldehydes. Extremely electron rich substrates proved incompatible due to the oxidative and slightly acidic conditions required.

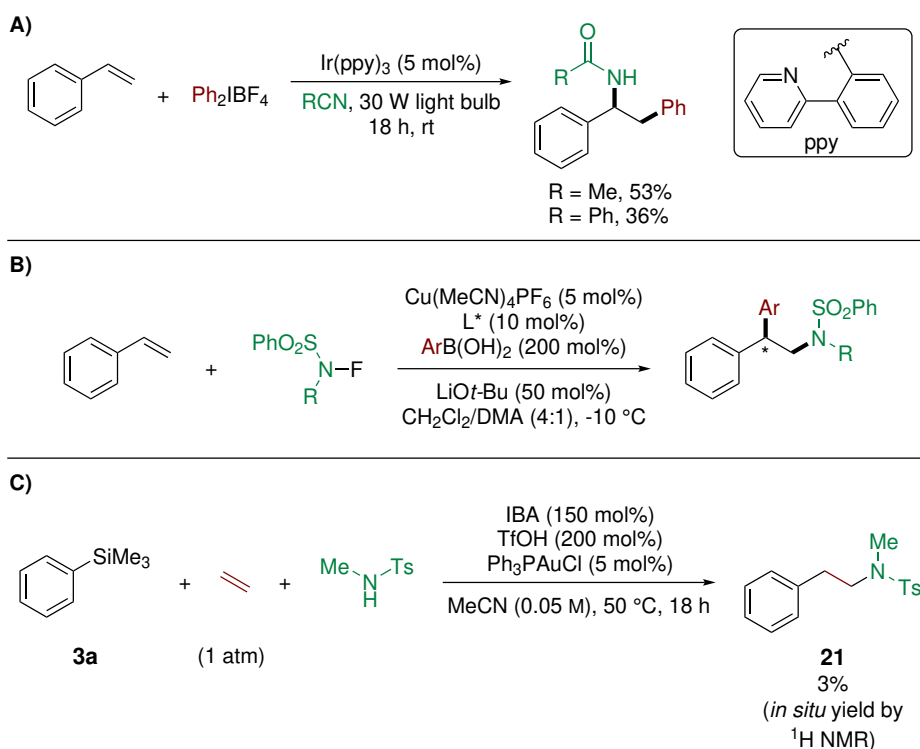
In contrast to most previous gold-catalysed oxyarylation methodologies, successful optimisation of the alcohol loading parameter allowed reduction of the alcohol component to as low as two equivalents. Furthermore, the procedure is operationally simple, occurring with equal efficiency in a sealed reaction vessel or under a balloon of ethylene.

2.11 Future Work

There have been a number of intramolecular aminoarylation reactions of alkenes reported in the literature, catalysed by gold,^{52,76,131,154,155} nickel,¹⁵⁶ and palladium.^{156–159} In addition, intra-⁸⁸ and intermolecular¹⁶⁰ aminoarylations of alkynes have been reported. However, only a few examples exist involving the addition of an amine and aryl group across an alkene in a three-component, intermolecular fashion. One such example was reported by Greaney *et al.* and employed diaryliodonium salts in combination with iridium pho-

photoredox catalysis to aminoarylate styrene (although only two examples were disclosed) (Scheme 2.25, A).¹⁶¹ Lie *et al.* reported a copper-catalysed enantioselective intermolecular aminoarylation of styrenes using *N*-fluoro-*N*-alkylsulfonamide as the amine component and arylboronic acids to deliver the aryl component (Scheme 2.25, B).¹⁶²

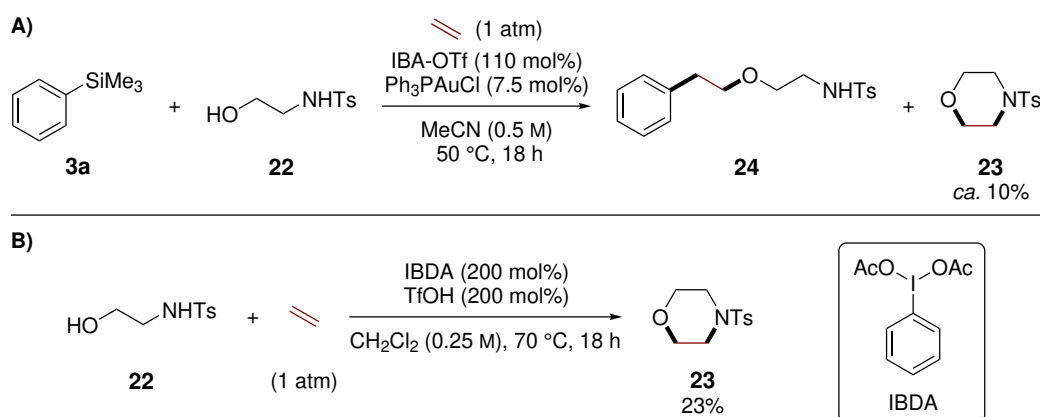
The intermolecular aminoarylation protocols discussed in the previous paragraph are limited to highly reactive styrenes as the alkene component. Expansion of our gold-catalysed 1,2-oxyarylation to use amines in place of the alcohol would be an avenue worth exploring. Preliminary results using *N*-methyl-tosylamine have proven the feasibility of such a reaction, whereby **21** was produced in 3% yield under unoptimised conditions (Scheme 2.25, C). Although the yield is extremely low, optimisation of this reaction would provide a useful modular route to homobenzylic amines.



Scheme 2.25: Intermolecular aminoarylation: photoredox catalysis using diaryliodonium salts (A);¹⁶¹ enantioselective aminoarylation (B);¹⁶² preliminary results for the gold-catalysed 1,2-aminoarylation of **3a** with *N*-methyl-tosylamine (C).

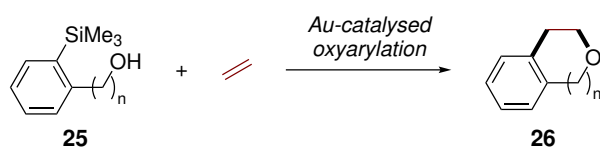
During alcohol scope exploration, submission of aminoalcohol **22** to oxyarylation conditions resulted in the detection of *N*-tosyl-morpholine **23**, an unexpected side product corresponding to oxidative oxyamination of ethylene (Scheme 2.26, A). A preliminary optimisation of this new annulation reaction revealed that a combination of IBDA and TfOH in CH₂Cl₂ gave the best results (Scheme 2.26, B). Interestingly, it was found that the presence of gold was not required.

Development of this reaction would provide a simple, atom economical route to biologically active morpholine scaffolds.¹⁶³ Previous methods to insert a bis-electrophilic ethylene unit include the use of bromo- or vinylsulfonium salts,^{164–166} and toxic 1,2-dibromoethane.^{167–169}



Scheme 2.26: Oxyarylation of **3a** with alcohol **22** resulted in formation of *N*-tosyl-morpholine **23** (A). Preliminary optimisation of the synthesis of **23** (B).

A further potential annulation reaction is to use ethylene as a two-carbon ring closing reagent (Scheme 2.27). For example, submission of alcohol tethered arylsilanes **25** to oxyarylation conditions could react to give cyclic ethers such as **26**. Varying the length of the alcohol bearing carbon chain could give access to a variety of ring sizes.



Scheme 2.27: Gold-catalysed oxyarylation as a tool for the ring closing of alcohol-tethered arylsilanes.

Chapter 3

Organometallic Steps with Gold

Abstract

Three-coordinate bipyridyl complexes of gold, $[(\kappa^2\text{-bipy})\text{Au}(\eta^2\text{-C}_2\text{H}_4)][\text{NTf}_2]$ are accessed by reaction of 2,2'-bipyridine (bipy), or its derivatives, with the homoleptic gold ethylene complex $[\text{Au}(\text{C}_2\text{H}_4)_3][\text{NTf}_2]$. These complexes undergo reversible oxidative addition with a range of aryl iodides to give the corresponding $[(\kappa^2\text{-bipy})\text{Au}(\text{aryl})\text{I}][\text{NTf}_2]$ complexes. Transmetalation of the gold(III) aryl iodides with arylzinc chlorides, followed by reductive elimination furnishes biaryl products in a process akin to a Negishi cross-coupling.

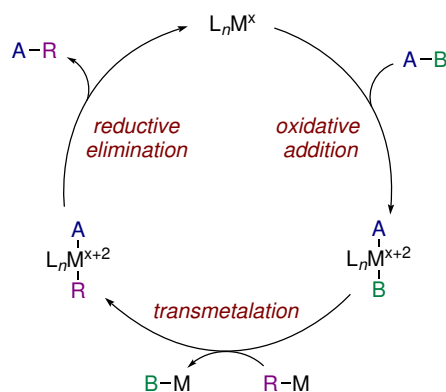
The contents of this chapter have been communicated:¹⁷⁰ Harper, M. J.; Arthur, C. J.; Crosby, J.; Emmett, E. J.; Falconer, R. L.; Fensham-Smith, A. J.; Gates, P. J.; Leman, T.; McGrady, J. E.; Bower, J. F.; Russell, C. A. *J. Am. Chem. Soc.* **2018**, *140*, 4440. Parts of this chapter have been reproduced from the aforementioned publication.

Author contributions for the publication are as follows: The manuscript was drafted by M.J.H. then refined and edited by M.J.H., J.F.B., C.A.R. and J.E.M. All non-computational experimental work was performed by M.J.H. Computational analysis was performed by J.E.M. at the University of Oxford. J.C., C.J.A., P.J.G., and T.L. assisted with

the collection of mass spectrometry data. A.J.F-S. synthesised $[(\kappa^2\text{-}2,2'\text{-bipyridine})\text{Au}(\eta^2\text{-C}_2\text{H}_4)][\text{NTf}_2]$ initially.¹⁷¹ E.J.E. was the industrial supervisor. R.L.F. assisted with the collection of X-ray diffraction data.

3.1 Introduction

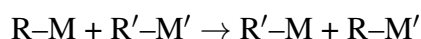
A cycle consisting of oxidative addition, transmetalation, and reductive elimination forms the basic mechanism of a metal-catalysed cross-coupling, as shown in Scheme 3.1.



Scheme 3.1: Oxidative addition, transmetalation, and reductive elimination at a metal centre, illustrated by a generic metal-catalysed cross-coupling.

Oxidative addition involves the addition of a species A–B to a metal complex, whereby the A–B bond is broken and two distinct M–A and M–B bonds are formed. In this process, both the coordination number and the oxidation state of the metal centre increase by two.^{172,173}

Transmetalation is the exchange of fragments between two metal centres, as described by the following equation:



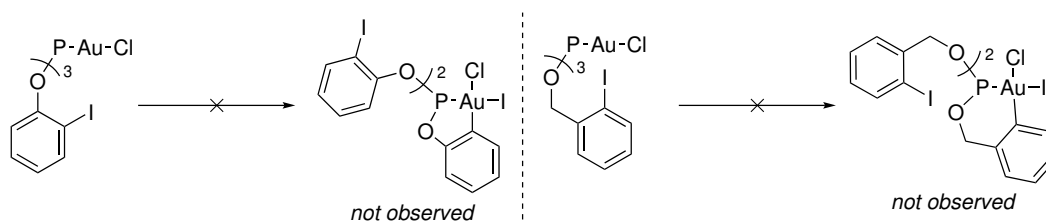
This process is commonly employed to transfer an organic moiety from a transmetalation reagent R–M (M = Li, Mg, Zn, B, Sn, Hg, and Si) to a transition metal.^{172,173}

Reductive elimination is the reverse of oxidative addition, whereby a new A–R bond is formed, and the coordination number and oxidation state of the metal centre decrease by two.^{172,173}

Transmetalation and reductive elimination are well established for gold and numerous examples exist in the literature; for more information the reader is directed to a recent review which summarises these topics in detail.¹⁷⁴ Oxidative addition with gold, however, is challenging.¹⁷⁵ This has largely prohibited gold from partaking in catalytic cycles such as that shown in Scheme 3.1, leading to considerable research effort towards solving the "redox gold problem" by overcoming the reluctance of gold(I) to undergo oxidative addition.

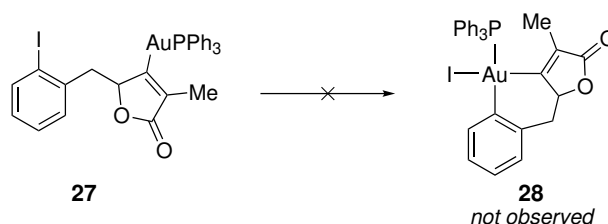
A comparison often cited in the literature is the diagonal relationship shared between gold(I) and palladium(0). As both are d^{10} metals, one might expect similar reactivity to be observed. For example, palladium(0) will undergo facile oxidative addition of aryl-X bonds, whereas gold(I) will not. A comparison of the standard reduction potentials (E^0 : $\text{Pd}^{\text{II}/0} = +0.92 \text{ V}$, $\text{Au}^{\text{III/I}} = +1.41 \text{ V}$)¹⁷⁶ reveals a significant energy cost for the oxidation of gold(I). This energy can, in part, be attributed to the increased effects of relativity that gold experiences (*vs* palladium) (see Chapter 1, Section 1.3 for further details). Relativistic contraction of the *s* and *p* orbitals leads to more diffuse *5d*-orbitals, whose electrons experience reduced electron/electron repulsion, leading to decreased nucleophilicity and a higher barrier towards oxidative addition.²²

Echavarren *et al.* synthesised a range of gold(I) complexes bearing tethered aryl-iodide bonds and found that even under these favourable intramolecular conditions, no oxidative addition was observed (Scheme 3.2).¹⁷⁵ Calculations were performed revealing prohibitively high barriers (approximately 40–49 kcal mol⁻¹) for the oxidative addition step. It was suggested that the origin for this is the energy required for gold(I) to deform from its strongly preferred 2-coordinate, linear conformation. This contrasts to the ability of palladium(0) to readily adopt 2- to 4-coordinate configurations.¹⁷²



Scheme 3.2: Attempted oxidative addition of gold(I) under intramolecular conditions.¹⁷⁵

The reluctance of gold to undergo oxidative addition was further demonstrated by Hashmi *et al.* in the synthesis of the vinyl gold(I) complex **27** bearing a tethered aryl iodide (Scheme 3.3).¹⁷⁷ Although a favourable 6-membered transition state was feasible, oxidative addition to **28** did not occur.



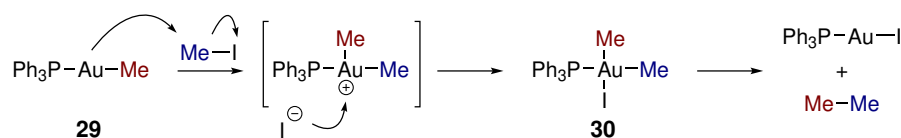
Scheme 3.3: Oxidative addition of the tethered aryl iodide to the vinyl gold(I) complex **27** does not occur.¹⁷⁷

3.1.1 Oxidative Addition to Gold(I)

As described in the previous section, oxidative addition to gold(I) is challenging. Despite this, a limited number of examples exist in the literature. Detailed in this section are achievements to date in this field.¹⁷⁴

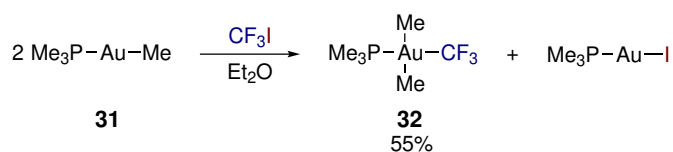
Oxidative addition to gold(I) was first reported in the early 1970s by Schmidbaur,¹⁷⁸ and was investigated shortly after by Kochi^{179,180} and Puddephatt.^{181,182} It was found that alkyl gold(I) complexes of the type LAuR (L = PMe₃, PPh₃; R = Me, neopentyl) **29** react with Me-X electrophiles (X = I or OTf) to produce LAuI and ethane (Scheme 3.4). The

reaction proceeds *via* S_N2-type oxidative addition to give a dimethyl gold(III) complex **30**. Complex **30** was not isolated, but its intermediacy was deduced from the products of its reductive elimination.



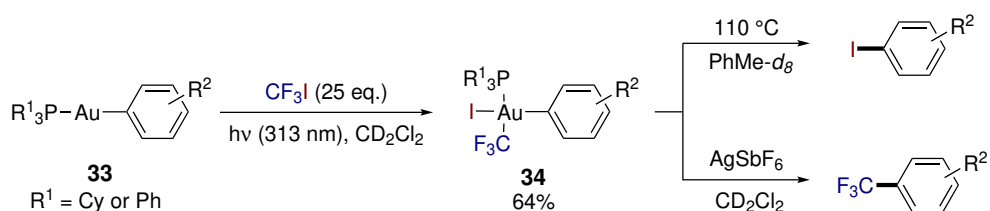
Scheme 3.4: S_N2-type oxidative addition of PPh₃AuMe with methyl iodide.^{178,180}

The intermediacy of complexes of type **30** was confirmed by Puddephatt.¹⁸¹ The stable gold(III) product of oxidative addition between **31** and CF₃I was isolated in 55% yield and characterised as *trans*-(Me)₂(Me₃P)Au(CF₃) **32**. Although formally an oxidative addition process, this S_N2-type nucleophilic addition is mechanistically distinct from oxidative addition of an aryl halide bond.



Scheme 3.5: Synthesis of *trans*-(Me)₂(Me₃P)Au(CF₃) **32** *via* oxidative addition of CF₃I.¹⁸¹

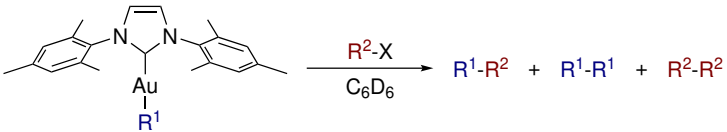
Toste *et al.* reported the oxidative addition of the highly electrophilic CF₃I to gold(I) facilitated by irradiation with 313 nm light (Scheme 3.6).¹⁸³ A range of phosphine supported gold(I) aryl complexes **33** undergo oxidative addition to the corresponding CF₃-ligated gold(III) complexes **34**. The reactions were proposed to proceed *via* a radical chain reaction initiated by the excitation of CF₃I. Activation of **34** by either heating (110 °C) or treatment with AgSbF₆ gave selectively the C_{aryl}-I or C_{aryl}-CF₃ reductive elimination products, respectively.



Scheme 3.6: Synthesis of **34** via photoinitiated oxidative addition of CF_3I to aryl gold(I) complex **33**.¹⁸³

In a report by Wendt *et al.*, NHC complexes of gold(I) bearing either σ -bound aryl or methyl ligands were found to react with Me-X ($\text{X} = \text{I}$ or OTf) or aryl iodides to give coupled products corresponding to an apparent oxidative addition/reductive elimination sequence (Table 3.1).¹⁸⁴ A significant weakness of the study is that in most cases symmetrical products are formed (in particular, entries 3, and 5–7), leaving the origin of each fragment unclear. This is compounded by the presence of homocoupling products originating from the gold-bound organic fragment (see entries 1 and 2). However, treatment of NHCAuPh with *p*-tol-I produces 85%ⁱ of the unsymmetrical cross-coupled product 4-Me-biphenyl (entry 4), suggestive of an oxidative addition/reductive elimination sequence at gold. Overall, the authors claim an oxidative addition mechanism for MeI and MeOTf , but cannot exclude the possibility of gold nanoparticles activating the aryl iodide substrates.

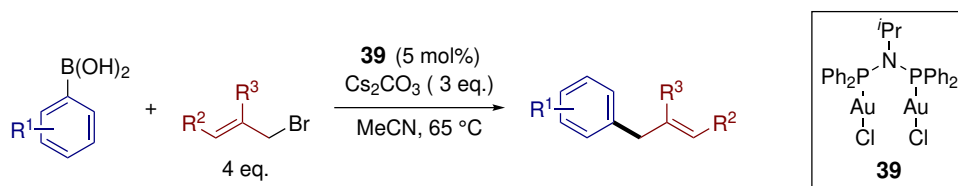
ⁱThis number corresponds to the relative product distribution and not absolute yield.

Table 3.1: Reactivity of IMesAuR with electrophiles.¹⁸⁴


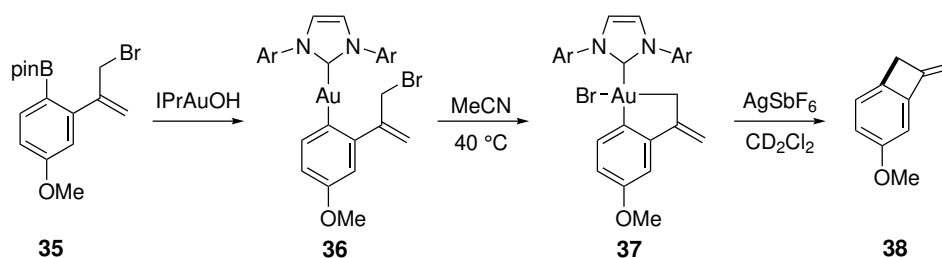
Entry	R ¹	R ² -X	Time (h)	Product distribution (%) ^a
1 ^b	Ph	MeOTf	7	Ph-Ph (54), Ph-Me (46), Me-Me
2 ^c	Ph	MeI	27	Ph-Ph (24), Ph-Me (76), Me-Me
3 ^c	Ph	PhI	50	Ph-Ph
4 ^c	Ph	<i>p</i> -tol-I	24	4,4'-bitolyl (3), 4-Me-biphenyl (85), Me-Me
5 ^c	Ph	PhOTf	100	Ph-Ph
6 ^c	Me	MeI	6	Me-Me
7 ^b	Me	MeOTf	3.5	Me-Me
8 ^c	Me	PhI	48	no reaction
9 ^c	Me	PhOTf	24	no reaction
10 ^b	<i>p</i> -tol	MeOTf	4.5	4,4'-bitolyl (60), <i>p</i> -xylene (40), Me-Me

^aProduct distributions determined by ¹H NMR or GC-MS. ^b25 °C. ^c110 °C.

In 2014, Toste *et al.* reported the first example of a gold-catalysed cross-coupling in the absence of an external oxidant (Scheme 3.7).¹⁸⁵ Catalytic allylation of aryl boronic acids was achieved using the dinuclear gold(I) catalyst **39**. It was proposed that oxidative addition of allylic C(sp²)-Br bonds was facilitated by the formation of a Au(II)-Au(II) intermediate, although experimental evidence to support this was not provided. However, a stoichiometric oxidative addition to gold(III) bromide **37** was realised starting from the gold(I) NHC complex **36** bearing a tethered allyl bromide (Scheme 3.8). Treatment of **37** with AgSbF₆ resulted in reductive elimination to furnish **38**, thus providing an elegant example of an oxidative addition/reductive elimination sequence at a gold centre.

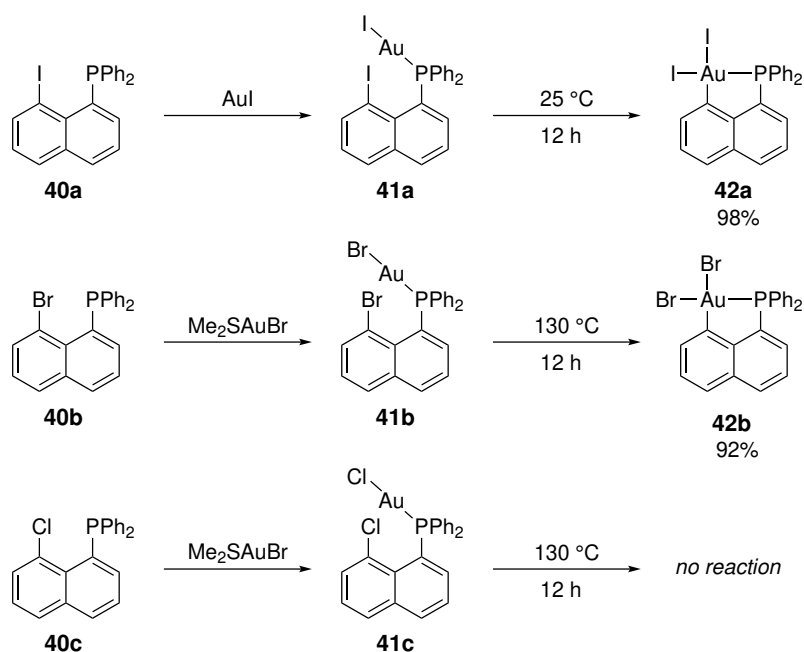


Scheme 3.7: External oxidant-free gold-catalysed cross-coupling of aryl boronic acids and allyl bromides.¹⁸⁵



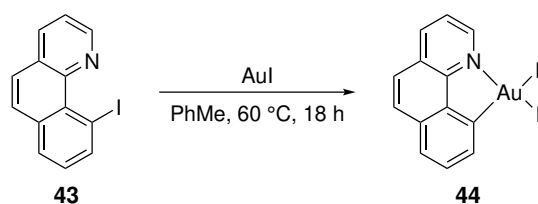
Scheme 3.8: Oxidative addition of **36** into a tethered allyl bromide and silver-induced reductive elimination to give cyclobutane **38**.¹⁸⁵ Ar = 2,6-diisopropylphenyl.

In 2014 the first direct evidence for oxidative addition of an aryl-halide to gold(I) was reported by Bourissou *et al.* (Scheme 3.9).¹⁸⁶ Using a template approach, gold(I) phosphine complexes bearing tethered C(sp²)-I (**40a**) or C(sp²)-Br (**40b**) bonds underwent oxidative addition at 25 °C and 130 °C, respectively. However, no oxidative addition of the chloro derivative (**40c**) was observed, even after 12 h at 130 °C. Cyclometalated gold(III) complexes **41a** and **41b** were isolated in excellent yields and the structure of **41a** was confirmed unambiguously by X-ray diffraction. This pioneering study confirmed that, at least with chelation assistance, oxidative addition of C(sp²)-I and -Br bonds to gold(I) is feasible.



Scheme 3.9: Synthesis of cyclometalated gold(III) complexes *via* phosphine-directed oxidative addition of aryl-iodide and -bromide bonds.¹⁸⁶

A further directing-group facilitated oxidative addition with gold(I) was reported by Ribas *et al.*^{187,188} Catalytic $\text{C}(\text{sp}^2)\text{-O}$ and -N bond formation was achieved using pyridyl directing groups and a cationic NHC-supported gold(I) catalyst. A stoichiometric oxidative addition was achieved using the rigid substrate **43** to furnish the gold(III) diiodo complex **44** (Scheme 3.10).¹⁸⁸



Scheme 3.10: Pyridyl-directed oxidative addition of gold(I) iodide into **43**.¹⁸⁸

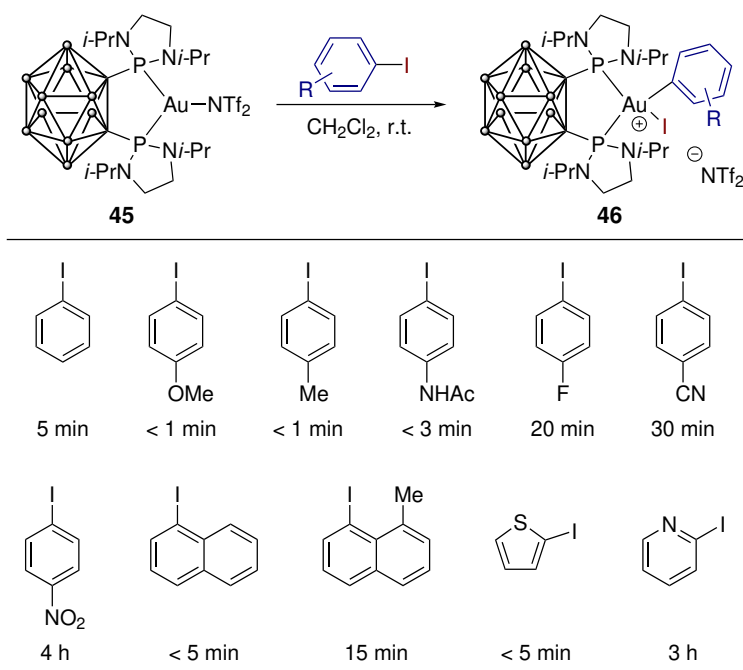
Pyridyl-directed oxidative addition to gold(I) was further exploited by Glorius *et al.*, however, this relied on the use of highly reactive aryl diazonium salts as the electrophile.⁷⁹

Moreover, undirected oxidative addition of aryl diazonium salts to gold(I) was reported by the groups of Hashmi⁷⁸ and Porcel.¹⁸⁹

In addition to aryl diazonium salts, gold(I) has been reported to undergo oxidative addition of C–C,¹⁹⁰ S–S,¹⁹¹ Si–Si,^{192,193} and Sn–Sn bonds.¹⁹⁴ However, these reactions are less relevant for catalytic applications and will not be discussed further.

The first general example of an intermolecular oxidative addition of aryl iodides to gold(I) was reported by Bourissou *et al.* in 2014 (Table 3.2).¹⁹⁵ Facilitated by a bidentate carboranyl diphosphine ligand,¹⁹⁶ complex **45** underwent oxidative addition of a range of (hetero)aryl iodides at room temperature. Interestingly, electron rich substrates were found to react faster,ⁱ which is in contrast to the reactivity trend observed for palladium(0). In addition to aryl iodides, complex **45** was found to undergo oxidative addition of the strained C–C bonds of biphenylene and benzocyclobutenone, however, extrapolation to aryl bromide bonds was not successful.¹⁹⁷

ⁱSee Section 3.7 for further discussion of this point.

Table 3.2: Oxidative addition of aryl iodides to carboranyl phosphine gold(I) complex **45**.^{195,a}

^aTimes to reach complete conversion using 5 equivalents of aryl iodide.

Key to the success of Bourissou's oxidative addition protocol is bending ($\text{P-Au-P} = 100.7^\circ$) of the gold(I) starting complex **45** away from the linear geometry normally preferred by gold(I) complexes. Two consequences of this bending lead to activation of the gold(I) centre towards oxidative addition. Firstly, the geometry of complex **45** is *preorganised* to more closely resemble the square-planar geometry of the gold(III) product. Secondly, inspection of a Walsh diagram for a d^{10} ML_2 complex (such as palladium(0), platinum(0), and gold(I)) reveals a change in the symmetry and energy of the HOMO (Figure 3.1).¹⁹⁸ In contrast to a linear complex, the HOMO of a bent ML_2 complex now possesses the correct symmetry for π -backdonation into the σ^* -orbital of the $\text{C}_{\text{aryl}}\text{-I}$ bond, the fundamental interaction required for oxidative addition.

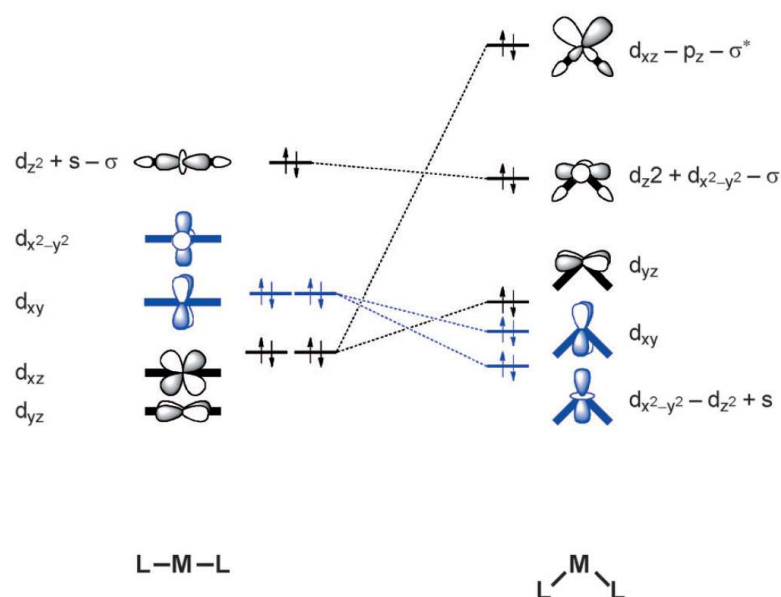
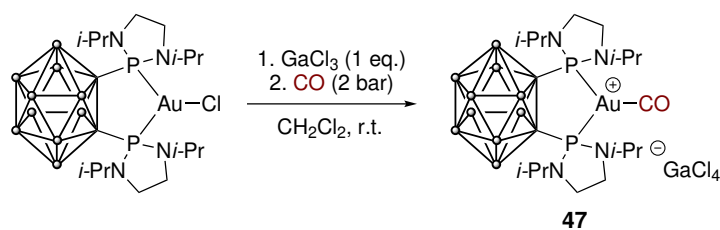


Figure 3.1: Simplified Walsh diagram for a linear (L) and bent (R) d^{10} ML_2 complex. Reproduced from Ref. 198.

The increased π -backdonation ability of a bent gold(I) species was demonstrated by Bourissou *et al.* upon the isolation of the first classicalⁱ gold(I) carbonyl complex **47** (Scheme 3.11).¹⁹⁹ Although several linear gold(I) carbonyl complexes have been isolated,^{200–204} complex **47** is the first that exhibits a CO stretching frequency ($\nu(\text{CO}) = 2113 \text{ cm}^{-1}$) that is redshifted when compared to free CO ($\nu(\text{CO}) = 2143 \text{ cm}^{-1}$). This is diagnostic of a weakened CO bond induced *via* π -backdonation from gold to the π^* bond of CO.

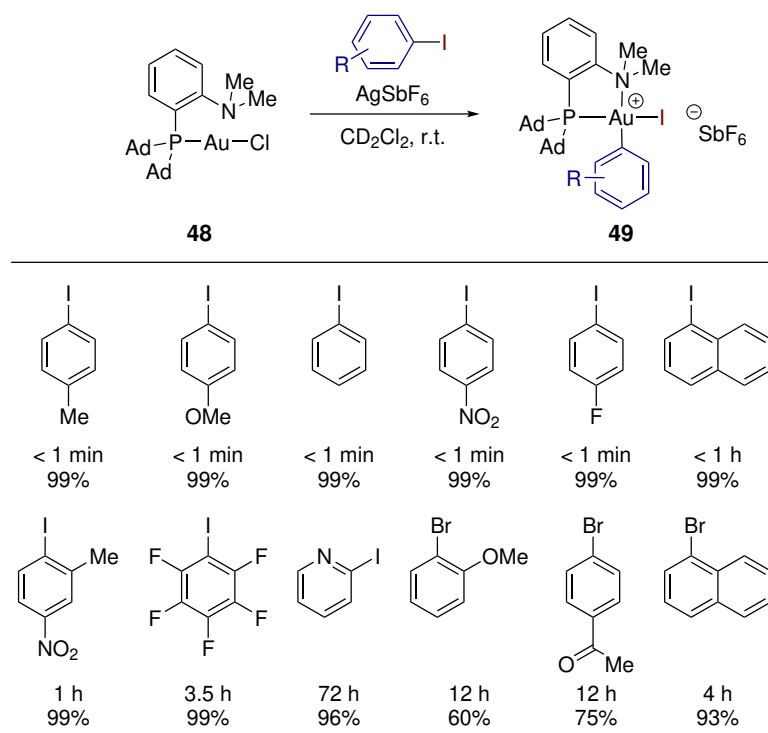
ⁱThe term classical carbonyl complex refers to a $L_nM\text{-CO}$ complex possessing a lower CO stretching frequency (redshifted) than that of free CO ($\nu(\text{CO}) = 2143 \text{ cm}^{-1}$)



Scheme 3.11: Synthesis and isolation of the first classical gold(I) carbonyl complex **47**.¹⁹⁹

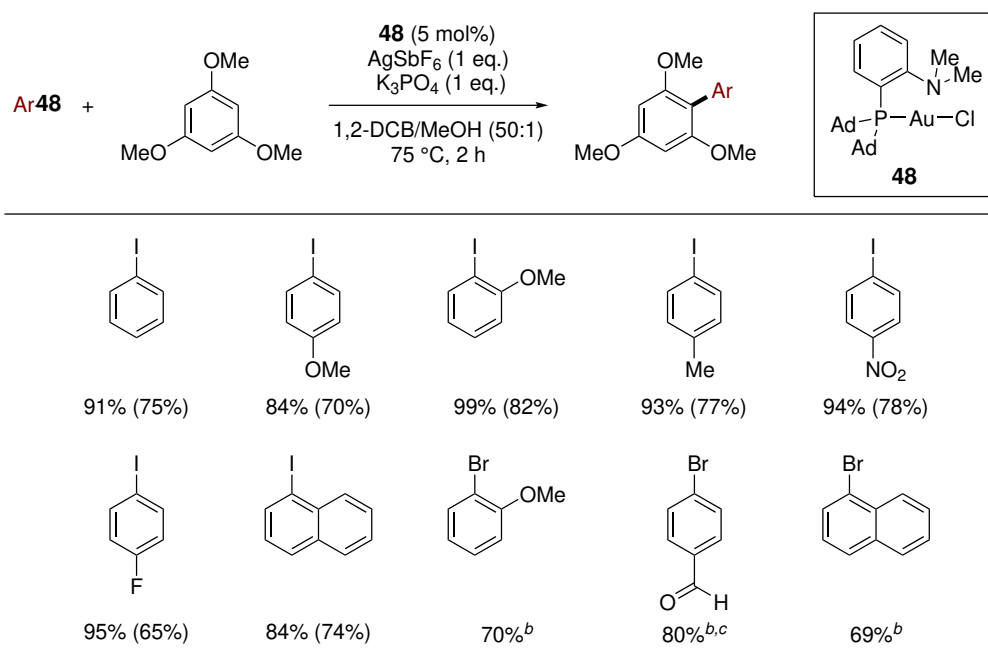
In 2017,ⁱ Bourissou *et al.* reported that (Me-Dalphos)AuCl **48** presented enhanced activity towards oxidative addition (Table 3.3).²⁰⁵ Me-Dalphos, a bulky phosphine ligand bearing a hemilabile pendant tertiary amine, facilitated oxidative addition to aryl iodides *and* bromides at room temperature. Mechanistically, computations suggest the reaction proceeds *via* a linear σ -coordinated gold(I) aryl halide adduct, followed by coordination of the pendant amine to facilitate the oxidative addition step.

ⁱThe research described in this chapter occurred prior to the publication of Ref. 205.

Table 3.3: Oxidative addition of aryl iodides and bromides to (Me-Dalpos)AuCl **48**.^{205,a}

^aSpectroscopic yields determined via ³¹P NMR spectroscopy.

It was found that complexes **49** reacted stoichiometrically with 1,3,5-trimethoxybenzene to slowly afford biaryl products. Addition of AgSbF₆ to abstract iodide and generate a more electrophilic gold(III) centre led to the development of a catalytic C–H arylation protocol (Table 3.4). This work represents the first gold-catalysed coupling reaction to use aryl halides as an internal oxidant in the absence of directing groups.²⁰⁵ Very recently, Spokoyny *et al.* demonstrated that complexes of type **46** (Table 3.2) and **49** (Table 3.3) act as robust reagents for chemoselective *S*-arylation of cysteine.²⁰⁶

Table 3.4: C–H arylation of 1,3,5-trimethoxybenzene catalysed by (Me-Dalpos)AuCl **48**.^{205,a}

^aYields determined by calibrated GC-MS, isolated yields shown in parentheses.

^b10 mol% **48** and 5 equivalents of aryl bromide. ^c 12 h reaction time.

3.1.2 Objectives

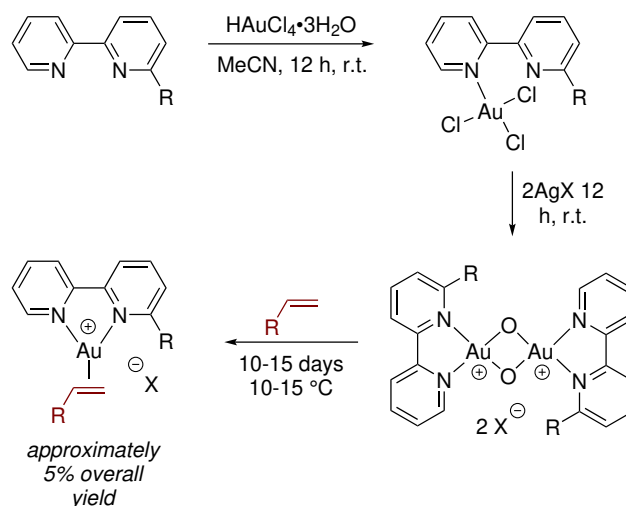
In the previous section, the results of Bourissou *et al.* illustrate that undirected, intermolecular oxidative addition of aryl halides to gold(I) complexes can be achieved through ligand design. Successful architectures are: a three-coordinate bent design enforced by a bidentate diphosphine with a small bite-angle (such as complex **45**, Table 3.2); or a mono-coordinate phosphine gold(I) complex bearing a pendant hemi-labile amine donor (such as complex **48**, Table 3.3).

In this chapter, the feasibility of an alternative three-coordinate bent design will be explored. Instead of the carboranyl diphosphine ligands used by Bourissou *et al.*, the effectiveness of what is perhaps the simplest small bite-angle bidentate ligand, 2,2'-bipyridine (bipy), will be explored. Three-coordinate gold(I) cations of the type $[(\kappa^2\text{-bipy})\text{Au}(\eta^2\text{-$

alkene)]⁺ will be targeted in order to enforce the π -backdonation required for oxidative addition.

3.2 Synthesis of $[(\kappa^2\text{-bipy})\text{Au}(\text{C}_2\text{H}_4)][\text{NTf}_2]$

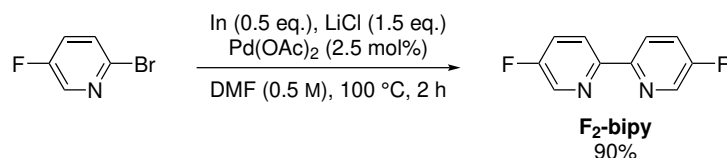
The only previous route to complexes of the type $[(\kappa^2\text{-bipy})\text{Au}(\eta^2\text{-alkene})]\text{X}$ was reported by Cinellu *et al.* (Scheme 3.12).^{207–209} The synthetic route was long and very low yielding, and substitution at the 6-position of bipy was required else the route would fail. Therefore, a shorter and more versatile route was sought.



Scheme 3.12: Synthetic route to complexes of the type $[(\kappa^2\text{-bipy})\text{Au}(\eta^2\text{-alkene})]\text{X}$ by Cinellu *et al.*^{207–209}

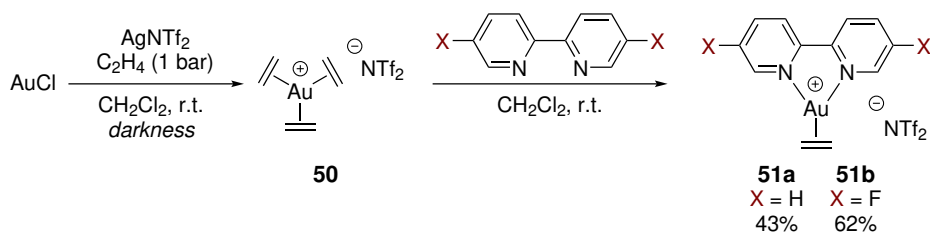
Cationic homoleptic gold(I) complexes were reported by Russell²¹⁰ and Dias²¹¹ and previous unpublished work in our group found that addition of bipy or its derivatives to these furnished the desired $[(\kappa^2\text{-bipy})\text{Au}(\eta^2\text{-alkene})]\text{X}$ complexes in a two step reaction.¹⁷¹ This route was selected for further investigation. A 2,2'-bipyridine derivative bearing fluorine substituents in the 5 and 5' positions was prepared in order to facilitate convenient reaction monitoring *via* ^{19}F NMR spectroscopy. To this end, 5,5'-difluoro-

2,2'-bipyridine (F₂-bipy) was prepared *via* the reductive palladium-catalysed homocoupling procedure of Lee *et al.* (Scheme 3.13).^{212,213}



Scheme 3.13: Synthesis of F₂-bipy *via* Pd-catalysed reductive homocoupling.^{212,213}

With F₂-bipy to hand, the bipy gold(I) ethylene complex [(κ²-bipy)Au(η²-C₂H₄)]-[NTf₂] **51a** and fluorinated analogue [(κ²-F₂-bipy)Au(η²-C₂H₄)]-[NTf₂] **51b** were synthesised (Scheme 3.14). Treatment of a CH₂Cl₂ suspension of AuCl with AgNTf₂ under an atmosphere of ethylene in the absence of light gave, after filtration of the AgCl by-product, the homoleptic gold(I) tris-ethylene complex [Au(C₂H₄)₃][NTf₂] **50**.²¹¹ Complex **50** is extremely fragile, although isolation is not necessary (and was not attempted) and rapid addition of bipy results in displacement of two ethylene ligands to furnish the desired gold(I) ethylene complexes **51a** and **51b** in 43% and 62% yields, respectively, after purification by recrystallisation.



Scheme 3.14: Synthesis of **51a** and **51b** *via* addition of 2,2'-bipyridine and F₂-bipy to [Au(C₂H₄)₃][NTf₂] **50**, respectively.

Single crystals of **51a**ⁱ and **51b** were grown by layering CH₂Cl₂ solutions of the gold

ⁱComplex **51a** was first synthesised by Dr. Andrew Fensham-Smith, and is reported in his PhD thesis.¹⁷¹ The crystal structure of **51a** (Figure 3.2) was acquired and solved by him, and is also reported in his thesis.

complexes with Et_2O , and the solid-state structures were determined by X-ray diffraction analysis (Figure 3.2 and Figure 3.3, respectively). However, due to the poor crystal quality of **51a** as a result of twinning, only bond metrics for **51b** will be discussed.

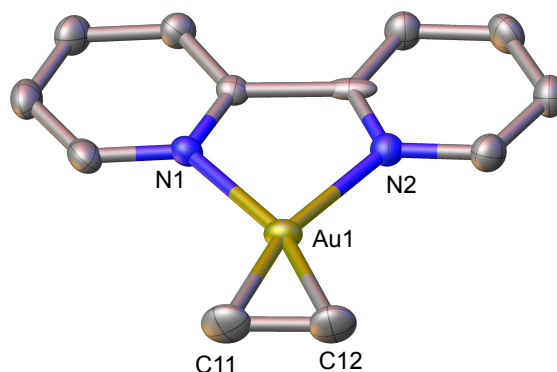


Figure 3.2: Molecular structure of **51a**, thermal ellipsoids are shown at the 30% probability level. Hydrogen atoms and the NTf_2 anion have been omitted for clarity. Selected bond lengths (\AA) and angles ($^\circ$): Au1-N1 2.174(4), Au1-N2 2.184(4), Au1-C12 2.090(6), Au1-C1 2.080(5), C11-C12 1.407(9), N1-Au1-N2 74.89(14). See Section 5.5, Table 5.3 for full crystallographic details.

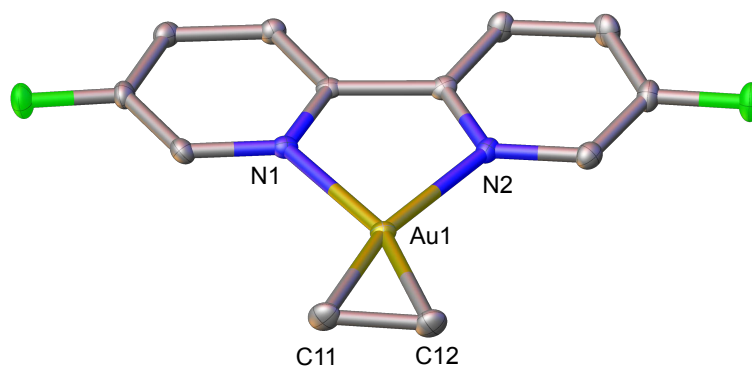


Figure 3.3: Molecular structure of **51b**, thermal ellipsoids are shown at the 50% probability level. Hydrogen atoms and the NTf_2 anion have been omitted for clarity. Selected bond lengths (\AA) and angles ($^\circ$): Au1-N1 2.178(2), Au1-N2 2.210(2), Au1-C12 2.092(3), Au1-C11 2.086(3), C11-C12 1.399(5), N1-Au1-N2 74.57(9). See Section 5.5, Table 5.4 for full crystallographic details.

Complex **51b** adopts a distorted trigonal planar geometry around the gold centre with the $\text{F}_2\text{-bipy}$ ligand binding in the symmetric κ^2 -mode with a bite angle of 75° . Impor-

tantly, the alkene C=C bond length (1.399(5) Å) is elongated when compared to other cationic gold(I) alkene complexes (Figure 3.4). For example in complexes of the type [LAu(η^2 -alkene)]⁺, the alkene C=C bond length is 1.349(14) Å when L = Pt-Bu₃ (**52**),²¹⁴ and 1.331(7) Å when L = IPr (**54**);²¹⁵ the C=C bond length is 1.351(7) Å in the homoleptic gold(I) tris-ethylene complex **54**.²¹¹

The ethylene carbon of **51b** exhibits a resonance at δ 63.8 in the ¹³C NMR spectrum (Figure 3.4). This is significantly upfield shifted when compared to the alkene CH₂ carbons of **52**, **53**, and **54**, which exhibit resonances at δ 96.2, δ 88.2, and δ 92.7, respectively (Figure 3.4).

The elongated C=C bond length of **55**, in addition to the shielded ethylene carbon in the ¹³C NMR spectrum, is consistent with increased sp³-character as a result of π -backdonation from the gold centre to the π^* orbital of ethylene. This suggests that the F₂-bipy ligand system does indeed enforce the desired enhanced π -backdonation character from gold(I), and could be effective for oxidative addition.

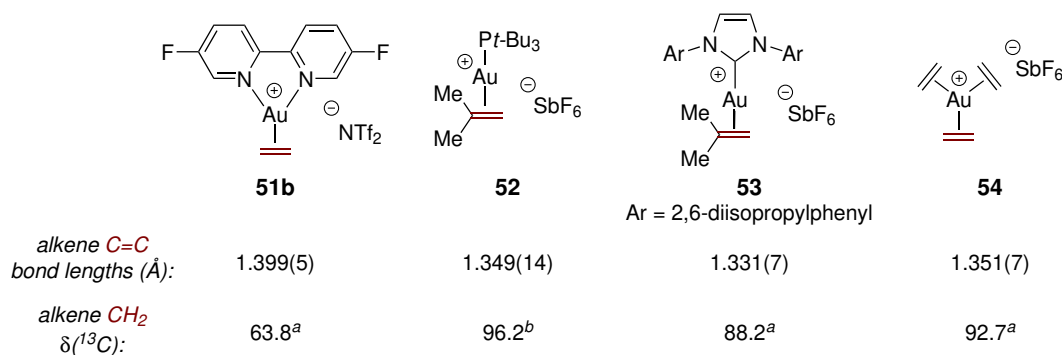
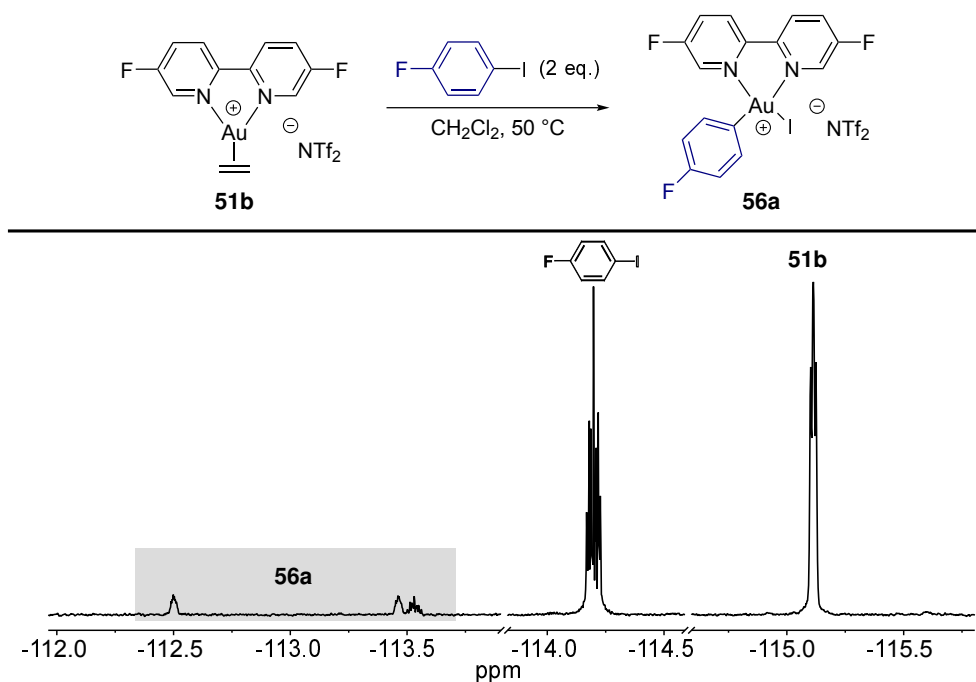


Figure 3.4: Alkene C=C bond lengths of cationic gold(I) alkene complexes **51b**, **52**,²¹⁴ **53**,²¹⁵ and **54**.²¹¹ ^aCD₂Cl₂ NMR solvent. ^bCDCl₃ NMR solvent.

3.3 Oxidative Addition: Initial Results

With ample quantities of **51b** to hand, investigations towards aryl-halide oxidative addition were commenced. Initially, **51b** was exposed to two equivalents of 4-fluoroiodobenzene in CH_2Cl_2 at 50°C (Scheme 3.15). Excitingly, the solution changed rapidly from colourless to pale yellow, a colour often indicative of Au(III). Analysis of the reaction mixture by ^{19}F NMR spectroscopy after 1 h revealed three new multiplets integrating in a 1:1:1 ratio (Scheme 3.15, highlighted in grey). This is consistent with desymmetrisation of the F_2 -bipy system which would accompany oxidative addition to $[(\kappa^2\text{-F}_2\text{-bipy})\text{Au}(4\text{-F-C}_6\text{H}_4\text{I})][\text{NTf}_2]$ **56a**. Confirmation that **56a** had formed was obtained by analysis of the reaction mixture using high-resolution electrospray ionisation mass spectrometry (ESI-HRMS); an ion was observed with m/z 610.9482, which is in agreement with the calculated m/z for the $[(\kappa^2\text{-F}_2\text{-bipy})\text{Au}(4\text{-F-C}_6\text{H}_4\text{I})]^+$ cation (610.9501).



Scheme 3.15: Oxidative addition of 4-fluoroiodobenzene to bipy gold(I) ethylene **51b** and accompanying ^{19}F NMR spectrum. The spectrum has been truncated for clarity.

Using only two equivalents of 4-fluoriodobenzene, attempts to isolate **56a** were hampered by poor (<10%) conversion at 50 °C. Increasing the aryl iodide loading to 20 equivalents increased conversion to 35% after 6 hours, however, reaction progress stalled after this point. This behaviour prompted the investigation of reaction progress as a function of temperature, monitored by ^{19}F NMR spectroscopy (Figure 3.5). At temperatures between 40-60 °C, conversion to **56a** increased with temperature then reached a plateau after approximately 3-6 hours. Increasing the reaction temperature to 70-80 °C saw conversion increase to a maximum of 75%, although this was followed by gradual decomposition.

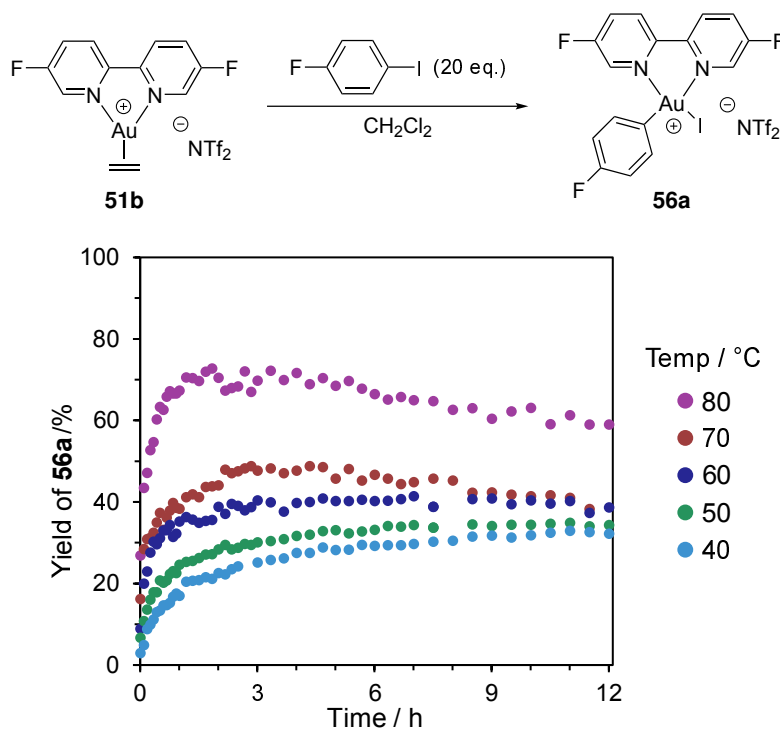
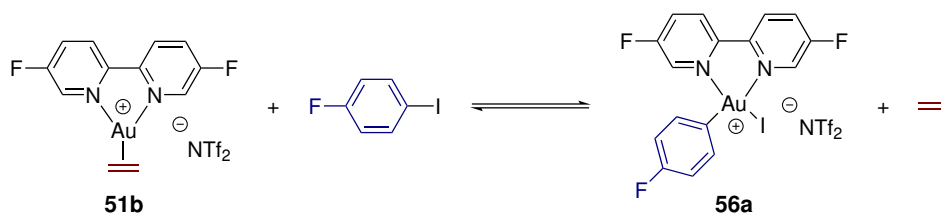


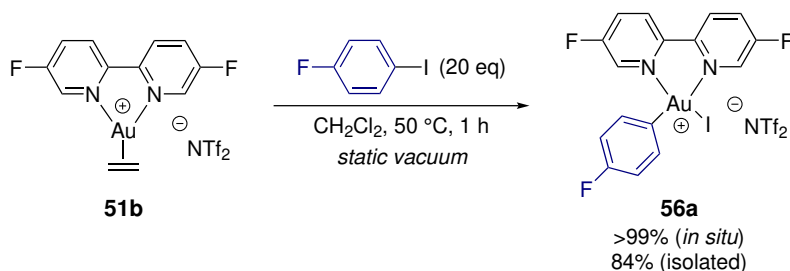
Figure 3.5: Effect of varying the temperature on the oxidative addition of 4-fluoriodobenzene to **51b**. Reaction progress monitored by ^{19}F NMR spectroscopy.

The data in Figure 3.5 suggests that **56a** may be in equilibrium with **51b**, a consequence of reversible oxidative addition (Scheme 3.16). The feasibility of such a $\text{C}(\text{sp}^2)\text{-I}$ reductive elimination process at gold has been previously demonstrated by the groups of Ribas¹⁸⁷ and Toste.¹⁸³



Scheme 3.16: Reversible oxidative addition to **51b** and subsequent C(sp²)-I reductive elimination from **56a**.

If the equilibrium depicted in Scheme 3.16 is in operation, then application of Le Chatelier's principle suggests the equilibrium can be shifted towards **56a** by either addition of 4-fluoriodobenzene, or removal of ethylene from the reaction mixture. To this end, exploiting the fact that ethylene is a gas at room temperature, a reaction mixture of **51b** and 4-fluoriodobenzene in CH₂Cl₂ was placed under a static vacuum (approximately 10⁻² mbar) in a sealed tube and then heated to 50 °C. Gratifyingly, analysis of the reaction mixture by ¹⁹F NMR spectroscopy revealed full conversion to **56a** after 1 h. Concentration of the reaction mixture to a minimum volume, followed by precipitation with hexane afforded pure **56a** in 84% yield as a bright yellow powder.



Scheme 3.17: Synthesis of **56a** via oxidative addition of 4-fluoriodobenzene to **51b**. *In situ* yield determined by ¹⁹F NMR spectroscopy.

Crystals of **56a** were grown from a CH₂Cl₂ solution layered with hexane; the solid-state structure was determined unambiguously by X-ray diffraction analysis and shows clear cleavage of the aryl C-I bond (Figure 3.6). Complex **56a** adopts a distorted square

planar geometry, as expected for a four-coordinate d^8 complex. The F₂-bipy ligand subtends a bite angle of 79° at the Au centre, with Au-N distances of 2.080(3) and 2.130(3), respectively.

In the solid state, complex **56a** is air stable for days at room temperature, and months at -20 °C. In solution (CD₂Cl₂), however, slow decomposition occurs at room temperature such that approximately 10% decomposition is observed after 16 h.

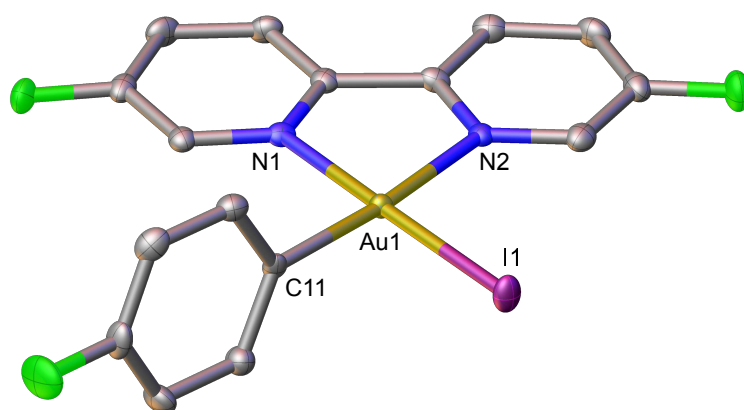
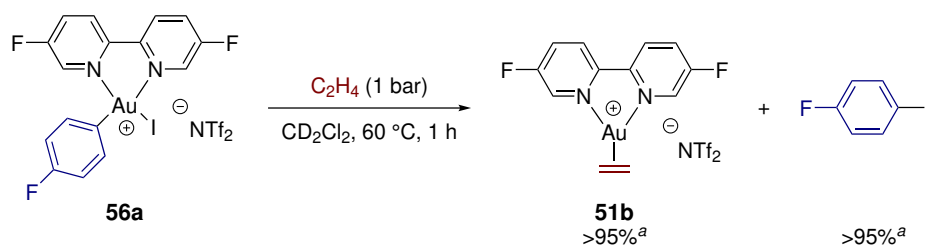


Figure 3.6: Molecular structure of **56a**, thermal ellipsoids are shown at the 50% probability level. Hydrogen atoms and the NTf₂ anion have been omitted for clarity. Selected bond lengths (Å) and angles (°): Au1–C1 2.011(3), Au1–I1 2.5357(3), Au1–N1 2.080(3), Au1–N2 2.130(3), N1–Au1–N2 78.92(12), N2–Au1–I(1) 99.37(8), N1–Au1–C11 95.17(14), C11–Au1–I1 86.54(11). See Section 5.5, Table 5.5 for full crystallographic details.

To confirm the reversibility of the oxidative addition process (Scheme 3.16), a solution of **56a** in CD₂Cl₂ was pressurised to 1 bar with ethylene and monitored by ¹⁹F NMR spectroscopy. After 1 h at 60 °C, clean and near quantitative (>95%) conversion of **56a** to **51b** and 4-fluoriodobenzene was observed (Scheme 3.18). This result provides unambiguous confirmation of the feasibility of C(sp²)-I reductive elimination from **56a**, and demonstrates that **56a** and **51b** lie in a finely balanced equilibrium.

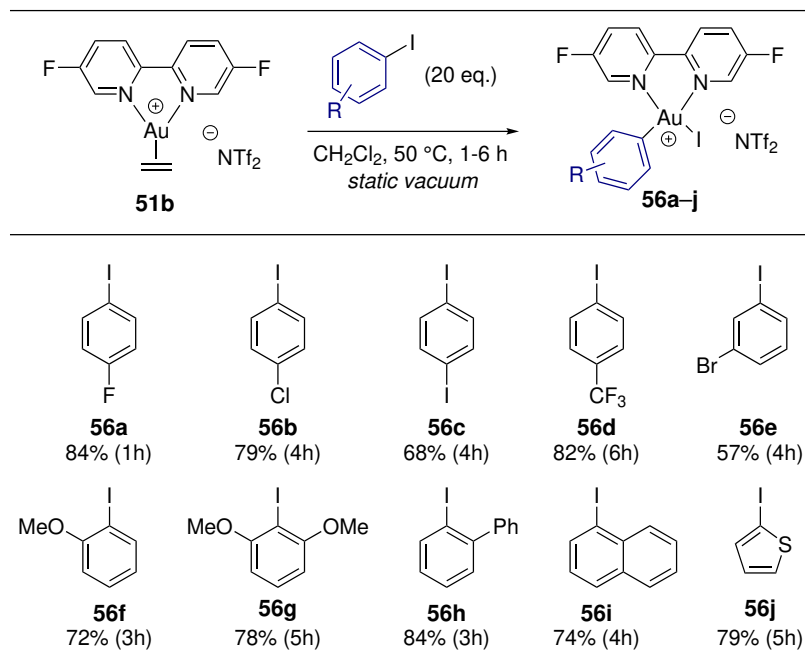
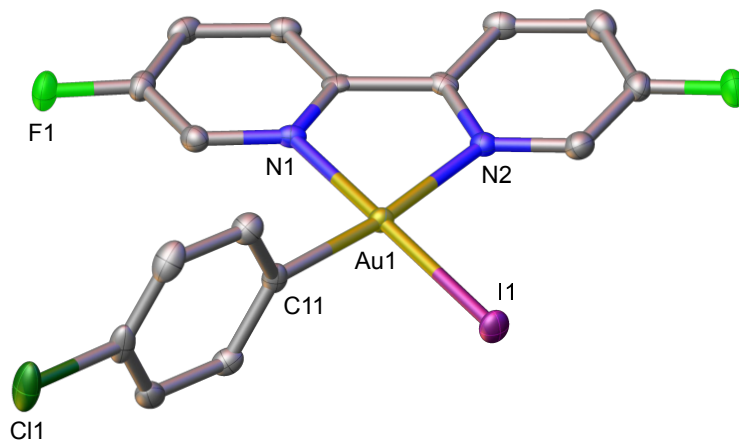


Scheme 3.18: Conversion of **56a** to **51b** via C(sp²)-I reductive elimination.^aConversion determined by ¹⁹F NMR spectroscopy.

3.4 Oxidative Addition: Aryl Iodide Scope

With conditions established for oxidative addition of 4-fluoriodobenzene to **51b**, the scope of the reaction was explored with respect to the aryl iodide component. Using 20 equivalents of the aryl iodide at 50 °C, full conversion to the corresponding gold(III)-complexes **56a–j** was observed with a range of aryl iodides, as determined by ¹⁹F NMR spectroscopy (Table 3.5). Both electron rich (**56f**, **56g**) and electron poor (**56d**) aryl iodides were tolerated, as well as substrates with bulky groups adjacent to iodine (**56f**, **56g**, **56h**). Furthermore, heteroaromatic (**56j**) and halide containing substrates (**56b**, **56l**, **56e**) were also compatible. For **56b** and **56e**, the high selectivity of **51b** towards the C–I bond is significant; no competing C–Cl/Br oxidative addition was observed. Oxidative addition products **56a–j** were isolated in good to excellent yields as yellow/orange solids, and were characterised by ESI-MS, ¹H NMR and ¹³C NMR spectroscopies. Crystals suitable for X-ray diffraction were grown and the solid-state structures were determined for complexes **56b** (Figure 3.7), **56c** (Figure 3.8), **56f** (Figure 3.9), **56h** (Figure 3.10), and **56j** (Figure 3.11), all of which adopt square-planar geometries analogous to that of **56a**.

All attempts to extend the methodology to the oxidative addition of other Ar-X (X = Br, Cl, OTf) or Alkyl-X (X = I) bonds resulted in no reaction. Furthermore, attempts to effect oxidative addition of **51b** into the strained C–C bond of biphenylene also resulted in no

reaction.^{190,197}**Table 3.5:** Scope of oxidative addition to **51b** with respect to the aryl iodide component.^a^aIsolated yields are quoted.**Figure 3.7:** Molecular structure of **56b**, thermal ellipsoids are shown at the 50% probability level. Hydrogen atoms and the NTf_2 anion have been omitted for clarity. Selected bond lengths (\AA) and angles ($^\circ$): $\text{Au1}-\text{C11}$ 2.014(3), $\text{Au1}-\text{I1}$ 2.5412(2), $\text{Au1}-\text{N(1)}$ 2.079(2), $\text{Au1}-\text{N(2)}$ 2.126(2), $\text{N1}-\text{Au1}-\text{N2}$ 78.63(10), $\text{N2}-\text{Au1}-\text{I1}$ 99.96(7), $\text{N1}-\text{Au1}-\text{C11}$ 96.03(11), $\text{C11}-\text{Au1}-\text{I1}$ 85.55(8). See Section 5.5, Table 5.7 for full crystallographic details.

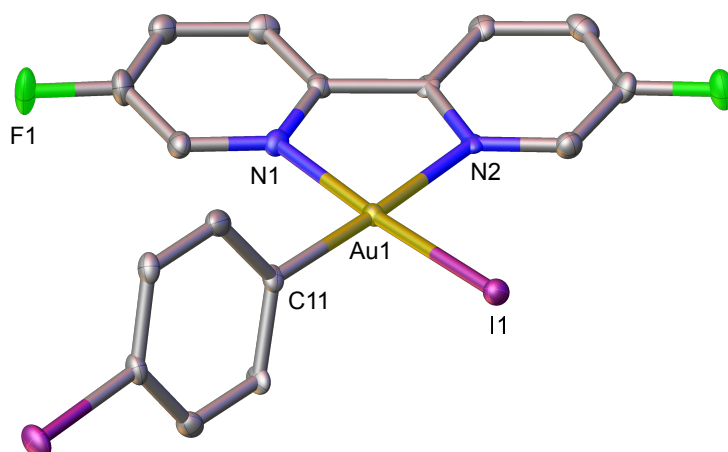


Figure 3.8: Molecular structure of **56c**, thermal ellipsoids are shown at the 50% probability level. Hydrogen atoms and the NTF₂ anion have been omitted for clarity. Selected bond lengths (Å) and angles (°): Au1–C11 2.012(5), Au1–I1 2.5442(4), Au1–N2 2.091(4), Au1–N1 2.142(5), N1–Au1–N2 78.78(18), N1–Au1–I1 99.23(12), N2–Au1–C11 97.6(2), C11–Au1–I1 84.42(15). See Section 5.5, Table 5.8 for full crystallographic details.

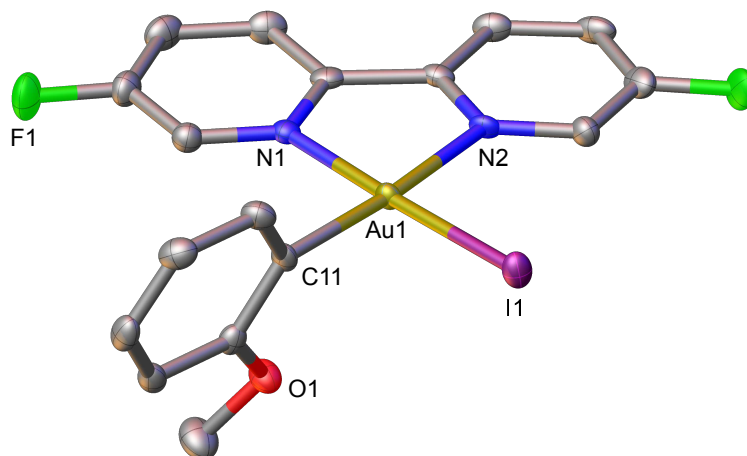


Figure 3.9: Molecular structure of **56f**, thermal ellipsoids are shown at the 50% probability level. Hydrogen atoms and the NTF₂ anion have been omitted for clarity. Selected bond lengths (Å) and angles (°): Au1–C11 2.019(3), Au1–I1 2.5373(2), Au1–N2 2.117(3), Au1–N1 2.091(3), N1–Au1–N2 78.30(10), N2–Au1–I1 99.75(7), N1–Au1–C11 95.86(12), C11–Au1–I1 86.10(9). See Section 5.5, Table 5.9 for full crystallographic details.

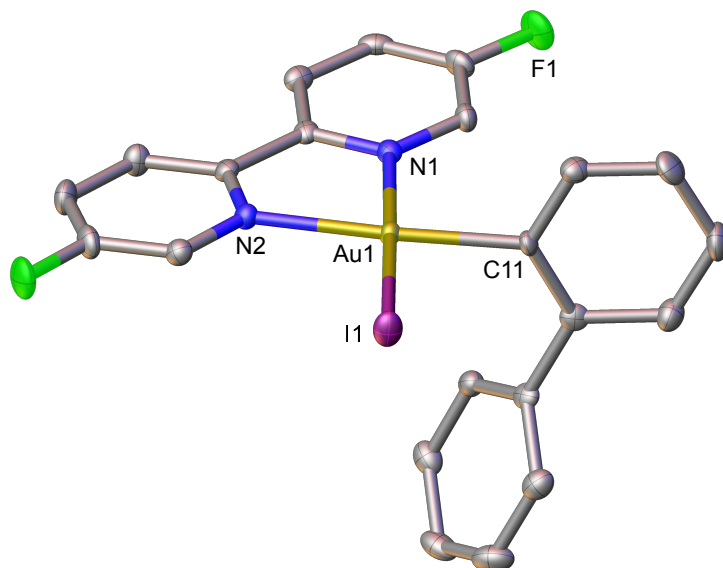


Figure 3.10: Molecular structure of **56h**, thermal ellipsoids are shown at the 50% probability level. Hydrogen atoms, a PhMe solvent molecule and the NTf₂ anion have been omitted for clarity. Selected bond lengths (Å) and angles (°): Au1-C11 2.028(3), Au1-I1 2.5455(2), Au1-N2 2.140(2), Au1-N1 2.083(2), N1-Au1-N2 78.21(9), N2-Au1-I1 100.80(6), C11-Au1-N1 94.91(10), C11-Au1-I1 86.13(8). See Section 5.5, Table 5.10 for full crystallographic details.

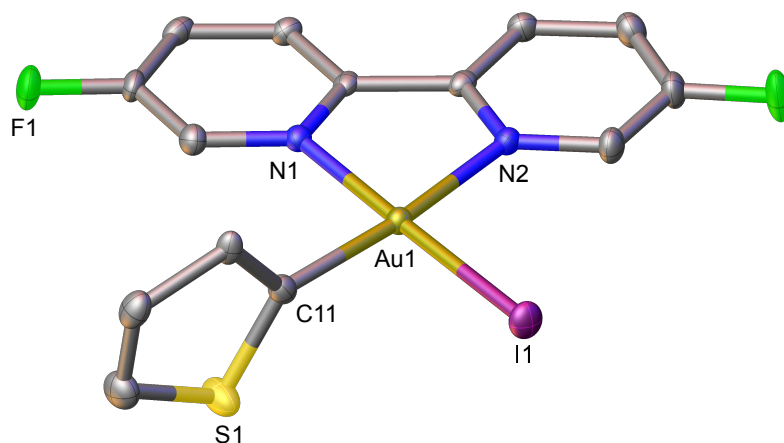
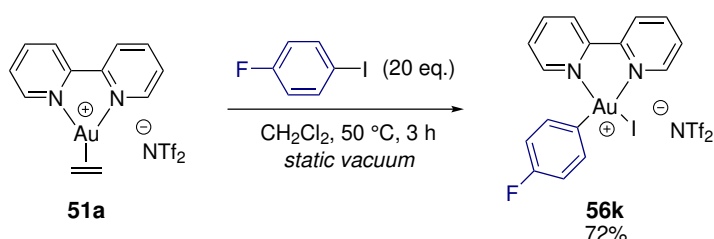


Figure 3.11: Molecular structure of **56j**, thermal ellipsoids are shown at the 50% probability level. Hydrogen atoms and the NTf₂ anion have been omitted for clarity. Selected bond lengths (Å) and angles (°): Au1-C11 1.998(3), Au1-I1 2.5530(2), Au1-N2 2.114(2), Au1-N1 2.084(2), N1-Au1-N2 78.70(9), N2-Au1-I1 100.29(6), C11-Au1-N1 93.94(10), C11-Au1-I1 87.07(8). See Section 5.5, Table 5.11 for full crystallographic details.

3.5 Oxidative Addition: 2,2'-Bipyridine System

In order to confirm that oxidative addition is not specific to the 5,5'-difluoro-substituted F₂-bipy ligand, the behaviour of the 2,2'-bipyridine-ligated complex **51a** towards aryl iodides was investigated. Pleasingly, the oxidative addition product **56k** was obtained in 72% isolated yield upon reaction of **51a** with 4-fluoriodobenzene at 50 °C for 3 h (Scheme 3.19). Thus, facile oxidative addition of aryl iodides to gold(I) is facilitated by the cheapⁱ and readily available bipy ligand.



Scheme 3.19: Oxidative addition of 4-fluoriodobenzene to **51a**. Isolated yield quoted.

Crystals of **56k** were grown from a CH₂Cl₂ solution layered with hexane; the solid-state structure is shown in Figure 3.12. Complex **56k** adopts a distorted square planar geometry, analogous to that observed for **56a**.

ⁱApproximately £0.70/g according to Sigma-Aldrich as of June 2018.

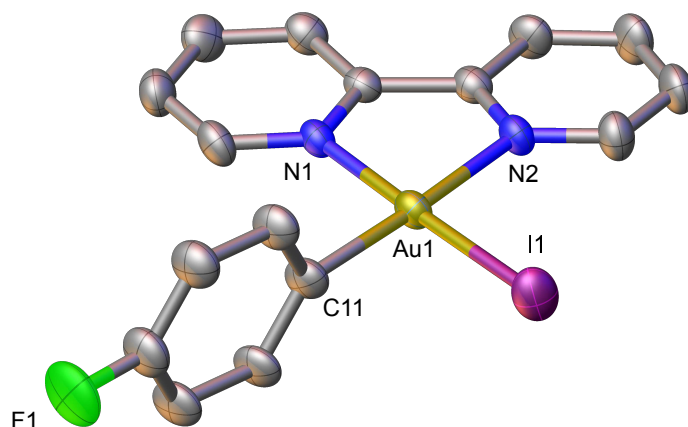
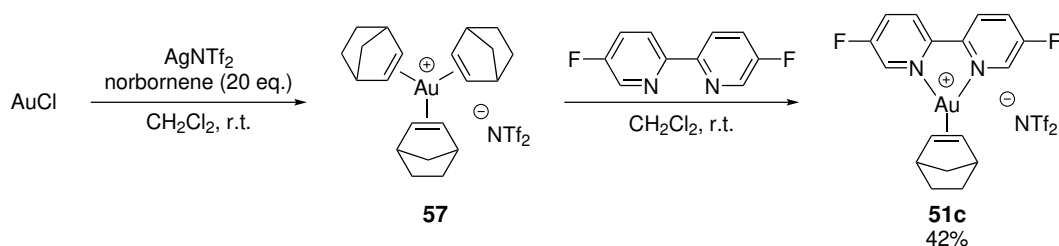


Figure 3.12: Molecular structure of **56k**, thermal ellipsoids are shown at the 30% probability level. Hydrogen atoms and the NTf₂ anion have been omitted for clarity. Selected bond lengths (Å) and angles (°): Au1–C11 2.000(4), Au1–I1 2.5420(5), Au1–N1 2.077(4), Au1–N2 2.128(4), N1–Au1–N2 78.52(14), N2–Au1–I1 99.81(11), N1–Au1–C11 96.6(5), C11–Au1–I1 85.0(5). See Section 5.5, Table 5.6 for full crystallographic details.

3.6 [(κ^2 -bipy)Au(η^2 -norbornene)][NTf₂]

The synthesis of **51a** and **51b** is challenging due to the fragility of the tris-ethylene gold(I) intermediate **50**. Homoleptic gold(I) complexes of norbornene, however, have previously been synthesised and are air- and moisture-stable.²¹⁰ Substitution of ethylene for norbornene in **51a** or **51b** would therefore simplify access to these complexes. The bipy gold(I) norbornene complex [(κ^2 -bipy)Au(η^2 -norbornene)][NTf₂] **51c** was prepared analogously to complexes **51a** and **51b** (see Scheme 3.14) by using an excess of norbornene (20 eq.) in place of ethylene (Scheme 3.20).



Scheme 3.20: Synthesis of $[(\kappa^2\text{-bipy})\text{Au}(\eta^2\text{-norbornene})][\text{NTf}_2]$ **51c** via addition of $\text{F}_2\text{-bipy}$ to $[\text{Au}(\text{norbornene})_3][\text{NTf}_2]$ **57**.

Crystals of **51c** were grown from a CH_2Cl_2 solution layered with hexane; the solid-state structureⁱ is shown in Figure 3.13. **51c** adopts a distorted trigonal planar geometry, with gold bound to the *exo* face of nbe.

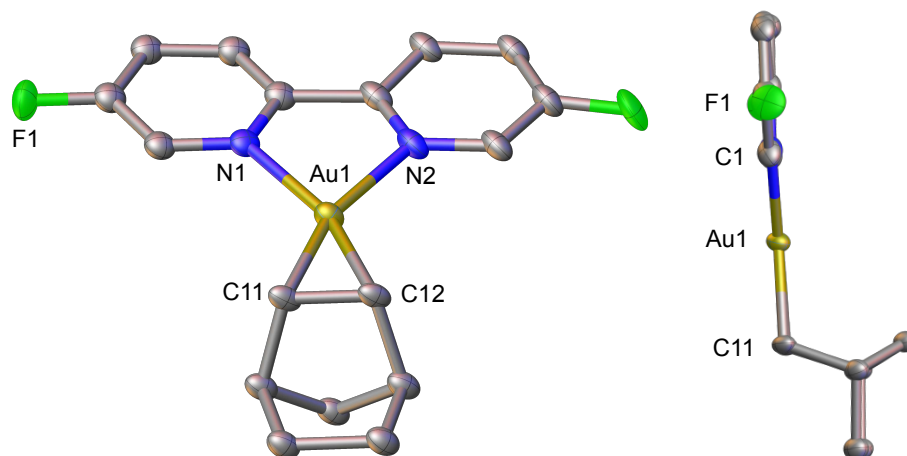
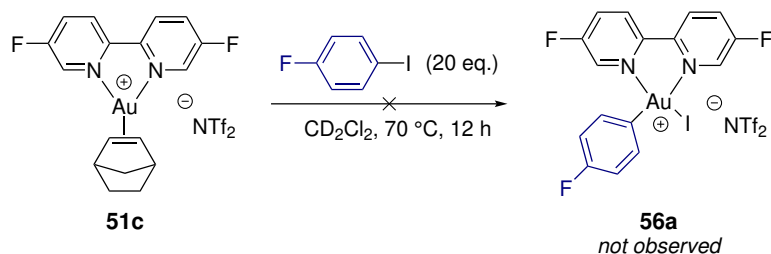


Figure 3.13: Molecular structure of **51c**, thermal ellipsoids are shown at the 50% probability level. Hydrogen atoms and the NTf_2 anion have been omitted for clarity. Selected bond lengths (\AA) and angles ($^\circ$): Au1-N1 2.189(11), Au1-N2 2.191(11), Au1-C11 2.081(12), Au1-C12 2.108(13), C11-C12 1.410(19), N1-Au1-N2 74.3(4). See Section 5.5, Table 5.12 for full crystallographic details.

Reaction of **51c** with 4-fluoriodobenzene in CD_2Cl_2 did not give any of the oxidative addition product **56a**. Even after 12 h at 70°C , only unreacted **51c** was observed via ^{19}F

ⁱCrystallographic data for **51c** were of insufficient quality for the discussion of bond metrics.

NMR spectroscopy. A plausible explanation for this lack of reactivity is that norbornene binds to gold more tightly than ethylene, and oxidative addition would require dissociation of the alkene (see Section 3.7).



Scheme 3.21: Attempted oxidative addition of 4-fluoriodobenzene to **51c**.

3.7 Oxidative Addition: Mechanism

Analysis of the relative reaction rates of oxidative addition to **51b** showed that electron rich aryl iodides react significantly faster than the electron poor counterparts (initial rate order for 4-**R**-C₆H₄I: **R** = OMe > H > CF₃; Figure 3.14). This order of reactivity is in agreement with the trend reported by Bourissou *et al.* for the process outlined in Table 3.2,¹⁹⁵ and contrasts to the reactivity of palladium(0) towards aryl iodides, where electron poor substrates have been shown to react faster.²¹⁶ Interestingly, calculations performed by Maseras and Echavarren suggest electron-deficient aryl halides should undergo faster oxidative addition to gold(I).¹⁷⁵ These results, however, were regarding a theoretical system for which there was no corresponding experimental evidence of oxidative addition.

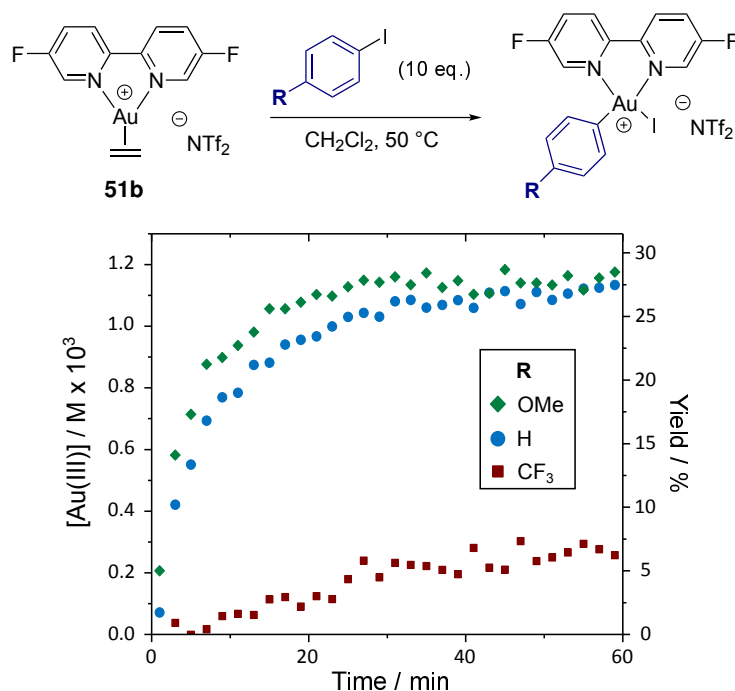


Figure 3.14: Reaction profiles for the oxidative addition of *para*-substituted aryl iodides to **51b**. Reactions monitored by ^{19}F NMR spectroscopy.

Although the relative rate order for electron rich *vs* electron poor aryl iodides is in agreement with the results reported by Bourissou *et al.*,¹⁹⁵ the reversibility of the oxidative addition to **51b** is in stark contrast. In order to investigate this further, the potential energy surface was computed using Density Functional Theory (DFT) (Figure 3.15).ⁱ Starting from the ethylene complex **51a**, the first step is an endothermic ($\Delta E = +16.2$ - 17.7 kcal/mol) substitution of ethylene by the aryl iodide to form an η^2 -arene complex; such η^2 -arene complexes of gold(I) are well known in the literature.²¹⁷⁻²²¹ From the η^2 -arene complex, oxidative addition is exothermic ($\Delta E = -12.0$ - 13.2 kcal/mol) with a barrier of $+9.5$ - 10.0 kcal/mol, proceeding *via* a transition state involving partial dissociation of bipy to the unsymmetrical κ^1 binding mode. The ability of bipy to partially dissociate presumably lowers the energy barrier by allowing gold(I) to maintain partial linear character throughout the transition state. The overall oxidative addition process is marginally en-

ⁱCalculations were performed by Prof. John E. McGrady at the University of Oxford.

dothemic ($\Delta E = +4.2\text{--}4.5$ kcal/mol). This observation, alongside the surmountable barrier for the reverse step, is consistent with the experimental evidence for an equilibrium. In contrast, the overall energy for Bourissou's oxidative addition is exothermic ($\Delta E = -12.9$ kcal/mol), which is in agreement with the observed irreversibility of their process.¹⁹⁵

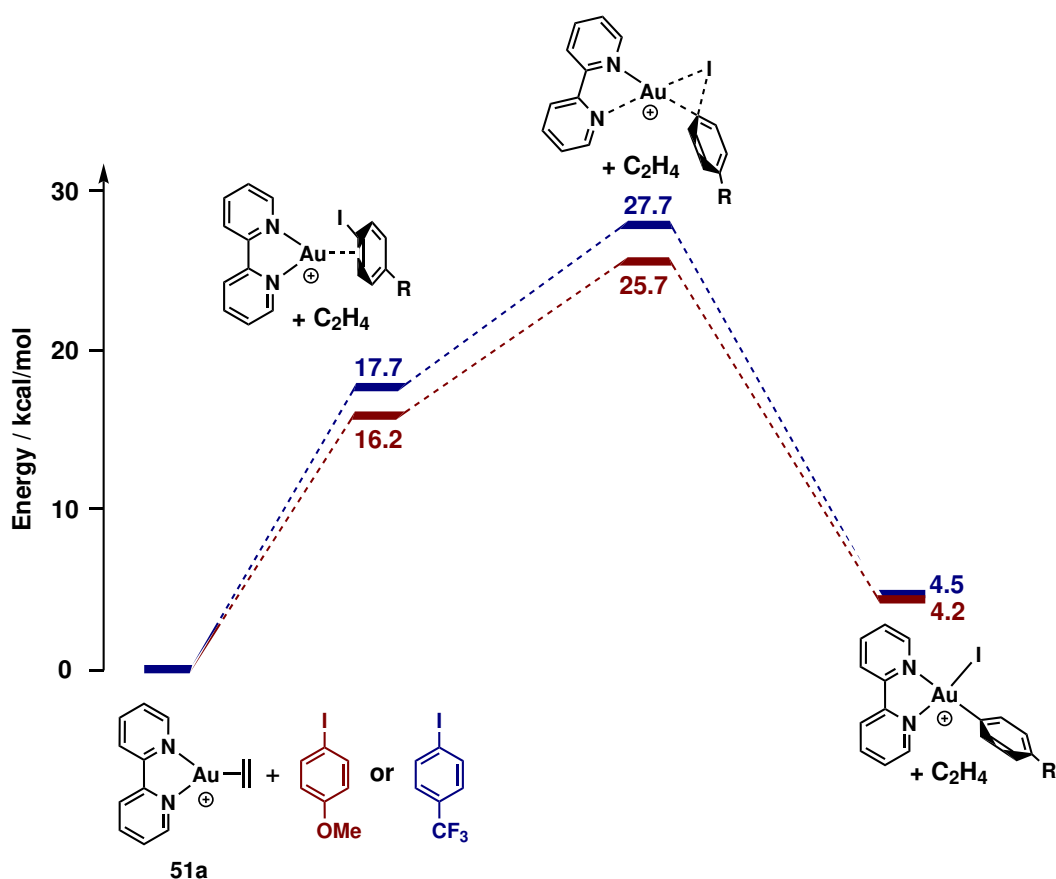


Figure 3.15: Computed potential energy surface for the oxidative addition. Calculations performed using the ω B97-XD functional, a def2-TZVP basis with associated 60-electron pseudopotential on Au, def2-SVP with associated 28-electron pseudopotential on I, def2-SVP on C/N and def2-SV on H/O/F. The effects of solvent were incorporated using the SMD solvation model (CH_2Cl_2 solvent). Energies shown include zero-point corrections. Calculations performed by Prof. John E. McGrady, University of Oxford.

The rate of oxidative addition of *para*-substituted aryl iodides to palladium(0) increases with the electron-withdrawing capabilities of the substituent.^{216,222–225} Theories to explain this include:

1) Electron-withdrawing substituents more efficiently stabilise a developing negative charge delocalised into the aromatic system in a three-centered transition state (Figure 3.16, A);^{216,225}

2) Electron withdrawing groups (either through inductive or resonative effects) can polarise the C-I bond resulting in a more electrophilic centre (or a more *oxidising* centre) (Figure 3.16, B), conversely, electron-donating groups will result in a more nucleophilic centre (a more *reducing* centre).²²²

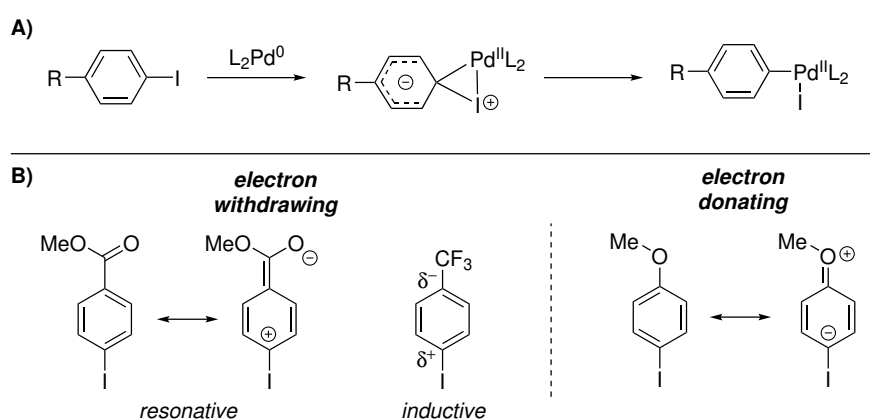


Figure 3.16: Delocalisation of negative charge during aryl iodide oxidative addition to palladium(0) (A) and electronic properties of aryl iodides bearing electron-withdrawing or -donating substituents (B).

With the available data, the inverse order of reactivity for the oxidative addition of aryl iodides to **51b** (*vs* palladium(0)) can be rationalised by examining the computed potential energy surface (Figure 3.15). The lower barrier calculated for the displacement of ethylene by an electron-rich aryl iodide (+16.2 kcal/mol for *p*-OMe *vs* +17.7 kcal/mol for *p*-CF₃) can be attributed simply to the greater coordinating ability of the more electron-rich arene. From the η²-arene complex, the barrier for oxidative addition of the electron-rich aryl iodide only is marginally lower (+9.5 kcal/mol for *p*-OMe *vs* +10.0 kcal/mol for *p*-CF₃) than that for the electron-poor system. However, examination of the transition states in more detail (Figure 3.17) reveals a significantly shorter Au-C_{ipso} bond distance

for the electron-rich system (2.16 Å vs 2.23 Å), suggesting a stronger aryl gold interaction for the electron-rich system. Overall, although the energetic differences for the two aryl iodides (*p*-OMe vs *p*-CF₃) are undeniably small, the calculated trend is consistent with the experimentally determined rates.

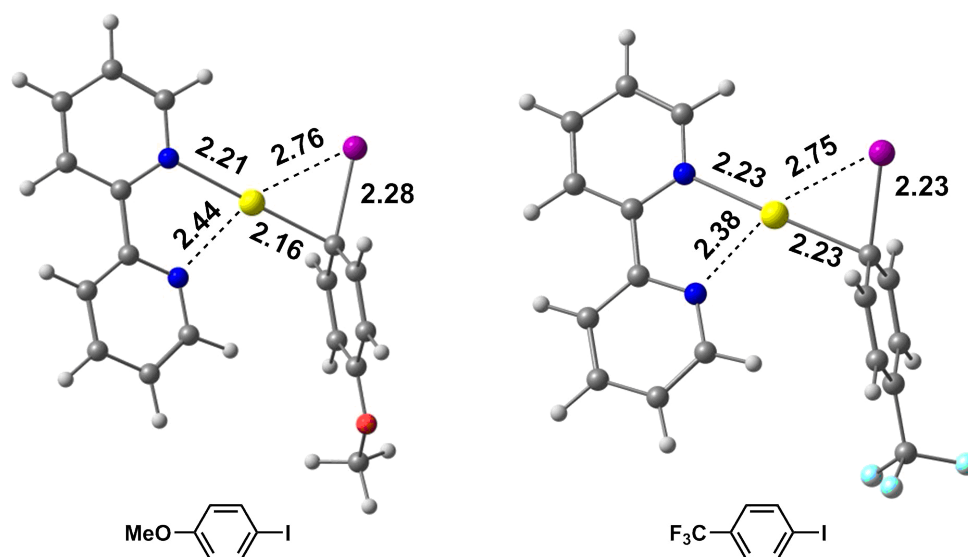


Figure 3.17: Computed transition states for the oxidative addition of *p*-MeO-iodobenzene (L) and *p*-CF₃-iodobenzene (R). Calculations performed using the ω B97-XD functional, a def2-TZVP basis with associated 60-electron pseudopotential on Au, def2-SVP with associated 28-electron pseudopotential on I, def2-SVP on C/N and def2-SV on H/O/F. The effects of solvent were incorporated using the SMD solvation model (CH₂Cl₂ solvent). Distances shown are in Å. Calculations performed by Prof. John E. McGrady, University of Oxford.

3.8 Transmetalation

The general mechanism of a classical transition-metal-catalysed biaryl cross-coupling consists of, in the following order: oxidative addition, transmetalation, and reductive elimination. With facile oxidative addition to **51b** established and with ample quantities of the aryl gold(III) iodide **56a** to hand, investigations commenced into the transmetalation of **56a** with organometallic aryl nucleophiles. To that end, CH₂Cl₂ solutions of **56a**

were exposed to a variety of 4-tolyl-substituted organometallic reagents and the temperature was raised until reactivity was observed (Table 3.6).

Aryl boronic acid, boronic acid pinacol ester, and trimethylsilane-based nucleophiles showed very little reactivity (Table 3.6, entries 1–3), and only reductive elimination to release 4-fluoroiodobenzene was observed (26–39% yield). $\text{Li}[4\text{-tolylB}(\text{pin})(t\text{-Bu})]^{\dagger}$ resulted in complete and rapid consumption of **56a**, and promisingly, 3% of the desired heterocoupled product **58** was formed (Table 3.6, entry 4). In this case, homocoupling predominated to generate 4,4'-difluorobiphenyl **59** in 36% yield. Nevertheless, the detection of **58**, albeit in low yield, prompted the investigation of other classes of organometallic reagents to favour the formation of the **58**. 4-Tollylithium did not give any of the desired product (Table 3.6, entry 6), but switching to 4-tolylMgBr gave **58** in 24% yield (Table 3.6, entry 5). Improvements were observed using 4-tolyl-Sn(*n*-Bu)₃ and -SnMe₃ to form **58** in 51% and 61% yield, respectively (Table 3.6, entries 7 and 8). Of all the organometallic reagents screened, 4-tolylZnCl provided the best reactivity and gave **58** in 72% yield, alongside 5% of **59** and 18% of 4-fluoroiodobenzene (Table 3.6, entry 9). Although the formation of 4-fluoroiodobenzene in 18% yield suggests reaction inefficiency, the consequences of regenerating the aryl iodide under catalytic conditions would be minor.

Overall, these results demonstrate the feasibility of C(sp²)-C(sp²) bond formation in the absence of an external oxidant, and they provide the first example of a Negishi cross-coupling at gold, albeit under stoichiometric conditions.

[†]Li[4-tolylB(pin)(*t*-Bu)] was kindly donated by Dr. Harry O'Brien, University of Bristol.²²⁶

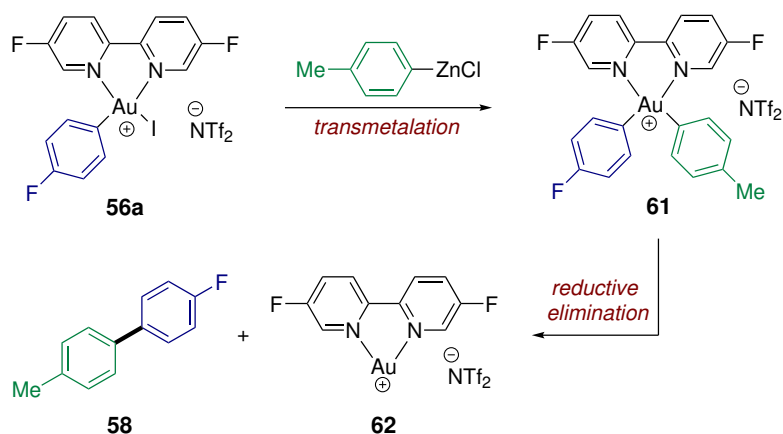
Table 3.6: Reaction of **56a** with organometallic nucleophiles.^a

Entry	[M]	T (°C)	56a (%)	58 (%)	59 (%)	ArI (%)
1	B(OH) ₂	60	53	0	0	26
2	Bpin	50	55	0	0	39
3	SiMe ₃	r.t.	58	0	0	30
4	[B(pin)(<i>t</i> -Bu)]Li	-78 to r.t.	0	3	36	4
5	MgBr	-78 to r.t.	0	24	21	0
6	Li	-78 to r.t.	0	0	0	35
7	Sn(<i>n</i> -Bu) ₃	-78 to r.t.	0	51	9	11
8	SnMe ₃	-78 to r.t.	0	61	0	7
9	ZnCl	-78 to r.t.	0	72	5	18

^aYields determined by ¹⁹F NMR spectroscopy.

3.9 Negishi Coupling Mechanism

For the gold-mediated Negishi cross-coupling process outlined in Table 3.6, entry 9, the most probable pathway involves transmetalation of the arylzinc reagent with **60** to give the bis-aryl gold(III) intermediate **61**, followed by reductive elimination to form **58** and the gold(I) complex **62** (Scheme 3.22).



Scheme 3.22: Probable pathway for the formation of **58** from **56a** and 4-tolylZnCl.

In order to confirm the pathway shown in Scheme 3.22, the reaction of **56a** with 4-tolylZnCl was monitored by variable-temperature ^{19}F NMR spectroscopy (Figure 3.18). A THF solution of 4-tolylZnCl (1 equivalent w.r.t **56a**) was added to a CD_2Cl_2 solution of **56a** at $-78\text{ }^\circ\text{C}$, which was accompanied by a colour change from yellow to orange. The sample temperature was maintained at $-78\text{ }^\circ\text{C}$ then rapidly transferred into a NMR spectrometer in which the probe had been pre-cooled to $-80\text{ }^\circ\text{C}$. Analysis by ^{19}F NMR spectroscopy at $-80\text{ }^\circ\text{C}$ revealed complete consumption of **56a** and the appearance of two new broad resonances, consistent with the formation of bis-aryl gold(III) **61** (Figure 3.18). This species was stable up to approximately $-40\text{ }^\circ\text{C}$, at which point it decomposed rapidly to form **58** and a small amount of 4,4'-difluorobiphenyl **59**.

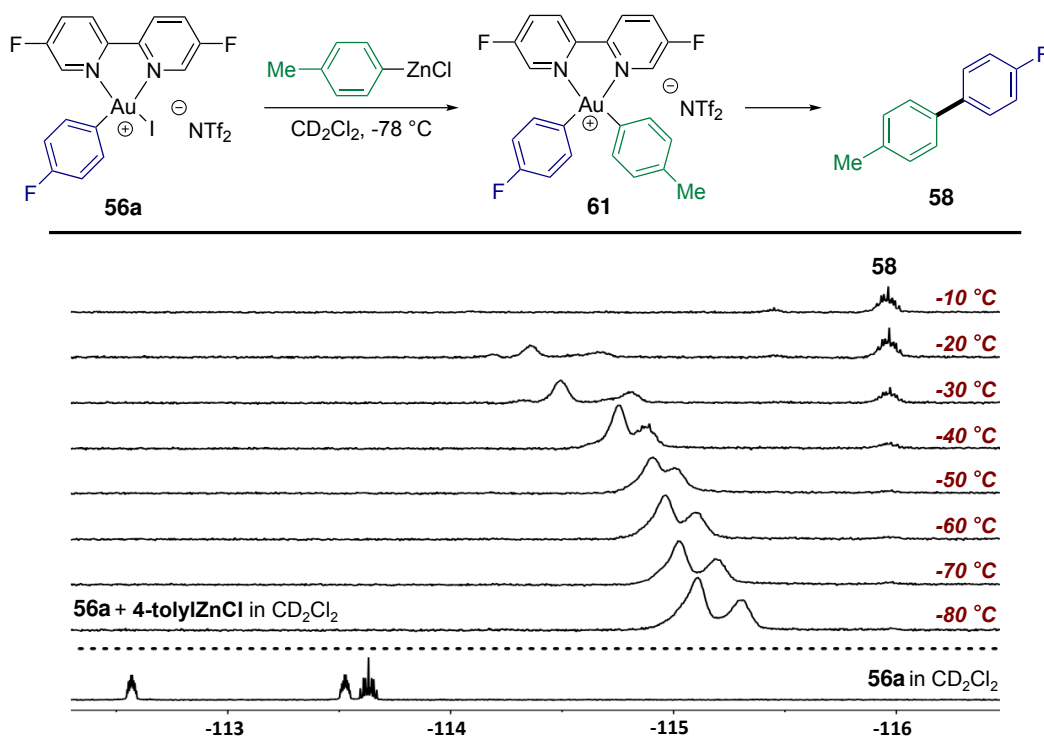


Figure 3.18: Reaction of **60** with 4-tolylZnCl monitored by variable-temperature ^{19}F NMR spectroscopy.

To confirm further the intermediacy of **61**, aliquots of the reaction mixture were analysed by ESI-HRMS (Figure 3.19). In order to prevent **61** from undergoing reductive elimination prior to detection by the mass spectrometer, the following steps were taken:

- 1) The reaction was conducted at the low concentration required (0.01 mg/mL) for ESI-MS, such that no further dilution was required.
- 2) The reaction was transported to the mass spectrometry laboratory in the original reaction flask whilst maintaining an inert atmosphere and cryogenic temperature.
- 3) The syringe and sample lines were pre-cooled by flushing with cold (-78°C) anhydrous CH_2Cl_2 immediately prior to injection.
- 4) Within the spectrometer, a reduced source voltage of 3 kV, a reduced source tempera-

ture of 45 °C and a reduced capillary temperature of 100 °C were used to minimise sample degradation.

To our delight, an ion was observed with m/z 575.0987, which agrees with the calculated m/z for the cation of **61** (575.1004). Furthermore, tandem mass spectrometryⁱ showed that this ion fragments to a new ion with m/z 389.0140, which corresponds to the calculated m/z for the cation of **62** (m/z 389.0159). These data amount to the direct observation of reductive elimination from **61** to give **62** and **58**.ⁱⁱ

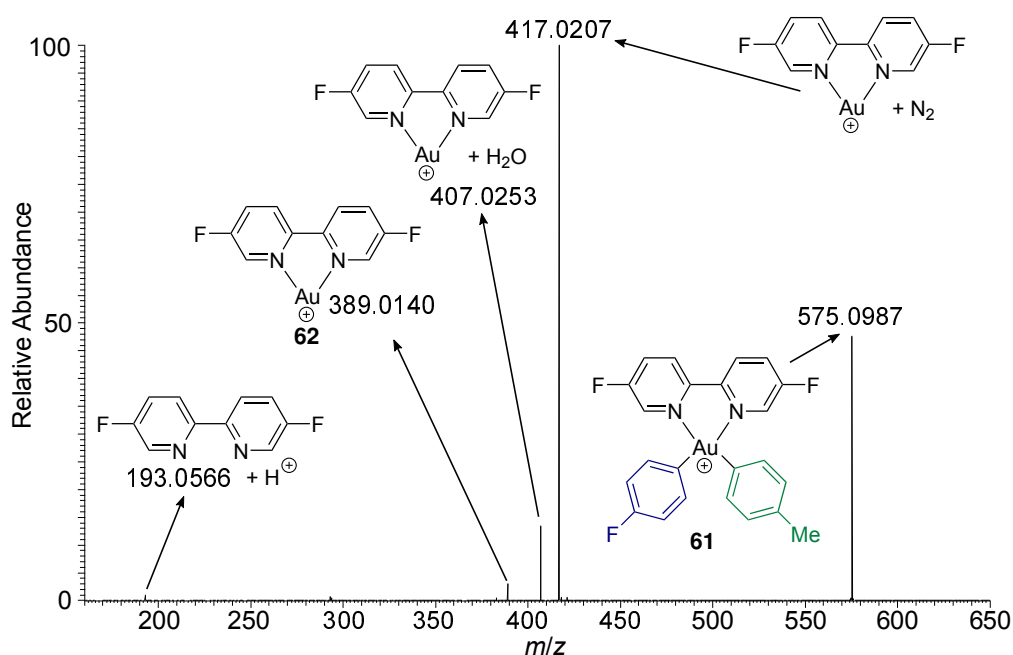


Figure 3.19: Tandem mass spectra for the reaction between 4-tolylZnCl and **56a**, isolated precursor ion m/z 575.

Additional ions of interest observed from the fragmentation of **61** include [F₂-bipy+H]⁺ at m/z 193.0566 (calculated m/z 193.0572), [62+H₂O]⁺ at m/z 407.0253 (calculated m/z 407.0265), and interestingly, [62+N₂]⁺ at m/z 417.0207 (calculated m/z 417.0221).

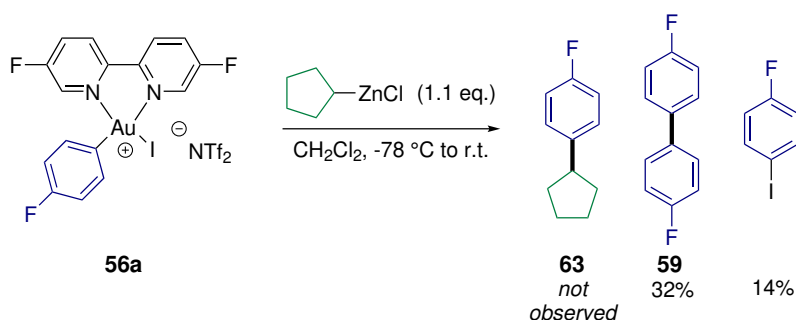
ⁱTandem mass spectra were recorded in the collision induced dissociation mode using N₂ collision gas at 20 eV on the isolated precursor ions (+/- 1 m/z isolation width). Mass spectrometry were performed with the assistance of Dr John Crosby, Dr Chris Arthur, and Dr Paul Gates.

ⁱⁱAnalogous results were obtained when this experiment was repeated using an alternative arylZnCl reagent. See Chapter 5, Section 5.3.5 for more details.

With respect to the observation $[62+N_2]^+$, this represents, to the best of our knowledge, the first example of a mono-metallic gold complex of dinitrogen. The closest existing example being the isolation of dinitrogen-bridged gold clusters by Sharp *et al.* in 1997.²²⁷ Although the gas-phase detection of $[62+N_2]^+$ under mass spectrometric conditions is exciting, we were unable to isolate it or gather any additional characterisation data. Thus, no conclusions can be drawn as to the nature and bonding of this proposed $[62+N_2]^+$ cation.²²⁸

3.10 Transmetalation of a C(sp³) Reagent

Given the known reluctance of gold complexes to undergo β -hydride elimination (which limits the use of sp³ coupling reagents in palladium-catalysed chemistry),^{229–231} the results described in this chapter hint towards the possibility of C(sp²)-C(sp³) cross-coupling. To test this hypothesis, a THF solution of cyclopentylZnCl was reacted with **56a** at -78 °C (Scheme 3.23). At low temperature the solution remained yellow and homogeneous then upon warming to r.t. a black suspension was obtained. Unfortunately, the desired cross-coupled product **63** was not observed *via* GC-MS or ¹⁹F NMR spectroscopy, only the formation of **59** and 4-fluoriodobenzene were detected.



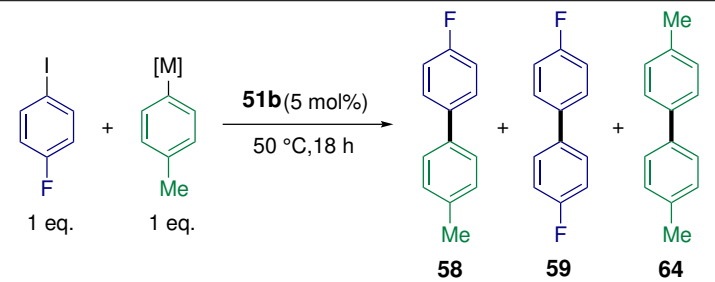
Scheme 3.23: Reaction of **56a** with cyclopentylZnCl. Yields determined by ¹⁹F NMR spectroscopy.

3.11 Investigations Toward Catalysis

Demonstrated in this chapter thus far has been the oxidative addition of aryl iodides to bipy gold(I) ethylene **51b**, transmetalation of the resulting aryl gold(III) **56a** with arylZnCl reagents to give bis-aryl gold(III) **61**, and subsequent reductive elimination to the cross-coupled product **58**. These steps amount to a *stoichiometric* Negishi cross-coupling; obviously progression to a catalytic protocol would be advantageous. This section will disclose investigations into the feasibility of catalytic biaryl cross-coupling using bipy-ligated gold species.

As shown in Section 3.8, Table 3.6, the most efficient transmetalation to **56a** was achieved using 4-tolylZnCl, therefore catalytic experiments commenced using this reagent. Unfortunately, reaction of 4-fluoriodobenzene and 4-tolylZnCl with 5 mol% **51b** in a range of solvents produced at most only 1% yield of the desired product **58** (Table 3.7, entries 1–5). In these cases, homocoupling of the aryl zinc reagent predominated to give **64** in 5–34% yield. In a control experiment, addition of 4-tolylZnCl to a CH₂Cl₂ solution of **51b** at r.t. resulted in the immediate decompositionⁱ of **51b** to an insoluble black precipitate. Accordingly, the aryl zinc reagent appears incompatible with **51b**. This is illustrated by the large disparity in temperature required for oxidative addition (50 °C) vs transmetalation (operating at -80 °C) (see Section 3.3 and Section 3.8, respectively). Less reactive transmetalating reagents were investigated next, however, the use of aryl-boronic acid, -boronic acid pinacol ester, and -SiMe₃ reagents did not lead to any improvement, even with addition of commonly used basic additives (Table 3.7, entries 6–14).

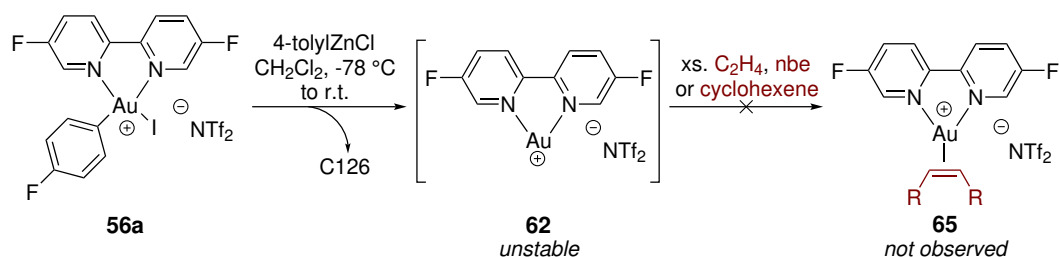
ⁱAnalysis of the mixture did not reveal any resonances in the Ar-F region of the ¹⁹F NMR spectrum, indicating that decomposition of **51b** facilitates the removal of F₂-bipy from solution.

Table 3.7: Attempted biaryl cross-couplings, catalysed by **51b**.^a


Entry	[M]	solvent	58 (%)	59 (%)	64 (%)	Additives
1	ZnCl	CH ₂ Cl ₂	<1	0	8	-
2	ZnCl	MeCN	<1	0	5	-
3	ZnCl	CHCl ₃	1	0	34	-
4	ZnCl	THF	1	0	8	-
5	ZnCl	Et ₂ O	<1	0	5	-
6 ^{b,c}	B(OH) ₂	CH ₂ Cl ₂	<1	0	52	-
7 ^{b,c}	SiMe ₃	CH ₂ Cl ₂	trace	<1	0	-
8 ^{b,c}	Bpin	CH ₂ Cl ₂	<1	trace	68	-
9 ^{b,c}	B(OH) ₂	CH ₂ Cl ₂	trace	0	0	Cs ₂ CO ₃ (2 eq.)
10 ^{b,c}	B(OH) ₂	CH ₂ Cl ₂	trace	2	0	LiOH (2 eq.)
11 ^d	B(OH) ₂	PhMe	<1	3	0	K ₃ PO ₄ (2 eq.)
12 ^e	B(OH) ₂	CH ₂ Cl ₂	<1	3	0	K ₂ CO ₃ (2 eq.)
13 ^d	B(OH) ₂	PhMe	<1	4	0	K ₂ CO ₃ (2 eq.)
14 ^e	B(OH) ₂	CHCl ₂	trace	4	0	LiOH (10 eq.)

^aYields determined by GC-FID using dodecane as internal standard. ^b60 °C. ^c2 equivalents of 4-fluoroiodobenzene. ^d110 °C. ^e80 °C.

A potential explanation for the poor results achieved in Table 3.7 is that in the absence of a stabilising ligand such as ethylene, decomposition of the [(F₂-bipy)Au]⁺ cation **62** is much faster than reoxidation to **56a**. It was expected that addition of ethylene should stabilise **62** by reforming **51b**. However, transmetalation in the presence of a large excess of alkene (ethylene, norbornene or cyclohexene) did not produce any of the expected bipy gold(I) alkene complexes **65** (Scheme 3.24).



Scheme 3.24: Transmetalation of **56a** with 4-tolylZnCl in the presence of excess ethylene, norbornene (nbe), or cyclohexene.

3.12 Conclusion

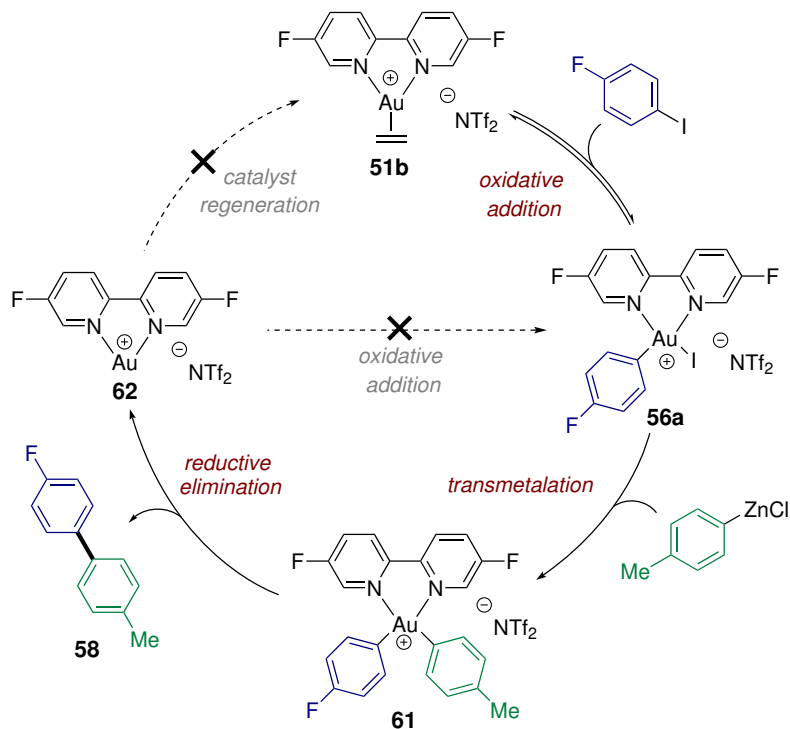
In summary (Scheme 3.25), the bipy gold(I) ethylene complex **51b** undergoes facile and reversible oxidative addition of aryl iodides. The resulting aryl gold(III) complex **56a** undergoes transmetalation with aryl zinc reagents to the bis aryl gold(III) complex **61**. Subsequent reductive elimination to form biaryl **58** provides the first example of a gold-mediated Negishi cross-coupling. Thus, elementary steps that are typical of palladium-catalysed biaryl formations have now been demonstrated from a simple mono-metallic gold centre in the absence of directing groups. The chemistry is switched on by the simple bipyridyl ligand framework, which enhances π -backdonation from gold to facilitate the key aryl iodide oxidative addition step.

In contrast to the reactivity of palladium, but in line with previous oxidative additions with gold,¹⁹⁵ electron-rich aryl iodides were found to undergo oxidative addition faster than the electron-poor counterparts.

The bis aryl gold(III) intermediate **61** was identified and characterised by ESI-HRMS and ¹⁹F NMR spectroscopy, and reductive elimination to form the cation of **62** was observed *via* tandem mass spectrometry.

Unfortunately, attempts to render the overall three-step oxidative addition, transmetala-

tion, reductive elimination process catalytic were unsuccessful. This is attributed to the instability of the bipy gold(I) cation **62**.



Scheme 3.25: Oxidative addition, transmetalation, and reductive elimination from a bipy-ligated gold centre.

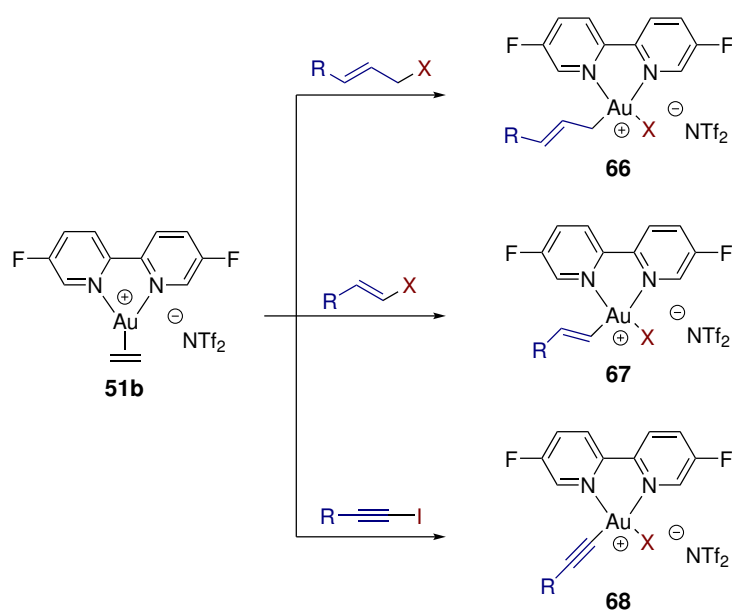
3.13 Future Work

3.13.1 Catalysis

Following the results described in this chapter, the most immediate task is to develop a catalytic protocol. As discussed in Section 3.1.1, the lack of catalytic turnover is attributed to the relative instability of the [(F₂-bipy)Au]⁺ cation **62**. Investigations towards addressing this problem *via* ligand design will be discussed in Chapter 4.

3.13.2 Oxidative Addition Scope

Section 3.4 described the oxidative addition of only aryl-iodides to **51b**; extension of this protocol to other aryl-X (X = Br, Cl, or OTf) or alkyl-X (X = I) bonds was unsuccessful. The reactivity of alternative C-X bonds such as vinyl-, allyl-, or alkynyl-X (X = Br, Cl, or OTf) were not evaluated. Access to complexes of the type **66**, **67**, and **68** (Scheme 3.26) should be investigated, and would broaden the scope of potential gold-catalysed cross-couplings.



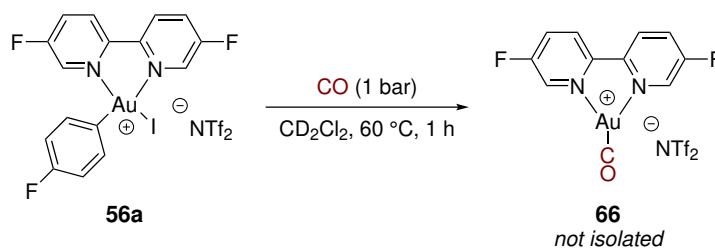
Scheme 3.26: Potential oxidative addition of vinyl- and allyl, or alkynyl-X (X = Br, Cl, or OTf) to **51b**.

3.13.3 Bipy Gold(I) Carbonyl

As discussed in Section 3.1.1, the amount of π -backdonation exhibited by gold(I) is enhanced by small bite-angle, bidentate ligands. A common method to quantify the degree of π -backdonation that a metal complex exhibits is to measure the CO stretching frequency of the corresponding L_nM -CO complex. In order to assess the degree to which bipy increases π -backdonation, it would be appealing to synthesise a bipy gold(I)

carbonyl, analogous to complex **47** prepared by Bourissou *et al.* (see Section 3.1.1, Scheme 3.11).

Pressurising a solution of aryl gold(III) **56a** with ethylene results in reductive elimination of the aryl iodide with concurrent ethylene coordination to form the ethylene complex **51b** (see Section 3.3, Scheme 3.18). To ascertain if this method would extend to CO, a solution of **56a** was pressurised with CO in an attempt to produce $[(\kappa^2\text{-F}_2\text{-bipy})\text{Au}(\text{CO})][\text{NTf}_2]$ **66** (Scheme 3.27). Interestingly, after 1 h at 60 °C the yellow colour of **56a** had faded almost to colourless, indicative of reduction to gold(I). Inspection of the ^{19}F NMR spectrum revealed approximately 70% consumption of **56a** and the presence of a new broad signal at $\delta = -177.7$ ppm. Furthermore, the ^1H NMR spectrum revealed a new set of F₂-bipy signals ($\delta = 8.78, 8.46, \text{ and } 8.04$ ppm) that did not correspond to either **56a** or free F₂-bipy. The aforementioned ^{19}F and ^1H NMR signals are *tentatively* assigned to the gold(I) carbonyl complex **66**.ⁱ In support of this, analysis of the reaction mixture by ESI-HRMS showed an ion with m/z 417.0117, which agrees with the calculated mass m/z for the cation $[(\text{F}_2\text{-bipy})\text{Au}(\text{CO})]^+$ (417.0108). Unfortunately, attempts to isolate **66** were unsuccessful, prohibiting the collection of further characterisation data such as IR. However, we believe that these preliminary results hint towards the feasibility of isolating a complex similar to **66**, and is worth pursuing further.



Scheme 3.27: Attempted synthesis of $[(\kappa^2\text{-F}_2\text{-bipy})\text{Au}(\text{CO})][\text{NTf}_2]$ **66** via reaction of **56a** with CO.

ⁱThe CO carbon signal of **66** could not be identified by ^{13}C NMR spectroscopy, even when ^{13}C labelled CO was used. Only a very broad signal was observed in the carbonyl region of the ^{13}C NMR spectrum, due to the large excess of ^{13}CO present.

Chapter 4

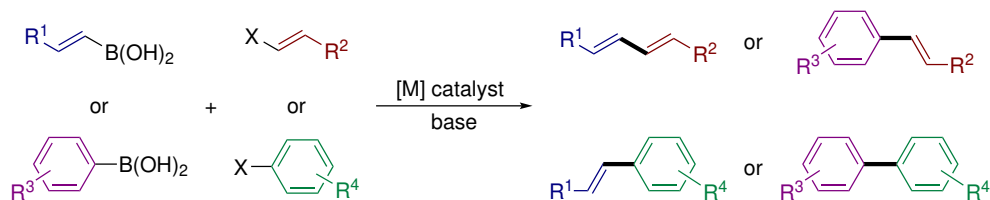
P,N-Ligands for Gold Catalysis

Abstract

A range of 8-quinolyl phosphine (8-QP) ligands with varying steric and electronic properties were synthesised and coordinated to gold(I). The resulting complexes were found to catalyse the Suzuki biaryl cross-coupling between 4-fluoriodobenzene and 4-tolylboronic acid. Optimum activity was achieved using an electron-withdrawing 8-QP ligand, giving the target product in 28% yield. Of particular note is that the reaction proceeds in the absence of an external base, in contrast to standard palladium-catalysed Suzuki conditions. The results described herein represent progress towards the development of a gold-catalysed Suzuki cross-coupling, however, further optimisation is required to achieve an attractive methodology.

4.1 Suzuki Coupling

The Suzuki reaction (also referred to as the Suzuki-Miyaura reaction) is the second most commonly used reaction in production level medicinal chemistry, second only to amide bond formation.^{232,233} It is the coupling of either aryl- or vinyl-boron reagents with aryl- or vinyl-electrophiles (Scheme 4.1).^{172,234,235} Suzuki couplings generally proceed under mild conditions, however, a base additive is required in order to activate the boron reagent towards transmetalation. The reaction is most commonly catalysed by palladium, although the more earth abundant nickel is also active.²³⁶ In addition, Suzuki biaryl cross-couplings catalysed by cobalt^{237,238} and iron²²⁶ have recently been reported, however, the latter requires the use of highly reactive *tert*-butyllithium-activated boronic esters. The general mechanism involves oxidative addition of the aryl- or vinyl-electrophile, transmetalation with the aryl- or vinyl-boron reagent, and reductive elimination to furnish the cross coupled product (see Chapter 3, Scheme 3.1).



Scheme 4.1: Generic Suzuki cross-coupling, scheme adapted from ref. 172.

4.2 Suzuki Coupling Catalysed by Gold

In 2006 and 2007, Corma *et al.* reported that Schiff base-supported trinuclear gold(I) complexes such as **69** and **70** (Figure 4.1) could catalyse the Suzuki and Sonogashira cross-couplings between aryl iodides and aryl boronic acids or terminal alkynes, respectively.^{239,240}

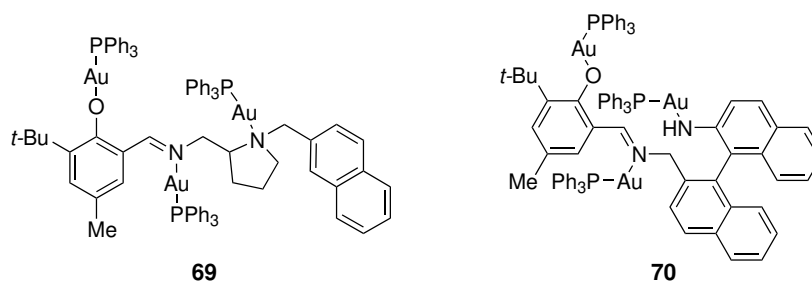


Figure 4.1: Schiff base-supported trinuclear gold(I) complexes **69** and **70** that reportedly catalysed Suzuki and Sonogoshira cross-couplings.^{239,240}

An implied suggestion of Corma's gold-catalysed Suzuki and Sonogashira cross-couplings is that gold(I) can undergo oxidative addition to aryl iodides; this sparked a lively debate in the literature. Echavarren *et al.* claimed that gold(I) was unable to undergo oxidative addition and that catalytic activity was instead due to trace palladium contamination. Furthermore, attempts to prepare complexes **69** and **70** by Echavarren *et al.* produced only mixtures of products,ⁱ leading to the assertion that the structures reported by Corma *et al.* were incorrectly characterised.²⁴¹

Corma *et al.* then countered stating that although the Sonogashira coupling may not be catalysed by a molecular gold species, Au₃₈ clusters formed *in situ* were responsible for activity.²⁴² Calculations found that the barrier for oxidative addition of iodobenzene to Au₃₈ was surmountable; 11.3 kcal/mol for Au₃₈ vs 31.6 kcal/mol for Me₃PAuI (Figure 4.2). O'Hair *et al.* further substantiated the propensity of gold clusters to undergo oxidative addition using combined mass-spectrometry and DFT studies.²²¹

ⁱThese mixtures of gold(I) products were found by Echavarren *et al.* to be inactive for the Suzuki and Sonogashira couplings reported by Corma *et al.*

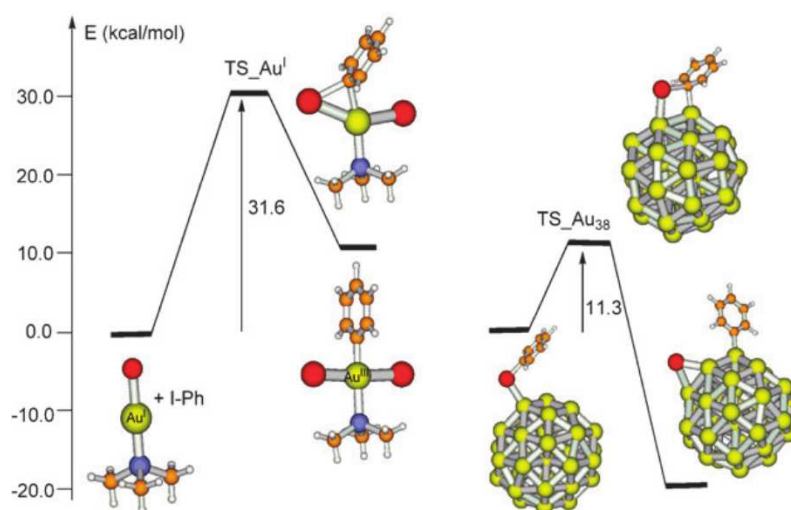


Figure 4.2: Calculated reaction profiles for the oxidative addition of iodobenzene to Me₃PAuI (left) and Au₃₈ clusters (right). Atom colours: Au (yellow), C (orange), H (white), I (red), P (purple). Reproduced from Ref. 242 with permission from The Royal Society of Chemistry.

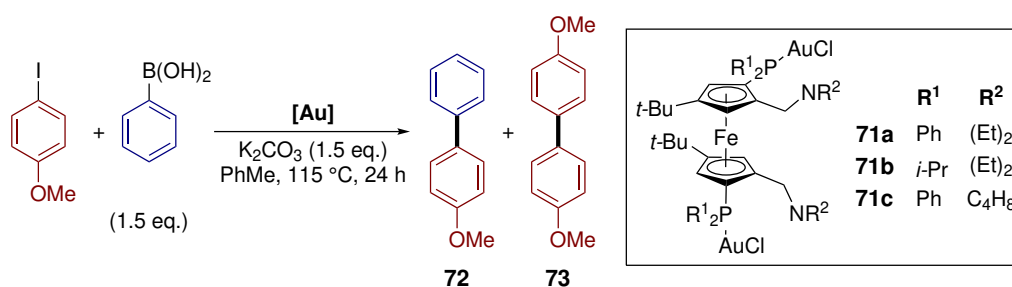
A further gold-catalysed Suzuki biaryl coupling was reported in 2017 by Hierso *et al.* using *N,N'*-diamino-*P,P'*-diphosphino ferrocene ligands (Table 4.1).²⁴³ Cross-coupling of 4-iodoanisole with phenylboronic acid to give biaryl **72** was achieved using the dinuclear complex **71b** as precatalyst. However, given the scrutiny and criticism that Corma's^{239,240} Suzuki and Sonogashira couplings attracted, there are some irregularities in this work that must be discussed.

Although a control experiment omitting gold did not give any product (Table 4.1, entry 1), it was intriguing that the use of 6 mol% AuCl or Me₂SAuCl produced **72** in 10% and 11% yields, respectively (Table 4.1, entries 2 and 3). That these extremely common gold sources are reported to catalyse a Suzuki coupling is surprising. The fact that this reactivity has not been previously reported by the many groups researching redox gold catalysis suggests, in the author's opinion, that perhaps adventitious palladium might be responsible for catalysis. Alternatively, gold nanoparticles, a likely consequence of heating AuCl

or Me_2SAuCl to 115 °C in the absence of an ancillary ligand, might be responsible for activity.

The authors claim that the use of "molecularly well-defined gold metal catalysts in pure form is a *guarantee* of the absence of other metal contaminants".²⁴³ However, previous reports of palladium-free Suzuki couplings were found to be catalysed by trace palladium present in the inorganic base.²⁴⁴ Interestingly, complex **71b** possesses a hemilabile amine donor in close proximity to the gold centre. Given the results described in Chapter 3, and the reports by Bourissou *et al.*,^{195,205} it is possible that this ligand could provide the chelative assistance required to undergo the initial oxidative addition step.

Table 4.1: Gold-catalysed Suzuki biaryl coupling reported by Hierso *et al.*^{243,a}



Entry	[Au]	[Au] (mol%)	72 (%)	73 (%)
1	none	-	0	0
2	AuCl	6	10	4
3	[Me ₂ SAuCl]	6	11	8
4	2[Me ₂ SAuCl]/ L71a	3	15	10
5	2[Me ₂ SAuCl]/ L71c	3	21	23
6	2[Me ₂ SAuCl]/ L71b	3	78	12
7	71b	3	81	-

^aYields determined by ¹H NMR and GC-MS.

4.3 Objectives

Chapter 3 describes a stoichiometric Negishi biaryl cross coupling enabled by the 2,2'-bipyridyl ligand. Efforts to make the process catalytic were unsuccessful; this was attributed in part to the instability of the $[(F_2\text{-bipy})Au]^+$ cation **62**, and subsequent decomposition to gold(0). A possibility is that by varying the ligand at gold, increased stability of the gold centre throughout this putative catalytic cycle can be achieved, which will allow a catalytic protocol to be developed.

While aiming to keep the essential small bite-angle that bipy subtends at the gold centre, introducing a phosphine donor might offer enhanced stability whilst still activating the gold centre towards oxidative addition. To that end, this chapter will investigate λ^3 -phosphinines, pyridyl phosphines, and quinolyl phosphines (Figure 4.3) to activate gold(I) towards oxidative addition, and ultimately for the development of gold-catalysed cross coupling in the absence of an external oxidant.

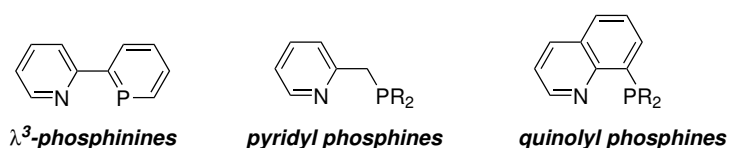


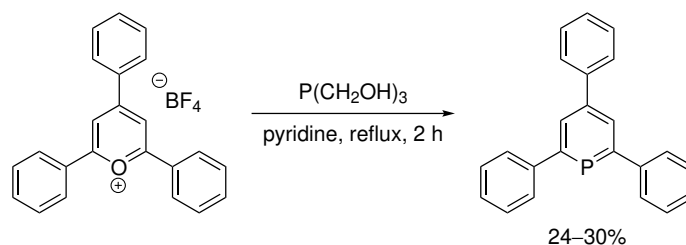
Figure 4.3: Target P,N-ligands to investigate.

4.4 λ^3 -phosphinines

Although synthetically challenging, direct substitution of a nitrogen atom for phosphorus appeared the obvious option to introduce phosphorus while maintaining the small bite angle of bipy.

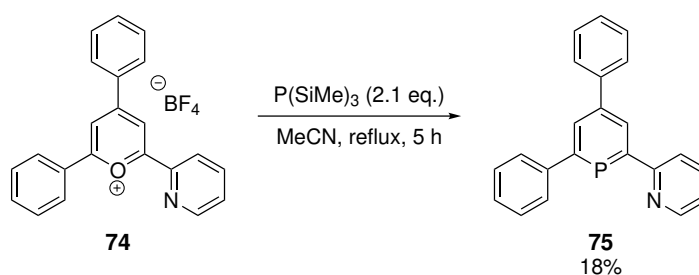
Phosphinines were first synthesised by Märkl in 1966 by reacting 2,4,6-triphenylpyrylium tetrafluoroborate with $P(CH_2OH)_3$ in refluxing pyridine (Scheme 4.2).^{245,246} Phos-

phosphinines are aromatic, and if compared to pyridine, they are poorer σ -donors yet better π -acceptors. Overall, phosphinines can be described as π -accepting electron withdrawing ligands, with electronic properties similar to that of phosphites.²⁴⁶



Scheme 4.2: Synthesis of 2,4,6-triphenylphosphinine *via* treatment of 2,4,6-triphenylpyrylium tetrafluoroborate with $\text{P(CH}_2\text{OH)}_3$.²⁴⁵

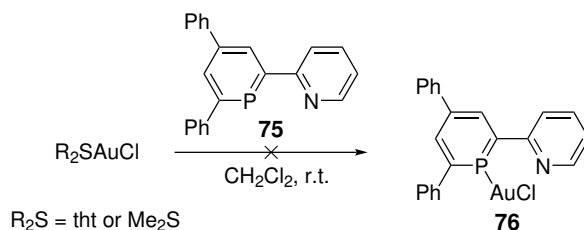
Phosphinine **75**, bearing a pendent pyridine ring, was synthesised according to the procedure reported by Müller *et al.* (Scheme 4.3).²⁴⁷ Reaction of 2-(2-pyridyl)-4,6-diphenylpyrylium tetrafluoroborate **74** with $\text{P(SiMe}_3)_3$ in MeCN afforded phosphinine **75** in a modest 18% yield. **75** is a red solid that exhibits a characteristic downfield ^{31}P resonance at $\delta = 187.4$ ppm in C_6D_6 .



Scheme 4.3: Synthesis of 2-(2-pyridyl)-4,6-diphenyl- λ^3 -phosphinine **75** *via* treatment of 2-(2-pyridyl)-4,6-diphenylpyrylium tetrafluoroborate **74** with $\text{P(SiMe}_3)_3$.²⁴⁷

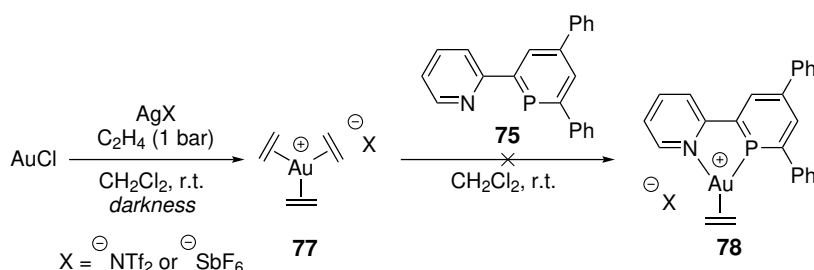
Initial attempts to coordinate **75** to gold involved treatment of either tHtAuCl or $\text{Me}_2\text{S-AuCl}$ with **75** in CH_2Cl_2 , but did not give any of the desired phosphinine gold(I) chloride **76** (Scheme 4.4). Analysis of the reaction mixtures by ^{31}P NMR spectroscopy revealed in

both cases a broad peak slightly upfield from free **75** at $\delta = 162$ ppm. However, attempts to isolate this species resulted in decomposition and a mixture of products.



Scheme 4.4: Attempted synthesis of **76** via reaction of **75** with either thtAuCl or Me₂SAuCl.

In order to ascertain if **75** would bind in the κ^2 -mode, **75** was reacted with both the NTf₂ and SbF₆ salts of tris-ethylene gold(I) cation **77** (Scheme 4.5), following the methodology outlined in Chapter 3, Scheme 3.14. Unfortunately, none of the target cation **78** was observed in either case; a mixture of compounds were obtained and no signals corresponding to ethylene were observed by ¹H NMR spectroscopy.



Scheme 4.5: Attempted synthesis of **78** via reaction of **75** with the homoleptic tris-ethylene gold(I).

In order to obtain evidence that **75** will coordinate to gold, it was reacted with [XPhos-Au-NCMe]SbF₆ **79** in CH₂Cl₂ at -78 °C. Analysis of the reaction mixture by low temperature ³¹P NMR spectroscopy (-80 °C) revealed two doublets coupled to each other at $\delta = 183$ and 42 ppm (²J_{PP} = 352 Hz), which are assigned to the phosphinine and XPhos phosphorus' of complex **80**, respectively (Figure 4.4).

Attempts to isolate **80** failed as rapid decomposition occurred upon warming to r.t., thus preventing the collection of more substantial characterisation data. Given the apparent instability of gold complexes of **75**, phosphinines were not investigated further.

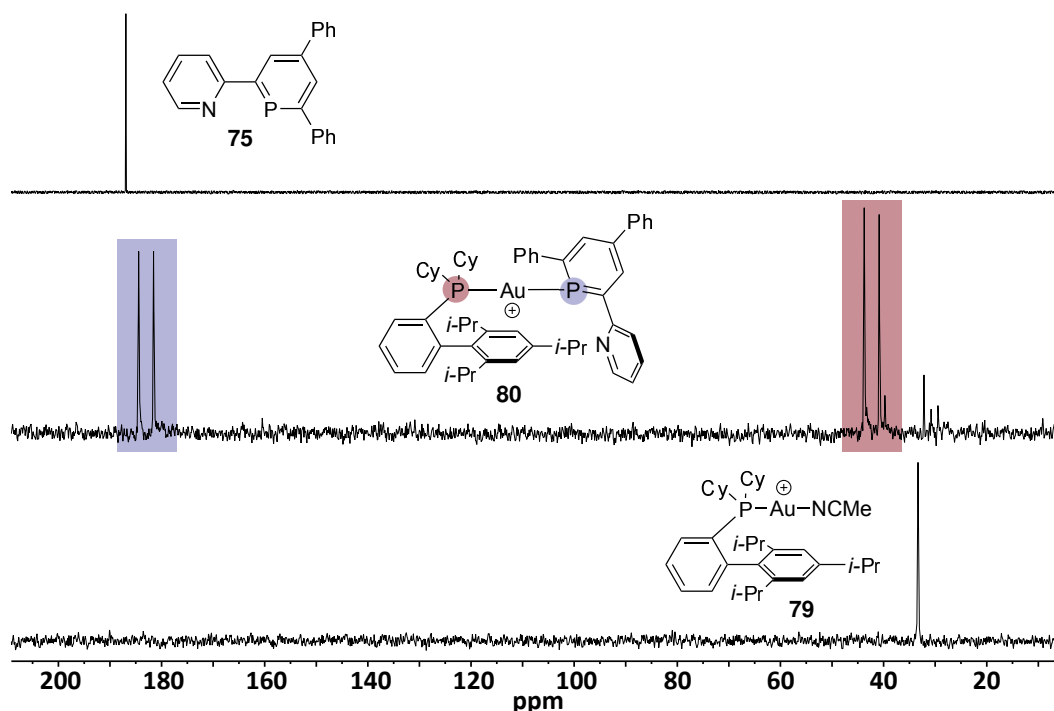
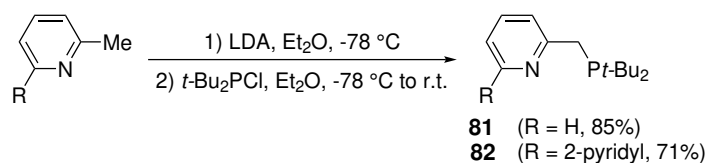


Figure 4.4: ^{31}P NMR spectra of free **75** (top), [XPhos-Au-NCMe] $^+$ [SbF $_6^-$] **79** (bottom), and **75** and **79** reacted together in a 1:1 stoichiometry (middle). The middle spectra was acquired at -80°C .

4.5 Pyridyl Phosphines

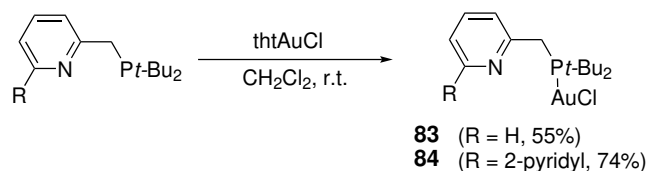
4.5.1 Pyridyl Phosphines: Synthesis

The di-*tert*-butyl phosphine ligands bearing pendent pyridyl (**81**) and bipyridyl (**82**) moieties were synthesised according to the literature procedures.^{248,249} Deprotonation of lutidine or 6-methyl-2,2'-bipyridine with LDA followed by addition of *t*-Bu $_2$ PCl gave **81** and **82** in 85% and 71% yields, respectively (Scheme 4.6).



Scheme 4.6: Synthesis of pyridyl phosphine **81** and bipyridyl phosphine **82**.^{248,249}

Coordination of ligands **81** and **82** to gold(I) was achieved *via* direct reaction with $\text{t}h\text{tAuCl}$ in CH_2Cl_2 . The resulting pyridyl phosphine gold(I) chloride complexes **83** and **84** were obtained in 55% and 74% yields, respectively (Scheme 4.7).



Scheme 4.7: Synthesis of the pyridyl phosphine gold(I) chloride complexes **83** and **84**.

Crystals of **84** suitable for X-ray diffraction analysis were grown from a CH_2Cl_2 solution layerd with hexane, the molecular structure is depicted in Figure 4.5. Complex **84** exhibits a linear geometry around gold, as is typical for a phosphine gold(I) chloride complex. The large distances between the gold centre and the bipyridyl nitrogens ($\text{Au1-N1} = 3.831(3) \text{ \AA}$, $\text{Au1-N2} = 3.029(2) \text{ \AA}$) is consistent with minimal gold-nitrogen interactions in the solid state.

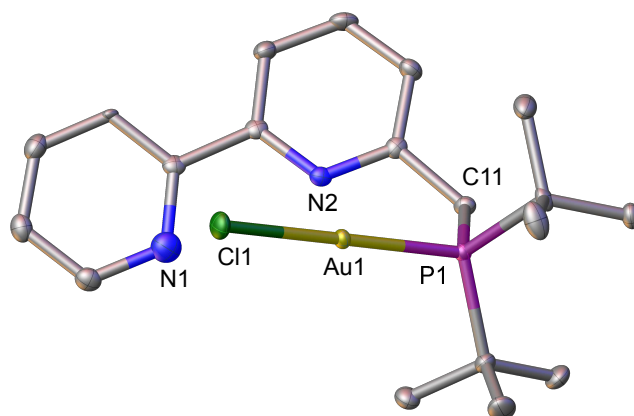
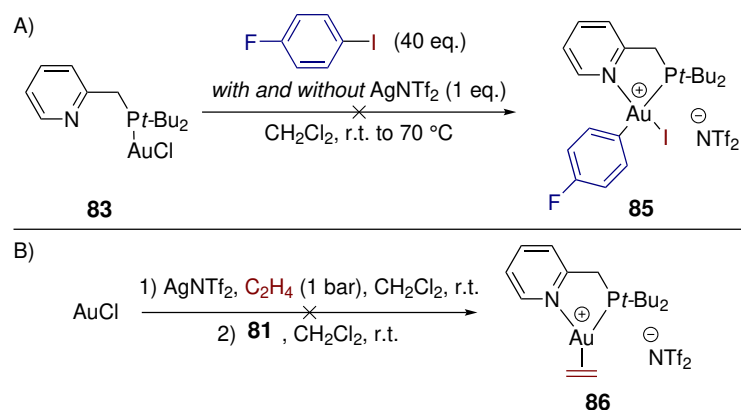


Figure 4.5: Molecular structure of **84**, thermal ellipsoids are shown at the 50% probability level. Hydrogen atoms have been omitted for clarity. Selected bond lengths (Å) and angles (°): Au1-P1 2.2472(7), Au1-C11 2.2973(7), P1-Au1-Cl1 178.81(2). Selected non-bonded distances (Å): Au1-N1 3.831(3), Au1-N2 3.029(2). See Section 5.5, Table 5.13 for full crystallographic details.

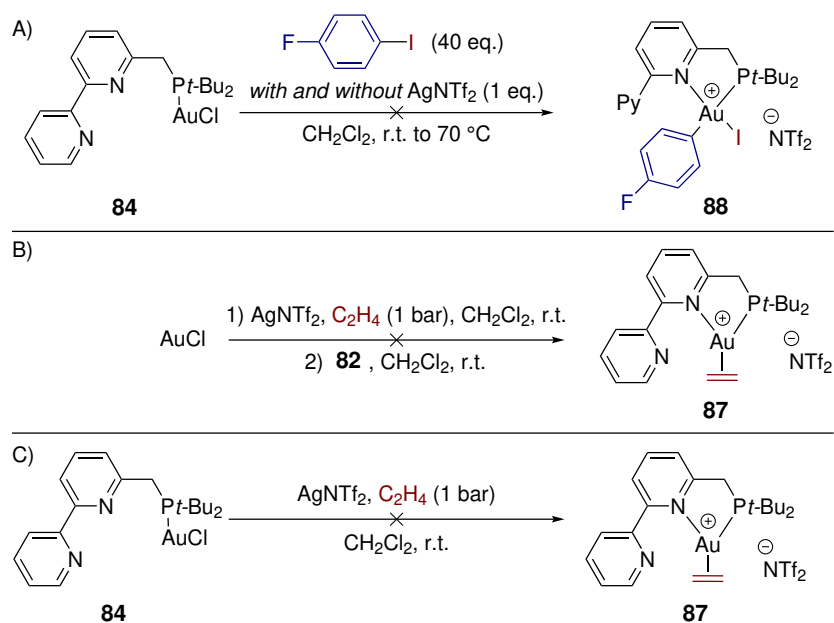
4.5.2 Pyridyl Phosphine Complexes: Reactivity

In order to assess if ligand **81** would activate gold(I) towards oxidative addition, **83** was reacted with 4-fluoriodobenzene in CH_2Cl_2 , with and without the addition of AgNTf_2 for chloride abstraction (Scheme 4.8, A). In both cases, none of the oxidative addition product was detected by ^{19}F or ^{31}P NMR. Additionally, attempts to replace the chloride of **83** by a more labile ligand, ethylene, did not result in the formation of **85** (Scheme 4.8, B).



Scheme 4.8: Attempted synthesis of **85** via oxidative addition of 4-fluoriodobenzene to **83** (A), and attempted synthesis of the gold(I) ethylene complex **86** (B).

Complex **84** was subjected to the same reactions as for **83**. Attempted oxidative addition of **84** to 4-fluoriodobenzene did not result in the detection of products consistent with complex **85**, with or without the addition of AgNTf₂ (Scheme 4.9, A). Furthermore, synthesis of the gold(I) ethylene complex **87** was attempted via the established route (Scheme 4.9, B) and via abstraction of chloride under an atmosphere of ethylene (Scheme 4.9, C). In both cases mixtures of products were obtained which did not exhibit signals corresponding to ethylene in the ¹H NMR spectrum.



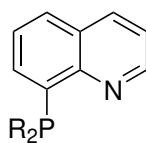
Scheme 4.9: Attempted synthesis of **88** *via* oxidative addition of 4-fluoriodobenzene to **84** (A), and attempted synthesis of the gold(I) ethylene complex **87** *via* the established route (B) and *via* abstraction of chloride from **84** under an atmosphere of ethylene.

4.6 Quinolyl Phosphines

In Section 4.5.2 it was found that the pyridyl phosphines ligands **81** and **82**, which have *flexible* methylene linkers between the two donor atoms, were not effective in facilitating oxidative addition to gold(I). Known examplesⁱ of undirected oxidative addition of gold(I) into aryl iodide bonds were all facilitated by *rigid* bidentate ligands. This ligand rigidity may be necessary in order for oxidative addition to occur.

8-Quinolyl phosphines (8-QP) (Figure 4.6), which possess a rigid two-carbon linker between the phosphine and amine moieties, were chosen as suitable candidates for further investigation.

ⁱSee Chapter 3 and references 195 and 205 by Bourissou *et al.*



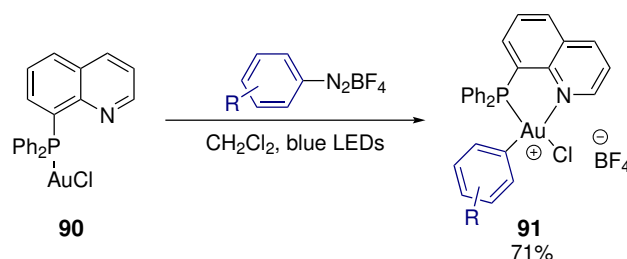
8-quinolyl phosphine

Figure 4.6: Generic structure of the 8-quinolyl phosphine (8-QP) class of ligands.

An 8-QP ligand, 8-(diphenylphosphino)quinoline **89**, was first used in conjunction with gold by Hashmi *et al.* in 2016.⁷⁸ It was found that under photochemical conditions, aryldiazonium salts undergo oxidative addition to (8-(diphenylphosphino)quinoline)AuCl **90** (Scheme 4.10). The corresponding aryl gold(III) complexes **91** were characterised by X-ray crystallography, showing that ligand **89** was coordinated in the κ^2 mode.

Although the reaction shown in Scheme 4.10 is formally an oxidative addition (the oxidation state of gold increases by two), the process is distinct from oxidative addition to an aryl halide. Oxidative addition of an aryl halide to a metal results in both the aryl *and* halide moieties ending up bonded to the metal. This contrasts with the process shown in Scheme 4.10, where only the aryl group is bonded to gold(III); N₂ is lost as a gas. In the author's opinion, the implication is that for this oxidative addition, instead of the ligand activating gold towards oxidative addition,ⁱ the oxidative addition is initiated by decomposition of the aryldiazonium salt.

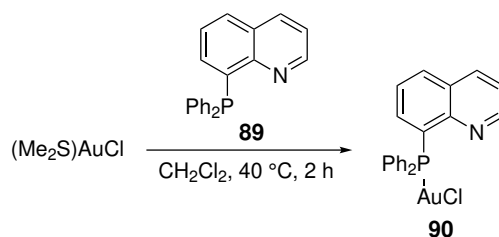
ⁱSee Chapter 3, Section 3.1.1 for a discussion of the effect that bidentate ligands have on the frontier orbitals of an ML₂ complex.



Scheme 4.10: Photochemical induced oxidative addition of aryldiazonium salts to **90** by Hashmi *et al.*⁷⁸

4.6.1 Initial Observations with (8-(Diphenylphosphino)quinoline)AuCl

8-(Diphenylphosphino)quinoline **89** was prepared *via* lithiation of 8-bromoquinoline and treatment with Ph_2PCl , according to the procedure by Leitner *et al.*²⁵⁰ Coordination of **89** to gold(I) can be achieved by reaction with either thtAuCl or Me_2SAuCl , however, the lower boiling point of Me_2S simplifies purification.ⁱ To that end, (8-(diphenylphosphino)quinoline)AuCl **90** was obtained in 87% yield by heating **89** and Me_2SAuCl at 40 °C in CH_2Cl_2 (Scheme 4.11).



Scheme 4.11: Synthesis of (8-(Diphenylphosphino)quinoline)AuCl **90** *via* reaction of Me_2SAuCl with 8-(Diphenylphosphino)quinoline **89**.

Crystals of **90** suitable for X-ray diffraction were grown from a CH_2Cl_2 solution layered with hexane, the solid state structure is shown in Figure 4.7. Complex **90** adopts a slightly

ⁱOccasionally when using thtAuCl , multiple hexane washes and/or reprecipitations were required in order to remove tht.

distorted linear geometry around the gold centre (P1-Au1-Cl1 173.78(13)°), and there is no significant interaction between the quinoline nitrogen and the gold centre in the solid state.

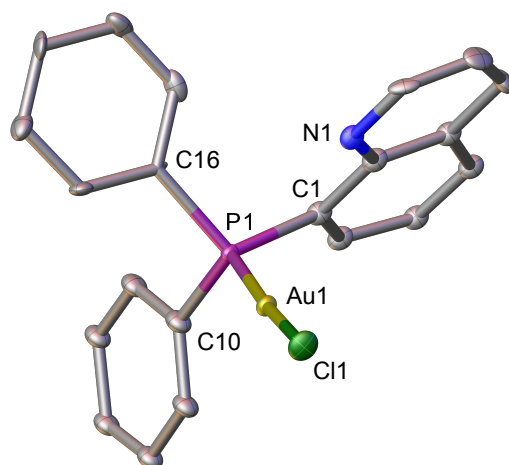
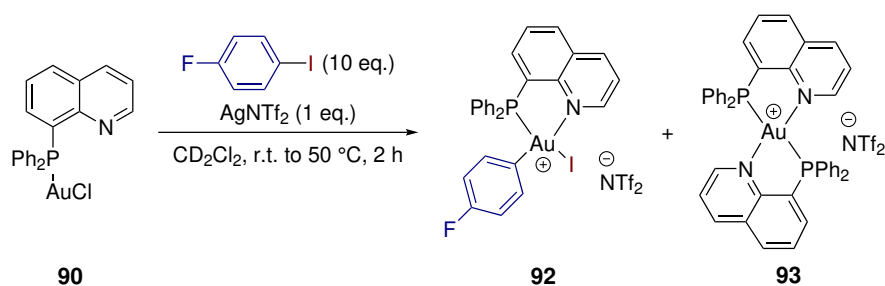


Figure 4.7: Molecular structure of **90**, thermal ellipsoids are shown at the 50% probability level. Hydrogen atoms have been omitted for clarity. Selected bond lengths (Å) and angles (°): Au1-P1 2.225(3), Au1-Cl1 2.285(3), P1-C1 1.806(13), P1-C16 1.824(12), P1-C10 1.827(13), P1-Au1-Cl1 173.78(13). See Section 5.5, Table 5.14 for full crystallographic details.

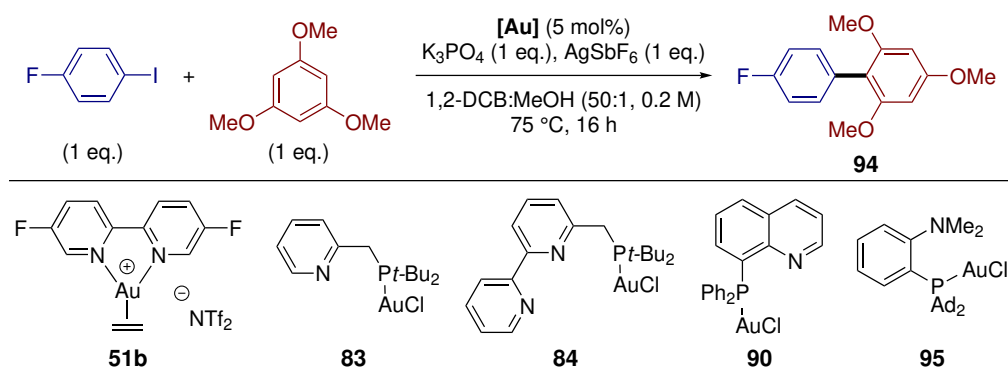
With **90** to hand, its reactivity towards aryl iodides was examined. Heating a CH₂Cl₂ solution of **90** with 10 equivalents of 4-fluoriodobenzene at 50 °C resulted in no reaction by ³¹P and ¹⁹F NMR spectroscopy. The same reaction, in the presence of one equivalent of AgNTf₂, resulted in a colour change from colourless to yellow, indicative of gold(III) formation (Scheme 4.12). Analysis of the ¹⁹F and ¹H NMR spectra revealed a mixture of products, which appeared to decompose to gold(0) upon standing. Although isolation and full characterisation was not possible, analysis of the reaction mixture prior to decomposition revealed an ion with *m/z* 732.0028, which is in agreement with the *m/z* calculated for the cation of the oxidative addition product **92** (*m/z* 732.0022). Additionally, an ion with *m/z* 823.1711 was observed, which is in agreement with that calculated for the bis-ligated cation **93** (*m/z* 823.1701).



Scheme 4.12: Reaction of **90** with AgNTf₂ and 4 fluoriodobenzene.

4.6.2 Catalysis with (8-(Diphenylphosphino)quinoline)AuCl

Given the mass spectrometry evidence supporting the possibility that **90** will undergo oxidative addition, **90** was evaluated for activity in a catalytic process. The C-H arylation methodology by Bourissou *et al.* was chosen as a benchmark reaction.²⁰⁵ Complex **90**, in addition to a selection of other gold complexes, were submitted to the conditions reported by Bourissou *et al.* (Table 4.2). The pyridyl phosphine complexes **83** and **84** did not exhibit any activity (Table 4.2, entries 3 and 4), whereas the bipy gold(I) ethylene complex **51b** produced **94** in 3% yield (Table 4.2, entry 1). Excitingly, complex **90** gave a promising 23% yield of **94** (Table 4.2, entry 4). Although far inferior to the 95% yield obtained by Bourissou *et al.* using complex **95**, this suggested that complex **90** should be investigated further.

Table 4.2: Evaluation of gold complexes for activity in the gold-catalysed C-H arylation conditions of Bourissou *et al.*²⁰⁵

Entry	[Au]	4-fluoriodobenzene (%)	94 (%)
1 ^a	51b	94	3
2 ^a	83	100	0
3 ^a	84	96	0
4 ^a	90	74	23
5 ^b	95	-	95

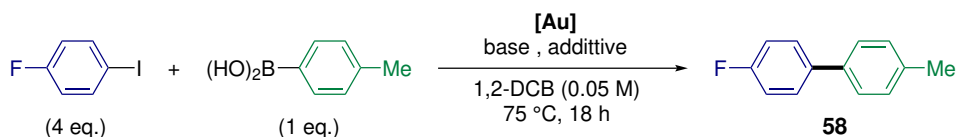
^aYields determined by ¹⁹F NMR spectroscopy. ^bYield taken from ref. 205.

The coupling of 4-fluoriodobenzene with 4-tolylboronic acid was chosen as a representative reaction to evaluate **90** as a catalyst for the Suzuki reaction (Table 4.3). Initial conditions were selected based on the C-H arylation conditions reported by Bourissou *et al.*²⁰⁵ Promisingly, **58** was produced in 10% yield using 5 mol% **90** with 100 mol% of both K_3PO_4 and $AgNTf_2$ in 1,2-DCB at 75 °C under air (Table 4.3, entry 1). Interestingly, a control experiment in the absence of base also resulted in a 10% yield of **58** (Table 4.3, entry 2). This surprising result represents a rare example of a base free Suzuki biaryl coupling. A small yield increase to 13% was obtained up increasing the $AgNTf_2$ loading to 150 % (Table 4.3, entry 3), however, a further yield increase was not observed upon increasing the $AgNTf_2$ loading to 200 mol% (Table 4.3, entry 4). The use of strictly anhydrous conditions did not benefit the process, thus simplifying the procedure significantly

(Table 4.3, entry 5). Attempts to achieve a higher turnover number by lowering the **90** loading resulted in diminished yields (Table 4.3, entries 6 and 7).

In an effort to rule out the possibility of catalysis by trace amounts of adventitious palladium, control experiments were conducted in the absence of AgNTf₂ and **90**, respectively (Table 4.3, entries 8 and 9). That these experiments did not result in any formation of **58** suggests that **90** is responsible for catalysis. However, the possibility of low level palladium contamination in **90** or AgNTf₂ cannot be ruled out with certainty.

Table 4.3: Suzuki biaryl coupling catalysed by the 8-QP-supported gold(I) complex **90**.^a

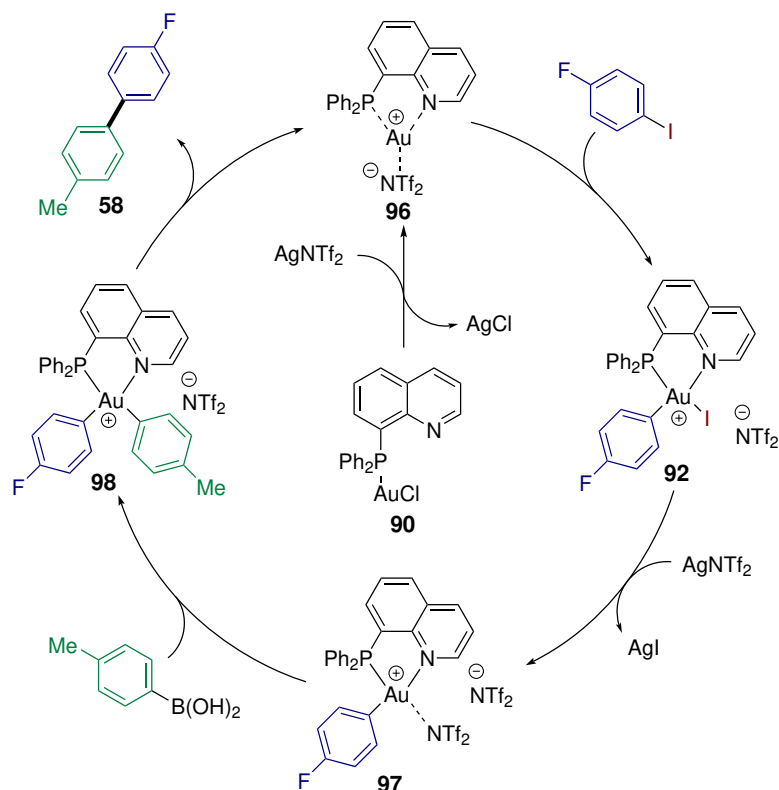


Entry	[Au] (%)	base (%)	additive (%)	58 yield (%)
1	90 (5)	K ₃ PO ₄ (100)	AgNTf ₂ (100)	10
2	90 (5)	-	AgNTf ₂ (100)	10
3	90 (5)	-	AgNTf ₂ (150)	13
4	90 (5)	-	AgNTf ₂ (200)	12
5 ^b	90 (5)	-	AgNTf ₂ (150)	13
6	90 (2.5)	-	AgNTf ₂ (150)	6
7	90 (1)	-	AgNTf ₂ (150)	4
8	-	-	AgNTf ₂ (150)	0
9	90 (5)	-	-	0

^aYields determined by calibrated GC-FID analysis using dodecane as internal standard and are an average of two experiments. ^bReaction conducted under an inert atmosphere with anhydrous reagents.

The requirement for stoichiometric quantities of a silver salt is unusual for a Suzuki cross coupling. Although a thorough mechanistic study is required to fully elucidate the role of silver, a speculative mechanism is shown in Scheme 4.13. Given the fact that **90** does not catalyse the reaction in the absence of silver (see Table 4.3, entry 9), it is

proposed that the first step is chloride abstraction from **90** to give a complex such as **96**. Oxidative addition of the aryl halide to **96** then forms **92**. A second halide abstraction from **92** renders the more electrophilic complex **97**, which then undergoes transmetalation to the bis aryl complex **98**. Reductive elimination to furnish the cross coupled biaryl **58** then closes the catalytic cycle.



Scheme 4.13: Speculative catalytic cycle for the Suzuki coupling of 4-fluoriodobenzene with 4-tolylboronic acid, using **90** as precatalyst.

Given the controversy surrounding previous reports of gold-catalysed Suzuki couplings (see Section 4.2), the possibility of palladium contamination in this work must be discussed. Although the author cannot rule out the presence of adventitious palladium, the following precautions were taken:

- All catalytic reactions were conducted in brand new vials.

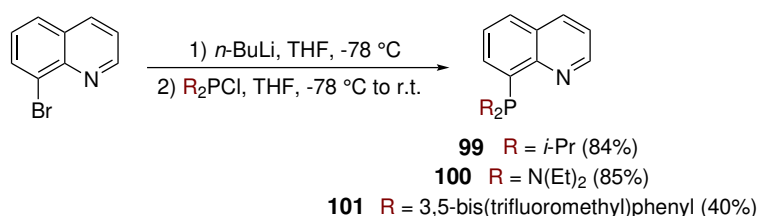
- New magnetic stirrer bars were obtained for catalytic reactions, and were cleaned with aqua regia in between uses and stored separately from other stirrer bars.

In addition to the precautions mentioned above, it must be noted that the most common source of palladium contamination arises from the inorganic base, which is absent in this methodology.

4.6.3 Synthesis of New 8-Quinoly Phosphine Ligands

The previous section describes initial investigations revealing a base-free Suzuki biaryl coupling using catalytic **90** (see Table 4.3). Although the catalytic performance of **90** is undeniably poor, the potential of 8-QP ligands to facilitate gold-catalysed processes is demonstrated. In this section, a range of new 8-QP ligands will be synthesised and their effectiveness for Suzuki coupling will be evaluated.

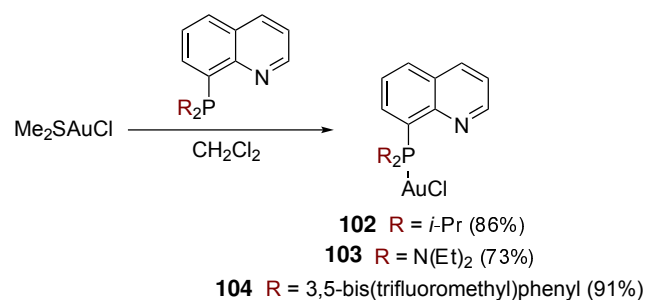
The newⁱ 8-QP ligands **99**, **100**, and **101** were prepared *via* lithiation of 8-bromoquinoline followed by reaction with the corresponding chlorophosphine (Scheme 4.14).



Scheme 4.14: Synthesis of 8-QP ligands *via* lithiation of 8-bromoquinoline followed by reaction with the corresponding chlorophosphine.

Coordination of **99**, **100**, and **101** to gold(I) proceeded cleanly in good yields to give the corresponding gold(I) complexes **102**, **103**, and **104** bearing *i*-Pr, N(Et)₂, and 3,5-bis(trifluoromethyl)phenyl substituents, respectively (Scheme 4.15).

ⁱPhosphine **100** was previously prepared by Consiglio *et al.*, however, it was used immediately in a subsequent reaction and not fully characterised.²⁵¹



Scheme 4.15: Coordination of ligands **99**, **100**, and **101** to gold(I).

The solid state structures of complexes **102**, **103**, and **104** were confirmed unambiguously by X-ray crystallography (Figure 4.8, Figure 4.9, and Figure 4.10, respectively). All three complexes adopt a slightly distorted linear geometry around gold(I), and there are no significant interactions between the quinoline nitrogen and gold in the solid state.

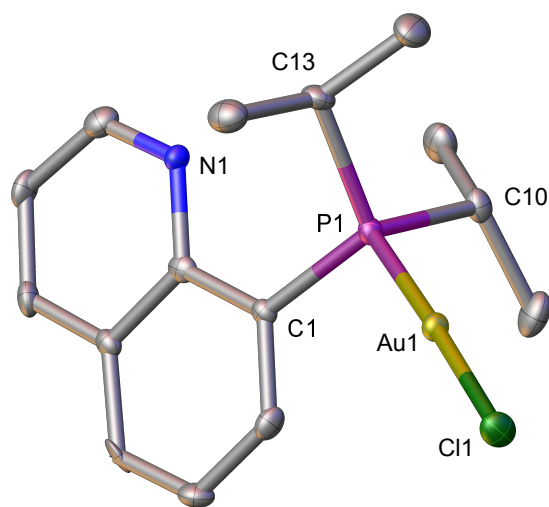


Figure 4.8: Molecular structure of **102**, thermal ellipsoids are shown at the 50% probability level. Hydrogen atoms have been omitted for clarity. Selected bond lengths (\AA) and angles ($^\circ$): Au1-P1 2.2434(13), Au1-Cl1 2.2879(12), P1-C1 1.831(5), P1-Au1-Cl1 178.10(5). See Section 5.5, Table 5.15 for full crystallographic details.

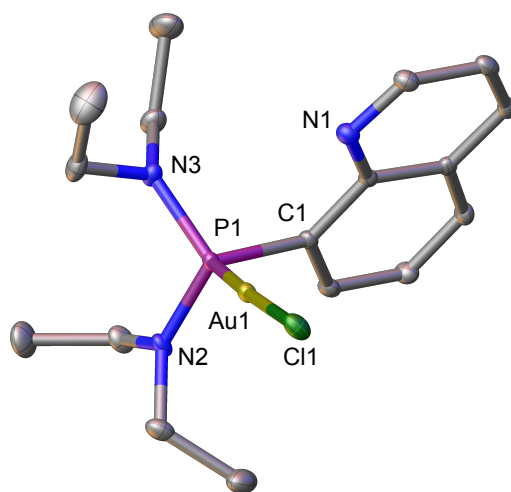


Figure 4.9: Molecular structure of **103**, thermal ellipsoids are shown at the 50% probability level. Hydrogen atoms have been omitted for clarity. Selected bond lengths (Å) and angles (°): Au1-P1 2.2335(5), Au1-Cl1 2.3003(5), P1-C1 1.819(2), P1-Au1-Cl1 174.43(2). See Section 5.5, Table 5.16 for full crystallographic details.

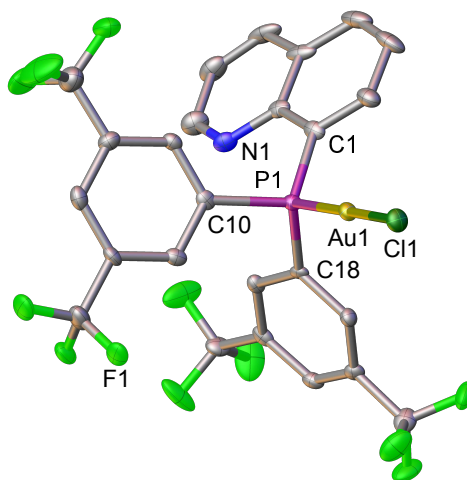
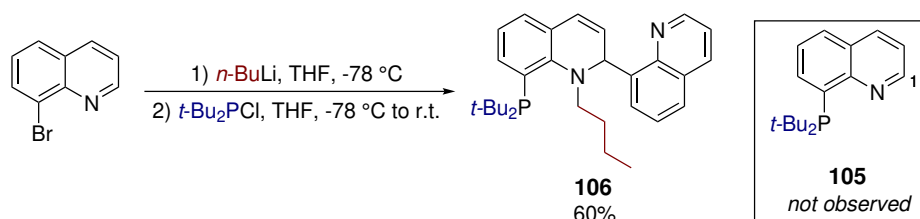


Figure 4.10: Molecular structure of **104**, thermal ellipsoids are shown at the 50% probability level. Hydrogen atoms have been omitted for clarity. Selected bond lengths (Å) and angles (°): Au1-P1 2.2315(13), Au1-Cl1 2.2886(13), P1-C1 1.820(5), P1-Au1-Cl1 175.56(4). See Section 5.5, Table 5.17 for full crystallographic details.

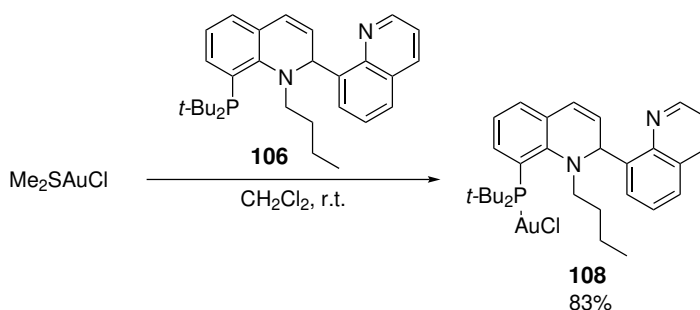
Attempts to synthesise the bulky di-*tert*-butyl substituted quinolyl phosphine **105** did not afford any of the desired product (Scheme 4.16). Instead, a mixture of products was

obtained, the major product being compound **106** which was isolated in 60% yield after flash column chromatography. Compound **106** is most likely formed *via* nucleophilic attack of 8-lithio-quinoline onto the 1-position of **105**, and quenching of the resultant amido anion with *n*-butyl bromide.



Scheme 4.16: Attempted synthesis of **105** resulting in the isolation of **106**.

Ligand **106** was coordinated to gold(I) to give complex **107** in 83% yield (Scheme 4.17). The solid state structure of **107** was confirmed by X-ray diffraction analysis and adopted a distorted linear geometry around the gold centre (Figure 4.11).



Scheme 4.17: Synthesis of complex **108** *via* reaction of **106** with Me₂SAuCl.

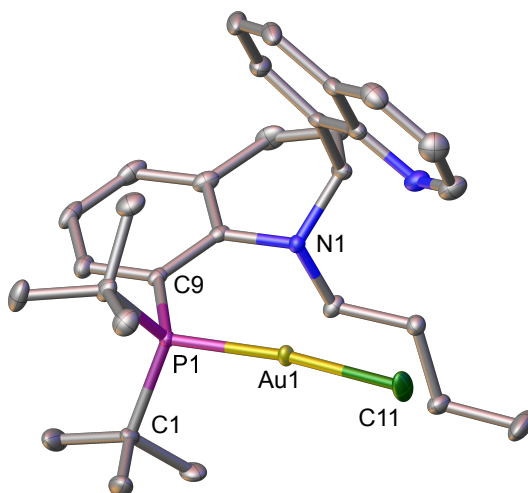
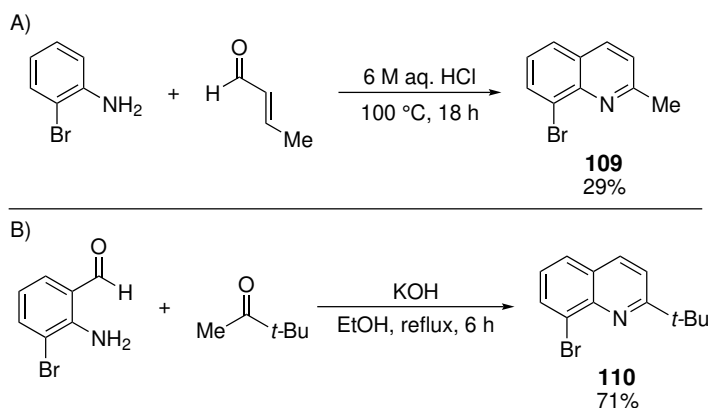


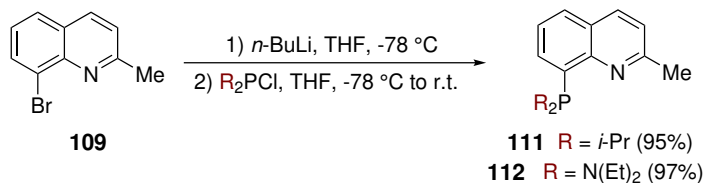
Figure 4.11: Molecular structure of **108**, thermal ellipsoids are shown at the 50% probability level. Hydrogen atoms have been omitted for clarity. Selected bond lengths (Å) and angles (°): Au1-P1 2.2484(5), Au1-Cl1 2.3011(6), P1-C9 1.831(2), P1-Au1-Cl1 173.15(2). See Section 5.5, Table 5.18 for full crystallographic details.

In section 4.6.1, the bis-chelated cation **93** was detected *via* mass spectrometry analysis (see Scheme 4.12). The formation of a species such as **93** is undesirable and would likely inhibit oxidative addition and subsequent entry into a catalytic cycle. Introduction of steric bulk at the 1-position of the quinoline ring should be effective at preventing bis-chelate formation. To that end, 8-bromoquinolines bearing methyl (**109**) and *tert*-butyl (**110**) substituents at the 1-positions were prepared as starting materials for subsequent ligand synthesis (Scheme 4.18).^{252,253}



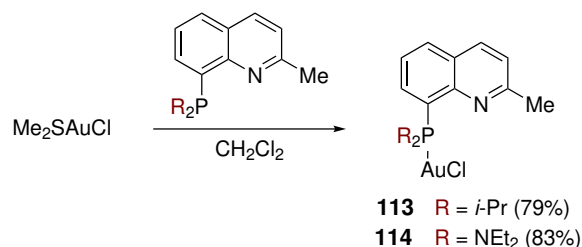
Scheme 4.18: Synthesis of methyl (**109**, A) and *tert*-butyl (**110**, B) substituted 8-bromoquinolines.^{252,253}

Lithiation of quinoline **109** followed by reaction with *i*-Pr₂PCl or (Et₂N)₂PCl furnished the corresponding ligands **111** and **112** in 95% and 97% yields, respectively (Scheme 4.19).



Scheme 4.19: Synthesis of ligands **111** and **112**.

Coordination of **111** and **112** to gold(I) afforded complexes **113** and **114** in 79% and 83% yields, respectively (Scheme 4.20). The structure of **114** was confirmed unambiguously by X-ray diffraction (Figure 4.12).



Scheme 4.20: Coordination of ligands **111** and **112** to gold(I).

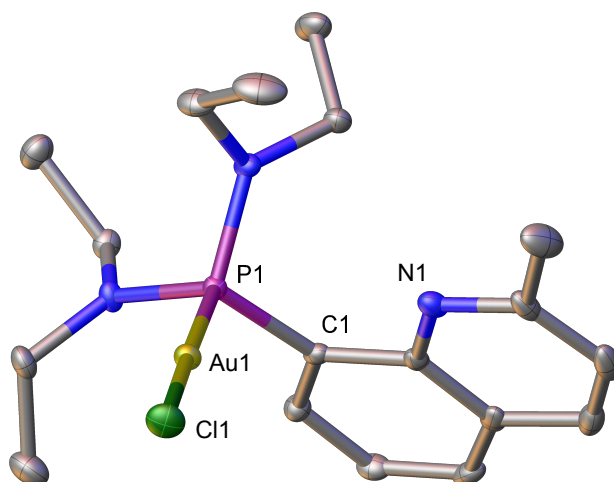
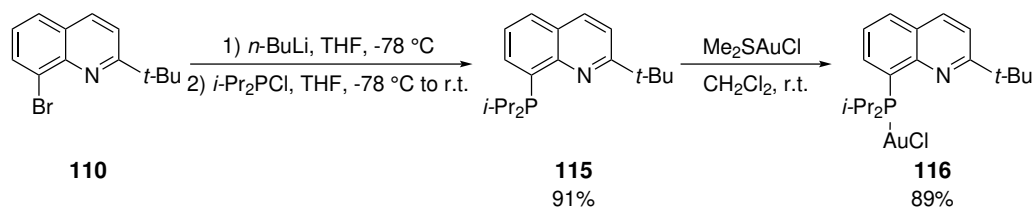


Figure 4.12: Molecular structure of **114**, thermal ellipsoids are shown at the 50% probability level. Hydrogen atoms have been omitted for clarity. Selected bond lengths (Å) and angles (°): Au1-P1 2.2342(8), Au1-Cl1 2.2960(8), P1-C1 1.821(3), P1-Au1-Cl2 176.72(3). See Section 5.5, Table 5.19 for full crystallographic details.

Lithiation of quinoline **110** followed by treatment with *i*-Pr₂P-Cl furnished ligand **115** in 91% yield (Scheme 4.19). Coordination to gold proceeded in 89% yield to afford the gold(I) complex **116** (Scheme 4.19). The structure of complex **116** was confirmed unambiguously by X-ray diffraction (Figure 4.13). In the solid state, the quinoline group is orientated at approximately 180° from the P–Au–Cl vector, suggesting that the *tert*-butyl group may be too bulky to accommodate gold in the κ²-P,N binding mode.



Scheme 4.21: Synthesis of ligand **115** and subsequent coordination to gold(I) to give complex **116**.

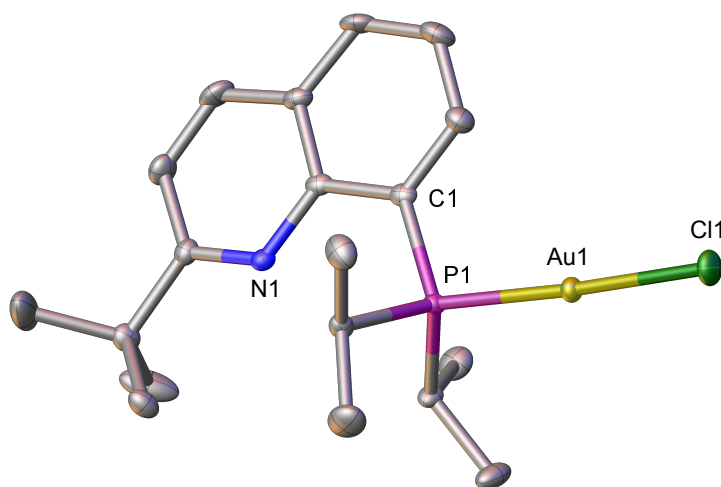
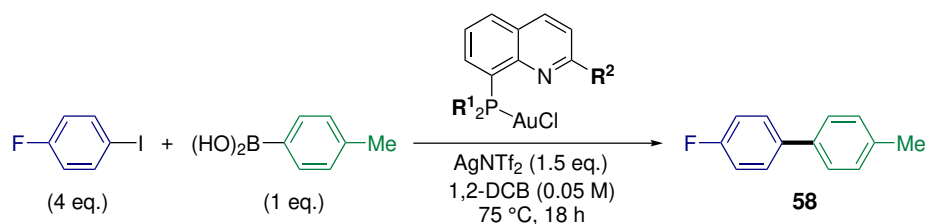


Figure 4.13: Molecular structure of **116**, thermal ellipsoids are shown at the 50% probability level. Hydrogen atoms have been omitted for clarity. Selected bond lengths (Å) and angles (°): Au1-P1 2.2439(6), Au1-Cl1 2.2934(6), P1-C1 1.822(3), P1-Au1-Cl1 177.06(2). See Section 5.5, Table 5.20 for full crystallographic details.

4.6.4 Evaluation of 8-QP Complexes in Catalysis

With a range of 8-QP-ligated gold(I) complexes to hand, their activity in the Suzuki coupling of 4-fluoriodobenzene and 4-tolylboronic acid was evaluated (Table 4.4). With respect to the initial yield of 13% of biaryl **58** using complex **90** (Table 4.4, entry 1), a small increase to 17% was observed using the *i*-Pr substituted complex **102** (Table 4.4, entry 2). The NEt₂ substituted complex **103** resulted in only 1% of the desired product (Table 4.4, entry 3). In all cases where substituents were present at the 1-position of quinoline, very low yields were obtained (Table 4.4, entries 5-8). In particular, complex **116** with the very bulky *t*-Bu group did not give any trace of cross-coupled product by GC-FID analysis. As stated in the previous section, this may be because the κ^2 -binding site of **116** is too sterically hindered to accommodate a gold centre. The best yield, at 28%, was obtained using complex **104**, bearing the electron withdrawing 3,5-bis-(CF₃)-C₆H₃ substituted phosphine (Table 4.4, entry 4).

Table 4.4: Suzuki biaryl coupling of 4-fluoroiodobenzene and 4-tolylboronic acid catalysed by 8-QP-supported gold complexes.^a

Entry	[Au] (mol%)	R ¹	R ²	58 yield (%)
1	90 (5)	H	H	13
2	102 (5)	<i>i</i> -Pr	H	17
3	103 (5)	NEt ₂	H	1
4	104 (5)	3,5-bis-(CF ₃)-C ₆ H ₃	H	28
5	113 (5)	<i>i</i> -Pr	Me	2
6	114 (5)	NEt ₂	Me	1
7	116 (5)	<i>i</i> -Pr	<i>t</i> -Bu	0
8	108 (5)	-	-	<1

^aYields determined by calibrated GC-FID analysis using dodecane as internal standard and are an average of two experiments.

Given that the most active catalyst gave only a 28% yield, it is clear that further optimisation of the reaction is required, however, time constraints led to the interruption of this project. Efforts to develop the protocol are under way by the Russell group.

4.7 Conclusion

In this chapter, a new class of small bite-angle P,N ligands were sought that would activate gold(I) towards oxidative addition of aryl iodides, with the goal of developing a gold catalysed cross-coupling using aryl iodides as the internal oxidant.

A phosphinine analogue of 2,2'-bipyridine (**75**) was synthesised, however, attempts to coordinate to gold(I) were unsuccessful; only rapid decomposition to gold(0) was ob-

served. Pyridyl (**81**) and bipyridyl (**82**) phosphines were synthesised and coordinated to gold(I), however, no evidence of oxidative addition with aryl iodides was observed.

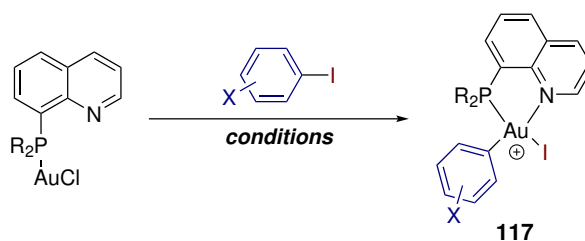
The 8-QP ligand **89** was prepared and coordinated to gold(I) to give complex **90**, which was characterised by X-ray crystallography. Evidence of oxidative addition into an aryl iodide bond was obtained *via* ESI-HRMS, although the product of oxidative addition was not isolated or fully characterised. Complex **90** was found to catalyse a Suzuki biaryl cross-coupling, albeit in low yield. However, contrary to standard Suzuki cross-coupling conditions, the reaction was found to proceed in the absence of an external base.

Aiming to improve the yield obtained with **90**, a range of new 8-QP ligands with varying steric and electronic properties were synthesised and coordinated to gold(I). The most active catalyst was found to be complex **104**, bearing an electron withdrawing 3,5-bis-(CF₃)-C₆H₃ substituted phosphine. The reaction was found to be intolerant of substituents at the 1-position of the quinoline. Work to optimise this reaction further is under way.

4.8 Future Work

The gold-catalysed Suzuki cross-coupling disclosed in this chapter requires further optimisation in order to become attractive. As shown in Section 4.6.4, Table 4.4, the nature of the ancillary ligand on gold has a large effect on catalytic activity. Electron-withdrawing substituents on the phosphine ligand resulted in the best yield, it would therefore be advantageous to investigate if introducing electron withdrawing substituents on the quinoline group would lead to further improvements. Additionally, alternative nucleophilic and electrophilic coupling partners should be investigated (for example Ar-Bpin and Ar-BF₃K as nucleophiles; Ar-OTf and Ar-Br/Cl as electrophiles). Furthermore, to exploit the reluctance of gold to undergo β -hydride elimination, sp³ coupling partners should be investigated.

In order to help confirm that gold is the active catalytic species, efforts should be undertaken to isolate and fully characterise the product of oxidative addition (**117**) of an 8-QP-supported gold complex to an aryl iodide (Scheme 4.22). This should be facilitated by careful choice of both ligand and aryl electrophile.



Scheme 4.22: Oxidative addition of an 8-QP-supported gold complex to an aryl iodide.

Chapter 5

Experimental

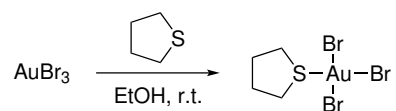
5.1 General Considerations

Reactions requiring inert conditions were conducted under an N₂ or Ar atmosphere using standard glovebox and Schlenk-line techniques. Anhydrous solvents were obtained from an Anhydrous Engineering alumina column drying system or from distillation following standard procedures. Trimethylsilyl chloride, trifluoromethanesulfonic anhydride, 2,6-lutidine, and 3-fluoriodobenzene were distilled prior to use. All other reagents were purchased from commercial suppliers and used as received. Reactions were monitored by TLC on Silica Gel 60 F254 (Merck) and visualised by examination under UV light (254 or 365 nm) and by treatment with basic KMnO₄ or phosphomolybdic acid solutions and heat. Infrared spectra were recorded using a Perkin Elmer Spectrum Two FT-IR spectrometer. NMR spectra were recorded on Bruker Advance III HD 500 Cryo, Varian VNMR500, Varian 400-MR, Jeol ECS 400 or JEOL ECS 300 spectrometers. Chemical shifts (δ) are quoted in parts per million (ppm) and are referenced to the residual solvent peak, coupling constants (J) are given in Hz. Multiplicities are abbreviated as: br (broad), s (singlet), d (doublet), t (triplet), q (quartet), m (multiplet) or combinations thereof. Assignments were made with the aid of COSY, HSQC, and HMBC experiments. Mass spectrometry was performed by the University of Bristol mass spectrometry service by either (EI⁺) using a VG Micromass Autospec spectrometer or by electrospray ionisation (ESI⁺) using a Bruker Daltonics MicrOTOF II spectrometer. GC-FID/MS analysis was performed on an Agilent 7820A equipped with a 5977B MSD.

5.2 Experimental Procedures Relevant to Chapter 2

5.2.1 Gold Complexes

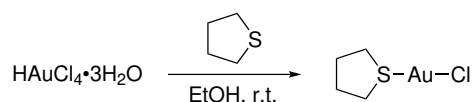
thtAuBr₃



To a solution of AuBr₃ (530 mg, 1.21 mmol) in EtOH (14 mL) was added a solution of tetrahydrothiophene (128 μ L, 1.46 mmol) in EtOH (1 mL) at room temperature. The resulting suspension was stirred for 15 minutes, then H₂O (1 mL) was added and the solid was filtered, washed with EtOH (3 \times 1 mL) then Et₂O (3 \times 1 mL), and dried *in vacuo* to afford the title compound (341 mg, 54%) as a red/brown powder.

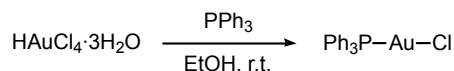
¹H NMR (400 MHz; C₆D₆) δ : 3.05 – 2.94 (m, 2H, CH₂), 1.82 – 1.72 (m, 2H, CH₂), 1.18 – 1.05 (m, 2H, CH₂), 0.75 – 0.63 (m, 2H, CH₂); ¹³C NMR (101 MHz; C₆D₆) δ : 41.5 (CH₂), 29.0 (CH₂). The spectroscopic properties of this compound were consistent with literature data.²⁵⁴

thtAuCl



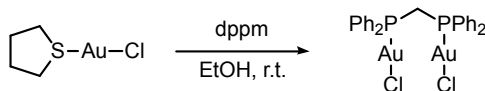
To a solution of H[AuCl₄·3H₂O] (2.32 g, 5.82 mmol) in EtOH (60 mL) was added tetrahydrothiophene (3.1 mL, 35.3 mmol) at room temperature. After stirring for 30 minutes, the solid was filtered, washed with cold EtOH (3 \times 30 mL) and dried *in vacuo* to afford the title compound (1.79 g, 95%) as a white amorphous solid.

¹H NMR (400 MHz; CDCl₃) δ : 3.79 – 3.07 (m, 4H, CH₂), 2.51 – 1.79 (m, 4H, CH₂); ¹³C NMR (126 MHz; CDCl₃) δ : 40.5 (CH₂), 30.7 (CH₂). The spectroscopic properties of this compound were consistent with literature data.²⁵⁵

Ph₃PAuCl

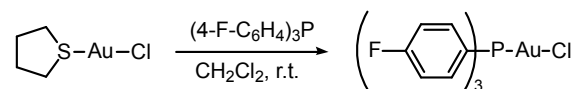
To a solution of $\text{HAuCl}_4 \cdot 3\text{H}_2\text{O}$ (1.00 g, 2.54 mmol) in EtOH (30 mL) was added triphenylphosphine (1.33 g, 5.08 mmol) at room temperature, resulting in immediate formation of a colourless precipitate. The suspension was stirred for 30 minutes then the solid was filtered off, washed with EtOH (2×5 mL) and Et₂O (2×5 mL) then dried *in vacuo*. Recrystallisation of the resulting fluffy colourless solid from $\text{CH}_2\text{Cl}_2/\text{Et}_2\text{O}$ afforded Ph_3PAuCl (993 mg, 79%) as colourless crystals.

¹H NMR (400 MHz; CDCl₃) δ: 7.56 – 7.43 (m, 15H, Ar-CH); ¹³C NMR (101 MHz; CDCl₃) δ: 134.3 (d, *J* = 13.7 Hz, Ar-CH), 132.1 (d, *J* = 2.6 Hz, Ar-CH), 129.4 (d, *J* = 11.7 Hz, Ar-CH), 128.8 (d, *J* = 62.4 Hz, Ar-CP); ³¹P{¹H} NMR (162 MHz; CDCl₃) δ: 33.8 (s). The spectroscopic properties of this compound were consistent with literature data.²⁵⁶

dppm(AuCl)₂

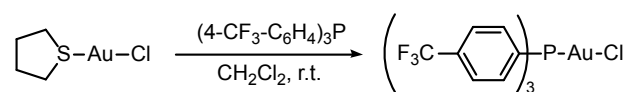
To a solution of thtAuCl (318 mg, 1.00 mmol) in EtOH (10 mL) was added dppm (190 mg, 0.500 mmol) at room temperature. After stirring for 30 minutes, pentane (5 mL) was added and the solid was filtered, washed with pentane (2×5 mL) and dried *in vacuo* to afford the title compound (375 mg, 88%) as a colourless powder.

¹H NMR (500 MHz; CDCl₃) δ: 7.74 – 7.63 (m, 8H, Ar-CH), 7.57 – 7.49 (m, 4H, Ar-CH), 7.48 – 7.40 (m, 8H, Ar-CH), 3.65 (t, *J* = 11.3 Hz, 2H, CH₂); ¹³C NMR (126 MHz; CDCl₃) δ: 133.6 (t, *J* = 7.2 Hz, Ar-CH), 132.8 (Ar-CH), 129.7 (t, *J* = 6.1 Hz, Ar-CH), 128.5 – 127.7 (m, Ar-CP), 29.6 (t, *J* = 31.1 Hz, CH₂). The spectroscopic properties of this compound were consistent with literature data.^{257,258}

(4-F-C₆H₄)₃PAuCl (118)

To a solution of tthAuCl (151 mg, 0.47 mmol) in CH₂Cl₂ (10 mL) was added tris(4-fluorophenyl)phosphine (149 mg, 0.47 mmol) at room temperature. After stirring for 45 minutes, the solution was concentrated to approx. 5 mL and hexane (20 mL) was added to precipitate a colourless solid. The solid was filtered, washed with hexane (2 × 10 mL) then dissolved in CH₂Cl₂, the solution was layered with hexane and allowed to stand overnight during which colourless crystals formed. The crystals were filtered, washed with pentane (2 × 10 mL) and dried *in vacuo* to afford the title compound (140 mg, 54%) as colourless crystals.

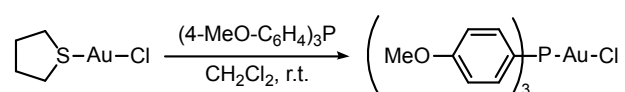
¹H NMR (400 MHz; CDCl₃) δ: 7.56 – 7.46 (m, 6H, Ar-CH), 7.24 – 7.16 (m, 6H, Ar-CH); ¹³C NMR (101 MHz; CDCl₃) δ: 165.3 (dd, *J* = 256, 2.6 Hz, Ar-CF), 136.4 (dd, *J* = 15.8, 8.9 Hz, Ar-CH), 124.4 (dd, *J* = 65, 3.6 Hz, Ar-CP), 117.1 (dd, *J* = 21.7, 13.3 Hz, Ar-CH); ¹⁹F NMR (377 MHz; CDCl₃) δ: -105.4 (m); ³¹P{¹H} NMR (162 MHz; CDCl₃) δ: 31.4 (s). The spectroscopic properties of this compound were consistent with literature data.²⁵⁹

(4-CF₃-C₆H₄)₃PAuCl (119)

To a solution of tthAuCl (146 mg, 0.46 mmol) in CH₂Cl₂ (15 mL) was added tris(4-trifluoromethylphenyl)phosphine (149 mg, 0.46 mmol) at room temperature. After stirring for 1 hour, the solution was concentrated to afford a colourless solid. The solid was dissolved in CH₂Cl₂ and the solution was layered with hexane and allowed to stand overnight during which colourless crystals formed. The crystals were filtered, washed with pentane (2 × 10 mL) and dried *in vacuo* to afford the title compound (280 mg, 87%) as colourless crystals.

$^1\text{H NMR}$ (500 MHz; CDCl_3) δ : 7.83 – 7.77 (m, 6H, Ar-CH), 7.72 – 7.64 (m, 6H, Ar-CH); $^{13}\text{C NMR}$ (125 MHz; CDCl_3) δ : 134.7 (qd, $J = 33, 2.7$ Hz, Ar-C(CF_3)), 134.6 (d, $J = 14.6$ Hz, Ar-CH), 131.7 (d, $J = 60.6$ Hz, Ar-CP), 126.6 (dq, $J = 12.2, 3.5$ Hz, Ar-CH), 123.5 (q, $J = 271.1$ Hz, CF_3); $^{19}\text{F NMR}$ (377 MHz; CDCl_3) δ : -63.3 (m); $^{31}\text{P}\{^1\text{H}\}$ NMR (162 MHz; CDCl_3) δ : 33.6 (s). The spectroscopic properties of this compound were consistent with literature data.²⁶⁰

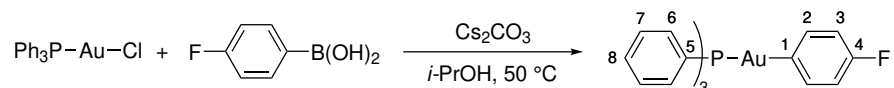
(4-MeO-C₆H₄)₃PAuCl (120)



To a solution of thtAuCl (237 mg, 0.74 mmol) in CH_2Cl_2 (25 mL) was added tris(4-methoxyphenyl)phosphine (261 mg, 0.74 mmol) at room temperature. After stirring for 1 hour, the solution was concentrated to afford a solid, which was washed with EtOH (10 mL), pentane (10 mL) then Et_2O (10 mL) then dried *in vacuo* to afford the title compound (274 mg, 63%) as a colourless solid.

$^1\text{H NMR}$ (400 MHz; CDCl_3) δ : 7.46 – 7.37 (m, 6H, Ar-CH), 6.97 – 6.91 (m, 6H, Ar-CH), 3.83 (s, 9H, OCH_3); $^{13}\text{C NMR}$ (101 MHz; CDCl_3) δ : 162.5 (d, $J = 2.4$ Hz, Ar-C(OMe)), 135.7 (d, $J = 15.4$ Hz, Ar-CH), 120.5 (d, $J = 68$ Hz, Ar-CP), 114.9 (d, $J = 13.1$ Hz, Ar-CH), 55.6 (OCH_3); $^{31}\text{P}\{^1\text{H}\}$ NMR (162 MHz; CDCl_3) δ : 29.8 (s). The spectroscopic properties of this compound were consistent with literature data.²⁵⁹

$\text{Ph}_3\text{PAu(4-F-C}_6\text{H}_4)$ (13)

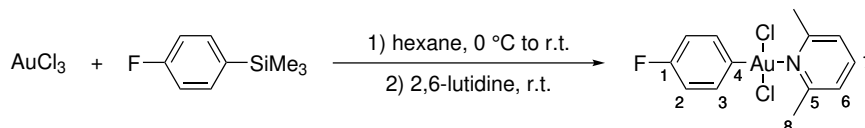


Adapted from the reported procedure.¹⁴⁷ To a flask containing Ph_3PAuCl (150 mg, 0.303 mmol), 4-fluorophenylboronic acid (82 mg, 0.585 mmol) and Cs_2CO_3 (184 mg, 0.564 mmol) was added anhydrous isopropanol (10 mL) and the resulting mixture was heated at 50 °C for 22 h. After cooling to room temperature, the reaction was concentrated

in vacuo. The resulting colourless solid was extracted with PhMe, filtered through a Celite plug, concentrated to dryness, washed with pentane and dried *in vacuo* to afford the title compound (154 mg, 92%) as a colourless solid. Single crystals suitable for X-ray diffraction were grown from a saturated solution in MeCN:MeOH (9:1).

$^1\text{H NMR}$ (400 MHz; C_6D_6) δ : 7.97 – 7.88 (m, 2H, Ar-CH), 7.46 – 7.37 (m, 6H, Ar-CH), 7.25 – 7.18 (m, 2H, Ar-CH), 7.03 – 6.88 (m, 9H, Ar-CH); $^{13}\text{C NMR}$ (126 MHz; C_6D_6) δ : 168.7 (dd, $J = 119, 4.2$ Hz, C1), 162.5 (d, $J = 243$ Hz, C4), 141.0 (d, $J = 5.3$ Hz, C3), 134.6 (d, $J = 13.8$ Hz, C6), 131.5 (d, $J = 49.0$ Hz, C5), 131.1 (d, $J = 2.5$ Hz, C8), 129.2 (d, $J = 10.6$ Hz, C7), 114.6 (dd, $J = 17.7, 6.7$ Hz, C2); $^{19}\text{F NMR}$ (470 MHz; C_6D_6) δ : -117.0 (m); $^{31}\text{P NMR}$ (202 MHz; C_6D_6) δ : 43.4; **HRMS**: (ESI) $^+$ Calculated for $[\text{C}_{24}\text{H}_{19}\text{AuFNAP}]^+ [\text{M}+\text{Na}]^+$: 577.0766. Found: 577.0766; ν_{max} (neat)/ cm^{-1} : 3046, 2923, 1573, 1479, 1434, 1213, 1159, 1098, 1025, 816, 738.

[*trans*-Au(4-F-C₆H₄)(2,6-lutidine)Cl₂] (16)

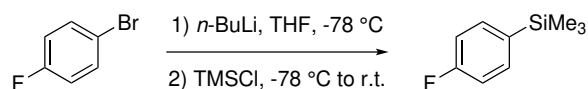


Adapted from the reported procedure.¹ Anhydrous AuCl_3 was used which was freshly prepared according to the literature procedure.⁹ To a rapidly stirred suspension of anhydrous AuCl_3 (51 mg, 0.18 mmol) in hexane (5.7 mL) was added distilled (4-fluorophenyl)-trimethylsilane **3b** (60 μL , 0.34 mmol) dropwise at 0 °C in the absence of light. The resulting red suspension was allowed to warm to room temperature and stirred for 2 hours, after which a light brown suspension was observed. Distilled 2,6-lutidine (40 μL , 0.34 mmol) was added and after stirring for 15 minutes at room temperature a yellow precipitate was observed. The mixture was concentrated *in vacuo* and the residue was purified by column chromatography (40% hexane/ CH_2Cl_2) to afford the title compound (26 mg, 33%) as a pale yellow solid. Single crystals suitable for X-ray diffraction analysis were grown by layering a CH_2Cl_2 solution of the title compound with hexane.

$^1\text{H NMR}$ (300 MHz; CDCl_3) δ : 7.74 (t, $J = 7.7$ Hz, 1H, C7-H), 7.29 (d, $J = 7.8$ Hz, 2H, C6-H), 7.26 – 7.20 (m, 2H, C3-H), 6.97 – 6.87 (m, 2H, C2-H), 3.04 (s, 3H, C8-H₃); $^{13}\text{C NMR}$ (126 MHz; CDCl_3) δ : 162.3 (d, $J = 245.0$ Hz, C1), 157.3 (C5), 140.1 (C7), 132.8 (d, $J = 7.1$ Hz, C3), 124.7 (C6), 124.5 (d, $J = 2$ Hz, C4), 115.8 (d, $J = 21.2$ Hz, C2), 24.7 (C8); $^{19}\text{F NMR}$ (282 MHz; CDCl_3) δ : -117.0 (m); **HRMS**: (ESI) Calculated for $[\text{C}_{13}\text{H}_{13}\text{Au}^{35}\text{Cl}_2\text{FNNa}]^+ [\text{M}+\text{Na}]^+$: 491.9967. Found: 491.9973; ν_{max} (neat)/ cm^{-1} : 2922, 1610, 1590, 1481, 1474, 1434, 1404, 1260, 1218, 1156.

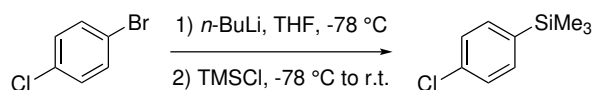
5.2.2 Arylsilanes

(4-fluorophenyl)trimethylsilane (3b)



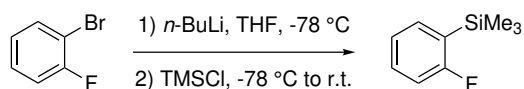
To a solution of 4-bromofluorobenzene (5.0 mL, 45.5 mmol) in anhydrous Et_2O (140 mL) at 78°C was added *n*-butyllithium (1.6 M in hexanes; 34.0 mL, 54.6 mmol) dropwise under an N_2 atmosphere. The solution was stirred at -78°C for 1.5 h, then trimethylsilyl chloride (8.7 mL, 68 mmol) was added dropwise at -78°C . The solution was stirred for 16 h at room temperature then quenched with H_2O (50 mL). The layers were separated then the aqueous layer was extracted with Et_2O (3×40 mL). The combined organic portions were washed with brine, dried over MgSO_4 , filtered and concentrated *in vacuo*. Following purification by Kugelrohr distillation ($65\text{--}70^\circ\text{C}$, 20 torr), the title compound (6.91g, 90%) was obtained as a colourless liquid.

$^1\text{H NMR}$ (400 MHz; CDCl_3) δ : 7.53 – 7.48 (m, 2H, Ar-CH), 7.09 – 7.03 (m, 2H, Ar-CH), 0.28 (s, 9H, $\text{Si}(\text{CH}_3)_3$); $^{13}\text{C NMR}$ (101 MHz; CDCl_3) δ : 163.7 (d, $J = 248$ Hz, Ar-CF), 136.0 (d, $J = 3.8$ Hz, Ar-CSi), 135.3 (d, $J = 7.3$ Hz, Ar-CH), 115.0 (d, $J = 19.6$ Hz, Ar-CH), -0.88 (s, $\text{Si}(\text{CH}_3)_3$); $^{19}\text{F NMR}$ (377 MHz; CDCl_3) δ : -112.5 (m). The spectroscopic properties of this compound were consistent with literature data.²⁶¹

(4-chlorophenyl)trimethylsilane (3c)

To a solution of 4-bromochlorobenzene (3.07 g, 16.0 mmol) in anhydrous THF (40 mL) at 78 °C was added *n*-butyllithium (1.6 M in hexanes; 10.6 mL, 17.0 mmol) dropwise under an N₂ atmosphere. The solution was stirred at -78 °C for 1 h, then trimethylsilyl chloride (2.40 mL, 19.2 mmol) was added dropwise at -78 °C. The solution was stirred for 18 h at room temperature then quenched with H₂O (50 mL). The layers were separated then the aqueous layer was extracted with Et₂O (3 × 30 mL). The combined organic portions were washed with brine (50 mL), dried over MgSO₄, filtered and concentrated *in vacuo* to afford the title compound (2.81 g, 95%) as a pale yellow liquid, which was used without further purification.

¹H NMR (400 MHz; CDCl₃) δ: 7.46 – 7.42 (m, 2H, Ar-CH), 7.35 – 7.31 (m, 2H, Ar-CH), 0.26 (s, 9H, Si(CH₃)₃); ¹³C NMR (101 MHz; CDCl₃) δ: 138.9 (Ar-C), 135.2 (Ar-C), 134.8 (Ar-CH), 128.1 (Ar-CH), -1.04 (Si(CH₃)₃); The spectroscopic properties of this compound were consistent with literature data.²⁶²

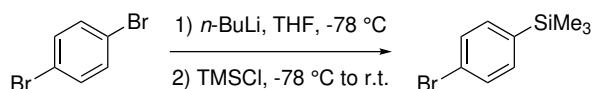
(2-fluorophenyl)trimethylsilane (3m)

To a solution of 2-bromofluorobenzene (2.2 mL, 20 mmol) in anhydrous THF (40 mL) at 78 °C was added *n*-butyllithium (1.6 M in hexanes; 15 mL, 24 mmol) dropwise under an N₂ atmosphere. The solution was stirred at -78 °C for 1 h, then trimethylsilyl chloride (3.8 mL, 30 mmol) was added dropwise at -78 °C. The solution was stirred for 18 h at room temperature then quenched with H₂O (40 mL). The layers were separated then the aqueous layer was extracted with Et₂O (3 × 25 mL). The combined organic portions were washed with brine, dried over MgSO₄, filtered and concentrated *in vacuo*. Following

purification by flash column chromatography (pentane), the title compound (2.16 g, 64%) was obtained as a colourless liquid.

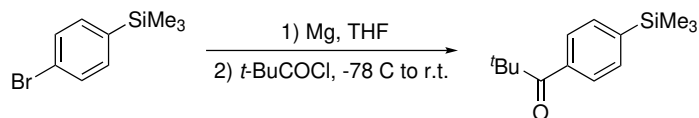
$^1\text{H NMR}$ (400 MHz; CDCl_3) δ : 7.42 – 7.37 (m, 1H, Ar-CH), 7.37 – 7.31 (m, 1H, Ar-CH), 7.16 – 7.10 (m, 1H, Ar-CH), 7.02 – 6.95 (m, 1H, Ar-CH), 0.32 (d, $J = 0.9$ Hz, 9H, $\text{Si}(\text{CH}_3)_3$); $^{13}\text{C NMR}$ (101 MHz, CDCl_3) δ : 167.6 (d, $J = 241$ Hz, Ar-CF), 135.2 (d, $J = 11$ Hz, Ar-CH), 131.3 (d, $J = 8$ Hz, Ar-CH), 126.3 (d, $J = 30$ Hz, Ar-CSi), 123.9 (d, $J = 3$ Hz, Ar-CH), 114.8 (d, $J = 26$ Hz, Ar-CH), -0.90 (d, $J = 2$ Hz, $\text{Si}(\text{CH}_3)_3$); $^{19}\text{F NMR}$ (377 MHz; CDCl_3) δ : -100.4 (m). The spectroscopic properties of this compound were consistent with literature data.²⁶³

(4-bromophenyl)trimethylsilane (3d)



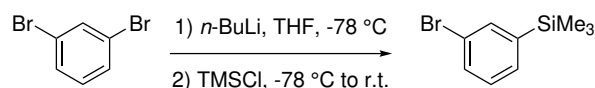
To a solution of 1,4-dibromobenzene (2.74 g, 11.6 mmol) in anhydrous THF (40 mL) at -78 °C was added *n*-butyllithium (1.6 M in hexanes; 7.25 mL, 11.6 mmol) dropwise under an N_2 atmosphere. The solution was stirred at -78 °C for 30 minutes, then trimethylsilyl chloride (1.77 mL, 13.9 mmol) was added dropwise at -78 °C. The solution was stirred for 18 h at room temperature then quenched with H_2O (40 mL). The layers were separated then the aqueous layer was extracted with Et_2O (3×20 mL). The combined organic portions were washed with brine, dried over MgSO_4 , filtered and concentrated *in vacuo*. The crude product was passed through a silica pad with hexane as eluent to afford the title compound (2.33 g, 87%) as a colourless liquid.

$^1\text{H NMR}$ (400 MHz; CDCl_3) δ : 7.50 – 7.47 (m, 2H, Ar-CH), 7.39 – 7.36 (m, 2H, Ar-CH), 0.26 (s, 9H, $\text{Si}(\text{CH}_3)_3$); $^{13}\text{C NMR}$ (101 MHz; CDCl_3) δ : 139.4 (Ar-C), 135.1 (Ar-CH), 131.0 (Ar-CH), 123.7 (Ar-C), -1.1 ($\text{Si}(\text{CH}_3)_3$). The spectroscopic properties of this compound were consistent with literature data.²⁶⁴

(4-pivaloylphenyl)trimethylsilane (3j)

A solution of (4-bromophenyl)trimethylsilane **3d** (0.85 g, 3.7 mmol) in THF (4 mL) was added dropwise to a flask containing Mg turnings (109 mg, 4.5 mmol) and a crystal of iodine in THF (4 mL). The rate of addition was controlled as to maintain a gentle reflux then the reaction was heated to 40 °C for 18 h. The reaction was cooled to -78 °C then a solution of pivaloyl chloride (1.4 mL, 11.1 mmol) in THF (8 mL) was added dropwise. The reaction was warmed to room temperature and then stirred at that temperature for 5 h, after which HCl (10% aqueous; 20 mL) and Et₂O (20 mL) were added. The layers were separated then the aqueous layer was extracted with Et₂O (3 × 15 mL). The combined organic portions were washed with sat. NaHCO₃ (20 mL), dried over MgSO₄, filtered and concentrated *in vacuo*. The crude product was purified by flash column chromatography (2% to 4% Et₂O/*n*-hexane) to afford the title compound (464 mg, 53%) as a colourless oil.

¹H NMR (400 MHz; CDCl₃) δ: 7.67 – 7.63 (m, 2H, Ar-CH), 7.57 – 7.53 (m, 2H, Ar-CH), 1.35 (s, 9H, C(CH₃)₃), 0.28 (s, 9H, Si(CH₃)₃); ¹³C NMR (101 MHz; CDCl₃) δ: 209.5 (C=O), 144.3 (Ar-C), 138.8 (Ar-C), 133.1 (Ar-CH), 127.0 (Ar-CH), 44.4 (C(CH₃)₃), 28.2 (C(CH₃)₃), -1.1 (Si(CH₃)₃). The spectroscopic properties of this compound were consistent with literature data.⁵⁶

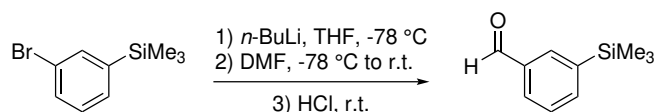
(3-bromophenyl)trimethylsilane (3p)

To a solution of 1,3-dibromobenzene (5.0 mL, 41 mmol) in anhydrous THF (140 mL) at 78 °C was added *n*-butyllithium (1.6 M in hexanes; 26 mL, 41 mmol) dropwise under an N₂ atmosphere. The solution was stirred at -78 °C for 30 minutes, then trimethylsilyl

chloride (6.2 mL, 49.2 mmol) was added dropwise at $-78\text{ }^{\circ}\text{C}$. The solution was stirred at r.t. for 18 h and then quenched with H_2O (80 mL). The layers were separated, then the aqueous layer was extracted with Et_2O ($3 \times 50\text{ mL}$). The combined organic portions were washed with brine, dried over MgSO_4 , filtered and concentrated *in vacuo*. The crude product was passed through a silica pad (eluent: pentane) to afford the title compound (8.81 g, 94%) as a colourless liquid.

$^1\text{H NMR}$ (400 MHz; CDCl_3) δ : 7.62 – 7.60 (m, 1H, Ar-CH), 7.49 – 7.46 (m, 2H, Ar-CH), 7.44 – 7.41 (m, 2H, Ar-CH), 7.25 – 7.20 (m, 1H, Ar-CH), 0.27 (s, 3H, $\text{Si}(\text{CH}_3)_3$); $^{13}\text{C NMR}$ (101 MHz; CDCl_3) δ : 143.8 (Ar-C), 136.0 (Ar-CH), 131.8 (Ar-CH), 131.7 (Ar-CH), 129.6 (Ar-CH), 123.0 (Ar-C), -1.2 ($\text{Si}(\text{CH}_3)_3$). The spectroscopic properties of this compound were consistent with literature data.²⁶⁵

3-(trimethylsilyl)benzaldehyde (3q)

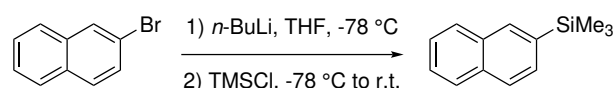


To a solution of (3-bromophenyl)trimethylsilane **3p** (2.08 g, 9.1 mmol) in THF (28 mL) at $78\text{ }^{\circ}\text{C}$ was added *n*-butyllithium (1.6 M in hexanes; 6.8 mL, 9.1 mmol) dropwise under an N_2 atmosphere. The solution was stirred at $-78\text{ }^{\circ}\text{C}$ for 1 h, then DMF (3.5 mL, 46 mmol) was added rapidly at $-78\text{ }^{\circ}\text{C}$. The reaction was stirred at $-78\text{ }^{\circ}\text{C}$ for 30 minutes, then at room temperature for 16 h. HCl (10% aqueous; 28 mL) was added and the reaction stirred for 1 h, after which the layers were separated and the aqueous layer was extracted with Et_2O ($3 \times 20\text{ mL}$). The combined organic portions were dried over MgSO_4 , filtered and concentrated *in vacuo*. Following purification by flash column chromatography (2% Et_2O /pentane) the title compound (861 mg, 53%) was obtained as a colourless oil.

$^1\text{H NMR}$ (400 MHz; CDCl_3) δ : 10.04 (s, 1H, CHO), 8.03 – 8.01 (m, 1H, Ar-CH), 7.85 (dt, $J = 7.4, 1.3\text{ Hz}$, 1H, Ar-CH), 7.78 (dt, $J = 7.4, 1.3\text{ Hz}$, 1H, Ar-CH), 7.52 (t, $J = 7.4$

Hz, 1H, Ar-CH), 0.31 (s, 1H, Si(CH₃)₃); ¹³C NMR (101 MHz; CDCl₃) δ: 193.0 (CHO), 142.0 (Ar-C), 139.5 (Ar-CH), 135.7 (Ar-C), 134.8 (Ar-CH), 130.2 (Ar-CH), 128.4 (Ar-CH), -1.2 (Si(CH₃)₃). The spectroscopic properties of this compound were consistent with literature data.²⁶⁵

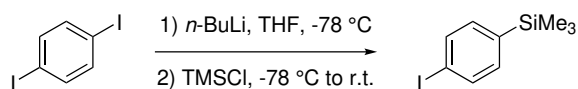
2-(trimethylsilyl)naphthalene (3s)



To a solution of 2-bromonaphthalene (2.05 g, 9.9 mmol) in anhydrous THF (20 mL) was added *n*-butyllithium (1.6 M in hexanes; 6.8 mL, 10.8 mmol) dropwise under an N₂ atmosphere. The solution was stirred at -78 °C for 1 hour, then trimethylsilyl chloride (1.90 mL, 14.9 mmol) was added dropwise at -78 °C. The solution was stirred for 18 h at room temperature and then quenched with H₂O (50 mL). The layers were separated and the aqueous layer was extracted with Et₂O (3 × 30 mL). The combined organic portions were washed with brine, dried over MgSO₄, filtered and concentrated *in vacuo* to afford the title compound (1.97 g, 99%) as a colourless oil, which was used without further purification.

¹H NMR (400 MHz; CDCl₃) δ: 8.02 (s, 1H, Ar-CH), 7.85 (m, 3H, Ar-CH), 7.62 (m, 1H, Ar-CH), 7.52 – 7.46 (m, 2H, Ar-CH), 0.37 (s, 9H, Si(CH₃)₃); ¹³C NMR (101 MHz; CDCl₃) δ: 138.1 (Ar-CH), 133.9 (Ar-CH), 133.8 (Ar-CH), 133.1 (Ar-CH), 130.0 (Ar-CH), 128.1 (Ar-CH), 127.8 (Ar-CH), 127.1 (Ar-CH), 126.3 (Ar-CH), 126.0 (Ar-CH), -0.93 (Si(CH₃)₃); The spectroscopic properties of this compound were consistent with literature data.⁵⁵

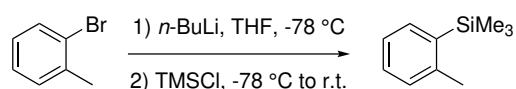
(4-iodophenyl)trimethylsilane (3e)



To a solution of 1,4-diodobenzene (2.99 g, 9.0 mmol) in anhydrous THF (20 mL) at 78 °C was added *n*-butyllithium (1.6 M in hexanes; 5.9 mL, 9.45 mmol) dropwise under an N₂ atmosphere. The solution was stirred at -78 °C for 1 hour, then trimethylsilyl chloride (1.70 mL, 13.5 mmol) was added dropwise at -78 °C. The solution was stirred for 18 h at room temperature and then quenched with H₂O (30 mL). The layers were separated, then the aqueous layer was extracted with Et₂O (3 × 20 mL). The combined organic portions were washed with sat. Na₂S₂O₃ (2 × 30 mL) then brine (1 × 20 mL), dried over MgSO₄, filtered and concentrated *in vacuo*. The crude product was passed through a silica pad (eluent: hexane) then purified by Kugelrohr distillation (2 torr, 100-125 °C) to afford the title compound (1.62 g, 65%) as a colourless liquid.

¹H NMR (400 MHz; CDCl₃) δ: 7.71 – 7.67 (m, 2H, Ar-CH), 7.27 – 7.22 (m, 2H, Ar-CH), 0.25 (s, 9H, Si(CH₃)₃); ¹³C NMR (101 MHz; CDCl₃) δ: 140.0 (Ar-C), 136.9 (Ar-CH), 135.1 (Ar-CH), 95.8 (Ar-C), -1.1 (Si(CH₃)₃). The spectroscopic properties of this compound were consistent with literature data.²⁶⁶

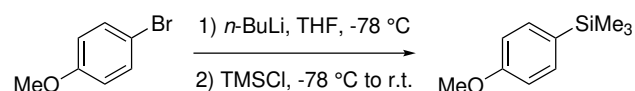
(*o*-tolyl)trimethylsilane (3I)



To a solution of 2-bromotoluene (2.40 mL, 20 mmol) in anhydrous THF (40 mL) was added *n*-butyllithium (1.6 M in hexanes; 13.8 mL, 22.0 mmol) dropwise under an N₂ atmosphere. The solution was stirred at -78 °C for 45 minutes, then trimethylsilyl chloride (3.05 mL, 24.0 mmol) was added dropwise at -78 °C. The solution was stirred at r.t. for 18 h, then the mixture was poured onto Et₂O (150 mL), washed with H₂O (3 × 50 mL) and then brine (1 × 50 mL), dried over MgSO₄, filtered and concentrated *in vacuo* to afford the title compound (3.09 g, 94%) as a colourless liquid, which was used without further purification.

$^1\text{H NMR}$ (400 MHz; CDCl_3) δ : 7.49 – 7.45 (m, 1H, Ar-CH), 7.30 – 7.25 (m, 1H, Ar-CH), 7.20 – 7.15 (m, 2H, Ar-CH), 2.47 (s, 3H, CH_3), 0.33 (s, 9H, $\text{Si}(\text{CH}_3)_3$); $^{13}\text{C NMR}$ (101 MHz; CDCl_3) δ : 143.7 (Ar-C), 138.5 (Ar-C), 134.4 (Ar-CH), 129.9 (Ar-CH), 129.3 (Ar-CH), 125.0 (Ar-CH), 23.1 (CH_3), 0.0 ($\text{Si}(\text{CH}_3)_3$). The spectroscopic properties of this compound were consistent with literature data.⁵⁶

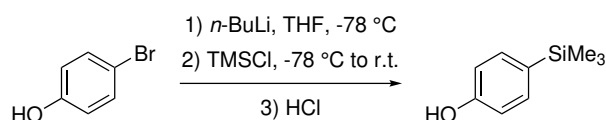
(4-methoxyphenyl)trimethylsilane (3i)



To a solution of 4-bromoanisole (3.13 mL, 25.0 mmol) in anhydrous THF (50 mL) at 78 °C was added *n*-butyllithium (1.6 M in hexanes; 17.2 mL, 27.5 mmol) dropwise under an N_2 atmosphere. The solution was stirred at -78 °C for 1.5 h, then trimethylsilyl chloride (3.81 mL, 30 mmol) was added dropwise at -78 °C. The solution was stirred for 18 h at room temperature, then quenched with H_2O (50 mL). The layers were separated and the aqueous layer was extracted with Et_2O (3×40 mL). The combined organic portions were washed with brine, dried over MgSO_4 , filtered and concentrated *in vacuo*. Following purification by Kugelrohr distillation (150 °C, 100 torr), the title compound (4.33 g, 96%) was obtained as a colourless liquid.

$^1\text{H NMR}$ (400 MHz; CDCl_3) δ : 7.49 – 7.44 (m, 2H, Ar-CH), 6.94 – 6.90 (m, 2H, Ar-CH), 3.82 (s, 3H, OCH_3), 0.26 (s, 9H, $\text{Si}(\text{CH}_3)_3$); $^{13}\text{C NMR}$ (101 MHz; CDCl_3) δ : 160.4 (Ar-C), 134.9 (Ar-CH), 131.5 (Ar-C), 113.7 (Ar-CH), 55.2 (OCH_3), -0.78 ($\text{Si}(\text{CH}_3)_3$). The spectroscopic properties of this compound were consistent with literature data.⁵⁵

4-trimethylsilylphenol (121)

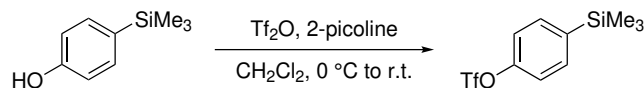


To a solution of 4-bromophenol (4.5 g, 26 mmol) in anhydrous THF (100 mL) at 78 °C was added *n*-butyllithium (1.6 M in hexanes; 37 mL, 59 mmol) dropwise under an N_2 at-

mosphere. The solution was stirred at $-78\text{ }^{\circ}\text{C}$ for 1 h, then trimethylsilyl chloride (8.6 mL, 68 mmol) was added dropwise at $-78\text{ }^{\circ}\text{C}$. The solution was stirred for 16 h at room temperature, then HCl (10% aqueous; 39 mL) was added and the reaction stirred vigorously for 1 h. The layers were separated and the aqueous layer was extracted with Et_2O (3×40 mL). The combined organic portions were washed with brine, dried over MgSO_4 , filtered and concentrated *in vacuo*. Following purification by flash column chromatography (10% to 20% EtOAc/n -hexane) the title compound (3.07 g, 71%) was obtained as a colourless solid.

$^1\text{H NMR}$ (400 MHz; CDCl_3) δ : 7.42 (d, $J = 8.4$ Hz, 2H, Ar-CH), 6.85 (d, $J = 8.4$ Hz, 2H, Ar-CH), 5.11 (s, 1H, OH), 0.25 (s, 9H, $\text{Si}(\text{CH}_3)_3$); $^{13}\text{C NMR}$ (101 MHz; CDCl_3) δ : 156.2 (Ar-C), 135.1 (Ar-CH), 131.9 (Ar-C), 115.1 (Ar-CH), -0.8 ($\text{Si}(\text{CH}_3)_3$). The spectroscopic properties of this compound were consistent with literature data.⁵³

(4-trimethylsilyl)phenyl trifluoromethanesulfonate (3f)

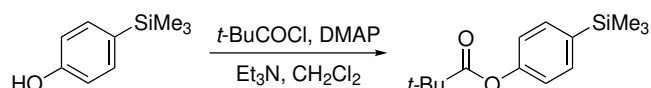


To a solution of 4-trimethylsilylphenol **121** (1.05 g, 6.3 mmol) and 2-picoline (1.2 mL, 12.6 mmol) in CH_2Cl_2 (16 mL) at $0\text{ }^{\circ}\text{C}$ was added trifluoromethanesulfonic anhydride (1.3 mL, 7.6 mmol) dropwise under an N_2 atmosphere. The reaction was stirred for 16 h at room temperature, then H_2O (25 mL) was added. The layers were separated, then the aqueous layer was extracted with Et_2O (3×10 mL). The combined organic portions were washed with HCl (10% aqueous; 20 mL) then sat. NaHCO_3 (20 mL) then brine (10 mL), dried over MgSO_4 , filtered and concentrated *in vacuo*. Following purification by flash column chromatography (hexanes) the title compound (1.69 g, 90%) was obtained as colourless liquid.

$^1\text{H NMR}$ (400 MHz; CDCl_3) δ : 7.60 – 7.56 (m, 2H, Ar-CH), 7.27 – 7.22 (m, 2H, Ar-CH), 0.28 (s, 9H, $\text{Si}(\text{CH}_3)_3$); $^{13}\text{C NMR}$ (101 MHz; CDCl_3) δ : 150.4 (Ar-C), 141.8 (Ar-C),

135.4 (Ar-CH), 120.6 (Ar-CH), 118.93 (q, $J = 321$ Hz, CF₃), -1.13 (Si(CH₃)₃); ¹⁹F NMR (470 MHz; CDCl₃) δ : -73.1 (s). The spectroscopic properties of this compound were consistent with literature data.⁵⁶

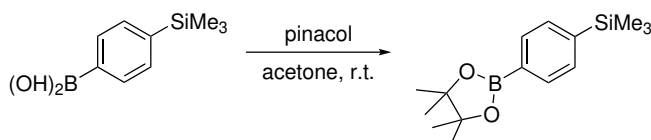
(4-trimethylsilyl)phenyl pivaloate (3k)



To a solution of 4-trimethylsilyl phenol **121** (516 mg, 3.10 mmol), triethylamine (0.65 mL, 4.65 mmol) and 4-(dimethylamino)pyridine (38 mg, 0.31 mmol) in CH₂Cl₂ (31 mL) at room temperature was added pivaloyl chloride (0.46 mL, 3.7 mmol) under an N₂ atmosphere. The reaction was stirred for 18 h at room temperature, then HCl (10% aqueous; 25 mL) was added. The layers were separated, then the aqueous layer was extracted with CH₂Cl₂ (3 × 20 mL). The combined organic portions were washed with sat. NaHCO₃ (20 mL), dried over MgSO₄, filtered and concentrated *in vacuo*. Following purification by flash column chromatography (2% to 3% Et₂O/*n*-hexane) the title compound (520 mg, 67%) was obtained as colourless solid.

¹H NMR (400 MHz; CDCl₃) δ : 7.54 – 7.50 (m, 2H, Ar-CH), 7.06 – 7.02 (m, 2H, Ar-CH), 1.36 (s, 9H, C(CH₃)₃), 0.26 (s, 9H, Si(CH₃)₃); ¹³C NMR (101 MHz; CDCl₃) δ : 177.2 (C=O), 151.9 (Ar-C), 137.8 (Ar-C), 134.6 (Ar-CH), 120.9 (Ar-CH), 39.2 (C(CH₃)₃), 27.3 (C(CH₃)₃), -0.9 (Si(CH₃)₃). The spectroscopic properties of this compound were consistent with literature data.⁶⁴

4-(trimethylsilyl)phenylboronic pinacol ester (3g)

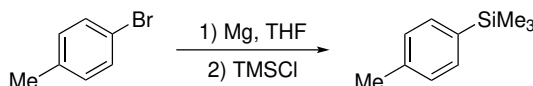


4-(trimethylsilyl)phenyl boronic acid (372 mg, 1.92 mmol) and pinacol (340 mg, 2.90 mmol) were stirred in acetone (4 mL) for 24 h at room temperature, then the reaction

mixture was concentrated *in vacuo*. Purification by flash column chromatography (20% EtOAc/*n*-hexane) afforded the title compound (531 mg, 66%) as a colourless solid.

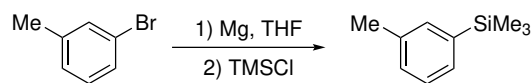
$^1\text{H NMR}$ (400 MHz; CDCl_3) δ : 7.82 – 7.77 (m, 1H, Ar-CH), 7.57 – 7.52 (m, 1H, Ar-CH), 1.35 (s, 12H, CH_3), 0.28 (s, 9H, $\text{Si}(\text{CH}_3)_3$); $^{13}\text{C NMR}$ (101 MHz; CDCl_3) δ : 144.4 (Ar-C), 134.0 (Ar-CH), 132.7 (Ar-CH), 83.9 ($\text{C}(\text{CH}_3)_2$), 25.0 ($\text{C}(\text{CH}_3)_2$), -1.1 ($\text{Si}(\text{CH}_3)_3$). The quaternary carbon attached to boron was not observed in the $^{13}\text{C NMR}$ spectrum. The spectroscopic properties of this compound were consistent with literature data.²⁶⁷

(*p*-tolyl)trimethylsilane (3h)



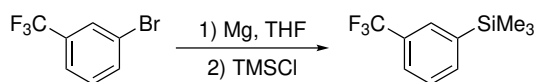
A solution of 4-bromotoluene (2.46 mL, 20.0 mmol) in THF (10 mL) was added dropwise to a flask containing Mg turnings (583 mg, 24.0 mmol) and a crystal of iodine in THF (approx. 10 mL). The rate of addition was controlled to maintain a gentle reflux. The reaction was stirred at room temperature for 1 h, then a solution of trimethylsilyl chloride (4.1 mL, 32 mmol) in THF (5 mL) was added dropwise. The reaction was stirred for 18 h at room temperature, then HCl (10% aqueous; 30 mL) was added. The layers were separated, then the aqueous layer was extracted with Et_2O (3×20 mL). The combined organic portions were washed with brine, dried over MgSO_4 , filtered and concentrated *in vacuo*. The crude product was purified by flash column chromatography (pentane) to afford the title compound (2.88 mg, 88%) as a colourless oil.

$^1\text{H NMR}$ (400 MHz; CDCl_3) δ : 7.46 – 7.41 (m, 2H, Ar-CH), 7.21 – 7.17 (m, 2H, Ar-CH), 2.36 (s, 3H, CH_3), 0.26 (s, 9H, $\text{Si}(\text{CH}_3)_3$); $^{13}\text{C NMR}$ (101 MHz; CDCl_3) δ : 138.8 (Ar-C), 137.0 (Ar-C), 133.5 (Ar-CH), 128.7 (Ar-CH), 21.6 (CH_3), -0.9 ($\text{Si}(\text{CH}_3)_3$). The spectroscopic properties of this compound were consistent with literature data.²⁶⁸

(*m*-tolyl)trimethylsilane (3o)

A solution of 3-bromotoluene (2.43 mL, 20.0 mmol) in THF (10 mL) was added dropwise to a flask containing Mg turnings (583 mg, 24.0 mmol) and a crystal of iodine in THF (approx. 10 mL). The rate of addition was controlled so as to maintain a gentle reflux. The reaction was stirred at room temperature for 1 h, then a solution of trimethylsilyl chloride (4.2 mL, 33 mmol) in THF (5 mL) was added dropwise. The reaction was stirred for 18 h at room temperature and then HCl (10% aqueous; 35 mL) was added. The layers were separated, then the aqueous layer was extracted with Et₂O (3 × 20 mL). The combined organic portions were washed with brine, dried over MgSO₄, filtered and concentrated *in vacuo*. The crude product was purified by flash column chromatography (pentane) to afford the title compound (2.95 mg, 90%) as a colourless oil.

¹H NMR (400 MHz; CDCl₃) δ: 7.36 – 7.32 (m, 2H, Ar-CH), 7.29 – 7.24 (m, 1H, Ar-CH), 7.20 – 7.16 (m, 1H, Ar-CH), 2.38 (s, 3H, CH₃), 0.28 (s, 9H, Si(CH₃)₃); ¹³C NMR (101 MHz; CDCl₃) δ: 140.5 (Ar-C), 137.2 (Ar-C), 134.1 (Ar-CH), 130.5 (Ar-CH), 129.7 (Ar-CH), 127.8 (Ar-CH), 21.7 (CH₃), -1.0 (Si(CH₃)₃). The spectroscopic properties of this compound were consistent with literature data.⁵⁵

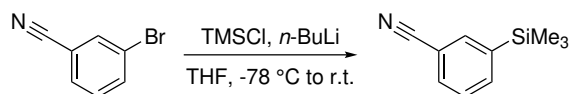
trimethyl(3-(trifluoromethyl)phenyl)silane (3n)

A solution of 3-bromobenzotrifluoride (2.80 mL, 20.0 mmol) in THF (10 mL) was added dropwise to a flask containing Mg turnings (583 mg, 24.0 mmol) and a crystal of iodine in THF (approx. 10 mL). The rate of addition was controlled as to maintain a gentle reflux. The reaction was stirred at room temperature for 1 h, then a solution of trimethylsilyl chloride (3.8 mL, 33 mmol) in THF (5 mL) was added dropwise. The reaction was stirred for 18 h at room temperature and then aqueous HCl (10%, 35 mL) was added. The

layers were separated, then the aqueous layer was extracted with Et₂O (3 × 20 mL). The combined organic portions were washed with brine, dried over MgSO₄, filtered and concentrated *in vacuo*. The crude product was purified by flash column chromatography (pentane) to afford the title compound (2.10 g, 48%) as a colourless oil.

¹H NMR (500 MHz; CDCl₃) δ: 7.76 – 7.73 (m, 1H, Ar-CH), 7.72 – 7.68 (m, 1H, Ar-CH), 7.62 – 7.58 (m, 1H, Ar-CH), 7.49 – 7.44 (m, 1H, Ar-CH), 0.31 (s, 9H, Si(CH₃)₃); ¹³C NMR (126 MHz; CDCl₃) δ: 141.8 (Ar-C), 136.6 (q, *J* = 1.5 Hz, Ar-CH), 129.9 (q, *J* = 31.5 Hz, Ar-CCF₃), 129.6 (q, *J* = 3.7 Hz, Ar-CH), 127.9 (Ar-CH), 125.5 (q, *J* = 3.7 Hz, Ar-CH), 124.4 (q, *J* = 273 Hz, C_F3), -1.30 (Si(CH₃)₃); ¹⁹F NMR (470 MHz; CDCl₃) δ: -62.61 (s). The spectroscopic properties of this compound were consistent with literature data.²⁶⁹

3-trimethylsilylbenzonitrile (3r)

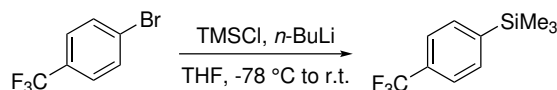


To a solution of 3-bromobenzonitrile (1.82 g, 10 mmol) and trimethylsilyl chloride (1.9 mL, 15 mmol) in anhydrous THF (50 mL) at 78 °C was added *n*-butyllithium (1.6 M in hexanes; 6.88 mL, 11 mmol) dropwise under an N₂ atmosphere. The solution was stirred at -78 °C for 15 min and then at room temperature for 1 h. H₂O (50 mL) was added, then the layers were separated and the aqueous layer was extracted with Et₂O (3 × 30 mL). The combined organic portions were washed with brine, dried over MgSO₄, filtered and concentrated *in vacuo*. Following purification by Kugelrohr distillation (150 °C, 120 torr), the title compound (1.06 g, 61%) was obtained as a colourless oil.

¹H NMR (400 MHz; CDCl₃) δ: 7.79 – 7.76 (m, 1H, Ar-CH), 7.75 – 7.69 (m, 1H, Ar-CH), 7.64 – 7.60 (m, 1H, Ar-CH), 7.47 – 7.42 (m, 1H, Ar-CH), 0.29 (s, 9H, Si(CH₃)₃); ¹³C NMR (101 MHz; CDCl₃) δ: 142.7 (Ar-C), 137.5 (Ar-CH), 137.0 (Ar-CH), 132.3

(Ar-CH), 128.4 (Ar-CH), 119.4 (Ar-CCN), 112.2 (Ar-CCN), -1.3 (Si(CH₃)₃). The spectroscopic properties of this compound were consistent with literature data.²⁷⁰

trimethyl(4-(trifluoromethyl)phenyl)silane (3t)

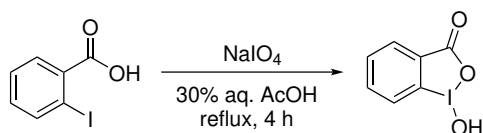


To a solution of 4-bromobenzotrifluoride (2.5 mL, 18 mmol) and trimethylsilyl chloride (3.4 mL, 27 mmol) in anhydrous THF (45 mL) at 78 °C was added *n*-butyllithium (1.6 M in hexanes; 13.1 mL, 21 mmol) dropwise under an N₂ atmosphere. The solution was stirred at 78 °C for 15 min and then at room temperature for 3 h. H₂O (100 mL) was added, then the layers were separated, and the aqueous layer was extracted with Et₂O (3 × 40 mL). The combined organic portions were washed with brine, dried over MgSO₄, filtered and concentrated *in vacuo*. Following purification by Kugelrohr distillation (135 °C, 180 torr), the title compound (2.81 g, 72%) was obtained as a colourless oil.

¹H NMR (400 MHz; CDCl₃) δ: 7.66 – 7.56 (m, 4H, Ar-CH), 0.30 (s, 9H, Si(CH₃)₃);
¹³C NMR (126 MHz; CDCl₃) δ: 145.6 (Ar-C), 133.7 (Ar-CH), 130.9 (q, *J* = 32 Hz, Ar-CCF₃), 124.4 (q, *J* = 3.8 Hz, Ar-CH), 124.5 (q, *J* = 272 Hz, C_F), -1.19 (Si(CH₃)₃);
¹⁹F NMR (377 MHz; CDCl₃) δ: -62.79. The spectroscopic properties of this compound were consistent with literature data.²⁶⁹

5.2.3 Iodine(III) Compounds

1-hydroxy-1,2-benzodioxol-3-(1*H*)-one (IBA)

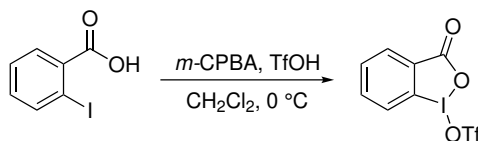


Adapted from the literature procedure.²⁷¹ A vigorously stirred suspension of NaIO₄ (2.25 g, 10.5 mmol) and 2-iodobenzoic acid (2.48 g, 10.0 mmol) in 30% aq. AcOH (15 mL)

was refluxed for 4 h. The reaction mixture was then diluted with ice-cold water (50 mL) then stirred at room temperature for 1 h. The solid was then filtered, washed with H₂O (3 × 10 mL), then acetone (3 × 10 mL), and air-dried in the dark to give the title compound (2.49 g, 94%) as a colourless solid.

¹H NMR (500 MHz; DMSO-*d*₆) δ: 8.24 – 7.83 (br s, 1H, OH), 8.01 (dd, *J* = 7.5, 1.5 Hz, 1H, Ar-CH), 7.96 (ddd, *J* = 8.3, 7.2, 1.5 Hz, 1H, Ar-CH), 7.84 (dd, *J* = 8.3, 1.0 Hz, 1H, Ar-CH), 7.70 (td, *J* = 7.2, 1.0 Hz, 1H, Ar-CH); ¹³C NMR (126 MHz; DMSO-*d*₆) δ: 167.7 (C=O), 134.5 (Ar-CH), 131.5 (Ar-C), 131.1 (Ar-CH), 130.4 (Ar-CH), 126.3 (Ar-CH), 120.4 (Ar-C). The spectroscopic properties of this compound were consistent with literature data.²⁷²

1-(trifluoromethanesulfonyloxy)-1,2-benziodoxol-3(1H)-one (IBA-OTf)



Adapted from the literature procedure,¹⁴⁴ to a solution of *m*-CPBA (approx. 75% active oxidant, dried under high vacuum for 1 h prior to use; 4.07 g, 17.7 mmol) in CH₂Cl₂ (80 mL) was added 2-iodobenzoic acid (3.99 g, 16.1 mmol). The resulting suspension was cooled to 0 °C then trifluoromethanesulfonic acid (2.57 mL, 29 mmol) was added dropwise then the orange solution was stirred at this temperature for 2-3 minutes. The solution was concentrated *in vacuo* to afford a yellow solid, which was further dried under high vacuum (0.5 torr) for a further 10 minutes. Et₂O was added (320 mL) and the mixture was stirred vigorously for 1 h, after which the solid was filtered, washed with Et₂O (3 × 15 mL) and dried under vacuum to afford the title compound (4.31 g, 62%) as the dihydrate (IBA-OTf·2H₂O), a beige solid.

¹H NMR (400 MHz; CD₃OD) δ: 8.20 – 8.16 (m, 1H, Ar-CH), 8.04 – 7.99 (m, 1H, Ar-CH), 7.91 – 7.87 (m, 1H, Ar-CH), 7.79 – 7.74 (m, 1H, Ar-CH); ¹³C NMR (126 MHz;

CD₃OD) δ : 172.1 (C=O), 136.7 (Ar-CH), 133.3 (Ar-CH), 132.1 (Ar-CH), 131.5 (Ar-C), 127.7 (Ar-CH), 121.6 (q, $J = 320$ Hz, CF₃), 120.4 (Ar-C). ¹⁹F NMR (377 MHz; CD₃OD) δ : -80.0 (s). The spectroscopic properties of this compound were consistent with literature data,¹⁴⁴ with the exception of the CF₃ signal in the ¹³C NMR data which was not reported in the original literature data.

5.2.4 Oxyarylation General Procedures

General Procedure 1 (GP-1: MeOH with *in-situ* hydrolysis)

It was found that the methyl ester of 2-iodobenzoic acid **8**, a by-product of IBA and IBA-OTf, had a similar R_F to many of the products. The procedure outlined below includes an *in situ* hydrolysis of the methyl ester to remove this by-product.

A J-Young's tube was charged with Ph₃PAuCl (0.05 eq.) and IBA-OTf (1.1 eq.), then anhydrous MeCN:MeOH (9:1; 0.05 M) was added. To this stirred mixture was added the appropriate arylsilane (1 eq.) then the tube was pressurised to 1 bar with ethylene, sealed, and stirred at 50–70 °C for the time specified, as monitored by TLC. The reaction mixture was then cooled to rt, MeOH (0.5 mL/0.1 mmol) and aq. 1 M NaOH (0.5 mL/0.1 mmol arylsilane) were added and the mixture was stirred at 40 °C for 4 h. After cooling to rt, the reaction mixture was diluted with H₂O (50 mL/mmol arylsilane) then extracted with Et₂O (3 × 30 mL/mmol arylsilane), the combined organic portions were washed with brine, dried over MgSO₄ and concentrated *in vacuo*. The crude mixture was purified by flash column chromatography (see specific compounds for eluent) to afford the desired products.

General Procedure 2 (GP-2: MeOH no *in-situ* hydrolysis)

A J-Young's tube was charged with Ph₃PAuCl (0.05 eq.) and IBA-OTf (1.1 eq.), then anhydrous MeCN:MeOH (9:1; 0.05 M) was added. To this stirred mixture was added

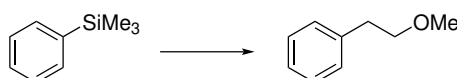
the appropriate arylsilane (1 eq.) then tube was then pressurised to 1 bar with ethylene, sealed, and stirred at 50–70 °C for the time specified, as monitored by TLC. The reaction was concentrated *in vacuo* then the crude mixture was purified by flash column chromatography (see specific compounds for eluent) to afford the desired products.

General Procedure 3 (GP-3: ROH with PhTMS)

A J-Young's tube was charged with Ph_3PAuCl (0.05–0.075 eq.), IBA-OTf (1.1 eq.) and, if solid, the appropriate alcohol (2–4 eq.). Anhydrous MeCN (0.25–1 M) was then added, followed by phenyltrimethylsilane (1 eq.) and, if liquid, the appropriate alcohol (2–4 eq.). The tube was then pressurised to 1 bar with ethylene, sealed, and stirred at 50 °C for the time specified, as monitored by TLC. The reaction was concentrated *in vacuo* then the crude mixture was purified by flash column chromatography (see specific compounds for eluent) to afford the desired products.

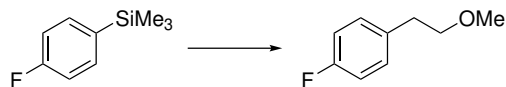
5.2.5 Oxyarylation Products

1-fluoro-4-(2-methoxyethyl)benzene (4a)



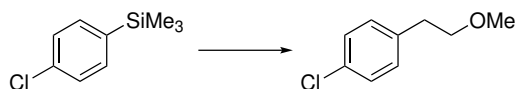
Subjecting phenyltrimethylsilane **3a** (68 μL , 0.40 mmol) to **GP-1** at 50 °C for 18 h afforded the title compound (39 mg, 72%) as a colourless oil (eluent: 5% to 10% Et₂O/pentane).

¹H NMR (400 MHz; CDCl₃) δ : 7.31 – 7.26 (m, 2H, Ar-CH), 7.23 – 7.18 (m, 3H, Ar-CH), 3.60 (t, $J = 7.1$ Hz, 2H, CH₂), 3.35 (s, 3H, CH₃), 2.88 (t, $J = 7.1$ Hz, 2H, CH₂). ¹³C NMR (101 MHz; CDCl₃) δ : 139.1 (Ar-C), 129.0 (Ar-CH), 128.5 (Ar-CH), 126.3 (Ar-C), 73.8 (CH₂), 58.8 (CH₃), 36.4 (CH₂). The spectroscopic properties of this compound were consistent with literature data.²⁷³

1-fluoro-4-(2-methoxyethyl)benzene (4b)

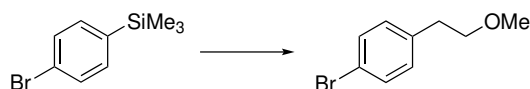
Subjecting (4-fluorophenyl)trimethylsilane **3b** (68 mg, 0.40 mmol) to **GP-1** at 50 °C for 18 h afforded the title compound (55 mg, 89%) as a colourless oil (eluent: 5% to 10% Et₂O/pentane).

¹H NMR (400 MHz; CDCl₃) δ: 7.21 – 7.15 (m, 2H, Ar-CH), 7.01 – 6.94 (m, 2H, Ar-CH), 3.58 (t, *J* = 6.9 Hz, 2H, CH₂), 3.35 (s, 3H, CH₃), 2.86 (t, *J* = 6.9 Hz, 2H, CH₂); ¹³C NMR (101 MHz; CDCl₃) δ: 161.7 (d, *J* = 244 Hz, Ar-CF), 134.8 (d, *J* = 3 Hz, Ar-C), 130.3 (d, *J* = 8 Hz, Ar-CH), 115.3 (d, *J* = 21 Hz, Ar-CH), 73.7 (CH₂), 58.8 (CH₃), 35.5 (CH₂); ¹⁹F NMR (377 MHz, CDCl₃) δ: -117.20 (m). The spectroscopic properties of this compound were consistent with literature data.²⁷⁴

1-chloro-4-(2-methoxyethyl)benzene (4c)

Subjecting (4-chlorophenyl)trimethylsilane **3c** (74 mg, 0.40 mmol) to **GP-1** at 70 °C for 18 h afforded the title compound (52 mg, 76%) as a colourless oil (eluent: 5% to 10% Et₂O/pentane).

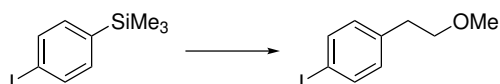
¹H NMR (400 MHz; CDCl₃) δ: 7.28 – 7.24 (m, 2H, Ar-CH), 7.18 – 7.13 (m, 2H, Ar-CH), 3.58 (t, *J* = 6.9 Hz, 2H, CH₂), 3.35 (s, 3H, CH₃), 2.85 (t, *J* = 6.9 Hz, 2H, CH₂); ¹³C NMR (101 MHz; CDCl₃) δ: 137.7 (Ar-C), 132.1 (Ar-C), 130.3 (Ar-CH), 128.6 (Ar-CH), 73.4 (CH₂), 58.8 (CH₃), 35.7 (CH₂). The spectroscopic properties of this compound were consistent with literature data.²⁷⁵

1-bromo-4-(2-methoxyethyl)benzene (4d)

Subjecting (4-bromophenyl)trimethylsilane **3d** (92 mg, 0.40 mmol) to **GP-1** at 50 °C for 18 h afforded the title compound (62 mg, 72%) as a colourless oil (eluent: 5% to 10% Et₂O/pentane).

¹H NMR (400 MHz; CDCl₃) δ: 7.43 – 7.39 (m, 2H, Ar-CH), 7.12 – 7.08 (m, 2H, Ar-CH), 3.58 (t, *J* = 6.8 Hz, 2H, CH₂), 3.34 (s, 3H, CH₃), 2.83 (t, *J* = 6.8 Hz, 2H, CH₂); ¹³C NMR (101 MHz; CDCl₃) δ: 138.0 (Ar-C), 131.4 (Ar-CH), 130.6 (Ar-CH), 120.0 (Ar-C), 73.2 (CH₂), 58.7 (CH₃), 35.6 (CH₂). The spectroscopic properties of this compound were consistent with literature data.²⁷⁶

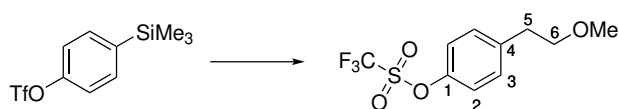
1-iodo-4-(2-methoxyethyl)benzene (**4e**)



Subjecting (4-iodophenyl)trimethylsilane **3e** (129 mg, 0.40 mmol) to **GP-1** at 70 °C for 18 h afforded the title compound (75 mg, 72%) as a colourless oil (eluent: 5% to 10% Et₂O/pentane).

¹H NMR (400 MHz; CDCl₃) δ: 7.63 – 7.58 (m, 2H, Ar-CH), 7.00 – 6.95 (m, 1H, Ar-CH), 3.57 (t, *J* = 6.8 Hz, 2H, CH₂), 3.37 – 3.31 (m, 3H, CH₃), 2.82 (t, *J* = 6.8 Hz, 2H, CH₂); ¹³C NMR (101 MHz; CDCl₃) δ: 138.8 (Ar-C), 137.5 (Ar-CH), 131.0 (Ar-CH), 91.5 (Ar-C), 73.2 (CH₂), 58.8 (CH₃), 35.8 (CH₂). The spectroscopic properties of this compound were consistent with literature data.²⁷⁴

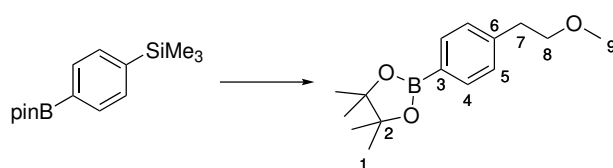
4-(2-methoxyethyl)phenyl trifluoromethanesulfonate (**4f**)



Subjecting (4-trimethylsilyl)phenyl trifluoromethanesulfonate **3f** (120 mg, 0.40 mmol) to **GP-2** at 70 °C for 18 h afforded the title compound (69 mg, 61%) as a colourless oil (eluent: 2.5% to 10% Et₂O/pentane).

$^1\text{H NMR}$ (400 MHz; CDCl_3) δ : 7.32 – 7.28 (m, 2H, C3-H), 7.21 – 7.17 (m, 2H, C2-H), 3.60 (t, $J = 6.7$ Hz, 2H, C6-H₂), 3.35 (s, 3H, CH₃), 2.90 (t, $J = 6.7$ Hz, 1H, C5-H₂); $^{13}\text{C NMR}$ (126 MHz; CDCl_3) δ : 148.2 (C1), 140.0 (C4), 130.7 (C3), 121.3 (C2), 118.9 (q, $J = 320$ Hz, CF₃), 73.1 (C6), 58.9 (CH₃), 35.6 (C5); $^{19}\text{F NMR}$ (377 MHz, CDCl_3) δ : -72.80 (s); **HRMS**: (ESI⁺) Calculated for $[\text{C}_{10}\text{H}_{11}\text{F}_3\text{NaO}_4\text{S}]^+$ $[\text{M}+\text{H}]^+$: 307.0222. Found: 307.0225; ν_{max} (neat)/ cm^{-1} : 2928, 1501, 1419, 1205, 1136, 1116, 886.

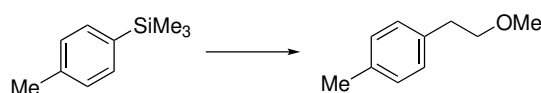
2-(4-(2-methoxyethyl)phenyl)-4,4,5,5-tetramethyl-1,3,2-dioxaborolane (4g)



Subjecting (4-bromophenyl)trimethylsilane **3g** (111 mg, 0.40 mmol) to **GP-2** at 70 °C for 18 h afforded the title compound (54 mg, 51%) as a colourless oil (eluent: 5% to 20% Et_2O /pentane).

$^1\text{H NMR}$ (400 MHz; CDCl_3) δ : 7.76 – 7.73 (m, 2H, C4-H), 7.25 – 7.22 (m, 2H, C5-H), 3.60 (t, $J = 7.1$ Hz, 2H, C8-H₂), 3.34 (s, 3H, C9-H₃), 2.90 (t, $J = 7.1$ Hz, 2H, C7-H₂), 1.34 (s, 12H, C1-H₃); $^{13}\text{C NMR}$ (126 MHz; CDCl_3) δ : 142.5 (C6), 135.0 (C4), 128.4 (C5), 83.8 (C2), 73.6 (C8), 58.8 (C9), 36.6 (C7), 25.0 (C1). The quaternary carbon attached to boron was not observed in the ^{13}C spectrum. **HRMS**: (ESI⁺) Calculated for $[\text{C}_{15}\text{H}_{23}\text{BNaO}_3]^+$ $[\text{M}+\text{Na}]^+$: 285.1635. Found: 285.1633; ν_{max} (neat)/ cm^{-1} : 2978, 1612, 1358, 1144, 1088, 856, 658.

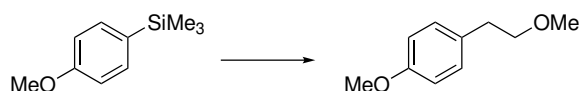
1-(2-methoxyethyl)-4-methylbenzene (4h)



Subjecting (*p*-tolyl)trimethylsilane **3h** (66 mg, 0.40 mmol) to **GP-1** at 50 °C for 18 h afforded the title compound (48 mg, 80%) as a colourless oil (eluent: 5% to 10% Et_2O /pentane).

$^1\text{H NMR}$ (400 MHz; CDCl_3) δ : 7.11 (s, 4H, Ar-CH), 3.58 (t, $J = 7.2$ Hz, 2H, CH₂), 3.36 (s, 3H, CH₃), 2.85 (t, $J = 7.2$ Hz, 2H, CH₂), 2.32 (s, 3H, CH₃); $^{13}\text{C NMR}$ (101 MHz; CDCl_3) δ : 136.0 (Ar-C), 135.8 (Ar-C), 129.2 (Ar-CH), 128.8 (Ar-CH), 74.0 (CH₂), 58.8 (CH₃), 35.9 (CH₂), 21.2 (CH₃). The spectroscopic properties of this compound were consistent with literature data.²⁷⁷

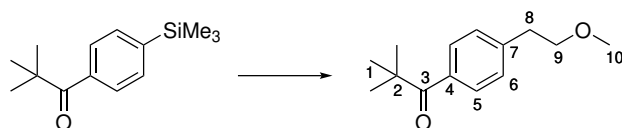
1-methoxy-4-(2-methoxyethyl)benzene (4i)



Subjecting (4-methoxyphenyl)trimethylsilane **3i** (72 mg, 0.40 mmol) to **GP-2** at 70 °C for 18 h afforded the title compound (6 mg, 9%) as a colourless oil (eluent: 2% to 10% Et_2O /pentane).

$^1\text{H NMR}$ (400 MHz; CDCl_3) δ : 7.16 – 7.12 (m, 2H, Ar-CH), 6.86 – 6.81 (m, 2H, Ar-CH), 3.79 (s, 3H, CH₃), 3.57 (t, $J = 7.1$ Hz, 2H, CH₂), 3.35 (s, 3H, CH₃), 2.83 (t, $J = 7.1$ Hz, 2H, CH₂); $^{13}\text{C NMR}$ (101 MHz; CDCl_3) δ : 158.2 (Ar-C), 131.1 (Ar-C), 129.9 (Ar-CH), 114.0 (Ar-CH), 74.0 (CH₂), 58.8 (CH₃), 55.4 (CH₃), 35.4 (CH₂). The spectroscopic properties of this compound were consistent with literature data.²⁷⁸

1-(2-methoxyethyl)-4-pivaloylbenzene (4j)



Subjecting (4-pivaloylphenyl)trimethylsilane **3j** (94 mg, 0.40 mmol) to **GP-2** at 70 °C for 18 h afforded the title compound (70 mg, 79%) as a colourless oil (eluent: 5% to 20% Et_2O /pentane).

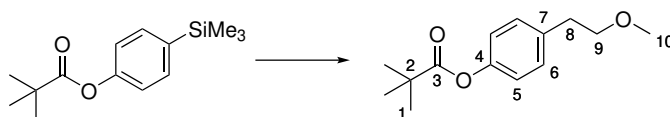
$^1\text{H NMR}$ (500 MHz; CDCl_3) δ : 7.72 – 7.69 (m, 2H, C5-H), 7.30 – 7.26 (m, 2H, C6-H), 3.64 (t, $J = 6.9$ Hz, 2H, C9-H₂), 3.38 (s, 3H, C10-H₃), 2.94 (t, $J = 6.9$ Hz, 2H, C8-H₂), 1.38 (s, 9H, C1-H₃); $^{13}\text{C NMR}$ (126 MHz; CDCl_3) δ : 208.5 (C3), 142.6 (C7), 136.3

(C4), 128.6 (C6), 128.5 (C5), 73.2 (C9), 58.9 (C10), 44.2 (C2), 36.2 (C8), 28.3 (C1);

HRMS: (ESI⁺) Calculated for [C₁₄H₂₀NaO₂]⁺ [M+Na]⁺: 243.1356. Found: 243.1358;

ν_{max} (neat)/ cm⁻¹: 2929, 1670, 1608, 1477, 1276, 1172, 1113, 961.

4-(2-methoxyethyl)phenyl pivalate (**4k**)



Subjecting (4-trimethylsilyl)phenyl pivaloate **3k** (75 mg, 0.3 mmol) to **GP-2** for 18 h afforded the title compound (54 mg, 76%) as a colourless oil (eluent: 2% to 10% EtOAc/pentane).

¹H NMR (400 MHz; CDCl₃) δ : 7.24 – 7.19 (m, 2H, C6-H), 7.00 – 6.95 (m, 2H, C5-H),

3.59 (t, $J = 7.1$ Hz, 2H, C9-H₂), 3.35 (s, 3H, C10-H₃), 2.87 (t, $J = 7.0$ Hz, 2H, C8-H₂),

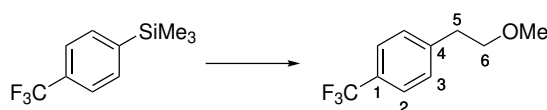
1.35 (s, 9H, C1-H₃); **¹³C NMR** (126 MHz; CDCl₃) δ : 177.3 (C3), 149.6 (C4), 136.4

(C7), 129.8 (C6), 121.4 (C5), 73.6 (C9), 58.7 (C10), 39.1 (C2), 35.7 (C8), 27.2 (C1);

HRMS: (ESI⁺) Calculated for [C₁₄H₂₀NaO₃]⁺ [M+Na]⁺: 259.1305. Found: 259.1312;

ν_{max} (neat)/ cm⁻¹: 2975, 1759, 1507, 1198, 1165, 1111.

1-(2-methoxyethyl)-4-(trifluoromethyl)benzene (**4t**)



Subjecting trimethyl(4-(trifluoromethyl)phenyl)silane **3k** (82 mg, 0.40 mmol) to **GP-1** at 70 °C for 18 h afforded the title compound (47 mg, 58%) as a colourless oil (eluent: 5% to 10% Et₂O/pentane).

¹H NMR (400 MHz; CDCl₃) δ : 7.55 (d, $J = 8.0$ Hz, 2H, C2-H), 7.34 (d, $J = 8.0$ Hz,

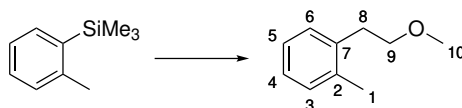
2H, C3-H), 3.63 (t, $J = 6.7$ Hz, 2H, C6-H₂), 3.36 (s, 3H, CH₃), 2.94 (t, $J = 6.7$ Hz, 2H,

C5-H₂); **¹³C NMR** (126 MHz; CDCl₃) δ : 143.5 (q, $J = 1.5$ Hz, C4), 129.3 (C3), 128.7

(q, $J = 32$ Hz, C1), 125.4 (q, $J = 3.8$ Hz, C2), 124.5 (q, $J = 272$ Hz, CCF₃), 73.1 (C6), 58.9

($\underline{\text{C}}\text{H}_3$), 36.3 (C5); ^{19}F NMR (377 MHz; CDCl_3) δ -62.30 (s); **HRMS**: (EI^+) Calculated for $[\text{C}_{10}\text{H}_{11}\text{F}_3\text{O}]^+ [\text{M}]^+$: 204.0762. Found: 204.0765; ν_{max} (neat)/ cm^{-1} : 2929, 1620, 1323, 1162, 1111, 1067, 1019, 843.

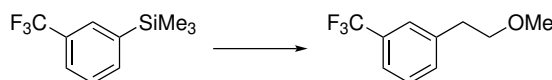
1-(2-methoxyethyl)-2-methylbenzene (4l)



Subjecting (*o*-tolyl)trimethylsilane **3l** (66 mg, 0.40 mmol) to **GP-1** at 70 °C for 18 h afforded the title compound (26 mg, 43%) as a colourless oil (eluent: 5% to 10% Et_2O /pentane).

^1H NMR (400 MHz; CDCl_3) δ : 7.20 – 7.09 (m, 4H, C3- $\underline{\text{H}}$, C4- $\underline{\text{H}}$, C5- $\underline{\text{H}}$, C6- $\underline{\text{H}}$), 3.57 (t, J = 7.5 Hz, 2H, C9- $\underline{\text{H}}_2$), 3.38 (s, 3H, C10- $\underline{\text{H}}_3$), 2.90 (t, J = 7.5 Hz, 2H, C8- $\underline{\text{H}}_2$), 2.34 (s, 3H, C1- $\underline{\text{H}}_3$); ^{13}C NMR (126 MHz; CDCl_3) δ : 136.8 (C7), 136.3 (C2), 130.2, 129.3, 126.4, 126.0 (C3, C4, C5, C6), 72.6 (C9), 58.6 (C10), 33.4 (C8), 19.4 (C1); **HRMS**: (EI^+) Calculated for $[\text{C}_{10}\text{H}_{14}\text{O}]^+ [\text{M}]^+$: 150.1045. Found: 150.1040; ν_{max} (neat)/ cm^{-1} : 2924, 1493, 1460, 1381, 1113, 743.

1-(2-methoxyethyl)-3-(trifluoromethyl)benzene (4n)



Subjecting trimethyl(3-(trifluoromethyl)phenyl)silane **3n** (87 mg, 0.40 mmol) to **GP-1** at 70 °C for 18 h afforded the title compound (33 mg, 40%) as a colourless oil (eluent: 5% to 10% Et_2O /pentane).

^1H NMR (400 MHz; CDCl_3) δ : 7.51 – 7.37 (m, 4H, Ar- $\underline{\text{C}}\text{H}$), 3.63 (t, J = 6.8 Hz, 2H, $\underline{\text{C}}\text{H}_2$), 3.36 (s, 3H, $\underline{\text{C}}\text{H}_3$), 2.94 (t, J = 6.8 Hz, 2H, $\underline{\text{C}}\text{H}_2$); ^{13}C NMR (101 MHz; CDCl_3) δ : 140.1 (Ar- $\underline{\text{C}}$), 132.37 (q, J = 1.2 Hz, Ar- $\underline{\text{C}}\text{H}$), 130.7 (q, J = 32.0 Hz, Ar- $\underline{\text{C}}\text{CF}_3$), 128.8 (Ar- $\underline{\text{C}}\text{H}$), 125.6 (q, J = 3.8 Hz, Ar- $\underline{\text{C}}\text{H}$), 124.3 (q, J = 272 Hz, $\underline{\text{C}}\text{F}_3$), 123.2 (q, J = 3.9

Hz, Ar-CH), 73.1 (CH₂), 58.8 (CH₃), 36.1 (CH₂). The spectroscopic properties of this compound were consistent with literature data.²⁷⁹

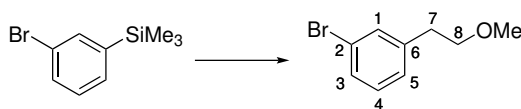
1-(2-methoxyethyl)-3-methylbenzene (4o)



Subjecting (*m*-tolyl)trimethylsilane **3o** (66 mg, 0.40 mmol) to **GP-1** at 50 °C for 18 h afforded the title compound (46 mg, 77%) as a colorless oil (eluent: 5% Et₂O/pentane).

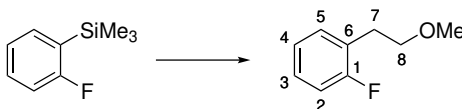
¹H NMR (400 MHz; CDCl₃) δ: 7.23 – 7.17 (m, 1H, Ar-CH), 7.08 – 7.01 (m, 3H, Ar-CH), 3.61 (t, *J* = 7.2 Hz, 1H, CH₂), 3.38 (s, 1H, CH₃), 2.87 (t, *J* = 7.2 Hz, 2H, CH₂), 2.35 (s, 3H, CH₃); ¹³C NMR (101 MHz; CDCl₃) δ: 138.9 (Ar-C), 138.0 (Ar-C), 129.8 (Ar-CH), 128.4 (Ar-CH), 127.1 (Ar-CH), 125.9 (Ar-CH), 73.8 (CH₂), 58.8 (CH₃), 36.3 (CH₂), 21.5 (CH₃). The spectroscopic properties of this compound were consistent with literature data.²⁷⁷

1-bromo-3-(2-methoxyethyl)benzene (4p)



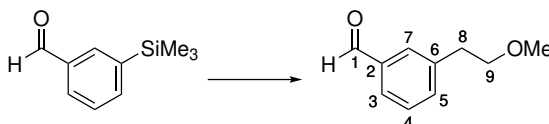
Subjecting (3-bromophenyl)trimethylsilane **3p** (92 mg, 0.40 mmol) to **GP-1** at 70 °C for 18 h afforded the title compound (30 mg, 35%) as a colourless oil (eluent: 5% to 10% Et₂O/pentane).

¹H NMR (500 MHz; CDCl₃) δ: 7.39 – 7.37 (m, 1H, C1-H), 7.36 – 7.32 (m, 1H, C3-H or C4-H), 7.17 – 7.14 (m, 2H, C3-H or C4-H, C5-H), 3.59 (t, *J* = 6.9 Hz, 2H, C8-H₂), 3.35 (s, 3H, CH₃), 2.85 (t, *J* = 6.9 Hz, 2H, C7-H₂); ¹³C NMR (126 MHz; CDCl₃) δ: 141.6 (C6), 132.0 (C1), 130.0 (C3 or C4), 129.5 (C3 or C4), 127.7 (C5), 122.5 (C2), 73.2 (C8), 58.9 (CH₃), 36.0 (C7); HRMS: (EI⁺) Calculated for [C₉H₁₁O⁷⁹Br]⁺ [M]⁺: 213.9993. Found: 213.9995; ν_{max} (neat)/ cm⁻¹: 2923, 1567, 1473, 1426, 1381, 1113, 1071, 778, 693.

1-fluoro-2-(2-methoxyethyl)benzene (4m)

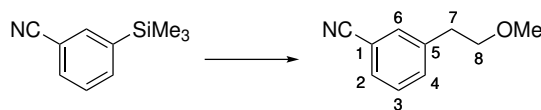
Subjecting (2-fluorophenyl)trimethylsilane **3m** (67 mg, 0.40 mmol) to **GP-1** 70 °C for 18 h afforded the title compound (14 mg, 23%) as a colourless oil (eluent: 5% to 10% Et₂O/pentane).

¹H NMR (400 MHz; CDCl₃) δ: 7.27 – 7.16 (m, 2H, C3-H, C5-H), 7.10 – 6.99 (m, 2H, C2-H, C4-H), 3.61 (t, *J* = 7.0, 2H, C8-H₂), 3.36 (s, 3H, CH₃), 2.93 (t, *J* = 7.0 Hz, 2H, C7-H₂); ¹³C NMR (101 MHz; CDCl₃) δ: 161.4 (d, *J* = 245 Hz, C1), 131.3 (d, *J* = 5.0 Hz, C5), 128.0 (d, *J* = 8.1 Hz, C3), 125.8 (d, *J* = 16 Hz, C6), 124.0 (d, *J* = 3.5 Hz, C4), 115.3 (d, *J* = 22 Hz, C2), 72.2 (d, *J* = 1.3 Hz, C8), 58.7 (CH₃), 29.5 (d, *J* = 2.2 Hz, C7); ¹⁹F NMR (283 MHz; CDCl₃) δ: -118.6 (m); HRMS: (ESI⁺) Calculated for [C₉H₁₁OF]⁺ [M]⁺: 154.0794. Found: 154.0782; *v*_{max} (neat)/ cm⁻¹: 2872, 1585, 1472, 1454, 1229, 1184, 1115, 755.

3-(2-methoxyethyl)benzaldehyde (4q)

Subjecting 3-(trimethylsilyl)benzaldehyde **3q** (71 mg, 0.40 mmol) to **GP-2** at 50 °C for 18 h afforded the title compound (49 mg, 75%) as a colourless oil (eluent: 2.5% to 5% acetone/pentane).

¹H NMR (400 MHz; CDCl₃) δ: 9.98 (s, 1H, CHO), 7.75 – 7.68 (m, 2H, C3-H, C7-H), 7.52 – 7.48 (m, 1H, C5-H), 7.47 – 7.43 (m, 1H, C4-H), 3.63 (t, *J* = 6.7 Hz, 2H, C9-H₂), 3.34 (s, 3H, CH₃), 2.95 (t, *J* = 6.7 Hz, 2H, C8-H₂); ¹³C NMR (101 MHz, CDCl₃) δ: 192.5 (CHO), 140.4 (C6), 136.7 (C2), 135.2 (C5), 129.9 (C7), 129.1 (C4), 128.0 (C3), 73.1 (C9), 58.8 (CH₃), 35.9 (C8); HRMS: (ESI⁺) Calculated for [C₁₀H₁₂NaO₂]⁺ [M+Na]⁺: 187.0730. Found: 187.0720; *v*_{max} (neat)/ cm⁻¹: 2924, 1697, 1585, 1240, 1113, 693.

3-(2-methoxyethyl)benzonitrile (4r)

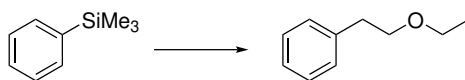
Subjecting 3-trimethylsilylbenzonitrile **3r** (70 mg, 0.40 mmol) to **GP-2** at 70 °C for 18 h afforded the title compound (42 mg, 65%) as a colourless oil (eluent: 2.5% to 5.5% acetone/pentane).

$^1\text{H NMR}$ (500 MHz; CDCl_3) δ : 7.53 – 7.51 (m, 1H, C6-H), 7.51 – 7.48 (m, 1H, C2-H), 7.48 – 7.44 (m, 1H, C4-H), 7.38 (t, $J = 7.7$ Hz, 2H, C3-H), 3.60 (t, $J = 6.5$ Hz, 2H, C8-H₂), 3.34 (s, 3H, CH₃), 2.90 (t, $J = 6.5$ Hz, 2H, C7-H₂); $^{13}\text{C NMR}$ (126 MHz; CDCl_3) δ : 140.8 (C5), 133.6 (C4), 132.5 (C6), 130.1 (C2), 129.2 (C3), 119.1 (CN), 112.5 (C1), 72.7 (C8), 58.9 (C7), 35.8 (CH₃); **HRMS**: (ESI⁺) Calculated for $[\text{C}_{10}\text{H}_{11}\text{NNaO}]^+$ $[\text{M}+\text{Na}]^+$: 184.0733. Found: 184.0739; ν_{max} (neat)/ cm^{-1} : 2926, 2873, 2228, 1729, 1583, 1483, 1114, 795, 691.

2-(2-methoxyethyl)naphthalene (4s)

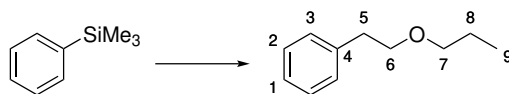
Subjecting 2-trimethylsilylnaphthalene **3s** (80 mg, 0.40 mmol) to **GP-1** at 50 °C for 18 h afforded the title compound (59 mg, 79%) as a colourless oil (eluent: 5% to 10% Et_2O /pentane).

$^1\text{H NMR}$ (400 MHz; CDCl_3) δ : 7.83 – 7.76 (m, 3H, Ar-CH), 7.69 – 7.66 (m, 1H, Ar-CH), 7.48 – 7.40 (m, 2H, Ar-CH), 7.37 (dd, $J = 8.4, 1.8$ Hz, 1H, Ar-CH), 3.70 (t, $J = 7.0$ Hz, 2H, CH₂), 3.38 (s, 3H, CH₃), 3.06 (t, $J = 7.0$ Hz, 2H, CH₂); $^{13}\text{C NMR}$ (101 MHz; CDCl_3) δ : 136.7 (Ar-C), 133.7 (Ar-C), 132.3 (Ar-C), 128.1 (Ar-CH), 127.8 (Ar-CH), 127.6 (Ar-CH), 127.6 (Ar-CH), 127.3 (Ar-CH), 126.1 (Ar-CH), 125.4 (Ar-CH), 73.7 (CH₂), 58.9 (CH₃), 36.5 (CH₂). The spectroscopic properties of this compound were consistent with literature data.²⁸⁰

(2-ethoxyethyl)benzene (6a)

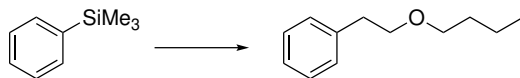
Subjecting phenyltrimethylsilane **3a** (68 μ L, 0.40 mmol) and ethanol (0.58 mL, 10 mmol) to **GP-3** for 36 h afforded, after *in situ* hydrolysis (see **GP-1**), the title compound (47 mg, 78%) as a colourless oil (eluent: 2.5% Et₂O/pentane).

¹H NMR (500 MHz; CDCl₃) δ : 7.35 – 7.30 (m, 2H, Ar-CH), 7.29 – 7.22 (m, 3H, Ar-CH), 3.67 (t, J = 7.4 Hz, 2H, CH₂), 3.54 (q, J = 7.0 Hz, 2H, CH₂), 2.93 (t, J = 7.4 Hz, 2H, CH₂), 1.24 (t, J = 7.0 Hz, 3H, CH₃). ¹³C NMR (126 MHz; CDCl₃) δ : 139.1 (Ar-C), 129.0 (Ar-CH), 128.5 (Ar-CH), 126.3 (Ar-CH), 71.7 (CH₂), 66.4 (CH₂), 36.6 (CH₂), 15.3 (CH₃). The spectroscopic properties of this compound were consistent with literature data.²⁸¹

(2-propoxyethyl)benzene (6b)

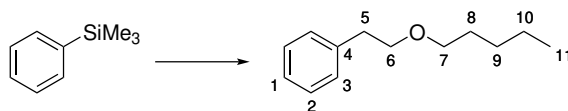
Subjecting phenyltrimethylsilane **3a** (68 μ L, 0.40 mmol) and *n*-propanol (0.75 mL, 10 mmol) to **GP-3** for 16 h afforded the title compound (47 mg, 78%) as a colourless oil (eluent: 2.5% to 5% Et₂O/pentane).

¹H NMR (400 MHz; CDCl₃) δ : 7.31 – 7.25 (m, 2H, C2-H), 7.24 – 7.17 (m, 3H, C1-H, C2-H), 3.62 (t, J = 7.3 Hz, 2H, C6-H₂), 3.40 (t, J = 6.7 Hz, 2H, C7-H₂), 2.89 (t, J = 7.3 Hz, 2H, C5-H₂), 1.66 – 1.52 (m, 2H, C8-H₂), 0.91 (t, J = 7.4 Hz, 3H, C9-H₃); ¹³C NMR (101 MHz; CDCl₃) δ : 139.3 (C4), 129.1 (C3), 128.5 (C2), 126.3 (C1), 72.8 (C7), 71.9 (C6), 36.5 (C5), 23.1 (C8), 10.7 (C9); HRMS: (EI⁺) Calculated for [C₁₁H₁₆O]⁺ [M]⁺: 164.1201. Found: 164.1208; ν_{max} (neat)/ cm⁻¹: 3028, 2935, 2855, 1731, 1496, 1454, 1107, 747, 698.

(2-butoxyethyl)benzene (6c)

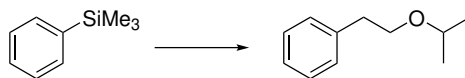
Subjecting phenyltrimethylsilane **3a** (68 μ L, 0.40 mmol) and *s*-butanol (0.92 mL, 10 mmol) to **GP-3** for 18 h afforded the title compound (48 mg, 67%) as a colourless oil (eluent: 0.5% to 2% Et₂O/pentane).

¹H NMR (400 MHz; CDCl₃) δ : 7.31 – 7.26 (m, 2H, Ar-CH), 7.24 – 7.17 (m, 3H, Ar-CH), 3.62 (t, J = 7.3 Hz, 2H, CH₂), 3.44 (t, J = 6.6 Hz, 2H, CH₂), 2.89 (t, J = 7.3 Hz, 2H, CH₂), 1.60 – 1.51 (m, 2H, CH₂), 1.41 – 1.30 (m, 2H, CH₂), 0.91 (t, J = 7.4 Hz, 3H, CH₃); ¹³C NMR (101 MHz; CDCl₃) δ : 139.3 (Ar-C), 129.0 (Ar-CH), 128.4 (Ar-CH), 126.3 (Ar-CH), 72.0 (CH₂), 70.9 (CH₂), 36.5 (CH₂), 32.0 (CH₂), 19.5 (CH₂), 14.1 (CH₃). The spectroscopic properties of this compound were consistent with literature data.²⁸¹

(2-(pentyloxy)ethyl)benzene (6d)

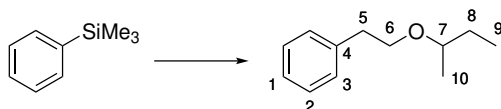
Subjecting phenyltrimethylsilane **3a** (68 μ L, 0.40 mmol) and *n*-pentanol (1.1 mL, 10 mmol) to **GP-3** (0.075 eq. Ph₃PAuCl, 0.25 M) for 18 h afforded the title compound (59 mg, 77%) as a colourless oil (eluent: 0.5% to 5% Et₂O/pentane).

¹H NMR (500 MHz; CDCl₃) δ : 7.32 – 7.27 (m, 2H, C2-H), 7.25 – 7.19 (m, 3H, C1-H, C3-H), 3.64 (t, J = 7.3 Hz, 2H, C6-H₂), 3.44 (t, J = 6.7 Hz, 2H, C7-H₂), 2.90 (t, J = 7.3 Hz, 2H, C5-H₂), 1.62 – 1.55 (m, 2H, C8-H₂), 1.37 – 1.28 (m, 4H, C9-H₂, C10-H₂), 0.91 (t, J = 7.0 Hz, 3H, C11-H₃); ¹³C NMR (126 MHz; CDCl₃) δ : 139.2 (C4), 129.0 (C3), 128.4 (C2), 126.2 (C1), 71.9 (C6), 71.2 (C7), 36.5 (C5), 29.6 (C8), 28.5 (C9), 22.7 (C10), 14.2 (C11); HRMS: (EI⁺) Calculated for [C₁₃H₂₀O]⁺ [M]⁺: 192.1514. Found: 192.1508; ν_{max} (neat)/ cm⁻¹: 3028, 2931, 2857, 1496, 1454, 1362, 1110, 748, 698.

(2-isopropoxyethyl)benzene (6e)

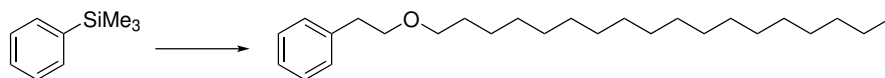
Subjecting phenyltrimethylsilane **3a** (68 μL , 0.40 mmol) and *i*-propanol (0.76 mL, 10 mmol) to **GP-3** (0.05 eq. Ph_3PAuCl , 0.25 M) for 18 h afforded the title compound (45 mg, 69%) as a colourless oil (eluent: 2.5% Et_2O /pentane).

$^1\text{H NMR}$ (400 MHz; CDCl_3) δ : 7.31 – 7.25 (m, 2H, Ar-CH), 7.24 – 7.17 (m, 3H, Ar-CH), 3.64 – 3.54 (m, 3H, CH₂, CH(CH_3)₂), 2.87 (t, $J = 7.5$ Hz, 2H, CH₂), 1.15 (d, $J = 6.1$ Hz, 2H, CH(CH_3)₂); $^{13}\text{C NMR}$ (101 MHz; CDCl_3) δ : 139.3 (Ar-C), 129.1 (Ar-CH), 128.4 (Ar-CH), 126.3 (Ar-CH), 71.7 (CH₂), 69.4 (CH(CH_3)₂), 37.0 (CH₂), 22.3 (CH(CH_3)₂). The spectroscopic properties of this compound were consistent with literature data.²⁸²

(2-(*s*-butoxy)ethyl)benzene (6f)

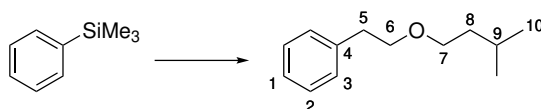
Subjecting phenyltrimethylsilane **3a** (68 μL , 0.40 mmol) and *s*-butanol (0.92 mL, 10 mmol) to **GP-3** (0.075 eq. Ph_3PAuCl , 0.25 M) for 18 h afforded the title compound (46 mg, 65%) as a colourless oil (eluent: 2.5% Et_2O /pentane).

$^1\text{H NMR}$ (400 MHz; CDCl_3) δ : 7.32 – 7.18 (m, 5H, C1-H, C2-H, C3-H), 3.73 – 3.65 (m, 1H, C6-HH), 3.61 – 3.54 (m, 1H, C6-HH), 3.33 (app h, $J = 6.1$ Hz, 1H, C7-H), 2.88 (t, $J = 7.4$ Hz, 2H, C5-H₂), 1.61 – 1.49 (m, 1H, C8-HH), 1.49 – 1.37 (m, 1H, C8-HH), 1.12 (d, $J = 6.1$ Hz, 3H, C10-H₃), 0.88 (t, $J = 7.5$ Hz, 3H, C9-H₃); $^{13}\text{C NMR}$ (101 MHz; CDCl_3) δ : 139.4 (C4), 129.1 (C3), 128.4 (C2), 126.2 (C1), 77.0 (C7), 69.6 (C6), 37.0 (C5), 29.4 (C8), 19.4 (C10), 9.9 (C9); **HRMS**: (EI^+) Calculated for $[\text{C}_{12}\text{H}_{18}\text{O}]^+$ $[\text{M}]^+$: 178.1358. Found: 178.1353; ν_{max} (neat)/ cm^{-1} : 2967, 2932, 2875, 1604, 1496, 1453, 1340, 1136, 1081, 748, 698.

(2-(octadecyloxy)ethyl)benzene (6h)

Subjecting phenyltrimethylsilane **3a** (68 μL , 0.40 mmol) and 1-octadecanol (216 mg, 0.8 mmol) to **GP-3** (0.075 eq. Ph_3PAuCl , 1 M) for 18 h afforded the title compound (57 mg, 57%) as a colourless oil (eluent: 10% to 20% PhMe/pentane).

$^1\text{H NMR}$ (500 MHz; CDCl_3) δ : 7.31 – 7.17 (m, 5H, Ar-CH), 3.62 (t, $J = 7.3$ Hz, 2H, ArCH₂CH₂), 3.43 (t, $J = 6.7$ Hz, 2H, Ar(CH₂)₂OCH₂), 2.89 (t, $J = 7.3$ Hz, 2H, ArCH₂CH₂), 1.54 (m, 2H, CH₂), 1.25 (s, 30H, 15 \times CH₂), 0.88 (t, $J = 6.7$ Hz, 3H, CH₃); $^{13}\text{C NMR}$ (101 MHz; CDCl_3) δ : 139.2 (Ar-C), 129.1 (Ar-CH), 128.5 (Ar-CH), 126.3 (Ar-CH), 72.0 (ArCH₂CH₂), 71.3 (Ar(CH₂)₂OCH₂), 36.6 (ArCH₂CH₂), 32.1 (CH₂), 29.9 – 29.8 (m, 10C, 10 \times CH₂), 29.8 (CH₂), 29.6 (CH₂), 29.5 (CH₂), 26.3 (CH₂), 22.9 (CH₂), 14.3 (CH₃); **HRMS**: (ESI⁺) Calculated for $[\text{C}_{26}\text{H}_{46}\text{NaO}]^+$ $[\text{M}+\text{Na}]^+$: 397.3441. Found: 397.3447; ν_{max} (neat)/ cm^{-1} : 2921, 2851, 1732, 1465, 1113.

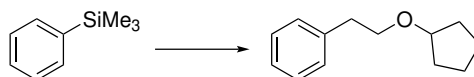
(2-(isopentyloxy)ethyl)benzene (6i)

Subjecting phenyltrimethylsilane **3a** (52 μL , 0.30 mmol) and isoamyl alcohol (131 μL , 1.2 mmol) to **GP-3** (0.075 eq. Ph_3PAuCl , 0.25 M) for 18 h afforded the title compound (50 mg, 87%) as a colourless oil (eluent: 1% to 2% Et_2O /pentane).

$^1\text{H NMR}$ (400 MHz; CDCl_3) δ : 7.33 – 7.18 (m, 5H, Ar-CH), 3.63 (t, $J = 7.3$ Hz, 2H, C6-H), 3.47 (t, $J = 6.9$ Hz, 2H, C7-H), 2.90 (t, $J = 7.3$ Hz, 2H, C5-H), 1.69 (septet, $J = 6.7$ Hz, 1H, C9-H), 1.48 (app q, $J = 6.9$ Hz, 2H, C8-H), 0.90 (d, $J = 6.6$ Hz, 6H, C10-H); $^{13}\text{C NMR}$ (101 MHz; CDCl_3) δ : 139.2 (Ar-C), 129.0 (Ar-CH), 128.4 (Ar-CH), 126.3 (Ar-CH), 72.0 (C6), 69.6 (C7), 38.7 (C8), 36.7 (C5), 25.2 (C9), 22.8 (C10); **HRMS**:

(EI⁺) Calculated for [C₁₃H₂₀O]⁺ [M]⁺: 192.1514. Found: 192.1510; ν_{max} (neat)/ cm⁻¹: 2953, 2925, 2865, 1496, 1466, 1453, 1366, 1108, 747, 698.

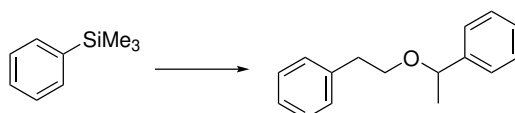
(2-(cyclopentyloxy)ethyl)benzene (6j)



Subjecting phenyltrimethylsilane **3a** (52 μ L, 0.30 mmol) and cyclopentanol (109 μ L, 1.2 mmol) to **GP-3** (0.075 eq. Ph₃PAuCl, 0.25 M) for 18 h afforded the title compound (45 mg, 79%) as a colourless oil (eluent: 5% Et₂O/pentane).

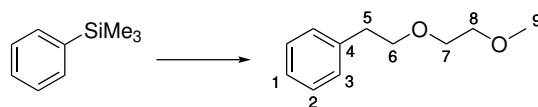
¹H NMR (400 MHz; CDCl₃) δ : 7.33 – 7.18 (m, 5H, Ar-CH), 3.92 (m, 1H, cyclopentyl-CH), 3.60 (t, J = 7.4 Hz, 2H, CH₂), 2.88 (t, J = 7.4 Hz, 2H, CH₂), 1.79 – 1.46 (m, 8H, 4 \times cyclopentyl-CH₂); ¹³C NMR (101 MHz; CDCl₃) δ : 139.3 (Ar-C), 129.0 (Ar-CH), 128.4 (Ar-CH), 126.2 (Ar-CH), 81.6 (cyclopentyl-CH), 70.0 (CH₂), 36.8 (CH₂), 32.4 (cyclopentyl-CH₂), 23.7 (cyclopentyl-CH₂). The spectroscopic properties of this compound were consistent with literature data.²⁸³

(1-phenethoxyethyl)benzene (6k)



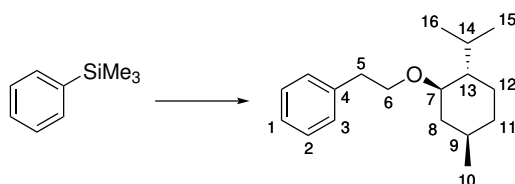
Subjecting phenyltrimethylsilane **3a** (68 μ L, 0.40 mmol) and 1-phenylethanol (145 μ L, 1.2 mmol) to **GP-3** (0.05 eq. Ph₃PAuCl, 1 M) for 18 h afforded the title compound (18 mg, 20%) as a colourless oil (eluent: 1% to 3% Et₂O/pentane).

¹H NMR (400 MHz; CDCl₃) δ : 7.36 – 7.16 (m, 10H, Ar-CH), 4.42 (q, J = 6.5 Hz, 1H, OCH(CH₃)(Ph)), 3.53 (t, J = 7.3 Hz, 2H, CH₂), 3.01 – 2.76 (m, 2H, CH₂), 1.44 (d, J = 6.5 Hz, 3H, CH₃); ¹³C NMR (126 MHz; CDCl₃) δ : 144.1 (Ar-C), 139.2 (Ar-C), 129.1 (Ar-CH), 128.5 (Ar-CH), 128.4 (Ar-CH), 127.5 (Ar-CH), 126.3 (Ar-CH), 126.2 (Ar-CH), 78.2 (OCH(CH₃)(Ph)), 69.7 (CH₂), 36.7 (CH₂), 24.3 (CH₃). The spectroscopic properties of this compound were consistent with literature data.²⁸⁴

(2-(2-methoxyethoxy)ethyl)benzene (6l)

Subjecting phenyltrimethylsilane **3a** (52 μ L, 0.30 mmol) and 2-methoxyethanol (95 μ L, 1.2 mmol) to **GP-3** (0.075 eq. Ph_3PAuCl , 0.25 M) for 18 h afforded the title compound (39 mg, 72%) as a colourless oil (eluent: 15% to 30% Et_2O /pentane).

$^1\text{H NMR}$ (400 MHz; CDCl_3) δ : 7.32 – 7.18 (m, 5H, Ar- $\underline{\text{C}}\text{H}$), 3.69 (t, $J = 7.7$ Hz, 2H, C6- $\underline{\text{H}}_2$), 3.63 – 3.59 (m, 2H, C7- $\underline{\text{H}}_2$), 3.57 – 3.53 (m, 2H, C8- $\underline{\text{H}}_2$), 3.39 (s, 3H, C9- $\underline{\text{H}}_3$), 2.93 (t, $J = 7.5$ Hz, 2H, C5- $\underline{\text{H}}_2$); $^{13}\text{C NMR}$ (101 MHz; CDCl_3) δ : 138.9 (Ar- $\underline{\text{C}}$), 129.0 (Ar- $\underline{\text{C}}\text{H}$), 128.4 (Ar- $\underline{\text{C}}\text{H}$), 126.3 (Ar- $\underline{\text{C}}\text{H}$), 72.6 (C6), 72.0 (C8), 70.3 (C7), 59.2 (C9), 36.4 (C5). The spectroscopic properties of this compound were consistent with literature data.²⁸⁵

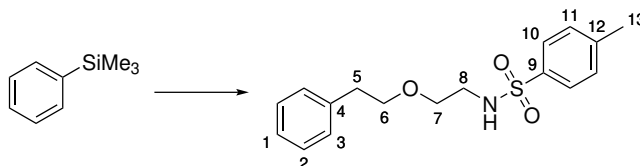
O-(2-phenylethyl)menthol (6m)

Subjecting phenyltrimethylsilane **3a** (52 μ L, 0.40 mmol) and DL-menthol (188 mg, 1.2 mmol) to **GP-3** (0.075 eq. Ph_3PAuCl , 0.25 M) for 18 h afforded the title compound (53 mg, 68%) as a colourless oil (eluent: 1% to 3% Et_2O /pentane).

$^1\text{H NMR}$ (500 MHz; CDCl_3) δ : 7.34 – 7.13 (m, 5H, Ar- $\underline{\text{C}}\text{H}$), 3.89 – 3.81 (m, 1H, C6- $\underline{\text{H}}_2$ -a), 3.53 – 3.44 (m, 1H, C6- $\underline{\text{H}}_2$ -b), 3.03 (td, $J = 10.6, 4.1$ Hz, 1H, C7- $\underline{\text{H}}$), 2.88 (t, $J = 7.5$ Hz, 2H, C5- $\underline{\text{H}}_2$), 2.22 – 2.04 (m, 2H, C8- $\underline{\text{H}}_{2a}$, C9- $\underline{\text{H}}$), 1.69 – 1.54 (m, 2H, C11- $\underline{\text{H}}_{2a}$, C12- $\underline{\text{H}}_{2a}$), 1.33 (m, 1H, C14- $\underline{\text{H}}$), 1.22 (ddt, $J = 12.2, 10.3, 3.1$ Hz, 1H, C13- $\underline{\text{H}}$), 1.03 – 0.77 (m, 9H, C8- $\underline{\text{H}}_{2b}$, C11- $\underline{\text{H}}_{2b}$, C12- $\underline{\text{H}}_{2b}$, C15- $\underline{\text{H}}_3$, C16- $\underline{\text{H}}_3$), 0.69 (d, $J = 6.9$ Hz, 3H, C10- $\underline{\text{H}}_3$); $^{13}\text{C NMR}$ (101 MHz; CDCl_3) δ : 139.4 (C4), 129.0 (Ar- $\underline{\text{C}}\text{H}$), 128.4 (Ar- $\underline{\text{C}}\text{H}$), 126.2 (Ar- $\underline{\text{C}}\text{H}$), 79.7 (C7), 69.8 (C6), 48.4 (C13), 40.7 (C8), 37.1 (C5), 34.7 (C11), 31.7

(C14), 25.7 (C9), 23.5 (C12), 22.5 (C15 or C16), 21.1 (C15 or C16), 16.3 (C10); **HRMS**: (ESI) Calculated for $[C_{18}H_{28}NaO]^+$ $[M+Na]^+$: 283.2032. Found: 283.2030; ν_{max} (neat)/ cm^{-1} : 3027, 2918, 2918, 2866, 1496, 1453, 1369, 1089, 1108, 747.

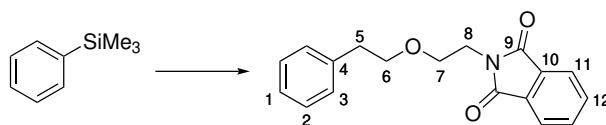
4-methyl-*N*-(2-phenethoxyethyl)benzenesulfonamide (6n)



Subjecting phenyltrimethylsilane **3a** (68 μ L, 0.40 mmol) and 4-methyl-*N*-(2-phenethoxyethyl)benzenesulfonamide (172 mg, 0.8 mmol) to **GP-3** (0.075 eq. Ph_3PAuCl , 1 M) for 18 h afforded the title compound (56 mg, 44%) as a colourless oil (eluent: 5% to 25% acetone/pentane).

1H NMR (400 MHz; $CDCl_3$) δ : 7.71 – 7.65 (m, 2H, Ar-CH), 7.33 – 7.26 (m, 4H, Ar-CH), 7.26 – 7.21 (m, 1H, Ar-CH), 7.19 – 7.15 (m, 2H, Ar-CH), 4.72 (t, $J = 6.0$ Hz, 1H, NH), 3.55 (t, $J = 6.9$ Hz, 2H, C6- H_2), 3.41 (t, $J = 5.0$ Hz, 2H, C7- H_2), 3.08 (m, 2H, C8- H_2), 2.81 (t, $J = 6.9$ Hz, 2H, C5- H_2), 2.42 (s, 3H, C13- H_3); ^{13}C NMR (101 MHz; $CDCl_3$) δ : 143.5 (C12), 138.8 (C4), 137.1 (C9), 129.8 (Ar-CH), 128.9 (Ar-CH), 128.6 (Ar-CH), 127.2 (Ar-CH), 126.5 (Ar-CH), 71.9 (C6), 68.7 (C7), 43.0 (C8), 36.2 (C5), 21.6 (C13); **HRMS**: (ESI) Calculated for $[C_{17}H_{22}NO_3S]^+$ $[M+H]^+$: 320.1315. Found: 320.1309; ν_{max} (neat)/ cm^{-1} : 3278, 2865, 1598, 1453, 1325, 1158, 1091.

2-(2-phenethoxyethyl)isoindoline-1,3-dione (6o)



Subjecting phenyltrimethylsilane **3a** (68 μ L, 0.40 mmol) and *N*-(2-hydroxyethyl)phthalimide (153 mg, 0.8 mmol) to **GP-3** (0.075 eq. Ph_3PAuCl , 1 M) for 18 h afforded the title compound (54 mg, 46%) as a colourless oil (eluent: 1% to 3% acetone/PhMe).

$^1\text{H NMR}$ (500 MHz; CDCl_3) δ : 7.84 (m, 2H, C11-H), 7.72 (m, 1H, C12-H), 7.18 – 7.07 (m, 5H, C1-H, C2-H, C3-H), 3.89 (t, $J = 5.8$ Hz, 2H, C8-H₂), 3.70 – 3.64 (m, 4H, C7-H₂, C6-H₂), 2.82 (t, $J = 7.0$ Hz, 2H, C5-H₂); $^{13}\text{C NMR}$ (101 MHz; CDCl_3) δ : 168.3 (C9), 138.8 (C4), 133.9 (C12), 132.1 (C10), 128.9 (Ar-CH), 128.2 (Ar-CH), 126.1 (Ar-CH), 123.3 (C11), 71.7 (C6), 67.5 (C7), 37.4 (C8), 36.2 (C5); **HRMS**: (ESI) Calculated for $[\text{C}_{18}\text{H}_{17}\text{NNaO}_3]^+$ $[\text{M}+\text{Na}]^+$: 318.1101. Found: 318.1099; ν_{max} (neat)/ cm^{-1} : 3027, 3863, 1773, 1707, 1391, 1111, 1025, 719.

5.2.6 Optimisation Procedure

Ethylene balloon procedure

To a reaction tube was added a stir bar, catalyst, oxidant and any other solid reagents (quantities depicted in Chapter 2, Table 2.1). The reaction tube was sealed with a rubber septum and Parafilm, then a needle-tipped ethylene balloon was pierced through the septum. An exit needle was pierced through the septum and the tube was purged with ethylene for 2–3 minutes. With stirring, the solvent (MeCN:MeOH, 9:1, 0.05 M with respect to phenyltrimethylsilane, unless otherwise stated), followed by phenyltrimethylsilane (0.25 mmol) and any other liquid reagents (quantities depicted in Chapter 2, Table 2.1) were added *via* syringe through the exit needle. Dodecane (100 μL , 0.44 mmol) was added as an internal standard, then the exit needle was sealed and the reaction tube was placed onto a pre-heated heating block (temperatures specified in Chapter 2, Table 2.1) for the specified time. Aliquots were removed *via* syringe through the exit needle and analysed by GC-FID.

Sealed tube procedure

To a J-Young's valve reaction tube was added a stir bar, catalyst, oxidant and any other solid reagents (quantities depicted in Chapter 2, Table 2.1). With stirring, the solvent

(MeCN:MeOH, 9:1, 0.05 M with respect to phenyltrimethylsilane, unless otherwise stated), followed by phenyltrimethylsilane (0.25 mmol) and any other liquid reagents (quantities depicted in Chapter 2, Table 2.1) were added via syringe. Dodecane (100 μ L, 0.44 mmol) was then added as an internal standard and the reaction tube was briefly purged, then pressurized to 1 bar with ethylene and sealed. The reaction tube was placed onto a pre-heated heating block (temperatures specified in Chapter 2, Table 2.1). After the specified time, an aliquot was removed and analysed by GC-FID.

5.2.7 Mechanistic Experiments

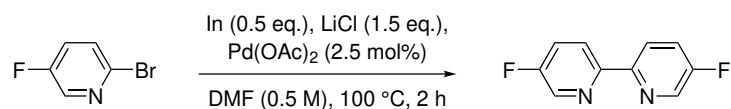
General Procedure For ^{19}F NMR Kinetics

To a 1.75 mL glass screw-top vial was added (4-fluorophenyl)trimethylsilane **3b** (100 μ L, 0.38 M in MeCN, 0.04 mmol), catalyst (400 μ L, 0.0050 M in MeCN, 0.002 mmol), hexafluorobenzene internal standard (50 μ L, 0.64 M in MeCN, 0.032 mmol), IBA-OTf (19 mg, 0.044 mmol), MeOH (80 μ L), and MeCN (170 μ L) to give an overall concentration of 0.05 M (MeCN:MeOH, 9:1) with respect to the arylsilane. The vial was sealed and the mixture was gently heated with shaking until homogeneous (approximately 40–50 $^{\circ}\text{C}$ for 15–30 seconds). The solution was then transferred to a J-Young's valve NMR tube, which was pressurised to 1 bar with ethylene and sealed. The reaction was then placed into a pre-heated NMR spectrometer (500 MHz) and data collection was started immediately. NMR parameters: nucleus = ^{19}F , frequency = 470 MHz, relaxation delay = 2 s, number of scans = 24, temperature = 50 $^{\circ}\text{C}$.

5.3 Experimental Procedures Relevant to Chapter 3

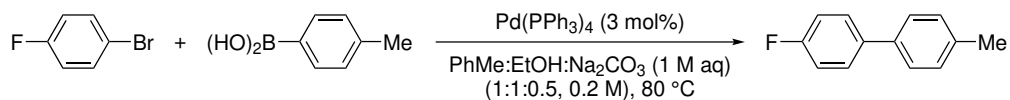
5.3.1 Organic Compounds

5,5'-difluoro-2,2'-bipyridine (F₂-bipy)



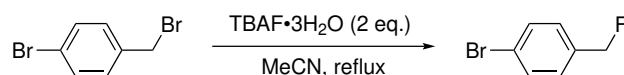
Adapted from the reported procedure.²¹² A mixture of 2-bromo-5-fluoropyridine (3.50 g, 19.9 mmol), Pd(OAc)₂ (112 mg, 0.50 mmol), LiCl (1.27 g, 29.9 mmol) and indium powder (1.15 g, 10 mmol) in anhydrous DMF (40 mL) was deoxygenated by purging the solution with N₂ for 10 minutes. The reaction was then heated to 100 °C for 2 h then cooled to r.t. and quenched with sat. NaHCO₃ (50 mL) and H₂O (100 mL). The layers were separated and the aqueous layer was extracted with EtOAc (3 × 50 mL). The combined organic portions were washed with H₂O (60 mL) then brine (40 mL), dried over MgSO₄, filtered and concentrated *in vacuo*. Purification by column chromatography (eluent: 5% EtOAc/*n*-hexane) afforded the title compound (1.72 g, 90%) as a colourless solid.

¹H NMR (400 MHz, CDCl₃) δ: 8.48 (d, *J* = 2.9 Hz, 2H, Ar-CH), 8.36 (dd, *J* = 8.9, 4.5 Hz, 2H, Ar-CH), 7.50 (td, *J* = 8.5, 2.9 Hz, 2H, Ar-CH); ¹³C{¹H} NMR (101 MHz, CDCl₃) δ: 159.9 (d, *J* = 260 Hz, Ar-CF), 151.7 (d, *J* = 4.1 Hz, Ar-C), 137.4 (d, *J* = 24 Hz, Ar-CH), 123.8 (d, *J* = 18 Hz, Ar-CH), 122.2 (d, *J* = 5.4 Hz, Ar-CH); ¹⁹F NMR (377 MHz, CDCl₃) δ -127.4 (m); HRMS: (ESI)⁺ Calculated for [C₁₀H₆F₂N₂Na]⁺ [M+Na]⁺: 215.0391. Found: 215.0397; *v*_{max} (neat)/ cm⁻¹: 3053, 1577, 1456, 1411, 1376, 1223, 1206, 1021, 907, 837. The ¹H and ¹³CNMR spectroscopic data for this compound were verified using 2D NMR spectroscopy methods and were *not* consistent with literature data.²¹²

4-fluoro-4'-methyl-1,1'-biphenyl (58)

Following the reported procedure,²⁸⁶ a genuine sample of **58** was prepared for GC-FID calibration and to confirm identity of products from transmetalation studies. A flask was charged with 1-bromo-4-fluorobenzene (1.5 g, 8.6 mmol), Pd(PPh₃)₄ (298 mg, 0.26 mmol), PhMe (10 ml), EtOH (10 mL), and 1 M aqueous Na₂CO₃ (10 mL) then stirred at room temperature for 15 minutes. *p*-Tolylboronic acid (1.4 g, 10.3 mmol) was added and the resulting mixture was stirred at 80 °C for 48 hours. After cooling to room temperature, the mixture was diluted with H₂O (60 mL) and extracted with EtOAc (3 × 30 mL). The combined organic portions were washed with brine (30 mL), dried over MgSO₄, filtered and concentrated *in vacuo*. Following purification by column chromatography (eluent: pentane) the title compound was obtained as a colourless solid (1.26 g, 79%).

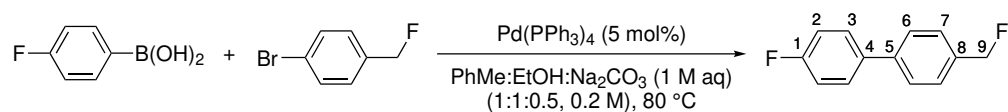
¹H NMR (400 MHz; CDCl₃) δ: 7.55 – 7.49 (m, 2H, Ar-CH), 7.46 – 7.40 (m, 2H, Ar-CH), 7.27 – 7.21 (m, 2H, Ar-CH), 7.13 – 7.07 (m, 2H, Ar-CH), 2.39 (s, 3H, CH₃); ¹³C NMR (101 MHz; CDCl₃) δ: 162.4 (d, *J* = 246 Hz, Ar-C-F), 137.5 (4° C), 137.4 (d, *J* = 3.3 Hz, 4° C), 137.2 (4° C), 129.7 (Ar-CH), 128.6 (d, *J* = 8.2 Hz, (Ar-CH), 127.0 (Ar-CH), 115.7 (d, *J* = 22 Hz, Ar-CH), 21.2 (CH₃); ¹⁹F NMR (377 MHz; CDCl₃) δ: -116.2 (m). The spectroscopic properties of this compound were consistent with literature data.²⁸⁷

1-bromo-4-(fluoromethyl)benzene (122)

Following the reported procedure.²⁸⁸ A solution of 4-bromobenzyl bromide (6.96 g, 11.0 mmol) and TBAF·3H₂O (6.96 g, 22.1 mmol) in MeCN (110 mL) was heated to reflux for 2 h. After cooling to room temperature the solvent was removed *in vacuo* to afford a yellow oil. Purification by column chromatography (25% Et₂O in hexane) afforded the title compound as a colourless oil (1.42 g, 68%), which solidified upon standing.

$^1\text{H NMR}$ (400 MHz; CDCl_3) δ : 7.55 – 7.50 (m, 2H, Ar-CH), 7.28 – 7.22 (m, 2H, Ar-CH), 5.33 (d, $J = 48$ Hz, 2H, CH_2F); $^{13}\text{C NMR}$ (101 MHz; CDCl_3) δ : 135.3 (d, $J = 17.3$ Hz, 4°C), 131.9 (Ar-C), 129.2 (d, $J = 5.9$ Hz, Ar-C), 123.0 (d, $J = 3.5$ Hz, 4°C), 83.91 (d, $J = 167$ Hz, CH_2F); $^{19}\text{F NMR}$ (377 MHz; CDCl_3) δ : -208.2 (t, $J = 48$ Hz). The spectroscopic properties of this compound were consistent with literature data.²⁸⁸

4-fluoro-4'-(fluoromethyl)-1,1'-biphenyl (**123**)



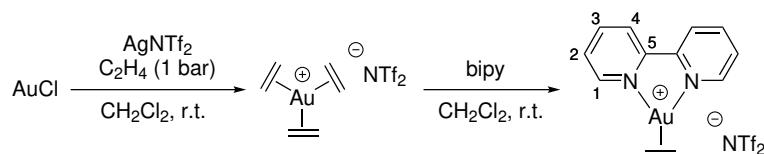
Adapted from the reported procedure,²⁸⁶ a genuine sample of **123** was required for GC-FID calibration and to confirm identity of products from transmetalation studies. A flask was charged with 1-bromo-4-(fluoromethyl)benzene **122** (400 mg, 2.12 mmol), $\text{Pd}(\text{PPh}_3)_4$ (122 mg, 0.11 mmol), PhMe (3 mL), EtOH (3 mL), and 1 M aqueous Na_2CO_3 (3 mL) then stirred at room temperature for 15 minutes. 4-Fluorophenylboronic acid (355 mg, 2.54 mmol) was added and the resulting mixture was stirred at 80°C for 18 hours. After cooling to room temperature, the mixture was diluted with H_2O (30 ml) and extracted with EtOAc (3×20 mL). The combined organic portions were washed with brine (20 mL), dried over MgSO_4 , filtered and concentrated *in vacuo*. Following purification by column chromatography (eluent: 5% to 20% PhMe/pentane) the title compound was obtained as a colourless solid (177 mg, 41%).

$^1\text{H NMR}$ (400 MHz; CDCl_3) δ : 7.60 – 7.53 (m, 4H, C3-H, C6-H), 7.46 (m, 2H, C7-H), 7.18 – 7.11 (m, 2H, C2-H), 5.43 (d, $J = 47.8$ Hz, 2H, C9-H); $^{13}\text{C NMR}$ (101 MHz; CDCl_3) δ : 162.8 (d, $J = 247$ Hz, C1), 140.90 (d, $J = 3.3$ Hz, C4), 136.9 (C5), 135.3 (d, $J = 17$ Hz, C8), 128.9 (d, $J = 7.9$ Hz, C3), 128.2 (d, $J = 5.8$ Hz, C7), 127.4 (C6), 115.9 (d, $J = 21$ Hz, C2), 84.5 (d, $J = 166$ Hz, C9); $^{19}\text{F NMR}$ (377 MHz; CDCl_3) δ : -115.3 (m, C1-F), -206.5 (t, $J = 48$ Hz, C9-F); **HRMS**: (EI)⁺ Calculated for $[\text{C}_{13}\text{H}_{10}\text{F}_2]^+$ [M]⁺:

204.0751. Found: 204.0750; ν_{max} (neat)/ cm^{-1} : 3035, 2897, 1603, 1524, 1498, 1378, 1236, 1194, 1161, 982, 908, 818, 734.

5.3.2 Gold Complexes

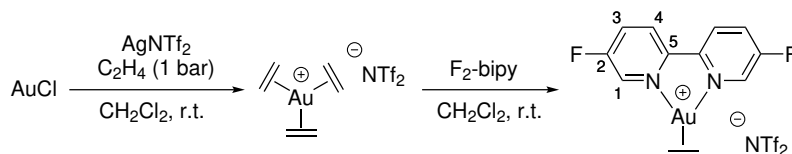
$[(\kappa^2\text{-}2,2'\text{-bipyridine})\text{Au}(\eta^2\text{-C}_2\text{H}_4)][\text{NTf}_2]$ (**51a**)



Under an inert atmosphere, a J-Young's valve reaction tube was charged with AuCl (100 mg, 0.43 mmol) and AgNTf₂ (167 mg, 0.43 mmol) then wrapped with foil to protect the contents from light. CH₂Cl₂ (9 mL) was added and the flask was pressurised with ethylene (1 bar) and stirred in the dark for 3 h at room temperature. While maintaining darkness, the reaction mixture was filtered (porosity 3, Celite, washed with 3 × 10 mL CH₂Cl₂) into a flask containing neat 2,2'-bipyridine (67 mg, 0.43 mmol). The colourless solution was concentrated to approx. 10 mL then Et₂O was added as a layer. Storage at -20 °C for 16 h gave a colourless crystalline solid. After decanting the solvent, the solid was washed with Et₂O (3 × 10 mL) and dried *in vacuo* to afford the title compound (120 mg, 43%) as colourless crystals. See Section 5.5, Table 5.3 for full crystallographic details.

¹H NMR (400 MHz; CD₂Cl₂) δ : 8.86 – 8.81 (m, 2H, C1-H), 8.49 (dt, $J = 8.2, 1.1$ Hz, 1H, C4-H), 8.31 (td, $J = 7.9, 1.7$ Hz, 2H, C3-H), 7.85 (ddd, $J = 7.7, 5.2, 1.2$ Hz, 2H, C2-H), 3.83 (s, 4H, ethylene-CH₂); ¹³C{¹H} NMR (126 MHz; CD₂Cl₂) δ : 152.5 (C5), 152.4 (C1), 142.4 (C3), 128.5 (C2), 124.4 (C4), 120.4 (q, $J = 322$ Hz, CF₃), 62.3 (ethylene-CH₂); HRMS: (ESI)⁺ Calculated for [C₁₂H₁₂AuN₂]⁺ [M-NTf₂]⁺: 381.0661. Found: 381.0645.

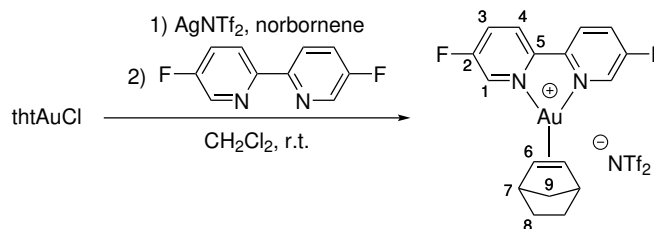
[(κ^2 -5,5'-difluoro-2,2'-bipyridine)Au(η^2 -C₂H₄)] [NTf₂] (51b)



Under an inert atmosphere, a J-Young's valve reaction tube was charged with AuCl (200 mg, 0.86 mmol) and AgNTf₂ (334 mg, 0.86 mmol) and wrapped with foil to protect the contents from light. CH₂Cl₂ (30 mL) was added then the flask was pressurised with ethylene (1 bar) and stirred in the dark for 3 h at room temperature. While maintaining darkness, the reaction mixture was filtered (porosity 3, Celite, washed with 3 × 10 mL CH₂Cl₂) into a flask containing neat 5,5'-difluoro-2,2'-bipyridine (165 mg, 0.86 mmol). The filtrate was concentrated to approximately 10 mL then the solution was layered with Et₂O. Storage at room temperature for 16 h afforded colourless crystals. The solvent was decanted, washed with Et₂O (3 × 10 mL) and dried *in vacuo* to afford the title compound (372 mg, 62%) as colourless crystals. See Section 5.5, Table 5.4 for full crystallographic details.

¹H NMR (400 MHz; CD₂Cl₂) δ: 8.68 (d, *J* = 2.7 Hz, 2H, C1-H), 8.56 (dd, *J* = 9.1, 4.2 Hz, 2H, C4-H), 8.03 (m, 2H, C3-H), 3.90 (s, 4H, ethylene-CH₂); ¹³C{¹H} NMR (126 MHz; CD₂Cl₂) δ: 161.1 (d, *J* = 260 Hz, C2), 147.8 (d, *J* = 3.1 Hz, C5), 140.6 (d, *J* = 30.3 Hz, C1), 129.0 (d, *J* = 18.6 Hz, C3), 125.7 (d, *J* = 7.4 Hz, C4), 119.8 (q, *J* = 320 Hz, CF₃), 63.81 (CH₂); HRMS: (ESI)⁺ Calculated for [C₁₂H₁₀AuF₂N₂]⁺ [M-NTf₂]⁺: 417.0472. Found: 417.0478; *v*_{max} (neat)/ cm⁻¹: 3073, 3053, 1591, 1479, 1349, 1329, 1181, 1198, 1137, 1048, 845.

[(κ^2 -5,5'-difluoro-2,2'-bipyridine)-Au-(η^2 -norbornene)][NTf₂] (51c)

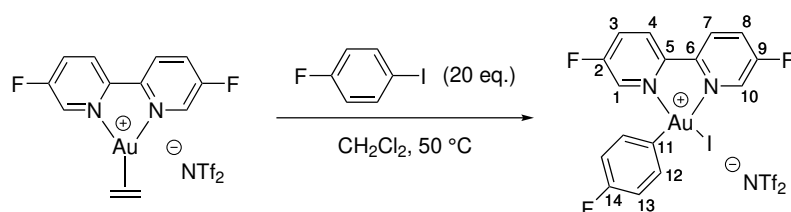


In a glovebox, a flask was charged with thtAuCl (204 mg, 0.64 mmol) and AgNTf₂ (247 mg, 0.64 mmol) then wrapped with foil to protect the contents from light. The flask was removed from the glovebox then placed under an N₂ atmosphere, norbornene (1.21 g, 12.8 mmol) was added, followed by CH₂Cl₂ (15 mL). The reaction was stirred in the dark at r.t. for 18 h, then filtered through a pad of Celite to give a colourless solution. 5,5'-difluoro-2,2'-bipyridine (F₂-bipy) (135 mg, 0.70 mmol) was added and the solution was stirred at room temperature for 6 hours. The solution was concentrated to a minimum volume, then hexane was added to precipitate a colourless solid, which was washed with Et₂O and hexane. The solid was dissolved in CH₂Cl₂ (approx. 5 mL), layered with hexane then stored at -20 °C for 24 h, after which a grey crystalline solid was observed. The solid was filtered, washed with hexane, and dried *in vacuo* to afford the title compound (207 mg, 42%) as a grey solid. Single crystals suitable for X-ray diffraction were grown from a CH₂Cl₂ solution layered with hexane. See Section 5.5, Table 5.12 for full crystallographic details.

¹H NMR (500 MHz; CD₂Cl₂) δ: 8.71 (d, *J* = 2.7 Hz, 2H, C1-H), 8.56 (dd, *J* = 9.1, 4.2 Hz, 2H, C4-H), 8.08 – 8.01 (m, 2H, C3-H), 4.35 (s, 2H, C6-H), 3.22 (s, 2H, C7-H), 1.78 – 1.71 (m, 2H, C8-H_a), 1.18 – 1.10 (m, 3H, C8-H_b, C9-H_a), 0.82 – 0.75 (m, 1H, C9-H_b); ¹³C NMR (126 MHz; CD₂Cl₂) δ: 161.7 (d, *J* = 262 Hz, C2), 148.2 (d, *J* = 3.3 Hz, C5), 140.8 (d, *J* = 30 Hz, C1), 129.4 (d, *J* = 18.6 Hz, C4), 126.2 (d, *J* = 7.4 Hz, C5), 120.5 (q, *J* = 321 Hz, CF₃), 86.2 (C6), 44.0 (C9), 43.0 (C7), 25.0 (C8); ¹⁹F NMR (377 MHz; CDCl₂) δ: -79.5 (s, 6F, CF₃), -118.6 (m, 2F, C2-F); HRMS: (ESI)⁺ Calculated for

$[\text{C}_{17}\text{H}_{16}\text{AuF}_2\text{IN}_2]^+ [\text{M-NTf}_2]^+$: 483.0942. Found: 483.0945.

$[(\kappa^2\text{-5,5'-difluoro-2,2'-bipyridine})\text{Au}(\text{4-F-C}_6\text{H}_4\text{I})][\text{NTf}_2]$ (56a**)**

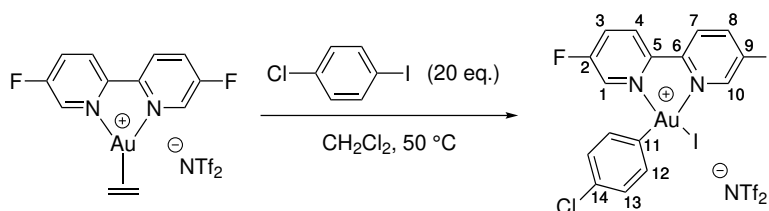


In a J-Young's valve reaction tube under an N_2 atmosphere, **51b** (82 mg, 0.118 mmol) was dissolved in CH_2Cl_2 (12 mL). 4-fluoroiodobenzene (0.27 mL, 2.35 mmol) was added then the flask was placed under a static vacuum (approx. 10^{-2} mbar), sealed, and stirred at 50°C . Every hour, the reaction was subjected to $3 \times$ freeze-pump-thaw cycles, before returning to stirring at 50°C under a static vacuum. After 1 h a yellow solution was observed, which was filtered and concentrated to approx. 2 mL. Hexane (approx. 15 mL) was added to precipitate a yellow solid which was filtered, washed with hexane (3×5 mL), and dried *in vacuo* to afford the title compound (88 mg, 84%) as a yellow solid. In the solid state, **3a** was found to be stable for months when stored at -20°C . Single crystals suitable for X-ray diffraction were grown from a CH_2Cl_2 solution layered with hexane. See Section 5.5, Table 5.5 for full crystallographic details.

$^1\text{H NMR}$ (400 MHz; CD_2Cl_2) δ : 9.49 (t, $J = 2.3$ Hz, 1H, C1-H or C10-H), 8.65 – 8.55 (m, 2H, C4-H, C7-H), 8.18 – 8.08 (m, 2H, C3-H, C8-H), 7.31 (t, $J = 2.4$ Hz, 1H, C1-H or C10-H), 7.22 – 7.16 (m, 2H, C12-H), 7.13 – 7.05 (m, 2H, C13-H); $^{13}\text{C}\{^1\text{H}\}$ NMR (126 MHz; CD_2Cl_2) δ : 164.1 (d, $J = 249$ Hz, C14), 162.8 (d, $J = 264$ Hz, C2 or C9), 161.4 (d, $J = 265$ Hz, C2 or C9), 151.6 (d, $J = 4.3$ Hz, C5 or C6), 150.2 (d, $J = 4.5$ Hz, C5 or C6), 140.7 (d, $J = 33$ Hz, C1 or C10), 136.3 (d, $J = 34$ Hz, C1 or C10), 134.9 (d, $J = 7.3$ Hz, C12), 132.1 (d, $J = 19.0$ Hz, C3 or C8), 131.0 (d, $J = 19.0$ Hz, C3 or C8), 128.4 (d, $J = 7.0$ Hz, C4 or C7), 128.3 (d, $J = 7.1$ Hz, C4 or C7), 120.2 (d, $J = 321$ Hz, $\underline{\text{C}}\text{F}_3$), 118.8 (d, $J = 21.7$ Hz, C13), 117.8 (d, $J = 1.2$ Hz, C11); $^{19}\text{F NMR}$ (377 MHz; CD_2Cl_2) δ : -79.3

(s, 6F, CF_3), -112.4 (m, 1F, C2-F or C9-F), -113.34 (m, 1F, C2-F or C9-F), -113.44 (m, 1F, C14-F); **HRMS**: (ESI)⁺ Calculated for $[\text{C}_{16}\text{H}_{10}\text{AuF}_3\text{IN}_2]^+$ $[\text{M-NTf}_2]^+$: 610.9501. Found: 610.9482.

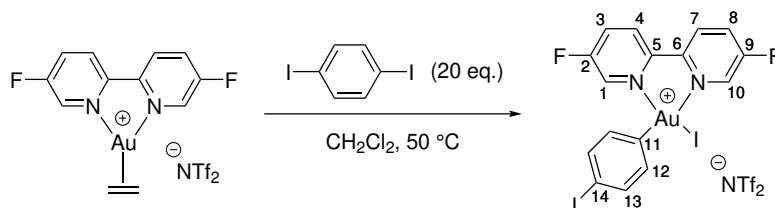
$[(\kappa^2\text{-5,5'-difluoro-2,2'-bipyridine)Au(4-Cl-C}_6\text{H}_4\text{)I][NTf}_2\text{]} (56b)$



Complex **56b** was synthesised analogously to **56a** using **51b** (25 mg, 0.036 mmol) and 1-chloro-4-iodobenzene (170 mg, 0.72 mmol). A total reaction time of 4 h was used and the title compound (26 mg, 79%) was obtained as a yellow solid. Single crystals suitable for X-ray diffraction were grown from a CH_2Cl_2 solution layered with pentane at $-20\text{ }^\circ\text{C}$. See Section 5.5, Table 5.7 for full crystallographic details.

$^1\text{H NMR}$ (500 MHz; CD_2Cl_2) δ : 9.60 – 9.52 (m, 1H, C1-H or C10-H), 8.69 (dd, $J = 9.1, 4.4$ Hz, 1H, C4-H or C7-H), 8.65 (dd, $J = 9.1, 4.6$ Hz, 1H, C4-H or C7-H), 8.27 – 8.12 (m, 2H, C3-H and C8-H), 7.44 (t, $J = 2.4$ Hz, 1H, C1-H or C10-H), 7.40 – 7.36 (m, 2H, C12-H or C13-H), 7.25 – 7.21 (m, 2H, C12-H or C13-H); **$^{13}\text{C}\{^1\text{H}\}$ NMR** (126 MHz; CD_2Cl_2) δ : 162.9 (d, $J = 264$ Hz, C2 or C9), 161.4 (d, $J = 264$ Hz, C2 or C9), 151.6 (d, $J = 4.1$ Hz, C5 or C6), 150.2 (d, $J = 4.4$ Hz, C5 or C6), 140.7 (d, $J = 33$ Hz, C1 or C10), 136.40 (d, $J = 33.9$ Hz, C1 or C10), 136.40 (C14), 135.0 (C12 or C13), 132.1 (d, $J = 19$ Hz, C3 or C8), 131.6 (C12 or C13), 131.1 (d, $J = 19$ Hz, C3 or C8), 128.5 – 128.1 (m 2C, C4 and C7), 122.1 (C11), 120.3 (q, $J = 322$ Hz, CF_3); **$^{19}\text{F NMR}$** (377 MHz; CD_2Cl_2) δ : -86.7 (s, 6H, CF_3), -119.7 (C2-F or C9-F), -120.7 (C2-F or C9-F); **HRMS**: (ESI)⁺ Calculated for $[\text{C}_{16}\text{H}_{10}\text{AuClF}_2\text{IN}_2]^+$ $[\text{M-NTf}_2]^+$: 626.9206. Found: 626.9210.

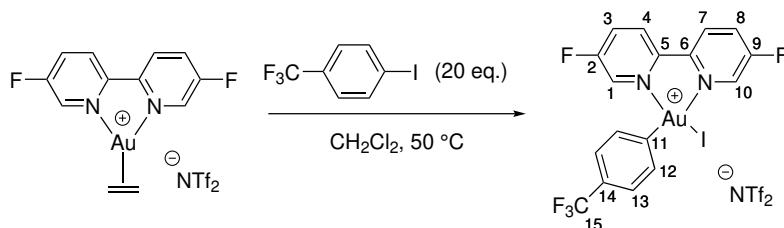
[(κ^2 -5,5'-difluoro-2,2'-bipyridine)Au(4-I-C₆H₄)I][NTf₂] (56c**)**



Complex **56c** was synthesised analogously to **56a** using **51b** (15 mg, 0.022 mmol) and 1,4-diiodobenzene (142 mg, 0.43 mmol). A total reaction time of 4 h was used and the title compound (15 mg, 68%) was obtained as a yellow solid. Single crystals suitable for X-ray diffraction were grown from a CH₂Cl₂ solution layered with pentane at -20 °C. See Section 5.5, Table 5.8 for full crystallographic details.

¹H NMR (500 MHz; CD₂Cl₂) δ : 9.60 (t, J = 2.2 Hz, 1H, C1-H or C10-H), 8.73 (dd, J = 9.1, 4.4 Hz, 1H, C4-H or C7-H), 8.69 (dd, J = 9.1, 4.6 Hz, 1H, C4-H or C7-H), 8.29 – 8.21 (m, 2H, C3-H, C8-H), 7.75 – 7.69 (m, 2H, C12-H), 7.51 (t, J = 2.4 Hz, 1H, C1-H or C10-H), 7.07 – 7.03 (m, 1H, C13-H); **¹³C{¹H} NMR** (126 MHz; CD₂Cl₂) δ : 162.8 (d, J = 264 Hz, C2 or C9), 161.4 (d, J = 265 Hz, C2 or C9), 151.6 (d, J = 4.3 Hz, C5 or C6), 150.2 (d, J = 4.3 Hz, C5 or C6), 140.7 (d, J = 33 Hz, C1 or C10), 140.4 (C12), 135.6 (C13), 136.5 (d, J = 34 Hz, C1 or C10), 132.14 (d, J = 19 Hz, C3 or C8), 131.0 (d, J = 19 Hz, C3 or C8), 128.6 – 128.0 (m, 2C, C4 or C7), 124.6 (C11), 120.28 (q, J = 322 Hz, CF₃), 96.0 (C14); **¹⁹F NMR** (377 MHz; CD₂Cl₂) δ : -79.2 (s, 6H, CF₃), -112.1 (C2-F or C9-F), -113.1 (C2-F or C9-F); **HRMS**: (ESI)⁺ Calculated for [C₁₆H₁₀AuF₂I₂N₂]⁺ [M-NTf₂]⁺: 718.8562. Found: 718.8594.

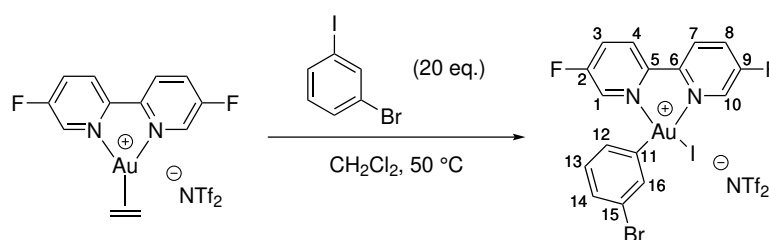
[(κ^2 -5,5'-difluoro-2,2'-bipyridine)Au(4-F₃C-C₆H₄)I][NTf₂] (56d**)**



Complex **56d** was synthesised analogously to **56a** using **51b** (24 mg, 0.034 mmol) and 4-iodobenzotrifluoride (101 μ L, 0.69 mmol). A total reaction time of 6 h was used and the title compound (26 mg, 82%) was obtained as a yellow solid.

$^1\text{H NMR}$ (500 MHz; CD_2Cl_2) δ : 9.59 (d, $J = 2.4$ Hz, 1H, C1-H or C10-H), 8.68 (dd, $J = 9.1, 4.5$ Hz, 1H, C4-H or C7-H), 8.64 (dd, $J = 9.1, 4.6$ Hz, 1H, C4-H or C7-H), 8.24 – 8.17 (m, 2H, C3-H, C8-H), 7.65 – 7.61 (m, 2H, C13-H), 7.50 – 7.46 (m, 2H, C12-H), 7.37 (t, $J = 2.4$ Hz, 1H, C1-H or C10-H); $^{13}\text{C}\{^1\text{H}\}$ NMR (126 MHz; CD_2Cl_2) δ : 162.8 (d, $J = 264$ Hz, C2 or C9), 161.3 (d, $J = 264$ Hz, C2 or C9), 151.7 (d, $J = 4.2$ Hz, C2 or C9), 150.3 (d, $J = 4.3$ Hz, C2 or C9), 140.8 (d, $J = 33$ Hz, C1 or C10), 136.4 (d, $J = 34$ Hz, C1 or C10), 134.8 (C12), 132.1 (d, $J = 19$ Hz, C3 or C8), 132.0 (q, $J = 33.2$ Hz, C14), 131.0 (d, $J = 19$ Hz, C3 or C8), 128.3 (m, 3C, C4, C7, C11), 128.0 (q, $J = 3.7$ Hz, C13), 124.0 (q, $J = 270$ Hz, C15), 120.3 (q, $J = 320$ Hz, CF_3); $^{19}\text{F NMR}$ (377 MHz; CD_2Cl_2) δ : -63.0 (s, 3H, C15-F₃) -79.3 (s, 6H, CF_3), -112.3 (C2-F or C9-F), -113.24 (C2-F or C9-F); **HRMS**: (ESI)⁺ Calculated for $[\text{C}_{17}\text{H}_{10}\text{AuF}_5\text{IN}_2]^+ [\text{M-NTf}_2]^+$: 660.9469. Found: 660.9442.

$[(\kappa^2\text{-}5,5'\text{-difluoro-}2,2'\text{-bipyridyl})\text{Au}(\text{3-Br-C}_6\text{H}_4)\text{I}][\text{NTf}_2]$ (56e**)**

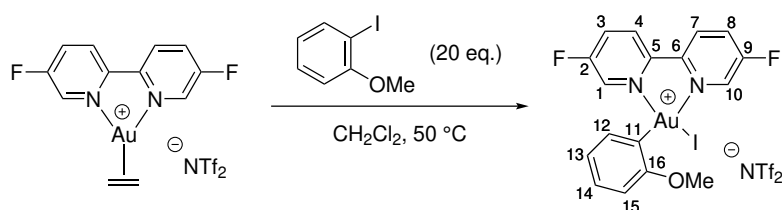


Complex **56e** was synthesised analogously to **56a** using **51b** (15 mg, 0.022 mmol) and 3-bromoiodobenzene (54 μ L, 0.43 mmol). A total reaction time of 4 h was used and the title compound (12 mg, 57%) was obtained as a yellow solid.

$^1\text{H NMR}$ (400 MHz; CD_2Cl_2) δ : 9.57 (t, $J = 2.2$ Hz, 1H, C1-H or C10-H), 8.73 – 8.64 (m, 2H, C4-H or C7-H), 8.27 – 8.17 (m, 2H, C3-H or C8-H), 7.52 (dt, $J = 7.4, 1.6$ Hz, 1H, 3-bromophenyl-H), 7.45 (t, $J = 1.6$ Hz, 1H, 3-bromophenyl-H), 7.42 (t, $J = 2.4$ Hz,

^1H , C1-H or C10-H), 7.29 – 7.20 (m, 2H, 2 × 3-bromophenyl-H); $^{13}\text{C}\{^1\text{H}\}$ NMR (126 MHz; CD_2Cl_2) δ : 162.3 (d, $J = 264$ Hz, C2 or C9), 160.7 (d, $J = 265$ Hz, C2 or C9), 151.0 (d, $J = 4.2$ Hz, C5 or C6), 149.6 (d, $J = 4.5$ Hz, C5 or C6), 140.2 (d, $J = 33.2$ Hz, C1 or C10), 135.9 (d, $J = 33.9$ Hz, C1 or C10), 135.7 (3-bromophenyl-CH), 132.5 (3-bromophenyl-CH), 132.3 (3-bromophenyl-CH), 132.0 (3-bromophenyl-CH), 131.6 (d, $J = 19.0$ Hz, C3 or C8), 130.5 (d, $J = 19.1$ Hz, C3 or C8), 127.8 (d, $J = 7.0$ Hz, C4 or C7), 127.7 (d, $J = 7.3$ Hz, C4 or C7), 124.6 (C11 or C15), 124.1 (C11 or C15), 119.71 (q, $J = 321$ Hz, $\underline{\text{CF}}_3$); ^{19}F NMR (377 MHz; CD_2Cl_2) δ : -79.3 (s, 6H, $\underline{\text{CF}}_3$), -112.1 (C2-F or C9-F), -113.2 (C2-F or C9-F); HRMS: (ESI) $^+$ Calculated for $[\text{C}_{16}\text{H}_{10}\text{AuBrF}_2\text{IN}_2]^+$ $[\text{M-NTf}_2]^+$: 670.8706. Found: 670.8699.

$[(\kappa^2\text{-5,5' -difluoro-2,2' -bipyridyl)Au(2-MeO-C}_6\text{H}_4\text{)I][NTf}_2\text{]} (56\text{f})$

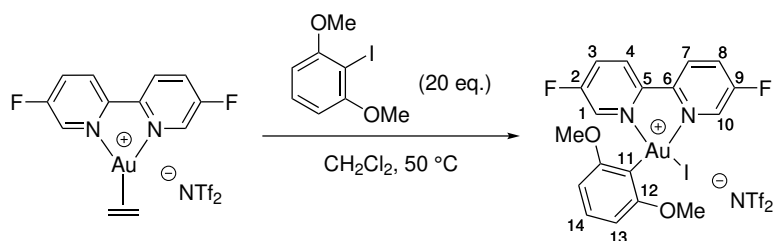


Complex **56f** was synthesised analogously to **56a** using **51b** (26 mg, 0.037 mmol) and 2-iodoanisole (100 μL , 0.74 mmol). A total reaction time of 3 h was used and the title compound (24 mg, 72%) was obtained as an orange solid. Single crystals suitable for X-ray diffraction were grown from a CH_2Cl_2 solution layered with pentane at -20 °C. See Section 5.5, Table 5.9 for full crystallographic details.

^1H NMR (500 MHz; CD_2Cl_2) δ 9.58 (t, $J = 2.3$ Hz, 1H, C1-H or C10-H), 8.80 (dd, $J = 9.1, 4.4$ Hz, 1H, C4-H or C7-H), 8.75 (dd, $J = 9.1, 4.6$ Hz, 1H, C4-H or C7-H), 8.26 – 8.20 (m, 2H, C3-H and C8-H), 7.41 (t, $J = 2.4$ Hz, 1H, C1-H or C10-H), 7.37 (ddd, $J = 8.3, 7.4, 1.4$ Hz, 1H, C13-H or C14-H), 7.19 (dd, $J = 7.9, 1.4$ Hz, 1H, C12-H or C15-H), 6.97 (td, $J = 7.6, 1.5$ Hz, 1H, C13-H or C14-H), 6.92 (dd, $J = 8.2, 1.4$ Hz, 1H, C12-H or C15-H), 3.78 (s, 3H, $\underline{\text{CH}}_3$); $^{13}\text{C}\{^1\text{H}\}$ NMR (126 MHz; CD_2Cl_2) δ : 162.9 (d, $J = 264$ Hz,

C2 or C9), 161.4 (d, $J = 264$ Hz, C2 or C9), 158.0 (C16), 151.6 (d, $J = 4.1$ Hz, C5 or C6), 150.2 (d, $J = 4.4$ Hz, C5 or C6), 140.5 (d, $J = 33$ Hz, C1 or C10), 136.2 (d, $J = 34$ Hz, C1 or C10), 135.4 (C12 or C15), 132.2 (d, $J = 19$ Hz, C3 or C8), 131.3 (C13 or C14), 131.1 (d, $J = 19$ Hz, C3 or C8), 128.8 – 128.3 (m, 2C, C4 and C7), 123.2 (C13 or C14), 120.4 (q, $J = 322$ Hz, $\underline{\text{CF}}_3$), 114.2 (C13 or C14), 113.3 (C11), 56.5 ($\underline{\text{CH}}_3$); ^{19}F NMR (377 MHz; CD_2Cl_2) δ : -79.2 (s, 6H, $\underline{\text{CF}}_3$), -112.6 (C2- $\underline{\text{F}}$ or C9- $\underline{\text{F}}$), -113.2 (C2- $\underline{\text{F}}$ or C9- $\underline{\text{F}}$); **HRMS**: (ESI) $^+$ Calculated for $[\text{C}_{17}\text{H}_{13}\text{AuF}_2\text{IN}_2\text{O}]^+ [\text{M-NTf}_2]^+$: 622.9701. Found: 622.9697.

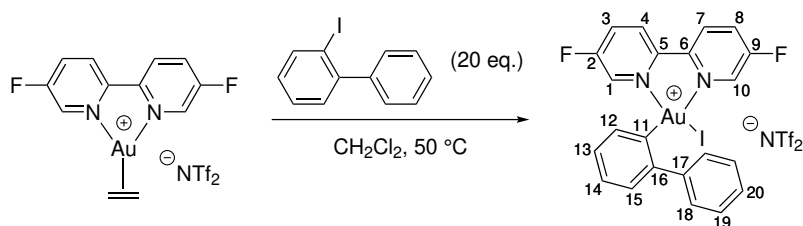
$[(\kappa^2\text{-5,5'-difluoro-2,2'-bipyridyl)Au(2,6-dimethoxyphenyl)I][\text{NTf}_2]$ (56g**)**



Complex **56g** was synthesised analogously to **56a** using **51b** (23 mg, 0.033 mmol) and 1-iodo-2,6-dimethoxybenzene (174 mg, 0.66 mmol). A total reaction time of 5 h was used and the title compound (24 mg, 78%) was obtained as an orange solid.

^1H NMR (500 MHz; CD_2Cl_2) δ : 9.63 (t, $J = 2.3$ Hz, 1H, C1- $\underline{\text{H}}$ or C10- $\underline{\text{H}}$), 8.85 (dd, $J = 9.1, 4.5$ Hz, 1H, C4- $\underline{\text{H}}$ or C7- $\underline{\text{H}}$), 8.80 (dd, $J = 9.1, 4.6$ Hz, 1H, C4- $\underline{\text{H}}$ or C7- $\underline{\text{H}}$), 8.30 – 8.20 (m, 2H, C3- $\underline{\text{H}}$ and C8- $\underline{\text{H}}$), 7.54 (t, $J = 2.4$ Hz, 1H, C1- $\underline{\text{H}}$ or C10- $\underline{\text{H}}$), 7.36 (t, $J = 8.3$ Hz, 1H, C14- $\underline{\text{H}}$), 6.57 (d, $J = 8.3$ Hz, 2H, C13- $\underline{\text{H}}$), 3.78 (s, 6H, $\underline{\text{CH}}_3$); $^{13}\text{C}\{^1\text{H}\}$ NMR (126 MHz, CD_2Cl_2) δ : 163.0 (d, $J = 264$ Hz, C2 or C9), 161.4 (d, $J = 264$ Hz, C2 or C9), 159.9 (C12), 151.7 (d, $J = 4.1$ Hz, C5 or C6), 150.4 (d, $J = 4.1$ Hz, C5 or C6), 140.6 (d, $J = 33$ Hz, C1 or C10), 136.2 (d, $J = 34$ Hz, C1 or C10), 132.7 (C14), 132.3 (d, $J = 19$ Hz, C3 or C8), 131.2 (d, $J = 19$ Hz, C3 or C8), 128.7 (m, 2C, C4 and C7), 120.4 (q, $J = 321$ Hz, $\underline{\text{CF}}_3$), 106.3 (C13), 100.2 (C11), 56.5 ($\underline{\text{CH}}_3$); ^{19}F NMR (377 MHz; CD_2Cl_2) δ : -79.4 ($\underline{\text{CF}}_3$), -112.8 (C2- $\underline{\text{F}}$ or C9- $\underline{\text{F}}$), -113.3 (C2- $\underline{\text{F}}$ or C9- $\underline{\text{F}}$); **HRMS**: (ESI) $^+$ Calculated for $[\text{C}_{18}\text{H}_{15}\text{AuF}_2\text{IN}_2\text{O}_2]^+ [\text{M-NTf}_2]^+$: 652.9807. Found: 652.9799.

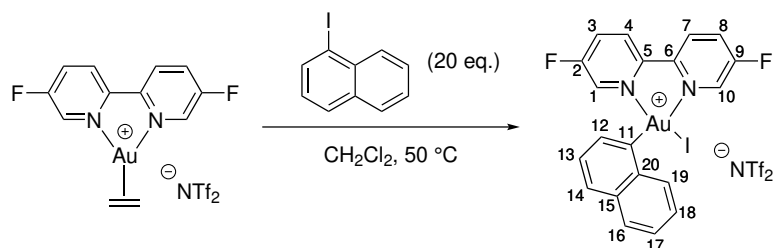
[(κ^2 -5,5'-difluoro-2,2'-bipyridine)Au(2-(C₆H₅)-C₆H₄)I][NTf₂] (56h**)**



Complex **56h** was synthesised analogously to **56a** using **51b** (14 mg, 0.020 mmol) and 2-iodobiphenyl (70 μ L, 0.40 mmol). A total reaction time of 3 h was used and the title compound (16 mg, 84%) was obtained as a yellow solid. Single crystals suitable for X-ray diffraction were grown from a saturated PhMe solution at -20 °C. See Section 5.5, Table 5.10 for full crystallographic details.

¹H NMR (500 MHz; CD₂Cl₂) δ : 9.53 – 9.49 (t, J = 2.2 Hz, 1H, C1-H or C10-H), 8.74 (dd, J = 9.1, 4.4 Hz, 1H, C4-H or C7-H), 8.70 (dd, J = 9.1, 4.6 Hz, 1H, C4-H or C7-H), 8.27 – 8.17 (m, 2H, C3-H, C8-H), 7.56 – 7.43 (m, 6H, C1-H or C10-H, 5 \times biphenyl-H), 7.39 – 7.25 (m, 4H, 4 \times biphenyl-H); ¹³C{¹H} NMR (126 MHz; CD₂Cl₂) δ : 162.2 (d, J = 264 Hz, C2 or C9), 160.6 (d, J = 264 Hz, C2 or C9), 150.8 (d, J = 4.1 Hz, C5 or C6), 149.2 (d, J = 4.5 Hz, C5 or C6), 143.5 (C16 or C17), 141.3 (C16 or C17), 140.0 (d, J = 33.1 Hz, C1 or C10), 135.5 (d, J = 34.1 Hz, C1 or C10), 135.3 (biphenyl-CH), 133.0 (biphenyl-CH), 131.7 (d, J = 18.8 Hz, C3 or C8), 130.5 (d, J = 18.9 Hz, C3 or C8), 129.6 (biphenyl-CH), 129.2 (biphenyl-CH), 129.1 (C18 or C19), 129.0 (C18 or C19), 128.2 (biphenyl-CH), 128.0 (d, J = 7.1 Hz, C4 or C7), 127.9 (d, J = 7.2 Hz, C4 or C7), 126.1 (C11), 119.8 (q, J = 321.7 Hz, CF₃); ¹⁹F NMR (377 MHz; CD₂Cl₂) δ : -79.3 (s, 6H, CF₃), -112.7 (C2-F or C9-F), -113.3 (C2-F or C9-F); HRMS: (ESI)⁺ Calculated for [C₂₂H₁₅AuF₂IN₂]⁺ [M-NTf₂]⁺: 668.9908. Found: 668.9901.

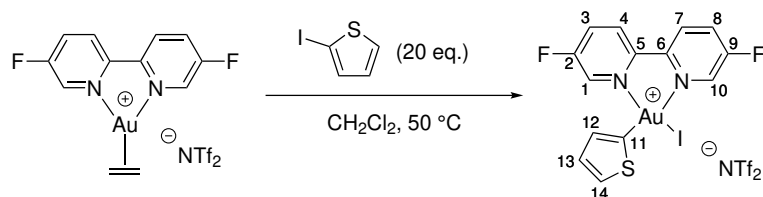
[(κ^2 -5,5'-difluoro-2,2'-bipyridine)Au(1-naphthyl)I][NTf₂] (56i**)**



Complex **56i** was synthesised analogously to **56a** using **51b** (15 mg, 0.022 mmol) and 1-iodonaphthalene (63 μ L, 0.43 mmol). A total reaction time of 4 h was used and the title compound (15 mg, 74%) was obtained as an orange solid.

¹H NMR (500 MHz; CD₂Cl₂) δ : 9.68 – 9.66 (br t, J = 2.3 Hz, 1H, C1-H or C10-H), 8.81 (dd, J = 9.1, 4.4 Hz, 1H, C4-H or C7-H), 8.73 (dd, J = 9.1, 4.6 Hz, 1H, C4-H or C7-H), 8.27 (m, 1H, C3-H or C8-H), 8.18 (m, 1H, C3-H or C8-H), 8.00 – 7.90 (m, 3H, 3 \times naphthyl-H), 7.64 (m, 1H, naphthyl-H), 7.57 (m, 1H, naphthyl-H), 7.52 – 7.44 (m, 2H, 2 \times naphthyl-H), 7.00 (br t, J = 2.4 Hz, 1H, C1-H or C10-H); **¹³C{¹H} NMR** (126 MHz; CD₂Cl₂) δ : 162.9 (d, J = 264 Hz, C2 or C9), 161.2 (d, J = 264 Hz, C2 or C9), 151.7 (d, J = 4.1 Hz, C5 or C6), 150.1 (d, J = 4.2 Hz, C5 or C6), 140.4 (d, J = 33.0 Hz, C1 or C10), 136.6 (C15 or C20), 136.2 (d, J = 33.9 Hz, C1 or C10), 135.4 (C15 or C20), 132.5 (naphthyl-CH), 132.1 (d, J = 19.1 Hz, C3 or C8), 131.1 (d, J = 18.9 Hz, C3 or C8), 130.1 (naphthyl-CH), 130.0 (naphthyl-CH), 128.9 (naphthyl-CH), 128.5 (d, J = 7.1 Hz, C4 or C7), 128.4 (d, J = 7.3 Hz, C4 or C7), 127.9 (naphthyl-CH), 127.7 (naphthyl-CH), 127.5 (naphthyl-CH), 126.5 (C11), 120.3 (q, J = 322 Hz, CF₃); **¹⁹F NMR** (377 MHz; CD₂Cl₂) δ : -79.3 (s, 6F, CF₃), -112.4 (m, C2-F or C9-F), -113.3 (m, C2-F or C9-F); **HRMS**: (ESI)⁺ Calculated for [C₂₀H₁₃AuF₂IN₂]⁺ [M-NTf₂]⁺: 642.9752. Found: 642.9773.

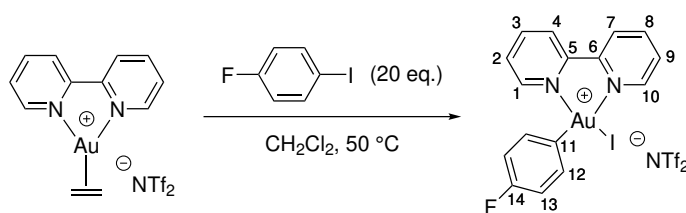
[(κ^2 -5,5'-difluoro-2,2'-bipyridyl)Au(2-thiophene)I][NTf₂] (56j**)**



Complex **56j** was synthesised analogously to **56a** using **51b** (27 mg, 0.039 mmol) and 2-iodothiophene (86 μ L, 0.78 mmol). A total reaction time of 5 h was used and the title compound (27 mg, 79%) was obtained as a yellow solid. Single crystals suitable for X-ray diffraction were grown from a CH₂Cl₂ solution layered with pentane at -20 °C. See Section 5.5, Table 5.11 for full crystallographic details.

¹H NMR (500 MHz; CD₂Cl₂) δ : 9.67 (t, J = 2.4 Hz, 1H, C1-H or C10-H), 8.75 (dd, J = 9.1, 4.5 Hz, 1H, C4-H or C7-H), 8.67 (dd, J = 9.1, 4.5 Hz, 1H, C4-H or C7-H), 8.26 – 8.21 (m, 2H, C3-H, C8-H), 7.84 – 7.81 (m, 1H, C12-H or C14-H), 7.44 (t, J = 2.4 Hz, 1H, C1-H or C10-H), 7.36 – 7.33 (m, 1H, C13-H), 7.02 – 6.99 (m, 1H, C12-H or C14-H); ¹³C{¹H} NMR (126 MHz; CD₂Cl₂) δ : 162.9 (d, J = 264 Hz, C2 or C9), 161.40 (d, J = 265 Hz, C2 or C9), 151.5 (d, J = 4.3 Hz, C5 or C6), 150.8 (d, J = 4.4 Hz, C5 or C6), 141.3 (d, J = 34 Hz, C1 or C10), 136.2 (d, J = 35 Hz, C1 or C10), 133.1 (C12 or C14), 132.4 (d, J = 19 Hz, C3 or C8), 132.2 (C12 or C14), 131.4 (d, J = 19 Hz, C3 or C8), 129.7 (C13), 128.7 (d, J = 7.2 Hz, C4 or C7), 128.3 (d, J = 7.2 Hz, C4 or C7), 120.5 (q, J = 321 Hz, CF₃), 109.0 (C11); ¹⁹F NMR (377 MHz; CD₂Cl₂) δ : -79.3 (CF₃), -111.8 (C2-F or C9-F), -112.8 (C2-F or C9-F); HRMS: (ESI)⁺ Calculated for [C₁₄H₉AuF₂IN₂S]⁺ [M-NTf₂]⁺: 597.9159. Found: 598.9157.

[(κ^2 -2,2'-bipyridine)Au(4-F-C₆H₄)I][NTf₂] (56k**)**



Complex **56k** was synthesised analogously to **56a** using **51a** (15 mg, 0.023 mmol) and 4-fluoriodobenzene (52 μL , 0.45 mmol). A total reaction time of 3 h was used and the title compound (14 mg, 72%) was obtained as a yellow solid. Single crystals suitable for X-ray diffraction were grown from a CH_2Cl_2 solution layered with hexane. See Section 5.5, Table 5.6 for full crystallographic details.

^1H NMR (500 MHz; CD_2Cl_2) δ : 9.75 – 9.70 (m, 1H, C1-H or C10-H), 8.67 (d, $J = 8.3$ Hz, 1H, C4-H or C7-H), 8.62 (d, $J = 8.1$ Hz, 1H, C4-H or C7-H), 8.48 (td, $J = 7.9, 1.6$ Hz, 2H, C3-H, C8-H), 7.97 (ddd, $J = 7.8, 5.5, 1.3$ Hz, 1H, C2-H or C9-H), 7.78 (ddd, $J = 7.4, 5.7, 1.4$ Hz, 1H, C2-H or C9-H), 7.56 (dd, $J = 5.8, 1.5$ Hz, 1H), 7.30 – 7.25 (m, 2H, C12-H), 7.19 – 7.14 (m, 2H, C13-H); $^{13}\text{C}\{^1\text{H}\}$ NMR (126 MHz; CD_2Cl_2) δ : 163.9 (d, $J = 248$ Hz, C14), 155.7 (C5 or C6), 154.3 (C5 or C6), 151.4 (C1 or C10), 147.0 (C1 or C10), 145.0 (C3 or C8), 143.9 (C3 or C8), 134.9 (d, $J = 7.3$ Hz, C12), 130.3 (C2 or C9), 129.2 (C2 or C9), 126.3 (C4 or C7), 126.2 (C4 or C7), 120.3 (q, $J = 321$ Hz, CF_3), 119.4 (C11), 118.5 (d, $J = 22$ Hz, C13); HRMS: (ESI) $^+$ Calculated for $[\text{C}_{16}\text{H}_{12}\text{AuFIN}_2]^+ [\text{M-NTf}_2]^+$: 574.9689. Found: 574.9663.

5.3.3 Reaction Profiles

Effect of Aryl Iodide Electronics on the Rate of Oxidative Addition to **51b**

In a J-Young's valve NMR tube under an inert atmosphere, 4-**R**- $\text{C}_6\text{H}_4\text{-I}$ (100 μL , 0.29 M in CH_2Cl_2 , 28.7 μmol) was added to a solution of **51b** (100 μL , 0.029 M in CH_2Cl_2 , 2.87 μmol) in CH_2Cl_2 (500 μL) at -78 $^\circ\text{C}$. The NMR tube was transferred into an NMR spectrometer (500 MHz) with the probe pre-heated to 50 $^\circ\text{C}$ and data collection was started immediately (Figure 5.1). NMR parameters: nucleus = ^{19}F , frequency = 470 MHz, relaxation delay = 2 s, number of scans = 24, temperature = 50 $^\circ\text{C}$.

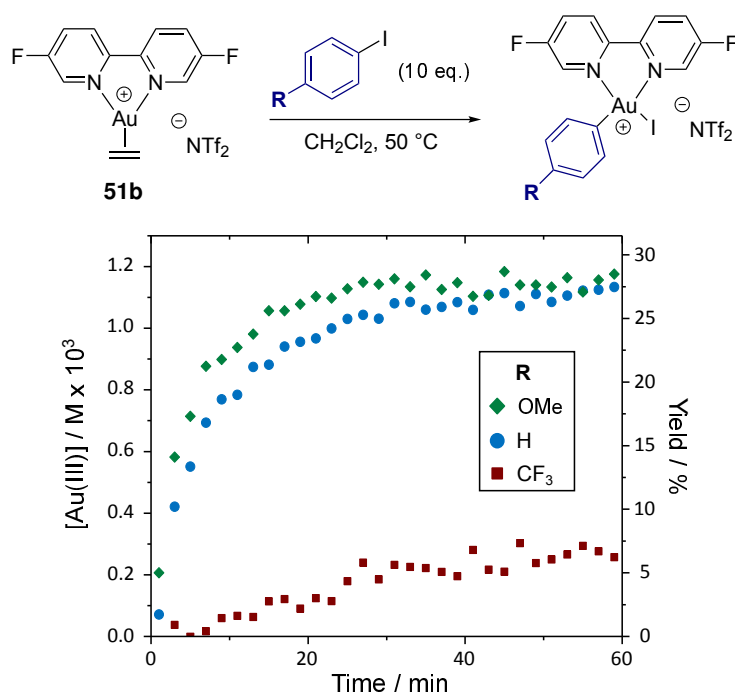


Figure 5.1: Reaction profiles for the oxidative addition of *para*-substituted aryl iodides to **51b**.

Effect of Temperature on the Oxidative Addition of 4-fluoriodobenzene to **51b**

In a J-Young's NMR tube under an inert atmosphere, 4-fluoriodobenzene (12 μL , 0.106 mmol) was added to a solution of **2b** (3.7 mg, 5.3 μmol) in CH_2Cl_2 (0.53 mL) at -78°C . The NMR tube was transferred into an NMR spectrometer (500 MHz) with the probe preheated to the designated temperature and data collection was started immediately (Figure 5.2). NMR parameters: nucleus = ^{19}F , frequency = 470 MHz, relaxation delay = 2 s, number of scans = 64.

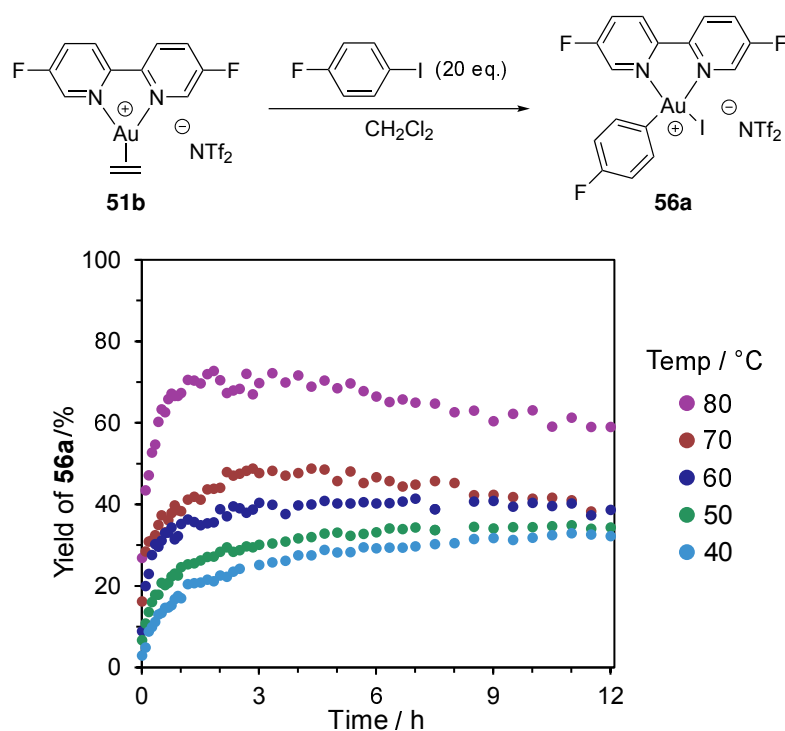


Figure 5.2: Effect of varying temperature on the oxidative addition of 4-iodobenzene to bipy the gold(I) ethylene complex **51b**.

5.3.4 Transmetalation: Low Temperature ^{19}F NMR Studies

Arylzinc reagents were prepared from the corresponding aryl bromides according to the literature procedure.²⁸⁹ 1-Bromo-4-(fluoromethyl)benzene was prepared according to the literature procedure.²⁸⁸

In a J-Young's valve NMR tube under an inert atmosphere at $-78\text{ }^\circ\text{C}$, *p*-tolylzinc chloride (74 μL , 0.05 M in THF/hexane, 3.71 μmol) was added to a solution of **3a** (340 μL , 0.01 M in CH_2Cl_2 , 3.71 μmol) and PhCF_3 (40 μL , 0.017 M in CH_2Cl_2 , internal standard) in CH_2Cl_2 (100 μL , total volume = 550 μL). The tube was rapidly transferred into an NMR spectrometer (300 MHz) with the probe pre-cooled to $-80\text{ }^\circ\text{C}$. The temperature was raised in $10\text{ }^\circ\text{C}$ increments and a ^{19}F NMR spectrum was recorded at each temperature (Figure 5.3).

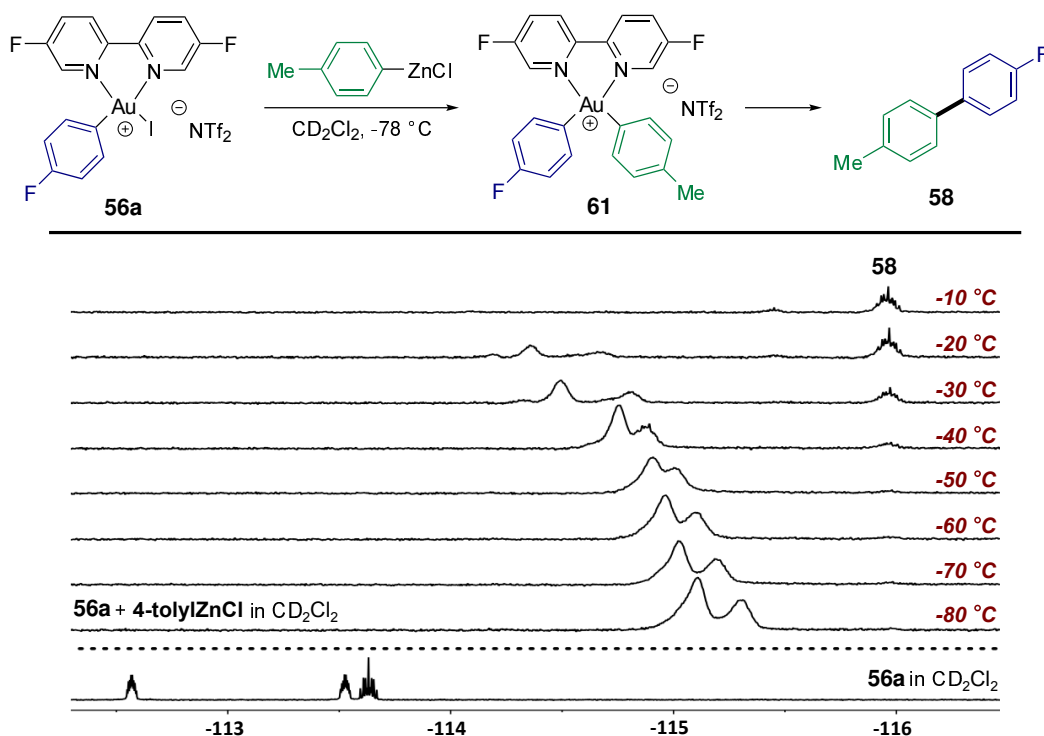


Figure 5.3: Reaction of **60** with 4-tolylZnCl monitored by variable-temperature ^{19}F NMR spectroscopy.

5.3.5 Mass Spectrometry

Under an inert atmosphere, equimolar quantities of **56a** and either 4-tolylZnCl (Figure 5.4) or 4-(fluoromethyl)benzeneZnCl (Figure 5.5) were mixed at -78°C in CH_2Cl_2 to give a total concentration of approximately 0.01 mg/mL. Mass spectrometric data was recorded by direct-infusion electrospray ionisation of the chilled reaction mixture on an Orbitrap Elite MS. All sample lines and the sample syringe were pre-chilled by flushing with cold solvent. A source voltage of 3 kV, source temperature of 45°C and a capillary temperature of 100°C were used to minimise sample degradation. Spectra were recorded in positive ion mode at 120000 resolution in the FTMS between 300 and 1000 Da. Tandem mass spectra were recorded in the collision induced dissociation mode using N_2 collision gas at 20 eV on the isolated precursor ions ($\pm 1 m/z$ isolation width).

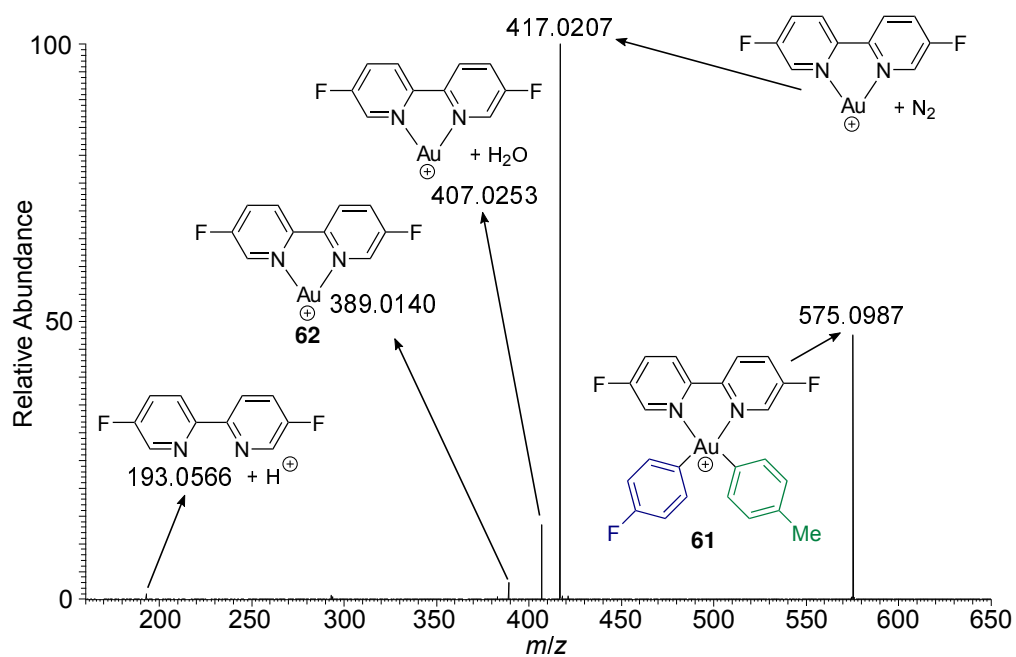


Figure 5.4: Tandem mass spectra for the reaction between 4-tolylZnCl and **56a**, isolated precursor ion m/z 575.

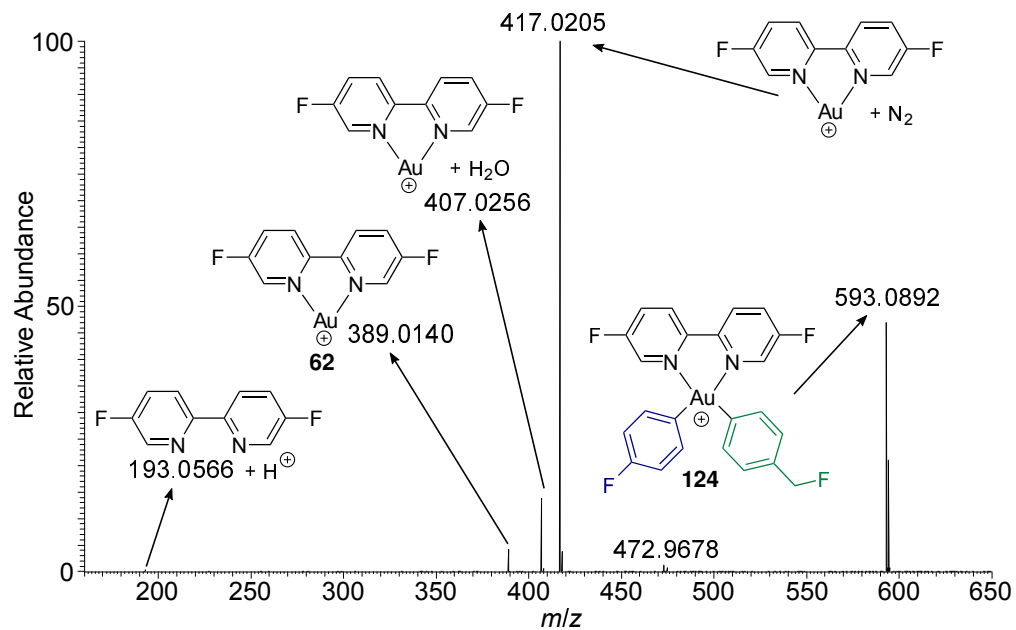


Figure 5.5: Tandem mass spectra for the reaction between 4-(fluoromethyl)benzeneZnCl and **56a**, isolated precursor ion m/z 593.

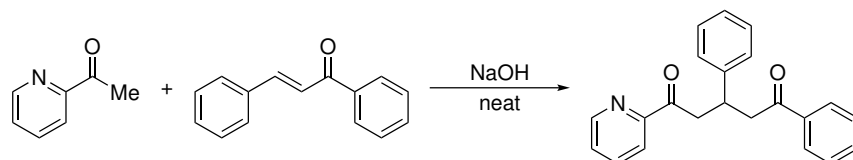
5.4 Experimental Procedures Relevant to Chapter 4

5.4.1 General Procedure for Suzuki Biaryl Coupling

The following procedure is relevant to the results reported in Table 4.3 and Table 4.4. A 7 mL vial was charged with 4-tolylboronic acid (13.6 mg, 0.1 mmol, 1 eq.) and a magnetic stirrer bar. The gold catalyst (see tables for quantities) was then added as a solid or as a stock solution in 1,2-DCB. 1,2-DCB was then added (total concentration 0.05 M with respect to the 4-tolylboronic acid) followed by 4-fluoroiodobenzene (46 μ L, 0.4 mmol, 4 eq.). The silver salt (see tables for quantities) was then added in a single portion then the vial was sealed and heated to 75 °C for 18 h. After cooling to room temperature, dodecane (100 μ L) was added as internal standard and the yield of **58** was determined by calibrated GC-FID analysis.

5.4.2 Ligands

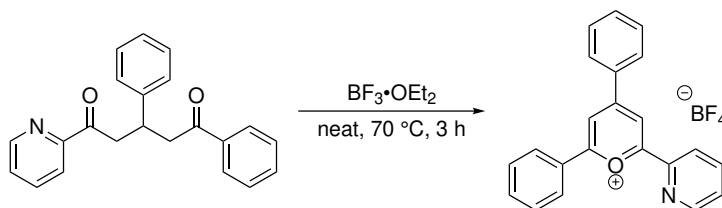
3,5-diphenyl-1-(2-pyridyl)pentane-1,5-dione (**125**)



Following the reported procedure,²⁴⁷ *trans*-chalcone (9.42 g, 45.2 mmol) and 2-acetylpyridine (5.1 mL, 45.2 mmol) were ground with NaOH (1.81 g, 45.2 mmol) in a pestle and mortar for approximately 10 minutes until a sticky yellow residue was obtained. The residue was transferred to a conical flask with hot EtOH:H₂O (250 mL, 2:1) and heated until full dissolution. The solution was then allowed to cool to r.t. with stirring, after which a white solid was observed. The solid was filtered, washed with EtOH:H₂O (2:1), and dried under vacuum to afford the title compound (10.1 g, 68%) as a white solid.

$^1\text{H NMR}$ (400 MHz; CDCl_3) δ : 8.57 – 8.52 (m, 1H, Ar-CH), 7.87 (d, $J = 7.9$ Hz, 1H, Ar-CH), 7.84 – 7.81 (d, $J = 7.7$ Hz, Ar-CH), 7.69 (td, $J = 7.7, 1.7$ Hz, 1H, Ar-CH), 7.46 – 7.40 (m, 1H, Ar-CH), 7.36 – 7.30 (m, 3H, Ar-CH), 7.27 – 7.21 (m, 2H, Ar-CH), 7.20 – 7.13 (m, 2H, Ar-CH), 7.09 – 7.03 (m, 1H, Ar-CH), 4.03 (q, $J = 7.1$ Hz, 1H, CH), 3.68 (dd, $J = 17.6, 7.4$ Hz, 1H, CHH), 3.54 (dd, $J = 17.6, 6.8$ Hz, 1H, CHH), 3.37 (dd, $J = 16.7, 6.9$ Hz, 1H, CHH), 3.27 (dd, $J = 16.7, 7.3$ Hz, 1H, CHH); $^{13}\text{C}\{^1\text{H}\}$ NMR (101 MHz, CDCl_3) δ : 200.1 (C=O), 198.7 (C=O), 153.5 (4°C), 149.0 (Ar-CH), 144.4 (4°C), 137.2 (4°C), 137.0 (Ar-CH), 133.1 (Ar-CH), 128.7 (Ar-CH), 128.6 (Ar-CH), 128.2 (Ar-CH), 127.7 (Ar-CH), 127.2 (Ar-CH), 126.6 (Ar-CH), 122.0 (Ar-CH), 45.4 (CH_2), 44.0 (CH_2), 36.7 (CH). The spectroscopic properties of this compound were consistent with literature data.²⁹⁰

2-(2-pyridyl)-4,6-diphenylpyrylium tetrafluoroborate (74)



Following the reported procedure,²⁴⁷ a flask was charged with **125** (5.0 g, 15.2 mmol) and chalcone (3.1 g, 15.2 mmol) then placed under an N_2 atmosphere. $\text{BF}_3\cdot\text{OEt}_2$ (15 mL, 21.4 mmol) was added dropwise then the mixture was stirred at 70°C for 3 h. After cooling to r.t. an orange solution with a sticky orange precipitate was obtained. Et_2O (100 mL) was added to precipitate a yellow solid, which was filtered then recrystallised from hot MeOH to afford the title compound (2.70 g, 45%) as small yellow needles.

$^1\text{H NMR}$ (400 MHz; $\text{DMSO}-d_6$) δ : 9.30 (d, $J = 1.8$ Hz, 1H, Ar-CH), 9.23 (d, $J = 1.7$ Hz, 1H, Ar-CH), 9.02 (dt, $J = 4.7, 1.4$ Hz, 1H, Ar-CH), 8.74 (dd, $J = 8.0, 1.1$ Hz, 1H, Ar-CH), 8.69 – 8.64 (m, 2H, Ar-CH), 8.60 – 8.54 (m, 2H, Ar-CH), 8.28 (td, $J = 7.8, 1.7$ Hz, 1H, Ar-CH), 7.94 – 7.74 (m, 7H, Ar-CH); $^{13}\text{C}\{^1\text{H}\}$ NMR (101 MHz, $\text{DMSO}-d_6$) δ :

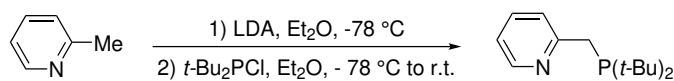
170.7 (4° C), 167.8 (4° C), 165.7 (4° C), 151.0 (Ar-CH), 146.4 (4° C), 138.6 (Ar-CH), 135.5 (Ar-CH), 135.5 (Ar-CH), 132.3 (4° C), 130.1 (Ar-CH), 129.9 (Ar-CH), 129.1 (Ar-CH), 129.0 (Ar-CH), 128.6 (Ar-CH), 124.6 (Ar-CH), 116.6 (Ar-CH), 115.3 (Ar-CH); ^{19}F NMR (376 MHz, DMSO- d_6) δ : -148.2. The spectroscopic properties of this compound were consistent with literature data.²⁴⁷

2-(2-pyridyl)-4,6-diphenyl- λ^3 -phosphinine (75)



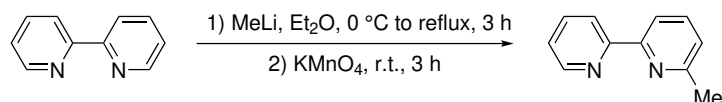
Following the reported procedure,²⁴⁷ a flask was charged with **74** (470 mg, 1.18 mmol) and MeCN (3 ml) under an N₂ atmosphere. P(SiMe₃) (0.72 ml, 2.48 mmol) was added dropwise at r.t. then the mixture was heated to 85 °C for 5 h, after which a deep red solution was obtained. After cooling to r.t., the mixture was concentrated *in vacuo* to afford a dark red solid. After purification by flash column chromatography on neutral alumina (eluent: 15% EtOAc in 40/60 petroleum ether) the title compound (71 mg, 18 %) was obtained as a red solid, which was stored in an Ar glovebox.

^1H NMR (400 MHz, C₆D₆) δ : 9.14 (dd, J = 5.7, 1.3 Hz, 1H, Ar-CH), 8.60 (ddd, J = 4.8, 1.9, 1.0 Hz, 1H, Ar-CH), 8.14 (dd, J = 6.0, 1.3 Hz, 1H, Ar-CH), 7.92 – 7.88 (m, 1H, Ar-CH), 7.70 – 7.60 (m, 2H, Ar-CH), 7.54 – 7.50 (m, 2H, Ar-CH), 7.26 – 7.15 (m, 6H, Ar-CH), 7.13 – 7.08 (m, 1H, Ar-CH), 6.67 (ddt, J = 7.5, 4.8, 0.8 Hz, 1H, Ar-CH); $^{13}\text{C}\{^1\text{H}\}$ NMR (126 MHz, C₆D₆) δ : 172.0 (d, J = 50.7 Hz, 4° C), 170.0 (d, J = 50.7 Hz, 4° C), 159.5 (d, J = 26.1 Hz, 4° C), 150.2 (Ar-CH), 144.7 (4° C), 144.6 (4° C), 144.2 (d, J = 25.0 Hz, 4° C), 142.6 (d, J = 3.1 Hz, 4° C), 136.6 (Ar-CH), 133.4 (d, J = 11.9 Hz, Ar-CH), 132.4 (d, J = 13.0 Hz, Ar-CH), 129.2 (Ar-CH), 122.8 (d, J = 1.9 Hz, Ar-CH), 121.5 (Ar-CH), 121.3 (Ar-CH); $^{31}\text{P}\{^1\text{H}\}$ NMR (162 MHz, C₆D₆) δ : 187.4. The spectroscopic properties of this compound were consistent with literature data.²⁴⁷

2-((di-*tert*-butylphosphino)methyl)pyridine (81)

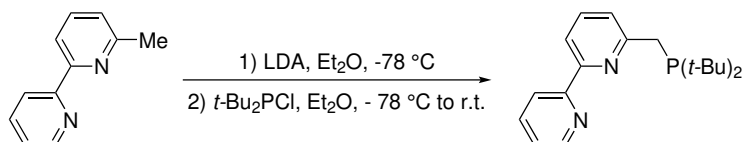
Following the reported procedure,²⁴⁸ to an oven dried flask under N₂ was charged Et₂O (15 mL) and diisopropylamine (566 μL, 4.04 mmol). The solution was cooled to -78 °C then *n*-butyllithium (1.62 M in hexanes, 2.47 mL, 4 mmol) was added. The reaction was warmed to r.t. and stirred for 15 minutes then cooled back down to -78 °C before a solution of 2-picoline (395 μL, 4 mmol) in Et₂O (8 mL) was added dropwise. After stirring at -78 °C for 45 minutes a solution of *t*-Bu₂PCl (760 μL, 4 mmol) in Et₂O (10 mL) was added dropwise. The resulting orange solution was allowed to warm to r.t. and stirred overnight. Degassed H₂O (20 mL) was added to the reaction and the reaction mixture turned from orange to colourless. The layers were separated and the aqueous layer was extracted with Et₂O (2 × 20 mL). The combined organic layers were dried over anhydrous Na₂SO₄ and concentrated *in vacuo* to afford a yellow oil, which was dissolved in hexane and filtered (porosity 3, Celite, washed with 3 × 15 mL hexane). Concentration of the filtrate *in vacuo* afforded the title compound (807 mg, 85%) as an air-sensitive orange oil.

¹H NMR (300 MHz; CDCl₃) δ: 8.50 – 8.41 (m, 1H, Ar-CH), 7.56 (td, *J* = 7.7, 1.9 Hz, 1H, Ar-CH), 7.43 (dq, *J* = 8.0, 1.2 Hz, 1H, Ar-CH), 7.10 – 6.98 (m, 1H, Ar-CH), 3.06 (d, *J* = 3.3 Hz, 2H, CH₂), 1.15 (d, *J* = 11.0 Hz, 18H, C(CH₃)₃); ¹³C{¹H} NMR (126 MHz; CDCl₃) δ: 162.2 (d, *J* = 13.7 Hz, 4 °C), 149.0 (Ar-CH), 136.1 (Ar-CH), 124.1 (d, *J* = 9.1 Hz, Ar-CH), 120.7 (d, *J* = 1.7 Hz, Ar-CH), 32.0 (d, *J* = 21.6 Hz, CH₂), 31.9 (d, *J* = 23.9 Hz, C(CH₃)₃), 29.8 (d, *J* = 13.2 Hz, C(CH₃)₃); ³¹P{¹H} NMR (122 MHz; CDCl₃) δ: 36.9. The spectroscopic properties of this compound were consistent with literature data.²⁴⁸

6-methyl-2,2'-bipyridine (126)

Following the reported procedure,²⁹¹ to an oven dried flask under an atmosphere of N₂ was charged 2,2'-bipyridine (4.00 g, 25.6 mmol) and Et₂O (85 mL). The solution was cooled to 0 °C then methyllithium (1.6 M in Et₂O, 16 mL, 25.6 mmol) was added dropwise over 30 minutes. The resulting red solution was refluxed for 3 h, then cooled to r.t. before the addition of H₂O (80 mL). The layers were separated and the aqueous layer was extracted with Et₂O (3 × 50 mL). The combined organic portions were dried over anhydrous Na₂SO₄ then the solvent was removed *in vacuo* to afford an orange oil. The orange oil was dissolved in a saturated solution of KMnO₄ in acetone (250 mL) and stirred at r.t. for 3 h. Following filtration, the filtrate was concentrated *in vacuo* then purified by column chromatography (eluent: 50% EtOAc/Hexane) to afford the title compound (1.64 g, 38%) as a colourless oil, which solidified upon standing.

¹H NMR (400 MHz; CDCl₃) δ: 8.69 – 8.65 (m, 1H, Ar-CH), 8.40 (d, *J* = 8.0 Hz, 1H, Ar-CH), 8.16 (d, *J* = 7.8 Hz, 1H, Ar-CH), 7.79 (td, *J* = 7.7, 1.8 Hz, 1H, Ar-CH), 7.69 (t, *J* = 7.7 Hz, 1H, Ar-CH), 7.30 – 7.25 (m, 1H, Ar-CH), 7.16 (d, *J* = 7.6 Hz, 1H, Ar-CH), 2.63 (s, 3H, CH₃); ¹³C{¹H} NMR (101 MHz; CDCl₃) δ: 158.1 (4 °C), 156.7 (4 °C), 155.7 (4 °C), 149.3 (Ar-CH), 137.2 (Ar-CH), 137.0 (Ar-CH), 123.6 (Ar-CH), 123.4 (Ar-CH), 121.3 (Ar-CH), 118.2 (Ar-CH), 24.8 (CH₃). The spectroscopic properties of this compound were consistent with literature data.²⁹¹

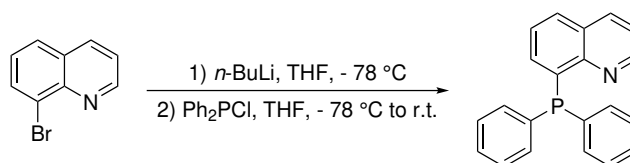
6-di-*tert*-butylphosphinomethyl-2,2'-bipyridine (82)

Adapted from the reported procedure,²⁴⁹ to an oven dried flask under N₂ was charged diisopropylamine (426 μL, 3.04 mmol) and Et₂O (7 mL). The solution was cooled to

-78 °C then *n*-butyllithium (1.62 M in hexanes, 1.56 mL, 2.54 mmol) was added dropwise. The reaction was warmed to r.t. and stirred for 15 minutes then cooled back down to -78 °C before a solution of **126** (287 mg, 1.69 mmol) in Et₂O (8 mL) was added dropwise. The reaction was warmed to r.t. for 10 minutes, then cooled back down to -78 °C before a solution of *t*-Bu₂PCl (514 μL, 2.71 mmol) in Et₂O (8 mL) was added dropwise. The resulting dark green solution was stirred at -78 °C for 45 minutes then allowed to warm to r.t. Degassed H₂O (20 mL) was added to the reaction then the layers were separated and the aqueous layer was extracted with Et₂O (2 × 10 mL). The combined organic layers were dried over anhydrous Na₂SO₄ then concentrated *in vacuo* to afford a yellow solid, which was dissolved in Et₂O and passed through a short silica column (eluent: Et₂O). The solvent was removed *in vacuo* to afford the title compound (379 mg, 71%) as a yellow solid.

¹H NMR (400 MHz; CDCl₃) δ: 8.66 – 8.64 (m, 1H, Ar-CH), 8.43 (dt, *J* = 8.0, 1.1 Hz, 1H, Ar-CH), 8.16 (d, *J* = 7.7 Hz, 1H, Ar-CH), 7.79 (td, *J* = 7.8, 1.8 Hz, 1H, Ar-CH), 7.70 (t, *J* = 7.8 Hz, 1H, Ar-CH), 7.42 (dt, *J* = 7.8, 1.1 Hz, 1H, Ar-CH), 7.27 (ddd, *J* = 7.5, 4.8, 1.2 Hz, 1H, Ar-CH), 3.15 (d, *J* = 3.3 Hz, 2H, CH₂), 1.19 (d, *J* = 11.0 Hz, 18H, C(CH₃)₃); ¹³C{¹H} NMR (126 MHz; CDCl₃) δ: 161.5 (d, *J* = 13.8 Hz, Ar-CH), 156.5 (4 °C), 155.0 (4 °C), 149.0 (Ar-CH), 137.0 (Ar-CH), 136.8 (Ar-CH), 123.9 (d, *J* = 8.5 Hz, Ar-CH), 123.4 (Ar-CH), 121.1 (Ar-CH), 117.8 (Ar-CH), 32.0 (d, *J* = 21.9 Hz, C(CH₃)₃), 31.8 (d, *J* = 24.3 Hz, CH₂), 29.7 (d, *J* = 13.3 Hz, C(CH₃)₃); ³¹P{¹H} NMR (121 MHz; CDCl₃) δ: 37.8. The spectroscopic properties of this compound were consistent with literature data.²⁴⁹

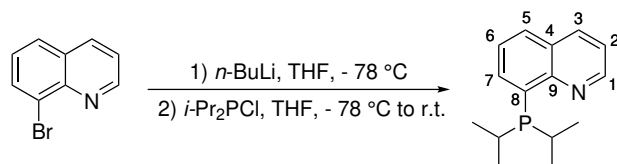
8-(Diphenylphosphino)quinoline (**89**)



Adapted from the reported procedure,²⁵⁰ to an oven dried flask under an atmosphere of N₂ was charged 8-bromoquinoline (3.67 g, 17.6 mmol) and THF (60 mL). The solution was cooled to -78 °C then *n*-butyllithium (2.37 M in hexane, 7.4 mL, 17.6 mmol) was added dropwise. The resulting orange solution was stirred at -78 °C for 15 minutes, then Ph₂PCl (3.25 mL, 17.6 mmol) was added dropwise. The reaction was allowed to stir at -78 °C for an additional 15 minutes then warmed to r.t. and stirred overnight. The resulting yellow suspension was concentrated *in vacuo* then the solid was extracted into PhMe and filtered through a plug of neutral alumina. The solvent was removed *in vacuo* and the resulting yellow solid was washed with pentane (3 × 20 mL) then dried *in vacuo* to afford the title compound (1.25 g, 23%) as a colourless solid.

¹H NMR (400 MHz; CDCl₃) δ: 8.87 (dd, *J* = 4.3, 1.8 Hz, 1H, Ar-CH), 8.16 (dd, *J* = 8.3, 1.8 Hz, 1H, Ar-CH), 7.81 (d, *J* = 8.1 Hz, 1H, Ar-CH), 7.45 – 7.41 (m, 1H, Ar-CH), 7.39 (dd, *J* = 8.3, 4.2 Hz, 1H, Ar-CH), 7.36 – 7.27 (m, 10H, Ar-CH), 7.13 (ddd, *J* = 7.1, 3.7, 1.4 Hz, 1H, Ar-CH); ¹³C NMR (126 MHz; CDCl₃) δ: 149.8 (d, *J* = 1.7 Hz, Ar-CH), 149.6 (d, *J* = 17.2 Hz, 4° C), 138.5 (d, *J* = 12.3 Hz, 4° C), 137.5 (d, *J* = 10.9 Hz, 4° C), 136.2 (d, *J* = 2.1 Hz, Ar-CH), 134.3 (Ar-CH), 134.2 (d, *J* = 20.2 Hz), 128.7 (Ar-CH), 128.5 (Ar-CH), 128.4 (Ar-CH), 128.3 (Ar-CH), 127.9 (d, *J* = 2.1 Hz, 4° C), 126.6 (Ar-CH), 121.4 (Ar-CH); ³¹P{¹H} NMR (162 MHz; CDCl₃) δ: -14.9. The spectroscopic properties of this compound were consistent with literature data.²⁵⁰

8-(diisopropylphosphino)quinoline (99)

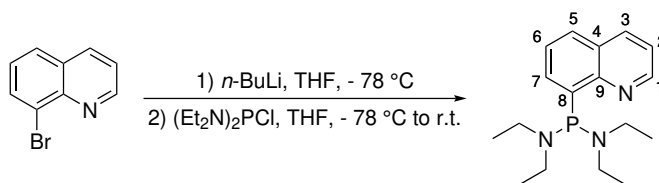


To an oven dried flask under an atmosphere of N₂ was charged 8-bromoquinoline (1.62 g, 7.79 mmol) and THF (30 mL). The solution was cooled to -78 °C then *n*-butyllithium (2.37 M in Hexane, 3.29 mL, 7.79 mmol) was added dropwise. The resulting orange

solution was stirred at $-78\text{ }^{\circ}\text{C}$ for 15 minutes, then $i\text{-Pr}_2\text{PCl}$ (1.24 mL, 7.79 mmol) was added dropwise. The reaction was warmed to r.t. and stirred for 5 h. The resulting yellow solution was concentrated *in vacuo* then passed through a short silica column. Two fractions were collected; the first eluted with hexane and the second eluted with THF. The THF fraction was concentrated *in vacuo* to afford the title compound (1.60 g, 84%, approx. 92% purity) as a yellow oil.

$^1\text{H NMR}$ (400 MHz; CDCl_3) δ : 8.97 (dd, $J = 4.2, 1.9$ Hz, 1H, C1-H), 8.12 (dd, $J = 8.3, 1.9$ Hz, 1H, C3-H), 7.85 – 7.74 (m, 2H, C7-H, C5-H), 7.58 – 7.48 (m, 1H, C6-H), 7.37 (dd, $J = 8.3, 4.1$ Hz, 1H, C2-H), 2.43 – 2.29 (m, 2H, $\text{CH}(\text{CH}_3)_2$), 1.14 (dd, $J = 14.0, 7.0$ Hz, 6H, $\text{CH}(\text{C}_a\text{H}_3)_2$), 0.96 (dd, $J = 12.2, 7.0$ Hz, 6H, $\text{CH}(\text{C}_b\text{H}_3)_2$); $^{13}\text{C NMR}$ (101 MHz; CDCl_3) δ : 151.5 (C9), 149.7 (C1), 137.0 (d, $J = 20.8$ Hz, C8), 136.3 (C3), 134.3 (C7), 128.6 (C5), 128.4 (d, $J = 2.3$ Hz, 1H, C4), 125.8 (C6), 121.0 (C2), 23.3 (d, $J = 13.8$ Hz, $\text{CH}(\text{CH}_3)_2$), 20.3 (d, $J = 17.6$ Hz, $\text{CH}(\text{C}_a\text{H}_3)_2$), 19.8 (d, $J = 11.6$ Hz, $\text{CH}(\text{C}_b\text{H}_3)_2$); $^{31}\text{P}\{^1\text{H}\}$ NMR (162 MHz; CDCl_3) δ : -0.5; HRMS: (ESI) $^+$ Calculated for $[\text{C}_{15}\text{H}_{21}\text{NP}]^+$ $[\text{M}+\text{H}]^+$: 246.1406. Found: 246.1404.

8-(bis(diethylamino)phosphino)quinoline (101)

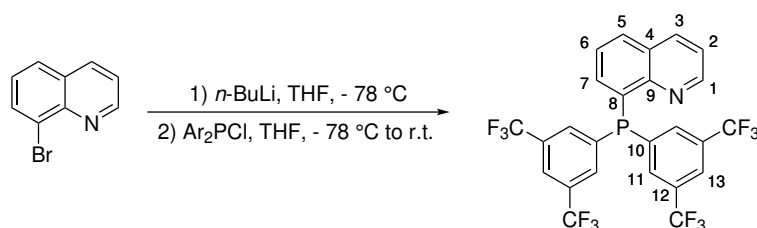


To an oven dried flask under an atmosphere of N_2 was charged 8-bromoquinoline (514 mg, 2.47 mmol) and THF (12 mL). The solution was cooled to $-78\text{ }^{\circ}\text{C}$ then n -butyllithium (2.37 M in hexane, 1.04 mL, 2.47 mmol) was added dropwise. The resulting orange solution was stirred at $-78\text{ }^{\circ}\text{C}$ for 15 minutes, then bis(diethylamino)chlorophosphine (0.520 mL, 2.47 mmol) was added dropwise. After stirring at $-78\text{ }^{\circ}\text{C}$ for 30 minutes, the reaction was warmed to r.t. and stirred for 1.5 h. The solution was concentrated *in vacuo* to afford a yellow solid, which was dissolved in PhMe and filtered (porosity 3, Celite,

washed with 3×10 mL PhMe). Concentration *in vacuo* afforded the title compound (640 mg, 85%) as a yellow oil.

$^1\text{H NMR}$ (400 MHz; CDCl_3) δ : 8.88 (dd, $J = 4.2, 1.9$ Hz, 1H, C1-H), 8.09 (dd, $J = 8.2, 1.9$ Hz, 1H, C3-H), 7.82 (ddd, $J = 7.0, 2.8, 1.5$ Hz, 1H, C7-H), 7.71 (dt, $J = 8.1, 1.7$ Hz, 1H, C5-H), 7.53 – 7.48 (m, 1H, C6-H), 7.34 (dd, $J = 8.2, 4.1$ Hz, 1H, C2-H), 3.11 – 3.01 (m, 8H, CH_2), 1.07 (t, $J = 7.1$ Hz, 12H, CH_3); $^{13}\text{C}\{^1\text{H}\}$ NMR (101 MHz; CDCl_3) δ : 149.1 (d, $J = 17.5$ Hz, C8 or C9), 149.0 (d, $J = 1.7$ Hz, C1), 141.9 (d, $J = 13.1$ Hz, C8 or C9), 135.9 (d, $J = 2.1$ Hz, C3), 131.8 (d, $J = 5.1$ Hz, C7), 128.1 (C4), 127.9 (d, $J = 2.0$ Hz, C5), 126.2 (C6), 120.9 (C2), 43.8 (d, $J = 19.0$ Hz, CH_2), 14.9 (d, $J = 3.1$ Hz, CH_3); $^{31}\text{P}\{^1\text{H}\}$ NMR (122 MHz, CDCl_3) δ : 96.8; HRMS: (ESI) $^+$ Calculated for $[\text{C}_{17}\text{H}_{27}\text{N}_3\text{P}]^+$ $[\text{M}+\text{H}]^+$: 304.1937. Found: 304.1932.

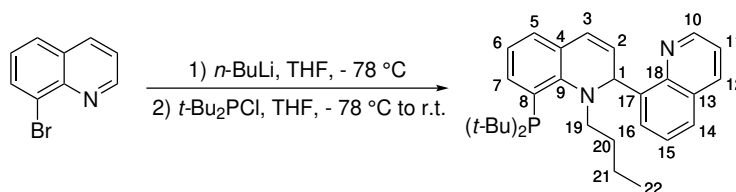
8-(bis(3,5-bis(trifluoromethyl)phenyl)phosphino)quinoline (100)



To an oven dried flask under an atmosphere of N_2 was charged 8-bromoquinoline (200 mg, 0.961 mmol) and THF (5 mL). The solution was cooled to -78 °C then *n*-butyllithium (2.37 M in hexane, 0.406 μL , 0.961 mmol) was added dropwise. The resulting orange solution was stirred at -78 °C for 15 minutes, then a solution of bis(3,5-di(trifluoromethyl)phenyl)chlorophosphine (430 mg, 0.870 mmol) in THF (5 mL) was added. After stirring at -78 °C for 30 minutes, the reaction was warmed to r.t. and stirred overnight. The solution was concentrated directly onto silica then purified by flash column chromatography on silica gel (eluent: 5% to 60% EtOAc in hexane) to afford the title compound (202 mg, 40%) as a pale orange solid.

$^1\text{H NMR}$ (400 MHz; CDCl_3) δ : 8.83 (dd, $J = 4.3, 1.7$ Hz, 1H, C1-H), 8.25 (dd, $J = 8.2, 1.7$ Hz, 1H, C3-H), 7.97 (d, $J = 8.2$ Hz, 1H, C5-H), 7.89 (s, 2H, C13-H), 7.73 (d, $J = 6.6$ Hz, 4H, C11-H), 7.58 – 7.51 (m, 1H, C6), 7.48 (dd, $J = 8.3, 4.2$ Hz, 1H, C2-H), 7.09 (ddd, $J = 7.1, 4.7, 1.4$ Hz, 1H, C7-H); $^{13}\text{C NMR}$ (126 MHz; CDCl_3) δ : 150.3 (d, $J = 1.6$ Hz, C1), 149.1 (d, $J = 16.8$ Hz, C9), 140.0 (d, $J = 18.0$ Hz, C10), 136.8 (d, $J = 2.0$ Hz, C3), 134.5 – 134.4 (m, 2C, C7, C8), 133.9 (dd, $J = 21.7, 3.8$ Hz, C11), 132.1 (qd, $J = 33.4, 6.6$ Hz, C12), 130.7 (C5), 128.3 (d, $J = 2.2$ Hz, C4), 127.1 (d, $J = 1.8$ Hz, C6), 123.5 – 123.3 (m, C13), 123.2 (q, $J = 273.1$ Hz, CF_3), 122.3 (C2); $^{31}\text{P}\{^1\text{H}\}$ NMR (162 MHz; CDCl_3) δ : -10.9; $^{19}\text{F NMR}$ (377 MHz; CDCl_3) δ : -62.9; HRMS: (ESI) $^+$ Calculated for $[\text{C}_{25}\text{H}_{13}\text{F}_{12}\text{NP}]^+$ $[\text{M}+\text{H}]^+$: 586.0589. Found: 586.0585.

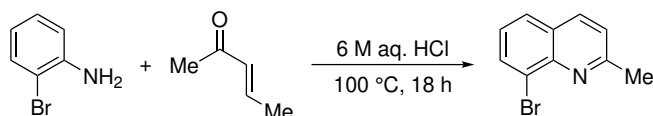
1-butyl-8-(di-*tert*-butylphosphino)-1,2-dihydro-2,8'-biquinoline (106)



To an oven dried flask under an atmosphere of N_2 was charged 8-bromoquinoline (2.08 mg, 10.0 mmol) and THF (15 mL). The solution was cooled to -78 °C then *n*-butyllithium (2.37 M in hexane, 4.22 mL, 10.0 mmol) was added dropwise. The resulting orange solution was stirred at -78 °C for 15 minutes, then *t*- Bu_2PCl (2.09 mL, 11.0 mmol) was added dropwise. After stirring at -78 °C for 30 minutes, the reaction was warmed to r.t. and stirred for 48 hours. Degassed H_2O (30 mL) was added to the reaction then the layers were separated and the aqueous layer was extracted with hexane (3×10 mL). The combined organic layers were dried over anhydrous Na_2SO_4 then concentrated *in vacuo* to afford a yellow oil. The oil was purified by flash column chromatography on silica gel (eluent: 15% EtOAc in hexane) to afford the title compound (1.39 mg, 60%) as a orange solid.

$^1\text{H NMR}$ (400 MHz; CDCl_3) δ : 8.99 (dd, $J = 4.2, 1.8$ Hz, 1H, C10-H), 8.05 (dd, $J = 8.3, 1.8$ Hz, 1H, C12-H), 7.56 (dd, $J = 8.2, 1.5$ Hz, 1H, C14-H), 7.45 (dt, $J = 7.6, 1.7$ Hz, 1H, C7-H), 7.40 (dd, $J = 7.2, 1.5$ Hz, 1H, C16-H), 7.36 (dd, $J = 8.2, 4.2$ Hz, 1H, C11-H), 7.22 – 7.18 (m, 1H, C15-H), 7.06 (dd, $J = 7.3, 1.7$ Hz, 1H, C5-H), 6.87 (t, $J = 7.5$ Hz, 1H, C6-H), 6.75 (dt, $J = 9.3, 1.0$ Hz, 1H, C3-H), 6.43 (d, $J = 5.9$ Hz, 1H, C1-H), 6.12 (dd, $J = 9.3, 5.9$ Hz, 1H, C2-H), 4.17 – 4.05 (m, 1H, C19-H_a), 3.62 – 3.50 (m, 1H, C19-H_b), 1.93 – 1.78 (m, 1H, C20-H_a), 1.72 – 1.57 (m, 1H, C20-H_b), 1.22 (d, $J = 11.5$ Hz, 11H, C(CH₃)₃, C21-H₂), 0.89 (t, $J = 7.4$ Hz, 3H, C22-H₃), 0.46 (d, $J = 11.6$ Hz, 9H, C(CH₃)₃); $^{13}\text{C NMR}$ (101 MHz; CDCl_3) δ : 151.5 (d, $J = 21.6$ Hz, C9), 149.5 (C10), 145.9 (C13 or C18 or C17), 139.3 (C13 or C18 or C17), 136.5 (d, $J = 2.8$ Hz, C7), 136.0 (C12), 131.1 (d, $J = 29.2$ Hz, C8), 129.4 (d, $J = 5.2$ Hz, C4), 128.7 (C13 or C18 or C17), 128.4 (C16), 128.2 (C2), 127.4 (C5), 127.1 (d, $J = 1.9$ Hz, C3), 126.9 (C14), 126.1 (C15), 120.7 (C11), 120.4 (C6), 61.2 (d, $J = 20.3$ Hz, C19), 54.9 (C1), 32.7 (d, $J = 25.2$ Hz, C_a(CH₃)₃), 32.1 (d, $J = 27.0$ Hz, C_b(CH₃)₃), 31.8 (d, $J = 15.9$ Hz, C(C_aH₃)₃), 30.5 (d, $J = 2.3$ Hz, C20), 29.4 (d, $J = 15.6$ Hz, C(C_bH₃)₃), 20.8 (C21), 14.5 (C22); $^{31}\text{P}\{^1\text{H}\}$ NMR (162 MHz; CDCl_3) δ : 18.46; **HRMS**: (ESI)⁺ Calculated for [C₃₀H₄₀N₂P]⁺ [M+H]⁺: 459.2924. Found: 459.2923.

8-bromo-2-methylquinoline (109)

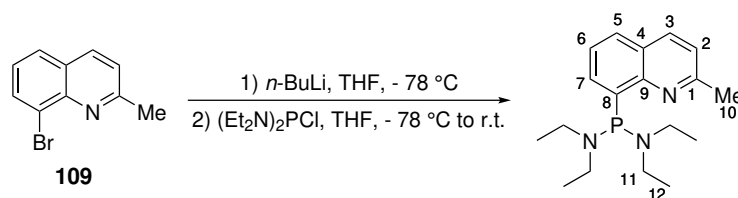


Adapted from the reported procedure,²⁵² a solution of 2-bromoaniline (9.70 g, 56.4 mmol) and crotonaldehyde (9.3 mL, 113 mmol) in 6 M aq. HCl (30 mL) was heated to 110 °C for 18 h. After cooling to r.t., the solution was basified (approximate pH = 10) by addition of 2.5 M aq. NaOH, then extracted with CH_2Cl_2 (4 × 25 mL). The combined organic layers were washed with H_2O and brine, dried over Na_2SO_4 , then filtered and concen-

trated *in vacuo*. Following purification by column chromatography (eluent: 2.5% to 20% EtOAc/hexane) the title compound (3.59 g, 29%) was obtained as a yellow solid.

$^1\text{H NMR}$ (400 MHz; CDCl_3) δ : 8.04 – 8.00 (m, 2H, Ar-CH), 7.74 (dd, $J = 8.1, 1.3$ Hz, 1H, Ar-CH), 7.36 – 7.30 (m, 2H, Ar-CH), 2.82 (s, 3H, CH_3); $^{13}\text{C}\{^1\text{H}\}$ NMR (101 MHz; CDCl_3) δ : 160.6 (4 °C), 145.0 (4 °C), 136.7 (Ar-CH), 133.2 (Ar-CH), 127.9 (4 °C), 127.6 (Ar-CH), 126.2 (Ar-CH), 124.3 (4 °C), 123.0 (Ar-CH), 25.9 (CH_3). The spectroscopic properties of this compound were consistent with literature data.^{252,292}

8-(bis(diethylamino)phosphino)-2-methylquinoline (112)

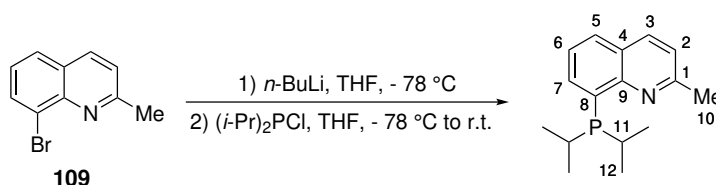


To an oven dried flask under an atmosphere of N_2 was charged 8-bromo-2-methylquinoline **109** (266 mg, 1.20 mmol) and THF (12 mL). The solution was cooled to -78 °C then *n*-butyllithium (2.37 M in hexane, 0.505 mL, 1.20 mmol) was added dropwise. The resulting orange solution was stirred at -78 °C for 15 minutes, then bis(diethylamino)chlorophosphine (252 μL , 1.20 mmol) was added dropwise. After stirring at -78 °C for 10 minutes, the reaction was warmed to r.t. and stirred for 3 h. The solution was concentrated *in vacuo* to afford a yellow oil, which was dissolved in PhMe and filtered (porosity 3, Celite, washed with 3×10 mL PhMe). Concentration *in vacuo* afforded the title compound (371 mg, 97%) as a yellow oil.

$^1\text{H NMR}$ (500 MHz; CDCl_3) δ : 7.96 (d, $J = 8.3$ Hz, 1H, C3-H), 7.76 (ddd, $J = 7.1, 3.0, 1.5$ Hz, 1H, C7-H), 7.68 – 7.64 (m, 1H, C5-H), 7.46 – 7.40 (m, 1H, C6-H), 7.22 (d, $J = 8.3$ Hz, 1H, C2-H), 3.14 – 2.96 (m, 8H, C12-H₂), 2.70 (s, 3H, C10-H₃), 1.10 (t, $J = 7.1$ Hz, 12H, C12-H₃); $^{13}\text{C}\{^1\text{H}\}$ NMR (126 MHz; CDCl_3) δ : 157.6 (d, $J = 1.6$ Hz, C1), 148.7 (d, $J = 17.0$ Hz, C8 or C9), 141.0 (d, $J = 12.1$ Hz, C8 or C9), 136.0 (d, $J = 2.1$ Hz, C3),

131.7 (d, $J = 5.5$ Hz, C7), 127.5 (d, $J = 2.1$ Hz, C5), 126.2 (C4), 125.3 (C6), 121.6 (C2), 44.2 (d, $J = 18.7$ Hz, C11), 25.5 (C10), 15.2 (d, $J = 3.1$ Hz, C12); $^{31}\text{P}\{^1\text{H}\}$ NMR (162 MHz; CDCl_3) δ : 97.2; **HRMS**: (ESI) $^+$ Calculated for $[\text{C}_{18}\text{H}_{29}\text{N}_3\text{P}]^+$ $[\text{M}+\text{H}]^+$: 318.2094. Found: 318.2085.

8-(diisopropylphosphino)-2-methylquinoline (111)

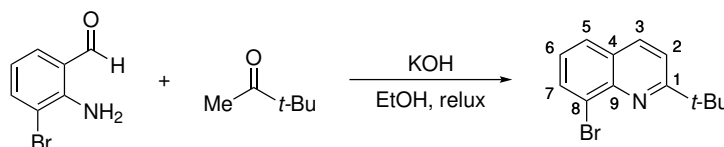


To an oven dried flask under an atmosphere of N_2 was charged 8-bromo-2-methylquinoline **109** (126 mg, 0.567 mmol) and THF (6 mL). The solution was cooled to -78 $^\circ\text{C}$ then *n*-butyllithium (2.37 M in hexane, 239 μL , 0.567 mmol) was added dropwise. The resulting orange solution was stirred at -78 $^\circ\text{C}$ for 30 minutes, then diisopropylchlorophosphine (90 μL , 0.567 mmol) was added dropwise. After stirring at -78 $^\circ\text{C}$ for 10 minutes, the reaction was warmed to r.t. and stirred for 2 h. The solution was concentrated *in vacuo* and the residue was extracted with PhMe and filtered (porosity 3, Celite, washed with 3×10 mL PhMe). Concentration *in vacuo* afforded the title compound (156 mg, 95%) as a yellow oil.

^1H NMR (400 MHz; CDCl_3) δ : 7.98 (d, $J = 8.3$ Hz, 1H, C2-H or C3-H), 7.75 (ddd, $J = 7.0, 4.6, 1.5$ Hz, 1H, C7-H), 7.71 (dd, $J = 8.1, 1.5$ Hz, 1H, C5-H), 7.44 (d, $J = 7.2$ Hz, 1H, C6-H), 7.23 (d, $J = 8.3$ Hz, 1H, C2-H or C3-H), 2.74 (s, 3H, C10-H₃), 2.43 (sd, $J = 6.9, 2.0$ Hz, 2H, C11-H), 1.17 (dd, $J = 13.9, 7.0$ Hz, 6H, C12_a-H₃), 0.96 (dd, $J = 12.2, 6.9$ Hz, 6H, C12_b-H₃); $^{13}\text{C}\{^1\text{H}\}$ NMR (101 MHz; CDCl_3) δ : 158.0 (C1), 150.7 (C9), 136.3 (d, $J = 1.4$ Hz, C2 or C3), 136.1 (d, $J = 20.9$ Hz, C8), 134.4 (d, $J = 7.2$ Hz, C7), 128.2 (C5), 126.4 (C4), 124.9 (d, $J = 3.4$ Hz, C6), 121.8 (C2 or C3), 25.6 (C10), 23.1 (d, $J = 13.4$ Hz, C11), 20.5 (d, $J = 17.2$ Hz, C12_a), 19.9 (d, $J = 11.5$ Hz, C12_b); $^{31}\text{P}\{^1\text{H}\}$ NMR (162

MHz; CDCl₃) δ : 3.05; **HRMS**: (ESI)⁺Calculated for [C₁₆H₂₃NP]⁺ [M+H]⁺: 260.1563. Found: 260.1554.

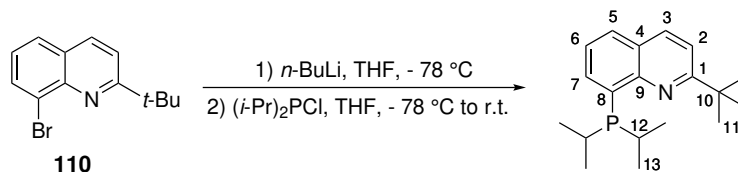
(8-bromo-2-(*tert*-butyl)quinoline (110)



Adapted from the reported procedure.²⁵³ To a solution of 2-amino-3-bromobenzaldehyde (4.84 g, 24.2 mmol) in EtOH (80 mL) was added 3,3-dimethyl-2-butanone (3.03 mL, 24.2 mmol) and powdered KOH (1.63 g, 29.0 mmol) portionwise. The reaction mixture was stirred at 95 °C for 6 hours, then cooled to r.t. and concentrated *in vacuo*. Purification by flash column chromatography (eluent: 2% to 4% Et₂O/hexane) afforded the title compound (4.55 g, 71%) as a colourless oil.

¹H NMR (400 MHz; CDCl₃) δ : 8.05 (d, J = 8.7 Hz, 1H, C2-H or C3-H), 8.01 (dd, J = 7.5, 1.4 Hz, 1H, C5-H or C7-H), 7.73 (dd, J = 8.1, 1.4 Hz, 1H, C5-H or C7-H), 7.56 (d, J = 8.6 Hz, 1H, C2-H or C3-H), 7.31 (t, J = 7.7 Hz, 1H, C6-H), 1.51 (s, 9H, C(CH₃)₃); ¹³C{¹H} NMR (101 MHz; CDCl₃) δ : 170.4 (C1), 144.3 (C9), 136.4 (C2 or C3), 132.8 (C5 or C7), 127.8 (C4 or C8), 127.2 (C5 or C7), 126.2 (C6), 125.7 (C4 or C8), 119.1 (C2 or C3), 38.8 (C(CH₃)₃), 30.2 (C(CH₃)₃); **HRMS**: (ESI)⁺Calculated for [C₁₃H₁₅BrN]⁺ [M+H]⁺: 264.0382. Found: 264.0379.

(8-(diisopropylphosphino)-2-(*tert*-butyl)quinoline (115)



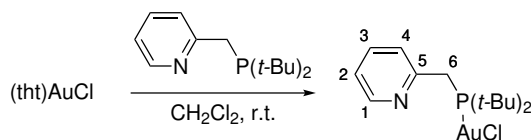
To an oven dried flask under an atmosphere of N₂ was charged 8-bromo-2-(*tert*-butyl)quinoline **110** (0.500 mL, 2.52 mmol) and THF (15 mL). The solution was cooled to -78 °C then *n*-butyllithium (2.37 M in hexane, 1.06 mL, 2.52 mmol) was added dropwise.

The resulting orange solution was stirred at $-78\text{ }^{\circ}\text{C}$ for 10 minutes, then diisopropylchlorophosphine (0.401 mL, 2.52 mmol) was added dropwise. After stirring at $-78\text{ }^{\circ}\text{C}$ for 10 minutes the reaction was warmed to r.t. and stirred for 3 h. The solution was concentrated *in vacuo* and the residue was dissolved in PhMe and filtered (porosity 3, Celite, washed with $3 \times 15\text{ mL}$ PhMe). Concentration *in vacuo* afforded the title compound (608 mg, 80%) as a pale yellow oil.

$^1\text{H NMR}$ (400 MHz; CDCl_3) δ : 8.05 (d, $J = 8.6\text{ Hz}$, 1H, C2-H or C3-H), 7.85 (td, $J = 7.2, 1.5\text{ Hz}$, 1H, C7-H), 7.74 (dd, $J = 8.0, 1.6\text{ Hz}$, 1H, C5-H), 7.51 (d, $J = 8.6\text{ Hz}$, 1H, C2-H or C3-H), 7.46 – 7.40 (m, 1H, C6-H), 2.77 – 2.64 (m, 2H, C12-H), 1.48 (s, 9H, C11-H₃), 1.19 (dd, $J = 13.7, 7.1\text{ Hz}$, 6H, C13_a-H₃), 0.96 (dd, $J = 13.5, 7.0\text{ Hz}$, 6H, C13_b-H₃); $^{13}\text{C}\{^1\text{H}\}\text{ NMR}$ (101 MHz; CDCl_3) δ : 168.2 (C1), 149.4 (d, $J = 6.8\text{ Hz}$, C8 or C9), 137.5 (d, $J = 21.5\text{ Hz}$, C8 or C9), 136.6 (C2 or C3), 136.0 (d, $J = 19.4\text{ Hz}$, C7), 128.5 (C5), 126.6 (d, $J = 1.6\text{ Hz}$, C4), 125.1 (d, $J = 7.2\text{ Hz}$, C6), 118.0 (C2 or C3), 38.9 (C10), 30.5 (C11), 23.7 (d, $J = 12.0\text{ Hz}$, C12), 21.0 (d, $J = 14.2\text{ Hz}$, C13_a), 20.7 (d, $J = 17.4\text{ Hz}$, C13_b); $^{31}\text{P}\{^1\text{H}\}\text{ NMR}$ (162 MHz; CDCl_3) δ : 12.3; **HRMS**: (ESI)⁺ Calculated for $[\text{C}_{19}\text{H}_{29}\text{NP}]^+ [\text{M}+\text{H}]^+$: 302.2032. Found: 302.2029.

5.4.3 Gold Complexes

(2-((di-*tert*-butylphosphino)methyl)pyridine)AuCl (**83**)

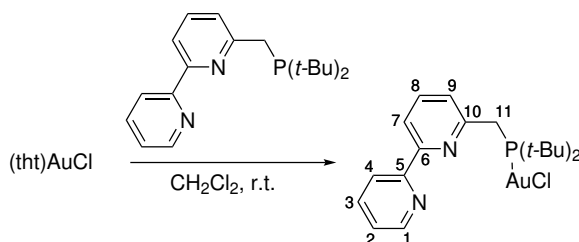


To an oven dried flask under an atmosphere of N_2 was charged tbtAuCl (192 mg, 0.598 mmol) and CH_2Cl_2 (6 mL), then a solution of **81** (171 mg, 0.717 mmol) in CH_2Cl_2 (6 mL) was added dropwise. After stirring overnight at r.t., the solution was concentrated to a minimum volume then hexane (approx. 15 mL) was added to precipitate a colourless

solid. The solid was washed with hexane (3×10 mL) then dried *in vacuo* to afford the title compound (260 mg, 55%) as a colourless solid.

$^1\text{H NMR}$ (400 MHz; CD_2Cl_2) δ : 8.49 (dt, $J = 4.9, 1.4$ Hz, 1H, C1-H), 7.72 – 7.65 (m, 2H, C2-H, C4-H), 7.22 – 7.18 (m, 1H, C3-H), 3.50 (d, $J = 11.5$ Hz, 2H, C6-H₂), 1.36 (d, $J = 15.1$ Hz, 18H, C(CH₃)₃); $^{13}\text{C}\{^1\text{H}\}$ NMR (126 MHz; CD_2Cl_2) δ : 156.3 (d, $J = 3.1$ Hz, C5), 149.3 (C1), 136.7 (C2), 125.2 (d, $J = 4.6$ Hz, C4), 122.1 (d, $J = 2.5$ Hz, C3), 36.0 (d, $J = 25.6$ Hz, C6), 30.7 (d, $J = 24.8$ Hz, C(CH₃)₃), 29.4 (d, $J = 4.8$ Hz, C(CH₃)₃); $^{31}\text{P}\{^1\text{H}\}$ NMR (162 MHz; CD_2Cl_2) δ : 75.8; HRMS: (ESI)⁺ Calculated for $[\text{C}_{14}\text{H}_{24}\text{AuNP}]^+ [\text{M-Cl}]^+$: 434.1312. Found: 434.1320.

(6-di-*tert*-butylphosphinomethyl-2,2'-bipyridine)AuCl (84)

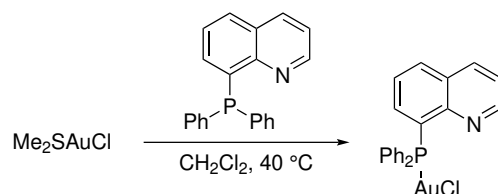


To an oven dried flask under an atmosphere of N_2 was charged tbtAuCl (68 mg, 0.212 mmol) and CH_2Cl_2 (3 mL), then **82** (80 mg, 0.250 mmol) was added in a single portion. After stirring overnight at r.t., the solution was concentrated to dryness to afford a colourless solid. The solid was washed with hexane (3×5 mL) then dried *in vacuo* to afford the title compound (110 mg, 80%) as a colourless solid. Single crystals suitable for X-ray diffraction were grown from a CH_2Cl_2 solution layered with hexane. See Section 5.5, Table 5.13 for full crystallographic details.

$^1\text{H NMR}$ (400 MHz; CD_2Cl_2) δ : 8.67 – 8.63 (m, 1H, C1-H), 8.60 (d, $J = 7.9$ Hz, 1H, C4-H), 8.35 (d, $J = 7.9$ Hz, 1H, C7-H), 7.85 (td, $J = 7.7, 1.8$ Hz, 1H, C3-H), 7.81 (t, $J = 7.8$ Hz, 1H, C8-H), 7.56 (d, $J = 7.7$ Hz, 1H, C9-H), 7.34 – 7.30 (m, 1H, C2-H), 3.58 (d, $J = 11.5$ Hz, 2H, C11-H₂), 1.39 (d, $J = 15.1$ Hz, 18H, C(CH₃)₃); $^{13}\text{C}\{^1\text{H}\}$ NMR (126

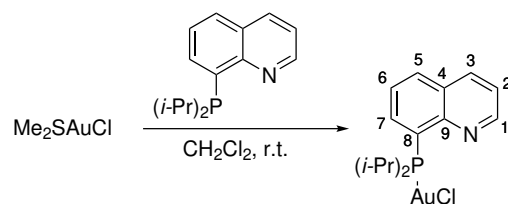
MHz; CD₂Cl₂) δ : 155.9 (C5 or C6), 155.4 (d, $J = 3.8$ Hz, C10), 155.4 (C5 or C6), 149.1 (C1), 137.7 (d, $J = 1.6$ Hz, C8), 137.0 (C3), 125.0 (d, $J = 4.7$ Hz, C9), 123.9 (C2), 121.3 (C4), 119.1 (d, $J = 2.3$ Hz, C7), 36.0 (d, $J = 25.6$ Hz, C(CH₃)₃), 30.7 (d, $J = 25.3$ Hz, C11), 29.5 (d, $J = 5.0$ Hz, C(CH₃)₃); ³¹P{¹H} NMR (122 MHz; CDCl₃) δ : 74.8; HRMS: (ESI)⁺ Calculated for [C₁₉H₂₈AuClN₂P]⁺ [M+H]⁺: 547.1339. Found: 547.1338.

(8-(diphenylphosphino)quinoline)AuCl (90)



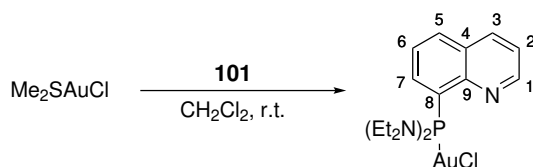
To an oven dried flask under an atmosphere of N₂ was charged Me₂SAuCl (649 mg, 2.07 mmol) and CH₂Cl₂ (30 mL), then **89** (649 mg, 2.03 mmol) was added in one portion. The solution was stirred at 40 °C for 2h then cooled to r.t. The reaction was concentrated to a minimum volume then hexane (approx. 30 mL) was added to precipitate a colourless solid. The solid was washed with hexane (3 × 10 mL) then dried *in vacuo* to afford the title compound (987 mg, 87%) as a colourless solid. Single crystals suitable for X-ray diffraction were grown from a CH₂Cl₂ solution layered with hexane. See Section 5.5, Table 5.14 for full crystallographic details.

¹H NMR (500 MHz; CD₂Cl₂) δ : 8.85 (dd, $J = 4.3, 1.8$ Hz, 1H, Ar-CH), 8.30 (dt, $J = 8.4, 1.7$ Hz, 1H, Ar-CH), 8.10 (d, $J = 8.2$ Hz, 1H, Ar-CH), 7.63 – 7.43 (m, 12H, Ar-CH), 7.27 (ddd, $J = 13.1, 7.2, 1.4$ Hz, 1H, Ar-CH); ¹³C{¹H} NMR (126 MHz; CD₂Cl₂) δ : 150.1 (4° C), 147.7 (d, $J = 7.1$ Hz, 4° C), 136.6 (d, $J = 1.7$ Hz, Ar-CH), 136.0 (d, $J = 6.4$ Hz, Ar-CH), 134.4 (d, $J = 14.2$ Hz, Ar-CH), 132.5 (d, $J = 2.4$ Hz, Ar-CH), 131.6 (d, $J = 2.6$ Hz, Ar-CH), 129.3 (d, $J = 64.0$ Hz, 4° C), 129.0 (d, $J = 12.0$ Hz, Ar-CH), 128.6 (d, $J = 5.5$ Hz, 4° C), 128.1 (d, $J = 64.8$ Hz, 4° C), 126.2 (d, $J = 11.1$ Hz, Ar-CH), 122.40 (Ar-CH); ³¹P{¹H} NMR (162 MHz; CDCl₃) δ : 26.2. The spectroscopic properties of this compound were consistent with literature data.⁷⁸

(8-(diisopropylphosphino)quinoline)AuCl (102)

To an oven dried flask under an atmosphere of N_2 was charged Me_2SAuCl (247 mg, 0.840 mmol) and CH_2Cl_2 (15 mL), then a solution of **99** (240 mg, 0.88 mmol) in CH_2Cl_2 (6 mL) was added dropwise. After stirring for 5 h at r.t., the solution was concentrated to a minimum volume then hexane (approx. 15 mL) was added to precipitate a colourless solid. The solid was washed with hexane (3×10 mL) then dried *in vacuo* to afford the title compound (260 mg, 55%) as a colourless solid.

1H NMR (400 MHz; $CDCl_3$) δ : 8.91 (dd, $J = 4.3, 1.8$ Hz, 1H, C1-H), 8.67 (ddd, $J = 17.2, 7.1, 1.5$ Hz, 1H, C7-H), 8.24 (dt, $J = 8.4, 1.7$ Hz, 1H, C3-H), 8.00 (dt, $J = 8.2, 1.7$ Hz, 1H, C6-H), 7.60 (ddd, $J = 8.4, 7.1, 1.4$ Hz, 1H, C5-H), 7.50 (dd, $J = 8.3, 4.2$ Hz, 1H, C2-H), 3.50 – 3.35 (m, 2H, $CH(CH_3)_2$), 1.40 (dd, $J = 20.0, 6.9$ Hz, 6H, $CH(C_aH_3)_2$), 0.82 (dd, $J = 18.7, 6.9$ Hz, 6H, $CH(C_bH_3)_2$); $^{13}C\{^1H\}$ NMR (126 MHz; $CDCl_3$) δ : 150.2 (C1), 148.5 (d, $J = 1.5$ Hz, C9 or C4), 143.3 (d, $J = 20.0$ Hz, C7), 137.1 (C3), 133.0 (d, $J = 2.6$ Hz, C6), 128.6 (d, $J = 5.3$ Hz, C9 or C4), 128.0 (d, $J = 51.5$ Hz, C8), 126.0 (d, $J = 14.7$ Hz, C5), 122.1 (C2), 27.1 (d, $J = 34.6$ Hz, $CH(CH_3)_2$), 21.5 (d, $J = 6.2$ Hz, $CH(C_aH_3)_2$), 20.6 (d, $J = 1.7$ Hz, $CH(C_bH_3)_2$); ^{31}P NMR (162 MHz; $CDCl_3$) δ : 74.78; HRMS: (ESI) $^+$ Calculated for $[C_{15}H_{20}AuClNNaP]^+$ $[M+Na]^+$: 500.0580. Found: 500.0578.

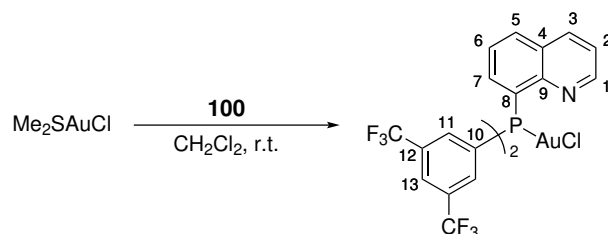
(8-(bis(diethylamino)phosphino)quinoline)AuCl (103)

To an oven dried flask under an atmosphere of N_2 was charged Me_2SAuCl (136 mg, 0.460 mmol) and CH_2Cl_2 (10 mL), then a solution of **101** (160 mg, 0.490 mmol) in CH_2Cl_2 (5

mL) was added dropwise. After stirring for 1.5 h at r.t., the solution was concentrated to a minimum volume then hexane (approx. 15 mL) was added to precipitate a colourless solid. The solid was washed with hexane (3×10 mL) then dried *in vacuo* to afford the title compound (179 mg, 73%) as a colourless solid. Crystals suitable for X-ray diffraction were grown from a CH_2Cl_2 solution layered with pentane at -20 °C. See Section 5.5, Table 5.16 for full crystallographic details.

$^1\text{H NMR}$ (500 MHz; CD_2Cl_2) δ : 8.98 (dd, $J = 4.2, 1.9$ Hz, 1H, C1-H), 8.23 (dt, $J = 8.3, 1.8$ Hz, 1H, C3-H), 8.01 (d, $J = 8.2$ Hz, 1H, C5-H), 7.86 (ddd, $J = 12.7, 7.1, 1.5$ Hz, 1H, C7-H), 7.65 – 7.59 (m, 1H, C6-H), 7.51 (dd, $J = 8.3, 4.1$ Hz, 1H, C2-H), 3.33 – 3.13 (m, 8H, CH_2), 1.16 (t, $J = 7.1$ Hz, 12H, CH_3); $^{13}\text{C}\{^1\text{H}\}$ NMR (126 MHz; CD_2Cl_2) δ : 150.5 (C1), 148.3 (d, $J = 9.5$ Hz, C9), 136.7 (d, $J = 2.0$ Hz, C3), 134.0 (d, $J = 6.7$ Hz, C7), 133.2 (d, $J = 80.8$ Hz, C8), 132.4 (d, $J = 2.1$ Hz, C5), 129.1 (d, $J = 5.8$ Hz, C4), 126.4 (d, $J = 10.8$ Hz, C6), 122.6 (C2), 43.1 (d, $J = 10.0$ Hz, CH_2), 14.5 (d, $J = 2.2$ Hz, CH_3); $^{31}\text{P}\{^1\text{H}\}$ NMR (162 MHz; CD_2Cl_2) δ : 93.7; HRMS: (ESI) $^+$ Calculated for $[\text{C}_{17}\text{H}_{27}\text{AuClN}_3\text{P}]^+$ $[\text{M}+\text{H}]^+$: 536.1291. Found: 536.1291.

(8-(bis(3,5-di(trifluoromethyl)phenyl)phosphino)quinoline)AuCl (**104**)

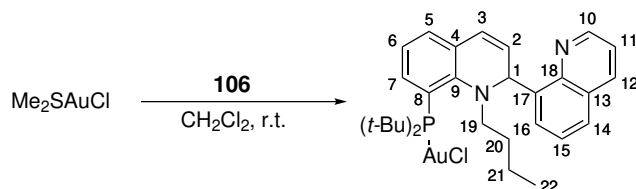


To an oven dried flask under an atmosphere of N_2 was charged Me_2SAuCl (81 mg, 0.273 mmol) and CH_2Cl_2 (6 mL), then a solution of **100** (240 mg, 0.287 mmol) in CH_2Cl_2 (6 mL) was added. After stirring at r.t. for 4 h, the solution was concentrated to a minimum volume then hexane (approx. 15 mL) was added to precipitate a colourless solid. The solid was washed with hexane (3×10 mL) then dried *in vacuo* to afford the title compound (213 mg, 91%) as a colourless solid. Crystals suitable for X-ray diffraction were

grown from a CH₂Cl₂ solution layered with pentane at -20 °C. See Section 5.5, Table 5.17 for full crystallographic details.

¹H NMR (400 MHz; CDCl₃) δ: 8.74 (dd, *J* = 4.3, 1.7 Hz, 1H, C1-H), 8.32 (dt, *J* = 8.3, 1.6 Hz, 1H, C3-H), 8.23 (dt, *J* = 8.3, 1.5 Hz, 1H, C5-H), 8.08 (d, *J* = 1.6 Hz, 2H, C13-H), 8.05 (s, 4H, C11-H), 7.94 (ddd, *J* = 16.4, 7.2, 1.4 Hz, 1H, C7-H), 7.74 (ddd, *J* = 8.2, 7.2, 2.4 Hz, 1H, C6-H), 7.55 (dd, *J* = 8.4, 4.3 Hz, 1H, C2-H); ¹³C{¹H} NMR (126 MHz; CDCl₃) δ: 150.7 (C1), 147.3 (d, *J* = 4.9 Hz, C9), 139.3 (d, *J* = 15.4 Hz, C7), 137.2 (d, *J* = 1.6 Hz, C3), 135.0 (d, *J* = 2.6 Hz, C5), 133.9 (d, *J* = 15.5 Hz, C13), 132.9 (qd, *J* = 34.2, 12.1 Hz, C12), 132.4 (d, *J* = 62.8 Hz, C10), 129.0 (d, *J* = 5.7 Hz, C4), 126.9 (d, *J* = 14.3 Hz, C6), 126.2 – 126.0 (m, C11), 124.4 (d, *J* = 66.0 Hz, C8), 123.3 (C2), 122.6 (q, *J* = 273.5 Hz, C_{F3}); ³¹P{¹H} NMR (162 MHz; CDCl₃) δ: 34.2; ¹⁹F NMR (377 MHz; CDCl₃) δ: -62.9; HRMS: (ESI)⁺Calculated for [C₂₅H₁₂AuClF₁₂NNaP]⁺ [M+Na]⁺: 839.9762. Found: 839.9767.

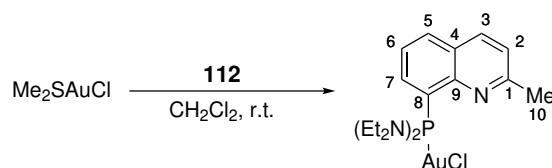
(1-butyl-8-(di-*tert*-butylphosphino)-1,2-dihydro-2,8'-biquinoline)AuCl (108)



To an oven dried flask under an atmosphere of N₂ was charged Me₂SAuCl (130 mg, 0.441 mmol) and CH₂Cl₂ (8 mL), then **106** (222 mg, 0.485 mmol) was added. After stirring at r.t. for 1.5 h, the solution was concentrated to a minimum volume then hexane (approx. 15 mL) was added to precipitate a colourless solid. The solid was washed with hexane (3 × 10 mL) then dried *in vacuo* to afford the title compound (252 mg, 83%) as a colourless solid. Single crystals suitable for X-ray diffraction were grown from a CH₂Cl₂ solution layered with pentane at -20 °C. See Section 5.5, Table 5.18 for full crystallographic details.

$^1\text{H NMR}$ (500 MHz; CD_2Cl_2) δ : 9.20 (dd, $J = 4.2, 1.8$ Hz, 1H, C10-H), 8.12 (dd, $J = 8.2, 1.8$ Hz, 1H, C11-H), 7.63 (dd, $J = 8.2, 1.5$ Hz, 1H, C14-H or C16-H), 7.49 (dd, $J = 8.0, 1.6$ Hz, 1H, C7-H or C5-H), 7.46 (dd, $J = 8.2, 4.2$ Hz, 1H, C12-H), 7.34 (dt, $J = 7.4, 1.3$ Hz, 1H, C7-H or C5-H), 7.29 (dd, $J = 7.2, 1.5$ Hz, 1H, C14-H or C16-H), 7.20 – 7.14 (m, 1H, C15-H), 7.14 (td, $J = 7.7, 1.4$ Hz, 1H, C6-H), 6.89 (d, $J = 9.3$ Hz, 1H, C3-H), 6.59 (d, $J = 5.6$ Hz, 1H, C1-H), 6.24 (dd, $J = 9.4, 5.6$ Hz, 1H, C2-H), 3.50 – 3.42 (m, 1H, C19-H_a), 3.41 – 3.33 (m, 1H, C19-H_b), 2.26 (ddd, $J = 21.7, 16.9, 5.0$ Hz, 1H, C20-H_a), 1.67 – 1.54 (m, 1H, C20-H_b), 1.44 (d, $J = 15.3$ Hz, 9H, C(CH₃)₃), 1.37 – 1.25 (m, 1H, C21-H_a), 1.23 – 1.13 (m, 1H, C21-H_b), 0.92 (t, $J = 7.4$ Hz, 3H, C22-H₃), 0.64 (d, $J = 15.6$ Hz, 9H, C(CH₃)₃); $^{13}\text{C}\{^1\text{H}\}$ NMR (126 MHz; CD_2Cl_2) δ : 151.7 (C10), 151.5 (d, $J = 6.9$ Hz, C4 or C9), 146.2 (C13 or C17 or C18), 137.2 (C13 or C17 or C18), 136.6 (C11), 134.9 (d, $J = 1.9$ Hz, C7 or C5), 133.1 (d, $J = 6.0$ Hz, C4 or C9), 130.4 – 130.3 (m, 2C, C2, C7 or C5), 129.2 (C13 or C17 or C18), 129.0 (C14 or C16), 128.2 (C14 or C16), 127.1 (C3), 125.9, (C15) 123.5 (d, $J = 7.6$ Hz, C6), 123.2 (d, $J = 44.3$ Hz, C8), 121.5 (C12), 63.6 (C19), 53.5 (C1), 38.4 (d, $J = 25.9$ Hz, C_a(CH₃)₃), 38.1 (d, $J = 25.7$ Hz, C_b(CH₃)₃), 32.1 (d, $J = 6.6$ Hz, C_a(CH₃)₃), 30.1 (C20), 30.0 (d, $J = 7.1$ Hz, C_a(CH₃)₃), 21.6 (C21), 14.5 (C22); $^{31}\text{P}\{^1\text{H}\}$ NMR (202 MHz; CD_2Cl_2) δ : 56.0; HRMS: (ESI)⁺ Calculated for $[\text{C}_{30}\text{H}_{40}\text{AuClN}_2\text{P}]^+$ $[\text{M}+\text{H}]^+$: 691.2278. Found: 691.2271.

(8-(bis(diethylamino)phosphino)-2-methylquinoline)AuCl (114)

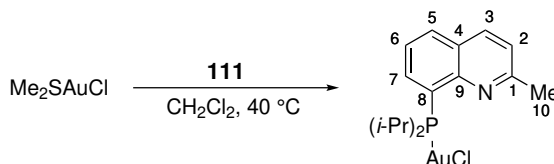


To an oven dried flask under an atmosphere of N_2 was charged Me_2SAuCl (310 mg, 1.05 mmol) and CH_2Cl_2 (20 mL), then a solution of **112** (351 mg, 1.11 mmol) in CH_2Cl_2 (10 mL) was added. After stirring for 1 h at r.t., the solution was concentrated to a minimum volume then pentane (approx. 25 mL) was added to precipitate a colourless solid. The solid was washed with hexane (2×10 mL) then dried *in vacuo* to afford the title

compound (479 mg, 83%) as a colourless solid. Single crystals suitable for X-ray diffraction were grown from a CH_2Cl_2 solution layered with Et_2O at $-18\text{ }^\circ\text{C}$. See Section 5.5, Table 5.19 for full crystallographic details.

$^1\text{H NMR}$ (400 MHz; CD_2Cl_2) δ : 8.09 (dd, $J = 8.4, 1.5$ Hz, 1H, C2-H or C3-H), 7.95 (dt, $J = 8.2, 1.3$ Hz, 1H, C5-H), 7.80 (ddd, $J = 12.4, 7.1, 1.4$ Hz, 1H, C7-H), 7.56 – 7.51 (m, 1H, C6-H), 7.36 (d, $J = 8.4$ Hz, 1H, C2-H or C3-H), 3.33 – 3.10 (m, 8H, CH₂), 2.75 (s, 3H, C10-H₃), 1.16 (t, $J = 7.1$ Hz, 12H, CH₃); $^{13}\text{C}\{^1\text{H}\}$ NMR (101 MHz; CD_2Cl_2) δ : 159.8 (C1), 147.8 (d, $J = 9.6$ Hz, C8), 136.7 (d, $J = 1.9$ Hz, C2 or C3), 133.5 (d, $J = 6.3$ Hz, C7), 132.7 (C4 or C9), 132.0 (d, $J = 2.0$ Hz, C5), 131.9 (C4 or C9), 125.5 (d, $J = 10.8$ Hz, C6), 123.4 (C2 or C3), 43.0 (d, $J = 10.1$ Hz, CH₂), 25.2 (C10), 14.2 (d, $J = 2.3$ Hz, CH₃); $^{31}\text{P}\{^1\text{H}\}$ NMR (162 MHz; CD_2Cl_2) δ : 93.6; **HRMS**: (ESI)⁺Calculated for $[\text{C}_{18}\text{H}_{29}\text{AuClN}_3\text{P}]^+ [\text{M}+\text{H}]^+$: 550.1448. Found: 550.1442.

(8-(diisopropylphosphino)-2-methylquinoline)AuCl (113)

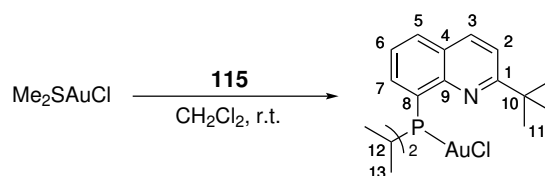


To an oven dried flask under an atmosphere of N_2 was charged Me_2SAuCl (136 mg, 0.463 mmol) and CH_2Cl_2 (10 mL), then a solution of **111** (126 mg, 0.486 mmol) in CH_2Cl_2 (5 mL) was added. After stirring for 30 mins at $40\text{ }^\circ\text{C}$, the solution was concentrated to a minimum volume then hexane (approx. 25 mL) was added to precipitate a colourless solid. The solid was washed with hexane (3×10 mL) then dried *in vacuo* to afford the title compound (180 mg, 79%) as a colourless solid.

$^1\text{H NMR}$ (400 MHz; CD_2Cl_2) δ : 8.54 (ddd, $J = 16.6, 7.1, 1.5$ Hz, 1H, C7-H), 8.14 (dd, $J = 8.4, 1.3$ Hz, 1H, C2-H or C3-H), 7.99 (dt, $J = 8.1, 1.7$ Hz, 1H, C5-H), 7.57 (ddd, $J = 8.3, 7.1, 1.5$ Hz, 1H, C6-H), 7.39 (d, $J = 8.4$ Hz, 1H, C2-H or C3-H), 3.45 – 3.31 (m, 2H, CH(CH_3)₂), 2.74 (s, 3H, C10-H₃), 1.39 (dd, $J = 19.8, 6.9$ Hz, 6H, C_aH (CH₃)₂), 0.87 (dd,

$J = 18.4, 7.0$ Hz, 6H, $C_bH(\underline{CH}_3)_2$); $^{13}C\{^1H\}$ NMR (126 MHz; CD_2Cl_2) δ : 159.9 (C1), 148.6 (d, $J = 1.8$ Hz, C4 or C9), 142.8 (d, $J = 18.5$ Hz, C7), 137.4 (C2 or C3), 133.0 (d, $J = 2.6$ Hz, C5), 127.3 (C4 or C9), 127.1 (d, $J = 47.9$ Hz, C8), 125.5 (d, $J = 14.3$ Hz, C6), 123.2 (C2 or C3), 27.5 (d, $J = 34.8$ Hz, $\underline{CH}(\underline{CH}_3)_2$), 25.6 (C10), 21.6 (d, $J = 6.1$ Hz, $C_dH(\underline{CH}_3)_2$), 20.6 (d, $J = 1.4$ Hz, $C_bH(\underline{CH}_3)_2$); $^{31}P\{^1H\}$ NMR (162 MHz; CD_2Cl_2) δ : 71.35; HRMS: (ESI)⁺ Calculated for $[C_{16}H_{23}AuClNP]^+$ $[M+H]^+$: 492.0917. Found: 492.0926.

(8-(diisopropylphosphino)-2-(tert-butyl)quinoline)AuCl (116)



To an oven dried flask under an atmosphere of N_2 was charged Me_2SAuCl (295 mg, 1.00 mmol) and CH_2Cl_2 (18 mL), then a solution of **115** (331 mg, 1.10 mmol) in CH_2Cl_2 (8 mL) was added. After stirring for 3 h at r.t., the solution was concentrated to a minimum volume then hexane (approx. 30 mL) was added to precipitate a colourless solid. The solid was washed with hexane (3×10 mL) then dried *in vacuo* to afford the title compound (475 mg, 89%) as a colourless solid. Single crystals suitable for X-ray diffraction were grown from a CH_2Cl_2 solution layered with hexane at -20 °C. See Section 5.5, Table 5.20 for full crystallographic details.

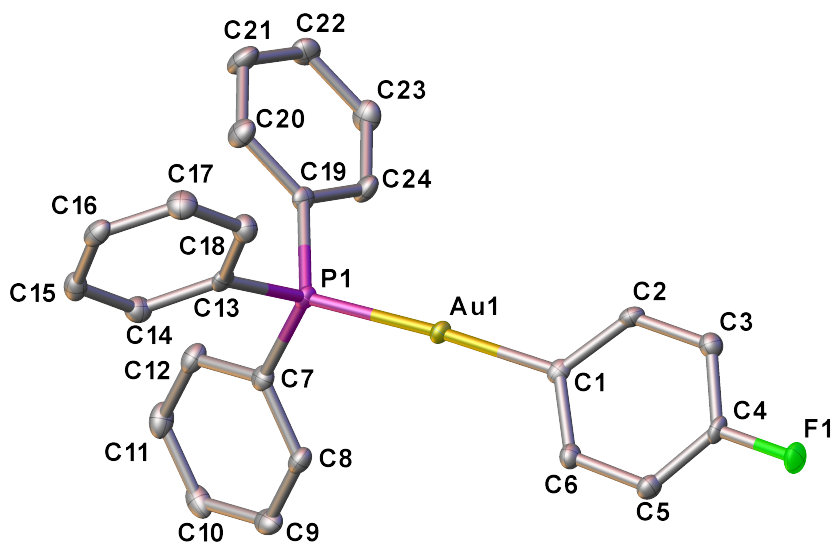
1H NMR (500 MHz; CD_2Cl_2) δ : 8.62 (ddd, $J = 17.3, 7.1, 1.5$ Hz, 1H, C7-H), 8.21 (dd, $J = 8.7, 1.4$ Hz, 1H, C2-H or C3-H), 8.00 (dt, $J = 8.1, 1.7$ Hz, 1H, C5-H), 7.65 (d, $J = 8.7$ Hz, 1H, C2-H or C3-H), 7.58 (ddd, $J = 8.2, 7.0, 1.4$ Hz, 1H, C6-H), 3.50 (dp, $J = 12.2, 6.9$ Hz, 2H, C12-H), 1.47 (s, 9H, C11-H₃), 1.42 (dd, $J = 19.7, 6.9$ Hz, 6H, C13_a-H₃), 0.84 (dd, $J = 18.7, 7.0$ Hz, 6H, C13_b-H₃); $^{13}C\{^1H\}$ NMR (126 MHz; CD_2Cl_2) δ : 170.5 (C1), 148.0 (d, $J = 1.4$ Hz, C9), 143.4 (d, $J = 17.0$ Hz, C7), 137.8 (C2 or C3), 133.1 (d, $J = 2.6$ Hz, C5), 127.7 (d, $J = 47.3$ Hz, C8), 127.4 (C4), 125.6 (d, $J = 14.7$ Hz, C6),

119.7 (C2 or C3), 39.4 (C10), 30.7 (C11), 27.3 (d, $J = 34.7$ Hz, C11), 21.8 (d, $J = 6.1$ Hz, C13_a), 20.9 (d, $J = 2.1$ Hz, C13_b); $^{31}\text{P}\{^1\text{H}\}$ NMR (162 MHz; CD_2Cl_2) δ : 74.7; **HRMS**: (ESI)⁺ Calculated for $[\text{C}_{19}\text{H}_{28}\text{AuCINNaP}]^+$ $[\text{M}+\text{Na}]^+$: 556.1206. Found: 556.1207.

5.5 Crystallographic Data

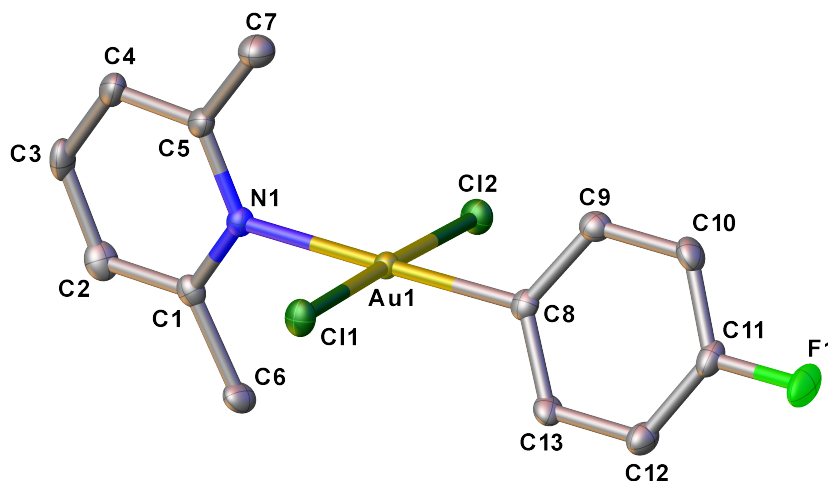
Single crystal X-ray diffraction experiments were carried out at 100(2) K on a Bruker APEX II CCD diffractometer using Mo-K α radiation ($\lambda = 0.71073$ Å). Intensities were integrated²⁹³ and absorption corrections were based on equivalent reflections using SAD-ABS.²⁹⁴ The structures were solved by direct methods (SHELXS-97)²⁹⁵ and refined against F^2 in SHELXL^{295,296} using Olex2.²⁹⁷ All of the non-hydrogen atoms were refined anisotropically, all of the hydrogen atoms were located geometrically and refined using a riding model.

Table 5.1: Crystallographic data for complex **13**, thermal ellipsoids are shown at the 50% probability level. Hydrogen atoms have been omitted for clarity. Selected bond lengths (Å) and angles (°): Au1-P1 2.2906(7), Au1-C1 2.043(3), P1-C7 1.818(3), C1-Au1-P1 176.51(8), C7-P1-Au1 113.09(9).



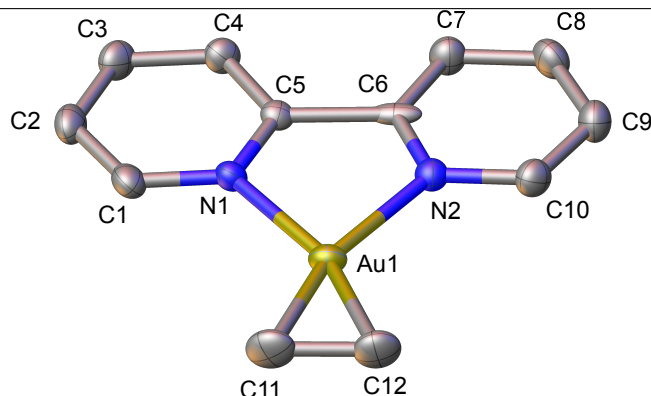
Empirical formula	C ₂₄ H ₁₉ AuFP
Formula weight	554.33
Temperature (K)	100(2)
Crystal system	Triclinic
Space group	<i>P</i> -1
<i>a</i> (Å), <i>b</i> (Å), <i>c</i> (Å)	8.6000(2), 14.9179(4), 15.1241(4)
α (°), β (°), γ (°)	88.5790(14), 89.7538(15), 86.1002(13)
Volume (Å³)	1935.24(9)
<i>Z</i>	4
Density_{calc} (g cm⁻³)	1.903
μ (mm⁻¹)	7.699
<i>F</i>(000)	1064
Crystal size (mm³)	0.361 × 0.219 × 0.136
Radiation	Mo K α (λ =0.71073)
2θ range for data collection (°)	3.794 to 55.984
Index ranges	-11 ≤ <i>h</i> ≤ 11, -19 ≤ <i>k</i> ≤ 19, -19 ≤ <i>l</i> ≤ 19
Reflections collected	25671
Independent reflections	9323 [<i>R</i> _{int} = 0.0281, <i>R</i> _{sigma} = 0.0260]
Data/restraints/parameters	9323/0/487
Goodness-of-fit on <i>F</i>²	1.029
Final <i>R</i> indexes [<i>I</i> > 2σ(<i>I</i>)]	<i>R</i> 1 = 0.0192, <i>wR</i> 2 = 0.0384
Final <i>R</i> indexes [all data]	<i>R</i> 1 = 0.0240, <i>wR</i> 2 = 0.0396
Largest diff. peak/hole (e Å⁻³)	1.20/-0.52

Table 5.2: Molecular structure of **16**, thermal ellipsoids are shown at the 50% probability level. Hydrogen atoms have been omitted for clarity. Selected bond lengths (Å) and angles (°): Au1-Cl1 2.2810(9), Au1-Cl2 2.2762(9), Au1-N1 2.150(3), Au1-C8 2.017(4), Cl2-Au1-Cl1 178.06(3), C8-Au1-N1 179.01(13), N1-Au1-Cl1 91.75(8), C8-Au1-Cl2 89.07(10).



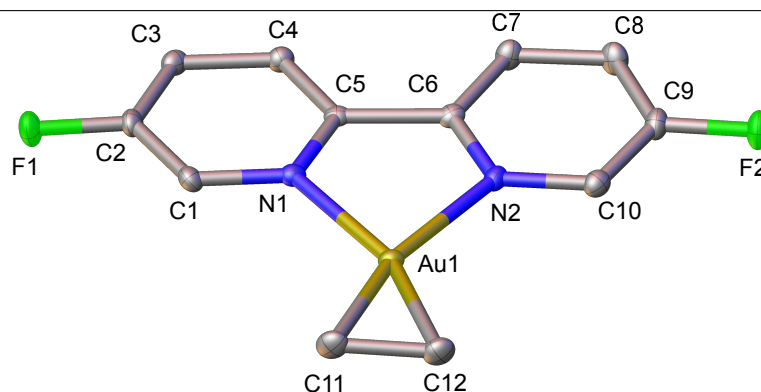
Empirical formula	C ₁₃ H ₁₃ AuCl ₂ FN
Formula weight	470.11
Temperature (K)	100(2)
Crystal system	Monoclinic
Space group	<i>P</i> ₁ / <i>n</i>
<i>a</i> (Å), <i>b</i> (Å), <i>c</i> (Å)	14.7841(3), 14.3018(2), 15.1278(3)
α (°), β (°), γ (°)	90, 117.4497(8), 90
Volume (Å³)	2838.50(9)
<i>Z</i>	8
Density_{calc} (g cm⁻³)	2.2000
μ (mm⁻¹)	10.734
<i>F</i>(000)	1760
Crystal size (mm³)	0.285 × 0.148 × 0.114
Radiation	Mo K α (λ =0.71073)
2θ range for data collection (°)	3.18 to 55.92
Index ranges	-11 ≤ <i>h</i> ≤ 11, -18 ≤ <i>k</i> ≤ 18, -19 ≤ <i>l</i> ≤ 18
Reflections collected	25671
Independent reflections	6818 [<i>R</i> _{int} = 0.0315]
Data/restraints/parameters	6818/0/329
Goodness-of-fit on <i>F</i>²	1.038
Final <i>R</i> indexes [<i>I</i> > 2σ(<i>I</i>)]	<i>R</i> 1 = 0.0238, <i>wR</i> 2 = 0.0511
Final <i>R</i> indexes [all data]	<i>R</i> 1 = 0.0353, <i>wR</i> 2 = 0.0551
Largest diff. peak/hole (e Å⁻³)	0.97/-1.04

Table 5.3: Molecular structure of **51a**, thermal ellipsoids are shown at the 30% probability level. Hydrogen atoms and the NTf_2 anion have been omitted for clarity. Selected bond lengths (Å) and angles (°): Au1-N1 2.174(4), Au1-N2 2.184(4), Au1-C12 2.090(6), Au1-C1 2.080(5), C11-C12 1.407(9), N1-Au1-N2 74.89(14).



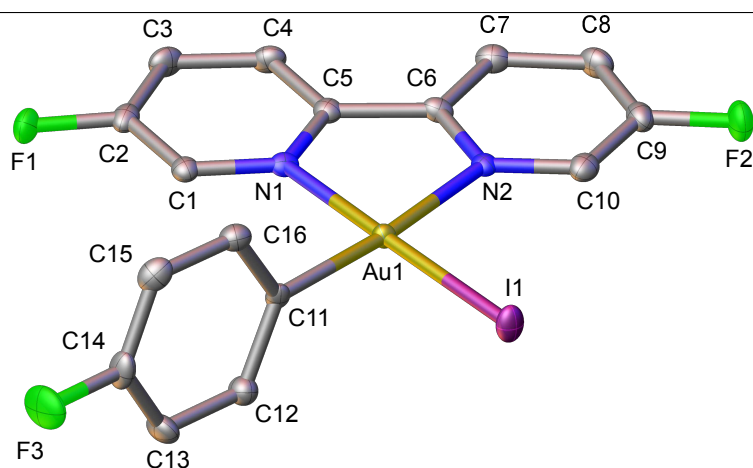
Empirical formula	$\text{C}_{14}\text{H}_{12}\text{AuF}_6\text{N}_3\text{O}_4\text{S}_2$
Formula weight	661.35
Temperature (K)	240
Crystal system	Monoclinic
Space group	$P2_1/c$
a (Å), b (Å), c (Å)	8.2217(15), 14.433(3), 17.223(3)
α (°), β (°), γ (°)	90, 92.689(9), 90
Volume (Å³)	2041.5(7)
Z	1
Density_{calc} (g cm⁻³)	0.538
μ (mm⁻¹)	1.873
$F(000)$	314.0
Crystal size (mm³)	$2.0 \times 0.29 \times 0.29$
Radiation	Mo $K\alpha$ ($\lambda=0.71073$)
2θ range for data collection (°)	3.684 to 55.948
Index ranges	$-10 \leq h \leq 10, -18 \leq k \leq 18, -20 \leq l \leq 22$
Reflections collected	19390
Independent reflections	4890 [$R_{int} = 0.0412$]
Data/restraints/parameters	4890/0/277
Goodness-of-fit on F^2	1.095
Final R indexes [$I > 2\sigma(I)$]	$R1 = 0.0349, wR2 = 0.0862$
Final R indexes [all data]	$R1 = 0.0432, wR2 = 0.0901$
Largest diff. peak/hole (e Å⁻³)	1.91/-2.18

Table 5.4: Molecular structure of **51b**, thermal ellipsoids are shown at the 50% probability level. Hydrogen atoms and the NTf_2 anion have been omitted for clarity. Selected bond lengths (\AA) and angles ($^\circ$): Au1-N1 2.178(2), Au1-N2 2.210(2), Au1-C12 2.092(3), Au1-C11 2.086(3), C11-C12 1.399(5), N1-Au1-N2 74.57(9).



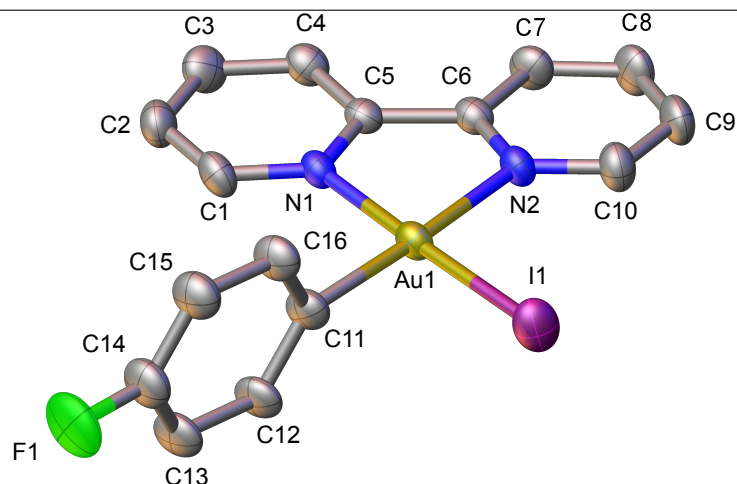
Empirical formula	$\text{C}_{14}\text{H}_{10}\text{AuF}_8\text{N}_3\text{O}_4\text{S}_2$
Formula weight	697.34
Temperature (K)	100.0
Crystal system	Monoclinic
Space group	$P2_1/c$
<i>a</i> (\AA), <i>b</i> (\AA), <i>c</i> (\AA)	8.1314(3), 14.0057(6), 17.5690(7)
α ($^\circ$), β ($^\circ$), γ ($^\circ$)	90, 90.710(2), 90
Volume (\AA^3)	2000.71(14)
<i>Z</i>	4
Density_{calc} (g cm^{-3})	2.315
μ (mm^{-1})	7.664
<i>F</i>(000)	1320.0
Crystal size (mm^3)	$0.3 \times 0.1 \times 0.1$
Radiation	Mo $\text{K}\alpha$ ($\lambda=0.71073$)
2θ range for data collection ($^\circ$)	3.72 to 55.198
Index ranges	$-10 \leq h \leq 10, -17 \leq k \leq 18, -22 \leq l \leq 22$
Reflections collected	34892
Independent reflections	4628 [$R_{int} = 0.0304$]
Data/restraints/parameters	4628/130/326
Goodness-of-fit on F^2	1.065
Final <i>R</i> indexes [$I > 2\sigma(I)$]	$R1 = 0.0179, wR2 = 0.0451$
Final <i>R</i> indexes [all data]	$R1 = 0.0204, wR2 = 0.0462$
Largest diff. peak/hole (e \AA^{-3})	1.45/-0.82

Table 5.5: Molecular structure of **56a**, thermal ellipsoids are shown at the 50% probability level. Hydrogen atoms and the NTf_2 anion have been omitted for clarity. Selected bond lengths (\AA) and angles ($^\circ$): Au1–C1 2.011(3), Au1–I1 2.5357(3), Au1–N1 2.080(3), Au1–N2 2.130(3), N1–Au1–N2 78.92(12), N2–Au1–I(1) 99.37(8), N1–Au1–C11 95.17(14), C11–Au1–I1 86.54(11).



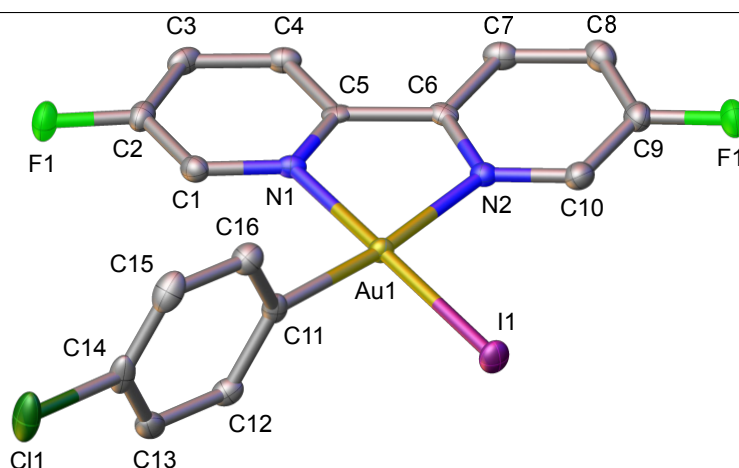
Empirical formula	$\text{C}_{18}\text{H}_{10}\text{AuF}_9\text{IN}_3\text{O}_4\text{S}_2$
Formula weight	891.28
Temperature (K)	100.0
Crystal system	Monoclinic
Space group	$P2_1/n$
<i>a</i> (\AA), <i>b</i> (\AA), <i>c</i> (\AA)	8.1391(3), 18.5972(8), 16.2536(7)
α ($^\circ$), β ($^\circ$), γ ($^\circ$)	90, 101.985(3), 90
Volume (\AA^3)	2406.59(17)
Z	4
Density_{calc} (g cm^{-3})	2.46
μ (mm^{-1})	7.672
<i>F</i>(000)	1664
Crystal size (mm^3)	0.298 × 0.088 × 0.077
Radiation	Mo $\text{K}\alpha$ ($\lambda=0.71073$)
2θ range for data collection ($^\circ$)	3.37 to 55.756
Index ranges	$-10 \leq h \leq 10, -24 \leq k \leq 24, -20 \leq l \leq 21$
Reflections collected	42606
Independent reflections	5754 [$R_{int} = 0.0586$]
Data/restraints/parameters	5754/0/343
Goodness-of-fit on F^2	1.014
Final <i>R</i> indexes [$I > 2\sigma(I)$]	$R1 = 0.0247, wR2 = 0.0424$
Final <i>R</i> indexes [all data]	$R1 = 0.0367, wR2 = 0.0452$
Largest diff. peak/hole (e \AA^{-3})	0.72/-0.92

Table 5.6: Molecular structure of **56k**, thermal ellipsoids are shown at the 30% probability level. Hydrogen atoms and the NTf₂ anion have been omitted for clarity. Selected bond lengths (Å) and angles (°): Au1–C11 2.000(4), Au1–I1 2.5420(5), Au1–N1 2.077(4), Au1–N2 2.128(4), N1–Au1–N2 78.52(14), N2–Au1–I1 99.81(11), N1–Au1–C11 96.6(5), C11–Au1–I1 85.0(5).



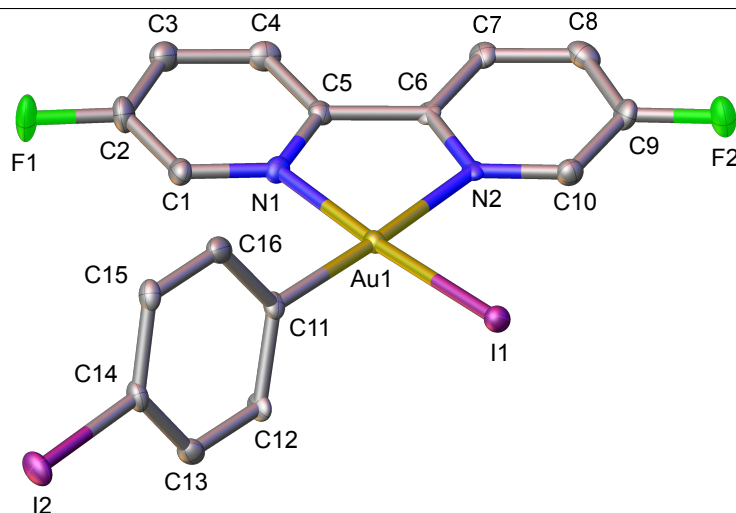
Empirical formula	C ₁₈ H ₁₂ AuF ₇ IN ₃ O ₄ S ₂
Formula weight	855.29
Temperature (K)	99.98
Crystal system	Monoclinic
Space group	<i>P</i> 2 ₁ / <i>c</i>
<i>a</i> (Å), <i>b</i> (Å), <i>c</i> (Å)	11.8370(7), 16.6292(10), 14.6146(8)
α (°), β (°), γ (°)	90, 95.625(3), 90
Volume (Å³)	2862.9(3)
<i>Z</i>	4
Density_{calc} (g cm⁻³)	1.984
μ (mm⁻¹)	6.435
<i>F</i>(000)	1600
Crystal size (mm³)	0.574 × 0.187 × 0.066
Radiation	Mo K α (λ =0.71073)
2θ range for data collection (°)	3.72 to 54.206
Index ranges	-15 ≤ <i>h</i> ≤ 15, -21 ≤ <i>k</i> ≤ 20, -18 ≤ <i>l</i> ≤ 18
Reflections collected	48777
Independent reflections	6314 [<i>R</i> _{int} = 0.0522]
Data/restraints/parameters	6314/770/501
Goodness-of-fit on <i>F</i>²	1.034
Final <i>R</i> indexes [<i>I</i> > 2σ(<i>I</i>)]	<i>R</i> 1 = 0.0299, <i>wR</i> 2 = 0.0704
Final <i>R</i> indexes [all data]	<i>R</i> 1 = 0.0704, <i>wR</i> 2 = 0.0758
Largest diff. peak/hole (e Å⁻³)	0.88/-1.21

Table 5.7: Molecular structure of **56b**, thermal ellipsoids are shown at the 50% probability level. Hydrogen atoms and the NTf_2 anion have been omitted for clarity. Selected bond lengths (\AA) and angles ($^\circ$): Au1–C11 2.014(3), Au1–I1 2.5412(2), Au1–N(1) 2.079(2), Au1–N2 2.126(2), N1–Au1–N2 78.63(10), N2–Au1–I1 99.96(7), N1–Au1–C11 96.03(11), C11–Au1–I1 85.55(8).



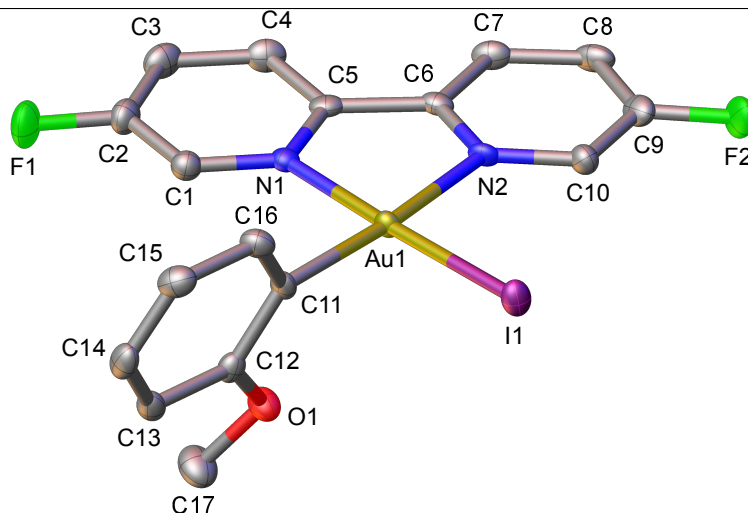
Empirical formula	$\text{C}_{18}\text{H}_{10}\text{AuClF}_8\text{IN}_3\text{O}_4\text{S}_2$
Formula weight	927.7
Temperature (K)	100.04
Crystal system	Monoclinic
Space group	$P2_1/c$
<i>a</i> (\AA), <i>b</i> (\AA), <i>c</i> (\AA)	8.2089(2), 16.0113(4), 19.2265(4)
α ($^\circ$), β ($^\circ$), γ ($^\circ$)	90, 97.1398(13), 90
Volume (\AA^3)	2507.44(10)
Z	4
Density_{calc} (g cm^{-3})	2.457
μ (mm^{-1})	7.862
<i>F</i>(000)	1731
Crystal size (mm^3)	$0.427 \times 0.232 \times 0.109$
Radiation	Mo $\text{K}\alpha$ ($\lambda=0.71073$)
2θ range for data collection ($^\circ$)	3.32 to 55.08
Index ranges	$-10 \leq h \leq 10, -20 \leq k \leq 20, -24 \leq l \leq 24$
Reflections collected	43569
Independent reflections	5781 [$R_{int} = 0.0431$]
Data/restraints/parameters	5781/0/343
Goodness-of-fit on F^2	1.04
Final <i>R</i> indexes [$I > 2\sigma(I)$]	$R1 = 0.0201, wR2 = 0.0398$
Final <i>R</i> indexes [all data]	$R1 = 0.0259, wR2 = 0.0413$
Largest diff. peak/hole (e \AA^{-3})	0.67/-0.55

Table 5.8: Molecular structure of **56c**, thermal ellipsoids are shown at the 50% probability level. Hydrogen atoms and the NTf₂ anion have been omitted for clarity. Selected bond lengths (Å) and angles (°): Au1–C11 2.012(5), Au1–I1 2.5442(4), Au1–N2 2.091(4), Au1–N1 2.142(5), N1–Au1–N2 78.78(18), N1–Au1–I1 99.23(12), N2–Au1–C11 97.6(2), C11–Au1–I1 84.42(15).



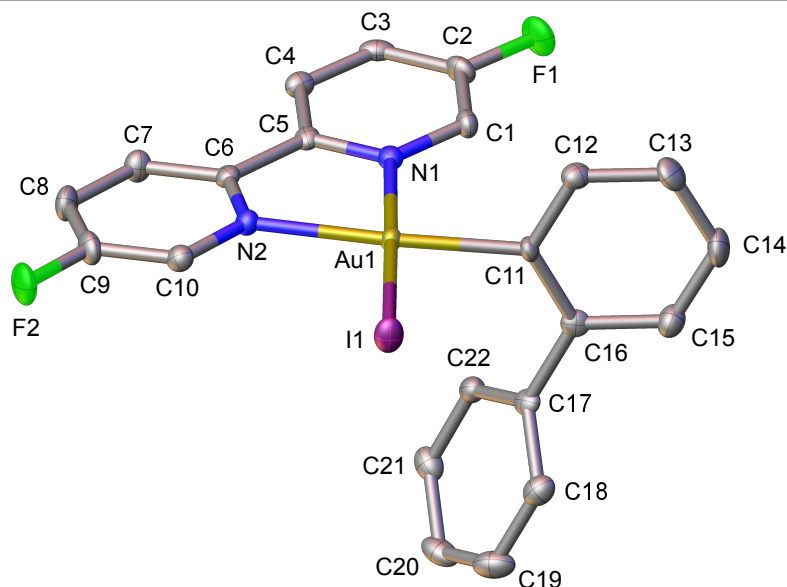
Empirical formula	C ₁₈ H ₁₀ AuF ₈ I ₂ N ₃ O ₄ S ₂
Formula weight	999.18
Temperature (K)	100
Crystal system	Monoclinic
Space group	<i>P</i> 2 ₁ / <i>n</i>
<i>a</i> (Å), <i>b</i> (Å), <i>c</i> (Å)	11.0172(3), 8.4253(2), 27.8416(7)
α (°), β (°), γ (°)	90, 100.3939(18), 90
Volume (Å³)	2541.94(11)
<i>Z</i>	4
Density_{calc} (g cm⁻³)	2.611
μ (mm⁻¹)	8.472
<i>F</i>(000)	1840
Crystal size (mm³)	0.229 × 0.219 × 0.086
Radiation	Mo K α (λ =0.71073)
2θ range for data collection (°)	2.974 to 55.008
Index ranges	-14 ≤ <i>h</i> ≤ 11, -10 ≤ <i>k</i> ≤ 10, -36 ≤ <i>l</i> ≤ 36
Reflections collected	42603
Independent reflections	5808 [<i>R</i> _{int} = 0.0890]
Data/restraints/parameters	5808/0/343
Goodness-of-fit on <i>F</i>²	1.048
Final <i>R</i> indexes [<i>I</i> > 2σ(<i>I</i>)]	<i>R</i> 1 = 0.0336, <i>wR</i> 2 = 0.0581
Final <i>R</i> indexes [all data]	<i>R</i> 1 = 0.0504, <i>wR</i> 2 = 0.0622
Largest diff. peak/hole (e Å⁻³)	0.97/-1.83

Table 5.9: Molecular structure of **56f**, thermal ellipsoids are shown at the 50% probability level. Hydrogen atoms and the NTf_2 anion have been omitted for clarity. Selected bond lengths (\AA) and angles ($^\circ$): Au1–C11 2.019(3), Au1–I1 2.5373(2), Au1–N2 2.117(3), Au1–N1 2.091(3), N1–Au1–N2 78.30(10), N2–Au1–I1 99.75(7), N1–Au1–C11 95.86(12), C11–Au1–I1 86.10(9).



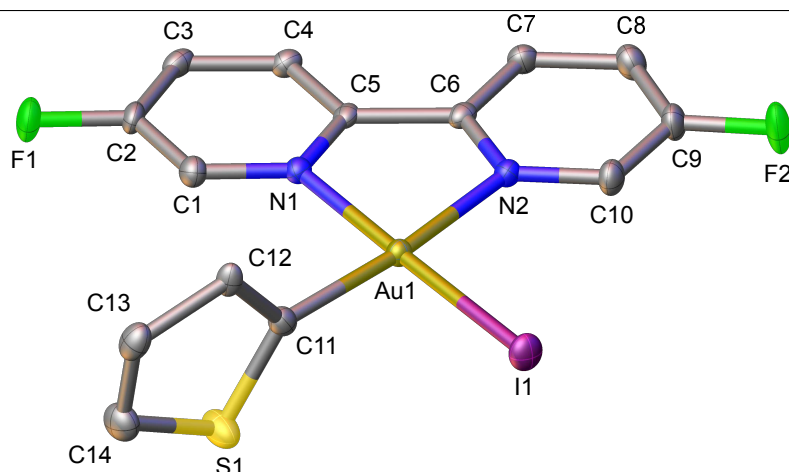
Empirical formula	$\text{C}_{19}\text{H}_{13}\text{AuF}_8\text{IN}_3\text{O}_5\text{S}_2$
Formula weight	903.31
Temperature (K)	100.01
Crystal system	Triclinic
Space group	$P\bar{1}$
a (\AA), b (\AA), c (\AA)	8.1277(3), 12.1214(4), 12.9584(4)
α ($^\circ$), β ($^\circ$), γ ($^\circ$)	102.8432(18), 96.108(2), 91.9896(19)
Volume (\AA^3)	1235.40(7)
Z	2
Density_{calc} (g cm^{-3})	2.428
μ (mm^{-1})	7.472
$F(000)$	848
Crystal size (mm^3)	$0.644 \times 0.318 \times 0.128$
Radiation	Mo $\text{K}\alpha$ ($\lambda=0.71073$)
2θ range for data collection ($^\circ$)	3.246 to 55.354
Index ranges	$-10 \leq h \leq 10, -15 \leq k \leq 15, -16 \leq l \leq 16$
Reflections collected	21994
Independent reflections	5747 [$R_{int} = 0.0399$]
Data/restraints/parameters	5747/0/353
Goodness-of-fit on F^2	1.042
Final R indexes [$I > 2\sigma(I)$]	$R1 = 0.0222, wR2 = 0.0559$
Final R indexes [all data]	$R1 = 0.0246, wR2 = 0.0571$
Largest diff. peak/hole (e \AA^{-3})	1.21/-1.16

Table 5.10: Molecular structure of **56h**, thermal ellipsoids are shown at the 50% probability level. Hydrogen atoms, a PhMe solvent molecule and the NTf₂ anion have been omitted for clarity. Selected bond lengths (Å) and angles (°): Au1-C11 2.028(3), Au1-I1 2.5455(2), Au1-N2 2.140(2), Au1-N1 2.083(2), N1-Au1-N2 78.21(9), N2-Au1-I1 100.80(6), C11-Au1-N1 94.91(10), C11-Au1-I1 86.13(8).



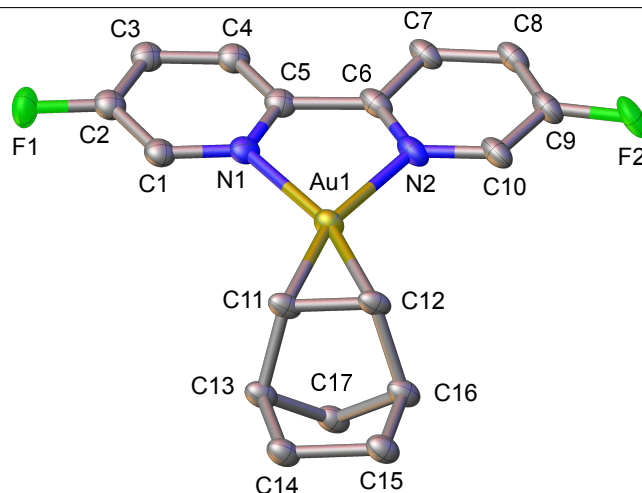
Empirical formula	C ₃₁ H ₂₃ AuF ₈ IN ₃ O ₄ S ₂
Formula weight	1041.51
Temperature (K)	101.13
Crystal system	Triclinic
Space group	<i>P</i> -1
<i>a</i> (Å), <i>b</i> (Å), <i>c</i> (Å)	9.7482(4), 18.0342(6), 20.0241(7)
α (°), β (°), γ (°)	92.573(2), 102.927(2), 95.368(2)
Volume (Å³)	3408.1(2)
<i>Z</i>	4
Density_{calc} (g cm⁻³)	2.030
μ (mm⁻¹)	5.430
<i>F</i>(000)	1992.0
Crystal size (mm³)	0.477 × 0.265 × 0.249
Radiation	Mo K α (λ =0.71073)
2θ range for data collection (°)	2.274 to 56.024
Index ranges	-12 ≤ <i>h</i> ≤ 12, -23 ≤ <i>k</i> ≤ 21, -26 ≤ <i>l</i> ≤ 26
Reflections collected	57496
Independent reflections	16334 [<i>R</i> _{int} = 0.0369]
Data/restraints/parameters	16334/111/975
Goodness-of-fit on <i>F</i>²	1.011
Final <i>R</i> indexes [<i>I</i> > 2σ(<i>I</i>)]	<i>R</i> 1 = 0.0233, <i>wR</i> 2 = 0.0453
Final <i>R</i> indexes [all data]	<i>R</i> 1 = 0.0303, <i>wR</i> 2 = 0.0469
Largest diff. peak/hole (e Å⁻³)	0.83/-0.66

Table 5.11: Molecular structure of **56j**, thermal ellipsoids are shown at the 50% probability level. Hydrogen atoms and the NTf₂ anion have been omitted for clarity. Selected bond lengths (Å) and angles (°): Au1-C11 1.998(3), Au1-I1 2.5530(2), Au1-N2 2.114(2), Au1-N1 2.084(2), N1-Au1-N2 78.70(9), N2-Au1-I1 100.29(6), C11-Au1-N1 93.94(10), C11-Au1-I1 87.07(8).



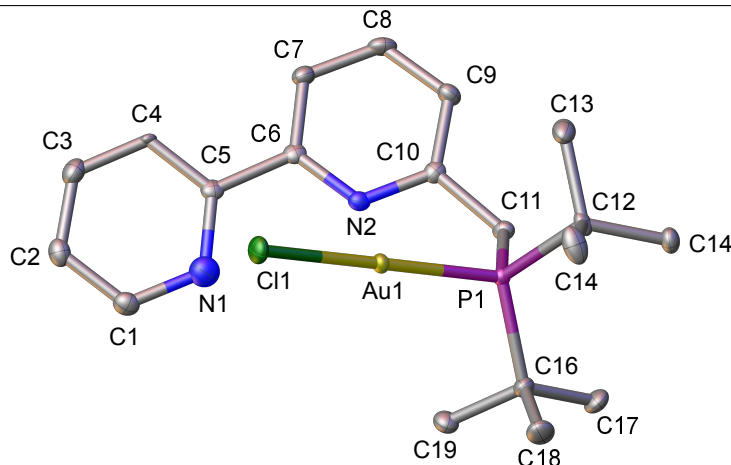
Empirical formula	C ₁₆ H ₉ AuF ₈ IN ₃ O ₄ S ₃
Formula weight	879.31
Temperature (K)	100.02
Crystal system	Monoclinic
Space group	<i>P</i> 2 ₁ / <i>c</i>
<i>a</i> (Å), <i>b</i> (Å), <i>c</i> (Å)	14.6761(3), 10.1045(2), 16.7196(3)
α (°), β (°), γ (°)	90, 108.4823(10), 90
Volume (Å³)	2351.54(8)
<i>Z</i>	4
Density_{calc} (g cm⁻³)	2.484
μ (mm⁻¹)	7.930
<i>F</i>(000)	1640.0
Crystal size (mm³)	0.201 × 0.145 × 0.084
Radiation	Mo K α (λ =0.71073)
2θ range for data collection (°)	4.78 to 60.22
Index ranges	-20 ≤ <i>h</i> ≤ 20, -14 ≤ <i>k</i> ≤ 14, -23 ≤ <i>l</i> ≤ 23
Reflections collected	52232
Independent reflections	6907 [<i>R</i> _{int} = 0.0409]
Data/restraints/parameters	6907/222/389
Goodness-of-fit on <i>F</i>²	1.023
Final <i>R</i> indexes [<i>I</i> > 2σ(<i>I</i>)]	<i>R</i> 1 = 0.0208, <i>wR</i> 2 = 0.0435
Final <i>R</i> indexes [all data]	<i>R</i> 1 = 0.0264, <i>wR</i> 2 = 0.0452
Largest diff. peak/hole (e Å⁻³)	1.83/-0.58

Table 5.12: Molecular structure of **51c**, thermal ellipsoids are shown at the 50% probability level. Hydrogen atoms and the NTf₂ anion have been omitted for clarity. Selected bond lengths (Å) and angles (°): Au1-N1 2.189(11), Au1-N2 2.191(11), Au1-C11 2.081(12), Au1-C12 2.108(13), C11-C12 1.410(19), N1-Au1-N2 74.3(4).



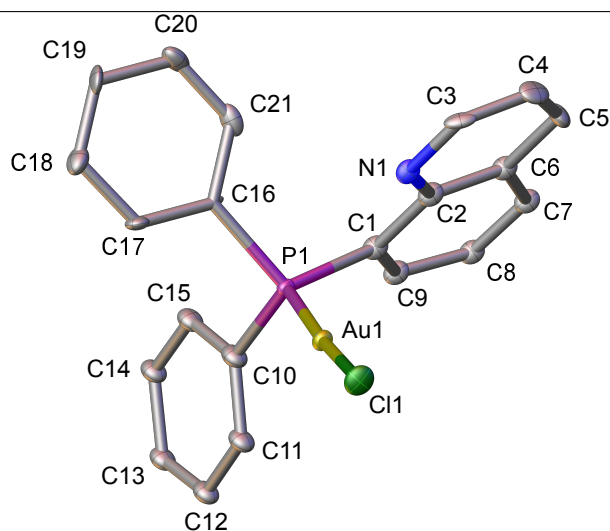
Empirical formula	C ₁₉ H ₁₆ AuF ₈ N ₃ O ₄ S ₂
Formula weight	763.43
Temperature (K)	100(2)
Crystal system	Triclinic
Space group	<i>P</i> -1
<i>a</i> (Å), <i>b</i> (Å), <i>c</i> (Å)	8.6437(7), 12.2625(10), 22.8213(18)
α (°), β (°), γ (°)	91.160(5), 89.967(6), 94.667(5)
Volume (Å³)	2410.4(3)
<i>Z</i>	4
Density_{calc} (g cm⁻³)	2.104
μ (mm⁻¹)	6.371
<i>F</i>(000)	1464.0
Crystal size (mm³)	0.579 × 0.14 × 0.087
Radiation	Mo K α (λ =0.71073)
2θ range for data collection (°)	3.334 to 50.054
Index ranges	-10 ≤ <i>h</i> ≤ 10, -14 ≤ <i>k</i> ≤ 14, 0 ≤ <i>l</i> ≤ 27
Reflections collected	8355
Independent reflections	8355 [<i>R</i> _{sigma} = 0.1095]
Data/restraints/parameters	8355/322/767
Goodness-of-fit on <i>F</i>²	1.031
Final <i>R</i> indexes [<i>I</i> > 2σ(<i>I</i>)]	<i>R</i> 1 = 0.0579, <i>wR</i> 2 = 0.1145
Final <i>R</i> indexes [all data]	<i>R</i> 1 = 0.1005, <i>wR</i> 2 = 0.1326
Largest diff. peak/hole (e Å⁻³)	2.24/-2.23

Table 5.13: Molecular structure of **84**, thermal ellipsoids are shown at the 50% probability level. Hydrogen atoms have been omitted for clarity. Selected bond lengths (Å) and angles (°): Au1-P1 2.2472(7), Au1-Cl1 2.2973(7), P1-Au1-Cl1 178.81(2). Selected non-bonded distances (Å): Au1-N1 3.831(3), Au1-N2 3.029(2).



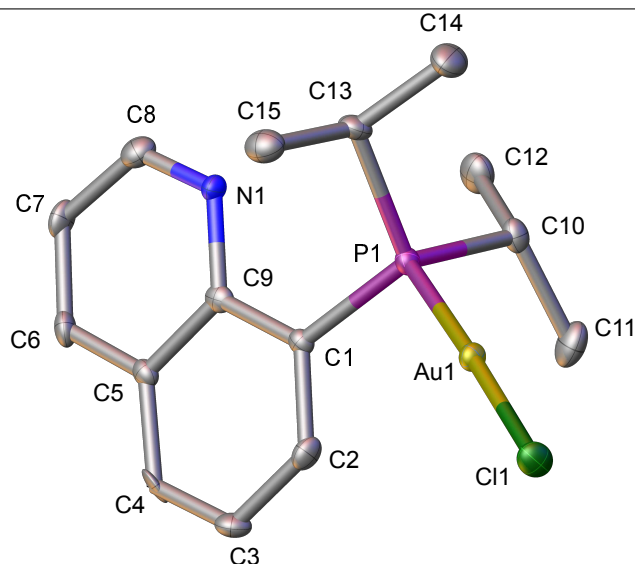
Empirical formula	C ₁₉ H ₂₈ AuClN ₂ P
Formula weight	547.82
Temperature (K)	100.0
Crystal system	Monoclinic
Space group	<i>P</i> 2 ₁ / <i>c</i>
<i>a</i> (Å), <i>b</i> (Å), <i>c</i> (Å)	11.2342(2), 11.2342(2), 11.2342(2)
α (°), β (°), γ (°)	90, 99.7421(11), 90
Volume (Å³)	1950.46(7)
<i>Z</i>	4
Density_{calc} (g cm⁻³)	1.866
μ (mm⁻¹)	7.765
<i>F</i>(000)	1068.0
Crystal size (mm³)	0.385 × 0.264 × 0.144
Radiation	Mo K α (λ =0.71073)
2θ range for data collection (°)	4.372 to 55.198
Index ranges	-14 ≤ <i>h</i> ≤ 14, -17 ≤ <i>k</i> ≤ 17, -17 ≤ <i>l</i> ≤ 17
Reflections collected	33966
Independent reflections	4524 [<i>R</i> _{sigma} = 0.0201]
Data/restraints/parameters	4524/0/223
Goodness-of-fit on <i>F</i>²	1.041
Final <i>R</i> indexes [<i>I</i> > 2σ(<i>I</i>)]	<i>R</i> 1 = 0.0178, <i>wR</i> 2 = 0.0404
Final <i>R</i> indexes [all data]	<i>R</i> 1 = 0.0215, <i>wR</i> 2 = 0.0415
Largest diff. peak/hole (e Å⁻³)	0.87/-0.98

Table 5.14: Molecular structure of **90**, thermal ellipsoids are shown at the 50% probability level. Hydrogen atoms have been omitted for clarity. Selected bond lengths (Å) and angles (°): Au1-P1 2.225(3), Au1-Cl1 2.285(3), P1-C1 1.806(13), P1-C16 1.824(12), P1-C10 1.827(13), P1-Au1-Cl1 173.78(13).



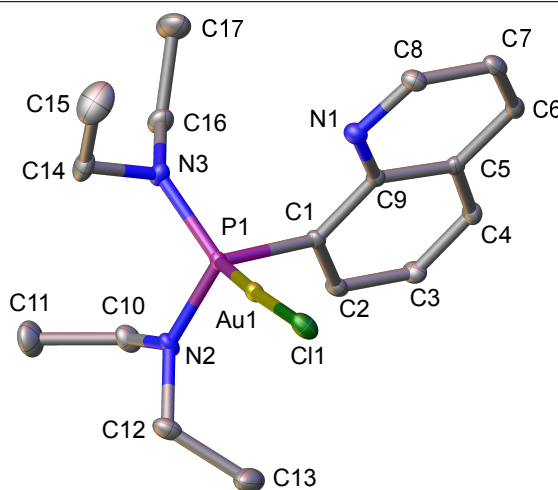
Empirical formula	C ₂₁ H ₁₆ AuClNP
Formula weight	545.73
Temperature (K)	100.07
Crystal system	Triclinic
Space group	<i>P</i> 1
<i>a</i> (Å), <i>b</i> (Å), <i>c</i> (Å)	9.6901(3), 10.5319(3), 10.9555(4)
α (°), β (°), γ (°)	115.5617(16), 90.9355(18), 110.3098(18)
Volume (Å³)	927.52(5)
<i>Z</i>	2
Density_{calc} (g cm⁻³)	1.954
μ (mm⁻¹)	8.164
<i>F</i>(000)	520.0
Crystal size (mm³)	0.48 × 0.453 × 0.315
Radiation	Mo K α (λ =0.71073)
2θ range for data collection (°)	4.204 to 54.198
Index ranges	-12 ≤ <i>h</i> ≤ 12, -12 ≤ <i>k</i> ≤ 13, -14 ≤ <i>l</i> ≤ 14
Reflections collected	14787
Independent reflections	7624 [<i>R</i> _{sigma} = 0.0288]
Data/restraints/parameters	7624/3/343
Goodness-of-fit on <i>F</i>²	1.030
Final <i>R</i> indexes [<i>I</i> > 2σ(<i>I</i>)]	<i>R</i> 1 = 0.0168, <i>wR</i> 2 = 0.0352
Final <i>R</i> indexes [all data]	<i>R</i> 1 = 0.0190, <i>wR</i> 2 = 0.0358
Largest diff. peak/hole (e Å⁻³)	0.69/-0.83

Table 5.15: Molecular structure of **102**, thermal ellipsoids are shown at the 50% probability level. Hydrogen atoms have been omitted for clarity. Selected bond lengths (Å) and angles (°): Au1-P1 2.2434(13), Au1-I1 2.2879(12), P1-C1 1.831(5), P1-Au1-C11 178.10(5).



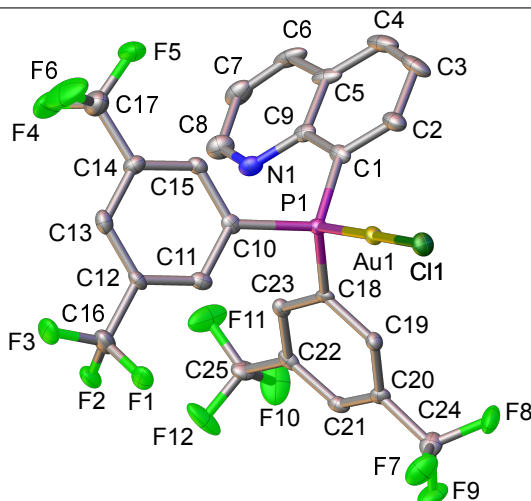
Empirical formula	C ₁₅ H ₂₀ AuClNP
Formula weight	477.71
Temperature (K)	100.0
Crystal system	Triclinic
Space group	<i>P</i> -1
<i>a</i> (Å), <i>b</i> (Å), <i>c</i> (Å)	7.4293(3), 10.4093(4), 11.2090(4)
α (°), β (°), γ (°)	109.047(2), 99.223(2), 94.949(2)
Volume (Å³)	799.81(5)
<i>Z</i>	2
Density_{calc} (g cm⁻³)	1.984
μ (mm⁻¹)	9.450
<i>F</i>(000)	456.0
Crystal size (mm³)	0.125 × 0.108 × 0.063
Radiation	Mo K α (λ =0.71073)
2θ range for data collection (°)	3.924 to 54.204
Index ranges	-9 ≤ <i>h</i> ≤ 9, -13 ≤ <i>k</i> ≤ 12, -14 ≤ <i>l</i> ≤ 14
Reflections collected	13616
Independent reflections	3536 [<i>R</i> _{sigma} = 0.0546]
Data/restraints/parameters	3536/0/176
Goodness-of-fit on <i>F</i>²	1.021
Final <i>R</i> indexes [<i>I</i> > 2σ(<i>I</i>)]	<i>R</i> 1 = 0.0288, <i>wR</i> 2 = 0.0472
Final <i>R</i> indexes [all data]	<i>R</i> 1 = 0.0391, <i>wR</i> 2 = 0.0496
Largest diff. peak/hole (e Å⁻³)	0.84/-1.17

Table 5.16: Molecular structure of **103**, thermal ellipsoids are shown at the 50% probability level. Hydrogen atoms have been omitted for clarity. Selected bond lengths (Å) and angles (°): Au1-P1 2.2335(5), Au1-Cl1 2.3003(5), P1-C1 1.819(2), P1-Au1-Cl1 174.43(2).



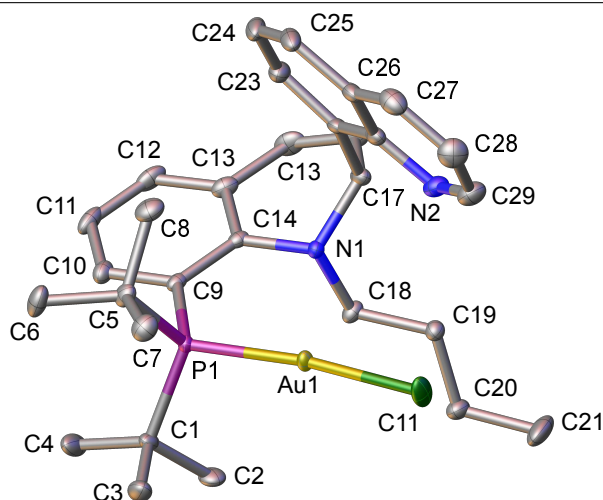
Empirical formula	$C_{17}H_{26}AuClN_3P$
Formula weight	535.79
Temperature (K)	100.0
Crystal system	Monoclinic
Space group	$P2_1/c$
<i>a</i> (Å), <i>b</i> (Å), <i>c</i> (Å)	7.96890(10), 18.6040(3), 13.4153(2)
α (°), β (°), γ (°)	90, 103.8601(8), 90
Volume (Å³)	1930.96(5)
Z	4
Density_{calc} (g cm⁻³)	1.843
μ (mm⁻¹)	7.842
<i>F</i>(000)	1040.0
Crystal size (mm³)	0.53 × 0.206 × 0.143
Radiation	Mo K α ($\lambda=0.71073$)
2θ range for data collection (°)	3.818 to 55.128
Index ranges	-10 ≤ <i>h</i> ≤ 10, -24 ≤ <i>k</i> ≤ 24, -17 ≤ <i>l</i> ≤ 17
Reflections collected	33800
Independent reflections	4467 [$R_{\text{sigma}} = 0.0166$]
Data/restraints/parameters	4467/0/212
Goodness-of-fit on <i>F</i>²	1.101
Final <i>R</i> indexes [<i>I</i> > 2σ(<i>I</i>)]	$R1 = 0.0156$, $wR2 = 0.0339$
Final <i>R</i> indexes [all data]	$R1 = 0.0168$, $wR2 = 0.0342$
Largest diff. peak/hole (e Å⁻³)	0.84/-0.93

Table 5.17: Molecular structure of **104**, thermal ellipsoids are shown at the 50% probability level. Hydrogen atoms have been omitted for clarity. Selected bond lengths (Å) and angles (°): Au1-P1 2.2315(13), Au1-Cl1 2.2886(13), P1-C1 1.820(5), P1-Au1-Cl1 175.56(4).



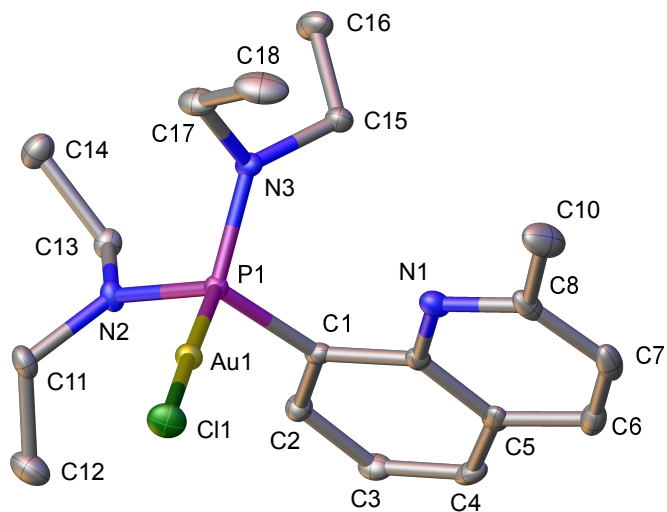
Empirical formula	C ₂₅ H ₁₂ AuClF ₁₂ NP
Formula weight	817.74
Temperature (K)	100.0
Crystal system	Triclinic
Space group	<i>P</i> -1
<i>a</i> (Å), <i>b</i> (Å), <i>c</i> (Å)	9.4520(2), 16.4219(5), 19.0813(5)
α (°), β (°), γ (°)	107.2523(17), 103.0629(16), 102.3216(17)
Volume (Å³)	2627.17(12)
<i>Z</i>	4
Density_{calc} (g cm⁻³)	2.067
μ (mm⁻¹)	5.865
<i>F</i>(000)	1552.0
Crystal size (mm³)	0.215 × 0.174 × 0.054
Radiation	Mo K α (λ =0.71073)
2θ range for data collection (°)	4.194 to 54.206
Index ranges	-12 ≤ <i>h</i> ≤ 12, -21 ≤ <i>k</i> ≤ 21, -24 ≤ <i>l</i> ≤ 23
Reflections collected	44871
Independent reflections	11579 [<i>R</i> _{sigma} = 0.0633]
Data/restraints/parameters	11579/102/794
Goodness-of-fit on <i>F</i>²	1.001
Final <i>R</i> indexes [<i>I</i> > 2σ(<i>I</i>)]	<i>R</i> 1 = 0.0334, <i>wR</i> 2 = 0.0552
Final <i>R</i> indexes [all data]	<i>R</i> 1 = 0.0599, <i>wR</i> 2 = 0.0620
Largest diff. peak/hole (e Å⁻³)	0.73/-1.18

Table 5.18: Molecular structure of **108**, thermal ellipsoids are shown at the 50% probability level. Hydrogen atoms have been omitted for clarity. Selected bond lengths (Å) and angles (°): Au1-P1 2.2484(5), Au1-C11 2.3011(6), P1-C9 1.831(2), P1-Au1-C11 173.15(2).



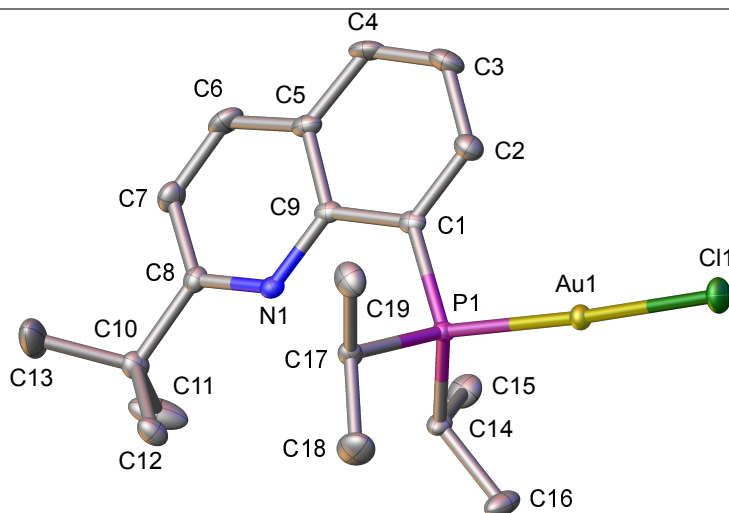
Empirical formula	C ₃₀ H ₃₉ AuClN ₂ P
Formula weight	691.02
Temperature (K)	100.0
Crystal system	Monoclinic
Space group	<i>P</i> 2 ₁ / <i>c</i>
<i>a</i> (Å), <i>b</i> (Å), <i>c</i> (Å)	9.913, 18.554, 15.731
α (°), β (°), γ (°)	90, 104.57, 90
Volume (Å³)	2800.5
<i>Z</i>	4
Density_{calc} (g cm⁻³)	1.639
μ (mm⁻¹)	5.427
<i>F</i>(000)	1376.0
Crystal size (mm³)	0.324 × 0.236 × 0.182
Radiation	Mo K α (λ =0.71073)
2θ range for data collection (°)	3.46 to 60.132
Index ranges	-13 ≤ <i>h</i> ≤ 13, -26 ≤ <i>k</i> ≤ 20, -22 ≤ <i>l</i> ≤ 22
Reflections collected	61021
Independent reflections	8188 [<i>R</i> _{sigma} = 0.0206]
Data/restraints/parameters	8188/266/403
Goodness-of-fit on <i>F</i>²	1.138
Final <i>R</i> indexes [<i>I</i> > 2σ(<i>I</i>)]	<i>R</i> 1 = 0.0214, <i>wR</i> 2 = 0.0416
Final <i>R</i> indexes [all data]	<i>R</i> 1 = 0.0257, <i>wR</i> 2 = 0.0424
Largest diff. peak/hole (e Å⁻³)	1.13/-0.83

Table 5.19: Molecular structure of **114**, thermal ellipsoids are shown at the 50% probability level. Hydrogen atoms have been omitted for clarity. Selected bond lengths (Å) and angles (°): Au1-P1 2.2342(8), Au1-Cl1 2.2960(8), P1-C1 1.821(3), P1-Au1-Cl2 176.72(3).



Empirical formula	C ₁₈ H ₂₈ N ₃ PClAu
Formula weight	549.82
Temperature (K)	99.99
Crystal system	Orthorhombic
Space group	<i>P</i> _{bca}
<i>a</i> (Å), <i>b</i> (Å), <i>c</i> (Å)	15.6501(3), 15.0007(3), 17.3929(4)
α (°), β (°), γ (°)	90, 90, 90
Volume (Å³)	4083.20(15)
<i>Z</i>	8
Density_{calc} (g cm⁻³)	1.789
μ (mm⁻¹)	7.420
<i>F</i>(000)	2144.0
Crystal size (mm³)	0.376 × 0.222 × 0.16
Radiation	Mo K α (λ =0.71073)
2θ range for data collection (°)	4.43 to 60.14
Index ranges	-22 ≤ <i>h</i> ≤ 22, -20 ≤ <i>k</i> ≤ 21, -24 ≤ <i>l</i> ≤ 15
Reflections collected	87151
Independent reflections	5982 [<i>R</i> _{sigma} = 0.0322]
Data/restraints/parameters	5982/0/222
Goodness-of-fit on <i>F</i>²	1.014
Final <i>R</i> indexes [<i>I</i> > 2σ(<i>I</i>)]	<i>R</i> 1 = 0.0228, <i>wR</i> 2 = 0.0390
Final <i>R</i> indexes [all data]	<i>R</i> 1 = 0.0508, <i>wR</i> 2 = 0.0463
Largest diff. peak/hole (e Å⁻³)	0.66/-0.99

Table 5.20: Molecular structure of **116**, thermal ellipsoids are shown at the 50% probability level. Hydrogen atoms have been omitted for clarity. Selected bond lengths (Å) and angles (°): Au1-P1 2.2439(6), Au1-Cl1 2.2934(6), P1-C1 1.822(3), P1-Au1-Cl1 177.06(2).



Empirical formula	C ₁₉ H ₂₈ AuClNP
Formula weight	533.81
Temperature (K)	293(2)
Crystal system	Orthorhombic
Space group	<i>P</i> _{bca}
<i>a</i> (Å), <i>b</i> (Å), <i>c</i> (Å)	14.2768(2), 15.7444(2), 17.7865(2)
α (°), β (°), γ (°)	90, 90, 90
Volume (Å³)	3998.04(9)
<i>Z</i>	8
Density_{calc} (g cm⁻³)	1.774
μ (mm⁻¹)	7.572
<i>F</i>(000)	2080.0
Crystal size (mm³)	0.555 × 0.28 × 0.214
Radiation	Mo K α (λ =0.71073)
2θ range for data collection (°)	4.48 to 55.122
Index ranges	-18 ≤ <i>h</i> ≤ 17, -20 ≤ <i>k</i> ≤ 20, -19 ≤ <i>l</i> ≤ 23
Reflections collected	36081
Independent reflections	4618 [<i>R</i> _{sigma} = 0.0210]
Data/restraints/parameters	4618/0/215
Goodness-of-fit on <i>F</i>²	1.039
Final <i>R</i> indexes [<i>I</i> > 2σ(<i>I</i>)]	<i>R</i> 1 = 0.0184, <i>wR</i> 2 = 0.0376
Final <i>R</i> indexes [all data]	<i>R</i> 1 = 0.0241, <i>wR</i> 2 = 0.0391
Largest diff. peak/hole (e Å⁻³)	0.49/-0.62

References

- [1] The World Gold Council, <https://www.gold.org/>, accessed 28th August 2018.
- [2] Belval, B. *Gold (Understanding the Elements of the Periodic Table)*; Rosen Central, 2006.
- [3] Reardon, A. C. *Metallurgy for the Non-Metallurgist*; ASM International, 2011.
- [4] Museums Victoria Collections, <https://collections.museumvictoria.com.au/specimens/23045>, accessed 29th August 2018.
- [5] InvestmentMine: Mining Markets & Investment, <http://www.infomine.com/investment/metal-prices/>, accessed 28th august 2018.
- [6] Housecroft, C. E.; Sharpe, A. G. *Inorganic Chemistry, Fifth Edition*; Pearson Education Limited, 2018.
- [7] Dietzel, P. D. C.; Jansen, M. *Chem. Commun.* **2001**, *1*, 2208.
- [8] Sommer, A. *Nature* **1943**, *152*, 215.
- [9] Preiß, S.; Förster, C.; Otto, S.; Bauer, M.; Müller, P.; Hinderberger, D.; Hashemi Haeri, H.; Carella, L.; Heinze, K. *Nat. Chem.* **2017**, *9*, 1249.
- [10] Hwang, I. C.; Seppelt, K. *Angew. Chem. Int. Ed.* **2001**, *40*, 3690.
- [11] Lin, J.; Zhang, S.; Guan, W.; Yang, G.; Ma, Y. *J. Am. Chem. Soc.* **2018**, *140*, 9545.
- [12] Gimeno, M. C.; Laguna, A. *Chem. Rev.* **1997**, *97*, 511.
- [13] Elschenbroich, C. *Organometallics*; Wiley-VCH Verlag GmbH & Co. KGaA, 2006.
- [14] Borissova, A. O.; Korlyukov, A. A.; Antipin, M. Y.; Lyssenko, K. A. *J. Phys. Chem. A* **2008**, *112*, 11519.
- [15] Teets, T. S.; Nocera, D. G. *J. Am. Chem. Soc.* **2009**, *131*, 7411.
- [16] Au, H.; Godfrey, S. M.; Ho, N.; Mcauliffe, C. A.; Pritchard, R. G. *Angew. Chem. Int. Ed.* **1996**, 2343.
- [17] Corti, C.; Holliday, R. *Gold: Science and Applications*; CRC Press, 2009.
- [18] Joost, M.; Gualco, P.; Coppel, Y.; Miqueu, K.; Kefalidis, C. E.; Maron, L.; Amgoune, A.; Bourissou, D. *Angew. Chem. Int. Ed.* **2014**, *53*, 747.
- [19] Durovic, M. D.; Bugarcic, Z. D.; van Eldik, R. *Coord. Chem. Rev.* **2017**, *338*, 186.

References

- [20] Kharasch, M.; Isbell, H. S. *J. Am. Chem. Soc.* **1931**, *53*, 3053.
- [21] Rocchigiani, L.; Fernandez-Cestau, J.; Budzelaar, P. H. M.; Bochmann, M. *Chem. Commun.* **2017**, *53*, 4358.
- [22] Gorin, D. J.; Toste, F. D. *Nature* **2007**, *446*, 395.
- [23] McKelvey, D. R. *J. Chem. Educ.* **1983**, *60*, 112.
- [24] Bartlett, N. *Gold Bull.* **1998**, *31*, 22.
- [25] Scherbaum, F.; Huber, B.; Grohmann, A.; Krüger, C.; Schmidbaur, H. *Angew. Chem. Int. Ed.* **1988**, *27*, 1544.
- [26] Emsley, J. *The Elements*; Oxford University Press, Inc., 1994.
- [27] Schwerdtfeger, P. *Heteroat. Chem.* **2002**, *13*, 578.
- [28] Schmidbaur, H. *Naturwiss. Rundsch.* **1995**, *4*, 48.
- [29] Nugent, W. A. *Angew. Chem. Int. Ed.* **2012**, *51*, 8936.
- [30] Hutchings, G. J.; Brust, M.; Schmidbaur, H. *Chem. Soc. Rev.* **2008**, *37*, 1759.
- [31] Takei, T.; Akita, T.; Nakamura, I.; Fujitani, T.; Okumura, M.; Okazaki, K.; Huang, J.; Ishida, T.; Haruta, M. *Adv. Catal.* **2012**, *55*, 1.
- [32] Hashmi, A. S. K.; Hutchings, G. J. *Angew. Chem. Int. Ed.* **2006**, *45*, 7896.
- [33] Hashmi, A. S. K.; Schwarz, L.; Choi, J. H.; Frost, T. M. *Angew. Chem. Int. Ed.* **2000**, *39*, 2285.
- [34] Brimble, M. A.; Quach, R.; Furkert, D. *Org. Biomol. Chem.* **2017**, *15*, 3098.
- [35] Shahzad, S. A.; Sajid, M. A.; Khan, Z. A.; Canseco-Gonzalez, D. *Synth. Commun.* **2017**, *47*, 735.
- [36] Li, Y.; Li, W.; Zhang, J. *Chem. Eur. J.* **2017**, *23*, 467.
- [37] Siva Kumari, A. L.; Siva Reddy, A.; Swamy, K. C. K. *Org. Biomol. Chem.* **2016**, *14*, 6651.
- [38] Zi, W.; Dean Toste, F. *Chem. Soc. Rev.* **2016**, *45*, 4567.
- [39] Pan, F.; Shu, C.; Ye, L.-W. *Org. Biomol. Chem.* **2016**, *14*, 9456.
- [40] Asiri, A. M.; Hashmi, A. S. K. *Chem. Soc. Rev.* **2016**, *45*, 4471.
- [41] Debrouwer, W.; Heugebaert, T. S. A.; Roman, B. I.; Stevens, C. V. *Adv. Synth. Catal.* **2015**, *357*, 2975.
- [42] Dorel, R.; Echavarren, A. M. *Chem. Rev.* **2015**, *115*, 9028.

- [43] Jia, M.; Bandini, M. *ACS Catal.* **2015**, *5*, 1638.
- [44] Yeom, H.-S.; Shin, S. *Acc. Chem. Res.* **2014**, *47*, 966.
- [45] Liu, L.-P.; Hammond, G. B. *Chem. Soc. Rev.* **2012**, *41*, 3129.
- [46] Hashmi, A. S. K. *Angew. Chem. Int. Ed.* **2010**, *49*, 5232.
- [47] Hashmi, A. S. K. *Gold Bull.* **2004**, *37*, 51.
- [48] Kar, A.; Mangu, N.; Kaiser, H. M.; Tse, M. K. *J. Organomet. Chem.* **2009**, *694*, 524.
- [49] Kar, A.; Mangu, N.; Kaiser, H. M.; Beller, M.; Tse, M. K. *Chem. Commun.* **2008**, 386.
- [50] Zhang, G.; Peng, Y.; Cui, L.; Zhang, L. *Angew. Chem. Int. Ed.* **2009**, *48*, 3112.
- [51] Peng, Y.; Cui, L.; Zhang, G.; Zhang, L. *J. Am. Chem. Soc.* **2009**, *131*, 5062.
- [52] Zhang, G.; Cui, L.; Wang, Y.; Zhang, L. *J. Am. Chem. Soc.* **2010**, *132*, 1474.
- [53] Brenzovich, Jr., W.; Brazeau, J.-F.; Toste, F. D. *Org. Lett.* **2010**, *12*, 4728.
- [54] Melhado, A. D.; Brenzovich, W. E.; Lackner, A. D.; Toste, F. D. *J. Am. Chem. Soc.* **2010**, *132*, 8885.
- [55] Ball, L. T.; Lloyd-Jones, G. C.; Russell, C. A. *Chem. Eur. J.* **2012**, *18*, 2931.
- [56] Ball, L. T.; Green, M.; Lloyd-Jones, G. C.; Russell, C. A. *Org. Lett.* **2010**, *12*, 4724.
- [57] De Haro, T.; Nevado, C. *J. Am. Chem. Soc.* **2010**, *132*, 1512.
- [58] Qian, D.; Zhang, J. *Beilstein J. Org. Chem.* **2011**, *7*, 808.
- [59] Pradal, A.; Toullec, P. Y.; Michelet, V. *Org. Lett.* **2011**, *13*, 6086.
- [60] Leyva-Pérez, A.; Doménech, A.; Al-Resayes, S. I.; Corma, A. *ACS Catal.* **2012**, *2*, 121.
- [61] Leyva-Pérez, A.; Doménech-Carbó, A.; Corma, A. *Nat. Commun.* **2015**, *6*, 6703.
- [62] Peng, H.; Xi, Y.; Ronaghi, N.; Dong, B.; Akhmedov, N. G.; Shi, X. *J. Am. Chem. Soc.* **2014**, *136*, 13174.
- [63] Ball, L. T.; Lloyd-Jones, G. C.; Russell, C. A. *J. Am. Chem. Soc.* **2014**, *136*, 254.
- [64] Ball, L. T.; Lloyd-Jones, G. C.; Russell, C. A. *Science* **2012**, *337*, 1644.
- [65] Cresswell, A. J.; Lloyd-Jones, G. C. *Chem. Eur. J.* **2016**, *22*, 12641.

References

- [66] Corrie, T. J.; Ball, L. T.; Russell, C. A.; Lloyd-Jones, G. C. *J. Am. Chem. Soc.* **2017**, *139*, 245.
- [67] Robinson, M. P.; Lloyd-Jones, G. C. *ACS Catal.* **2018**, *8*, 7484.
- [68] Corrie, T. J.; Lloyd-Jones, G. C. *Top. Catal.* **2017**, *60*, 570.
- [69] Hata, K.; Ito, H.; Segawa, Y.; Itami, K. *Beilstein J. Org. Chem.* **2015**, *11*, 2737.
- [70] Cambeiro, X. C.; Ahlsten, N.; Larrosa, I. *J. Am. Chem. Soc.* **2015**, *137*, 15636.
- [71] Marchetti, L.; Kantak, A.; Davis, R.; DeBoef, B. *Org. Lett.* **2015**, *17*, 358.
- [72] Yip, S. J.; Kawakami, T.; Murakami, K.; Itami, K. *Asian J. Org. Chem.* **2018**, *7*, 1372.
- [73] Zheng, Z.; Wang, Z.; Wang, Y.; Zhang, L. *Chem. Soc. Rev.* **2016**, *45*, 4448.
- [74] Hofer, M.; Genoux, A.; Kumar, R.; Nevado, C. *Angew. Chem. Int. Ed.* **2017**, *56*, 1021.
- [75] Akram, M. O.; Banerjee, S.; Saswade, S. S.; Bedi, V.; Patil, N. T. *Chem. Commun.* **2018**, DOI: 10.1039/c8cc05601c.
- [76] Sahoo, B.; Hopkinson, M. N.; Glorius, F. *J. Am. Chem. Soc.* **2013**, *135*, 5505.
- [77] Hopkinson, M. N.; Sahoo, B.; Glorius, F. *Adv. Synth. Catal.* **2014**, *356*, 2794.
- [78] Huang, L.; Rominger, F.; Rudolph, M.; Hashmi, A. S. K. *Chem. Commun.* **2016**, *52*, 6435.
- [79] Tlahuext-Aca, A.; Hopkinson, M. N.; Daniliuc, C. G.; Glorius, F. *Chem. Eur. J.* **2016**, *22*, 11587.
- [80] Kim, S.; Rojas-Martin, J.; Toste, F. D. *Chem. Sci.* **2016**, *7*, 85.
- [81] Tlahuext-Aca, A.; Hopkinson, M. N.; Sahoo, B.; Glorius, F. *Chem. Sci.* **2016**, *7*, 89.
- [82] Um, J.; Yun, H.; Shin, S. *Org. Lett.* **2016**, *18*, 484.
- [83] Tlahuext-Aca, A.; Hopkinson, M. N.; Aleyda Garza-Sanchez, R.; Glorius, F. *Chem. Eur. J.* **2016**, *22*, 5909.
- [84] Alcaide, B.; Almendros, P.; Busto, E.; Luna, A. *Adv. Synth. Catal.* **2016**, *358*, 1526.
- [85] Shu, X. Z.; Zhang, M.; He, Y.; Frei, H.; Toste, F. D. *J. Am. Chem. Soc.* **2014**, *136*, 5844.
- [86] He, Y.; Wu, H.; Toste, F. D. *Chem. Sci.* **2015**, *6*, 1194.

- [87] Xia, Z.; Khaled, O.; Mouriès-Mansuy, V.; Ollivier, C.; Fensterbank, L. *J. Org. Chem.* **2016**, *81*, 7182.
- [88] Qu, C.; Zhang, S.; Du, H.; Zhu, C. *Chem. Commun.* **2016**, *52*, 14400.
- [89] Bansode, A. H.; Shaikh, S. R.; Gonnade, R. G.; Patil, N. T. *Chem. Commun.* **2017**, *53*, 9081.
- [90] Akram, M. O.; Mali, P. S.; Patil, N. T. *Org. Lett.* **2017**, *19*, 3075.
- [91] Gauchot, V.; Lee, A.-L. *Chem. Commun.* **2016**, *52*, 10163.
- [92] Cornilleau, T.; Hermange, P.; Fouquet, E. *Chem. Commun.* **2016**, *52*, 10040.
- [93] Chakrabarty, I.; Akram, M. O.; Biswas, S.; Patil, N. T. *Chem. Commun.* **2018**, *54*, 7223.
- [94] Cai, R.; Lu, M.; Aguilera, E. Y.; Xi, Y.; Akhmedov, N. G.; Petersen, J. L.; Chen, H.; Shi, X. *Angew. Chem. Int. Ed.* **2015**, *54*, 8772.
- [95] Huang, L.; Rudolph, M.; Rominger, F.; Hashmi, A. S. K. *Angew. Chem. Int. Ed.* **2016**, *55*, 4808.
- [96] Witzel, S.; Xie, J.; Rudolph, M.; Hashmi, A. S. K. *Adv. Synth. Catal.* **2017**, 1522.
- [97] Callonnec, F. L.; Fouquet, E.; Felpin, F. X. *Org. Lett.* **2011**, *13*, 2646.
- [98] Harper, M. J.; Emmett, E. J.; Bower, J. F.; Russell, C. A. *J. Am. Chem. Soc.* **2017**, *139*, 12386.
- [99] Nguyen, T. *Chem. Eng. News* **2018**, 96.
- [100] *Chem. Eng. News* **2006**, *84*, 59.
- [101] Saini, V.; Stokes, B. J.; Sigman, M. S. *Angew. Chem. Int. Ed.* **2013**, *52*, 11206.
- [102] Ghanta, M.; Fahey, D.; Subramaniam, B. *Appl. Petrochemical Res.* **2013**, *4*, 167.
- [103] Heck, R. F.; Plevyak, J. E. *J. Org. Chem.* **1978**, *43*, 2454.
- [104] Mizoroki, T.; Mori, K.; Ozaki, A. *Bull. Chem. Soc. Jpn.* **1971**, *44*, 581.
- [105] DeVries, R. A.; Mendoza, A. *Organometallics* **1994**, *13*, 2405.
- [106] Kiji, J.; Okano, T.; Hasegawa, T. *J. Mol. Catal. A Chem.* **1995**, *97*, 73.
- [107] Matsubara, R.; Jamison, T. F. *J. Am. Chem. Soc.* **2010**, *132*, 6880.
- [108] Matsubara, R.; Gutierrez, A. C.; Jamison, T. F. *J. Am. Chem. Soc.* **2011**, *133*, 19020.
- [109] Bogdanović, B.; Henc, B.; Meister, B.; Pauling, H.; Wilke, G. *Angew. Chem. Int. Ed.* **1972**, *11*, 1023.

References

- [110] Bayersdorfer, R.; Ganter, B.; Englert, U.; Keim, W.; Vogt, D. *J. Organomet. Chem.* **1998**, *552*, 187.
- [111] Nomura, N.; Jin, J.; Park, H.; RajanBabu, T. V. *J. Am. Chem. Soc.* **1998**, *120*, 459.
- [112] Franciò, G.; Faraone, F.; Leitner, W. *J. Am. Chem. Soc.* **2002**, *124*, 736.
- [113] Grutters, M. M. P.; Van Der Vlugt, J. I.; Pei, Y.; Mills, A. M.; Lutz, M.; Spek, A. L.; Müller, C.; Moberg, C.; Vogt, D. *J. Am. Chem. Soc.* **2006**, *128*, 7414.
- [114] Liu, W.; Rajanbabu, T. V. *J. Org. Chem.* **2010**, *75*, 7636.
- [115] Page, J. P.; Rajanbabu, T. V. *J. Am. Chem. Soc.* **2012**, *134*, 6556.
- [116] Park, H.; Kumareswaran, R.; RajanBabu, T. V. *Tetrahedron* **2005**, *61*, 6352.
- [117] Jiang, G.; List, B. *Chem. Commun.* **2011**, *47*, 10022.
- [118] Ng, S. S.; Jamison, T. F. *J. Am. Chem. Soc.* **2005**, *127*, 14194.
- [119] Ng, S. S.; Ho, C. Y.; Jamison, T. F. *J. Am. Chem. Soc.* **2006**, *128*, 11513.
- [120] Park, B. Y.; Luong, T.; Sato, H.; Krische, M. J. *J. Org. Chem.* **2016**, *81*, 8585.
- [121] Ishii, Y.; Chatani, N.; Kakiuchi, F.; Murai, S. *Organometallics* **1997**, *16*, 3615.
- [122] Chatani, N.; Asaumi, T.; Ikeda, T.; Yorimitsu, S.; Ishii, Y.; Kakiuchi, F.; Murai, S. *J. Am. Chem. Soc.* **2000**, *122*, 12882.
- [123] Saini, V.; Sigman, M. S. *J. Am. Chem. Soc.* **2012**, *134*, 11372.
- [124] Saini, V.; Liao, L.; Wang, Q.; Jana, R.; Sigman, M. S. *Org. Lett.* **2013**, *15*, 5008.
- [125] Bidange, J.; Fischmeister, C.; Bruneau, C. *Chem. Eur. J.* **2016**, *22*, 12226.
- [126] Tobisu, M.; Chatani, N.; Asaumi, T.; Amako, K.; Ie, Y.; Fukumoto, Y.; Murai, S. *J. Am. Chem. Soc.* **2000**, *122*, 12663.
- [127] Chatani, N.; Tobisu, M.; Asaumi, T.; Murai, S. *Synthesis (Stuttg.)* **2000**, 925.
- [128] Jeong, N.; Hwang, S. H. *Angew. Chem. Int. Ed.* **2000**, *39*, 636.
- [129] Grigorjeva, L.; Daugulis, O. *Org. Lett.* **2014**, *16*, 4684.
- [130] Ohashi, M.; Shirataki, H.; Kikushima, K.; Ogoshi, S. *J. Am. Chem. Soc.* **2015**, *137*, 6496.
- [131] Brenzovich, W. E.; Benitez, D.; Lackner, A. D.; Shunatona, H. P.; Tkatchouk, E.; Goddard, W. a.; Toste, F. D. *Angew. Chem. Int. Ed.* **2010**, *49*, 5519.
- [132] Hatanaka, Y.; Hiyama, T. *J. Org. Chem.* **1988**, *53*, 918.

- [133] Dong, B.; Peng, H.; Motika, S. E.; Shi, X. *Chem. Eur. J.* **2017**, *23*, 11093.
- [134] Brooner, R. E.; Widenhoefer, R. A. *Angew. Chem. Int. Ed.* **2013**, *52*, 11714.
- [135] Norman, R. O. C.; Parr, W. J. E.; Thomas, C. B. *J. Chem. Soc., Perkin Trans. 1* **1976**, 818.
- [136] Rezsnyak, C. E.; Autschbach, J.; Atwood, J. D.; Moncho, S. *J. Coord. Chem.* **2013**, *66*, 1153.
- [137] Langseth, E.; Nova, A.; Tråseth, E. A.; Rise, F.; Øien, S.; Heyn, R. H.; Tilset, M. *J. Am. Chem. Soc.* **2014**, *136*, 10104.
- [138] Holmsen, M. S. M.; Nova, A.; Balcells, D.; Langseth, E.; Øien-Ødegaard, S.; Tråseth, E. A.; Heyn, R. H.; Tilset, M. *Dalton Trans.* **2016**, *45*, 14719.
- [139] Eaborn, C. *J. Organomet. Chem.* **1975**, *100*, 43.
- [140] Utimoto, K.; Otake, Y.; Yoshino, H.; Kuwahara, E.; Oshima, K.; Matsubara, S. *Bull. Chem. Soc. Jpn.* **2001**, *74*, 753.
- [141] Trummal, A.; Lipping, L.; Kaljurand, I.; Koppel, I. A.; Leito, I. *J. Phys. Chem. A* **2016**, *120*, 3663.
- [142] Koser, G. F.; Wettach, R. H. *J. Org. Chem.* **1980**, *45*, 1542.
- [143] Zhdankin, V. V.; Kuehl, C. J.; Bolz, J. T.; Formanek, M. S.; Simonsen, A. J. *Tetrahedron Lett.* **1994**, *35*, 7323.
- [144] Merritt, E. A.; Olofsson, B. *Eur. J. Org. Chem.* **2011**, 3690.
- [145] Tkatchouk, E.; Mankad, N. P.; Benitez, D.; Goddard, W.; Toste, F. D. *J. Am. Chem. Soc.* **2011**, *133*, 14293.
- [146] Fackler, J. P. *Inorg. Chem.* **2002**, *41*, 6959.
- [147] Hashmi, A. S. K.; Ramamurthi, T. D.; Rominger, F. *J. Organomet. Chem.* **2009**, *694*, 592.
- [148] Fuchita, Y.; Utsunomiya, Y.; Yasutake, M. *J. Chem. Soc., Dalt. Trans.* **2001**, 2330.
- [149] Schwerdtfeger, P.; Boyd, P. D. W.; Brienne, S.; Burrell, A. K. *Inorg. Chem.* **1992**, *31*, 3411.
- [150] Savjani, N.; Rosca, D. A.; Schormann, M.; Bochmann, M. *Angew. Chem. Int. Ed.* **2013**, *52*, 874.
- [151] Eisenberger, P.; Gischig, S.; Togni, A. *Chem. Eur. J.* **2006**, *12*, 2579.
- [152] Denton, R. M.; An, J.; Adeniran, B.; Blake, A. J.; Lewis, W.; Poulton, A. M. *J. Org. Chem.* **2011**, *76*, 6749.

References

- [153] Kuroboshi, M.; Yano, T.; Kamenoue, S.; Kawakubo, H.; Tanaka, H. *Tetrahedron* **2011**, *67*, 5825.
- [154] Shimogaki, M.; Fujita, M.; Sugimura, T. *Angew. Chem. Int. Ed.* **2016**, *55*, 15797.
- [155] Zhu, S.; Ye, L.; Wu, W.; Jiang, H. *Tetrahedron* **2013**, *69*, 10375.
- [156] Yang, H. B.; Pathipati, S. R.; Selander, N. *ACS Catal.* **2017**, *7*, 8441.
- [157] Yang, M. N.; Yan, D. M.; Zhao, Q. Q.; Chen, J. R.; Xiao, W. J. *Org. Lett.* **2017**, *19*, 5208.
- [158] Muriel, B.; Orcel, U.; Waser, J. *Org. Lett.* **2017**, *19*, 3548.
- [159] Faulkner, A.; Scott, J. S.; Bower, J. F. *J. Am. Chem. Soc.* **2015**, *137*, 7224.
- [160] Rabet, P. T.; Boyd, S.; Greaney, M. F. *Angew. Chem. Int. Ed.* **2017**, *56*, 4183.
- [161] Fumagalli, G.; Boyd, S.; Greaney, M. F. *Org. Lett.* **2013**, *15*, 4398.
- [162] Wang, D.; Wu, L.; Wang, F.; Wan, X.; Chen, P.; Lin, Z.; Liu, G. *J. Am. Chem. Soc.* **2017**, *139*, 6811.
- [163] Wijtmans, R.; Vink, M. K.; Schoemaker, H. E.; van Delft, F. L.; Blaauw, R. H.; Rutjes, F. P. *Synthesis (Stuttg.)* **2004**, *2004*, 641.
- [164] Yar, M.; McGarrigle, E. M.; Aggarwal, V. K. *Angew. Chem. Int. Ed.* **2008**, *47*, 3784.
- [165] Yar, M.; McGarrigle, E. M.; Aggarwal, V. K. *Org. Lett.* **2009**, *11*, 257.
- [166] Yar, M.; Fritz, S. P.; Gates, P. J.; McGarrigle, E. M.; Aggarwal, V. K. *Eur. J. Org. Chem.* **2012**, 160.
- [167] Bhatt, U.; Just, G. *Helv. Chim. Acta* **2000**, *83*, 722.
- [168] Samanta, S.; Mal, A.; Halder, S.; Ghorai, M. K. *Synth.* **2015**, *47*, 3776.
- [169] Kashima, C.; Harada, K. *J. Chem. Soc., Perkin Trans. 1* **1988**, 1521.
- [170] Harper, M. J.; Arthur, C. J.; Crosby, J.; Emmett, E. J.; Falconer, R. L.; Fensham-Smith, A. J.; Gates, P. J.; Leman, T.; Mcgrady, J. E.; Bower, J. F.; Russell, C. A. *J. Am. Chem. Soc.* **2018**, *140*, 4440.
- [171] Fensham-Smith, A. J. Reverse alchemy: Turning gold into a base metal. Ph.D. thesis, University of Bristol, 2017.
- [172] Hartwig, J. F. *Organotransition Metal Chemistry: From Bonding to Catalysis*; University Science Books, 2010.

- [173] Spessard, G. O.; Miessler, G. L. *Organometallic Chemistry*, 2nd ed.; Oxford University Press, Inc.: New York, 2010.
- [174] Joost, M.; Amgoune, A.; Bourissou, D. *Angew. Chem. Int. Ed.* **2015**, *54*, 15022.
- [175] Livendahl, M.; Goehry, C.; Maseras, F.; Echavarren, A. M. *Chem. Commun.* **2014**, *50*, 1533.
- [176] Bratsch, S. G. *J. Phys. Chem. Ref. Data* **1989**, *18*, 1.
- [177] Hashmi, A. S. K.; Lothschütz, C.; Döpp, R.; Ackermann, M.; De Buck Becker, J.; Rudolph, M.; Scholz, C.; Rominger, F. *Adv. Synth. Catal.* **2012**, *354*, 133.
- [178] Shiotani, A.; Schmidbaur, H. *J. Organomet. Chem.* **1972**, *37*, 24.
- [179] Tamaki, A.; Kochi, J. K. *J. Organomet. Chem.* **1972**, *40*, 81.
- [180] Tamaki, A.; Kochi, J. K. *J. Organomet. Chem.* **1974**, *64*, 411.
- [181] Johnson, A.; Puddephatt, R. J. *Inorg. Nucl. Chem. Lett.* **1973**, *9*, 1175.
- [182] Johnson, A.; Puddephatt, R. J. *J. Organomet. Chem.* **1975**, *85*, 115.
- [183] Winston, M. S.; Wolf, W. J.; Toste, F. D. *J. Am. Chem. Soc.* **2014**, *136*, 7777.
- [184] Johnson, M. T.; Marthinus Janse Van Rensburg, J.; Axelsson, M.; Ahlquist, M. S.; Wendt, O. F. *Chem. Sci.* **2011**, *2*, 2373.
- [185] Levin, M. D.; Toste, F. D. *Angew. Chem. Int. Ed.* **2014**, *53*, 6211.
- [186] Guenther, J.; Mallet-Ladeira, S.; Estevez, L.; Miqueu, K.; Amgoune, A.; Bourissou, D. *J. Am. Chem. Soc.* **2014**, *136*, 1778.
- [187] Serra, J.; Whiteoak, C. J.; Acuña-Parés, F.; Font, M.; Luis, J. M.; Lloret-Fillol, J.; Ribas, X. *J. Am. Chem. Soc.* **2015**, *137*, 13389.
- [188] Serra, J.; Parella, T.; Ribas, X. *Chem. Sci.* **2017**, *8*, 946.
- [189] Asomoza-Solís, E. O.; Rojas-Ocampo, J.; Toscano, R. A.; Porcel, S. *Chem. Commun.* **2016**, *52*, 7295.
- [190] Wu, C.-Y.; Horibe, T.; Jacobsen, C. B.; Toste, F. D. *Nature* **2015**, *517*, 449.
- [191] Bachman, R. E.; Bodolosky-Bettis, S. A.; Pyle, C. J.; Gray, M. A. *J. Am. Chem. Soc.* **2008**, *130*, 14303.
- [192] Gualco, P.; Ladeira, S.; Miqueu, K.; Amgoune, A.; Bourissou, D. *Angew. Chem. Int. Ed.* **2011**, *50*, 8320.
- [193] Gualco, P.; Ladeira, S.; Miqueu, K.; Amgoune, A.; Bourissou, D. *Organometallics* **2012**, *31*, 6001.

References

- [194] Lassauque, N.; Gualco, P.; Mallet-Ladeira, S.; Miqueu, K.; Amgoune, A.; Bourissou, D. *J. Am. Chem. Soc.* **2013**, *135*, 13827.
- [195] Joost, M.; Zeineddine, A.; Estévez, L.; Mallet-Ladeira, S.; Miqueu, K.; Amgoune, A.; Bourissou, D. *J. Am. Chem. Soc.* **2014**, *136*, 14654.
- [196] Crespo, O.; Gimeno, M. C.; Laguna, A.; Jones, P. G. **1992**, 1601.
- [197] Joost, M.; Estévez, L.; Miqueu, K.; Amgoune, A.; Bourissou, D. *Angew. Chem. Int. Ed.* **2015**, *54*, 5236.
- [198] Wolters, L. P.; Bickelhaupt, F. M. *ChemistryOpen* **2013**, *2*, 106.
- [199] Joost, M.; Estévez, L.; Mallet-Ladeira, S.; Miqueu, K.; Amgoune, A.; Bourissou, D. *Angew. Chem. Int. Ed.* **2014**, *53*, 14512.
- [200] Dash, C.; Kroll, P.; Yousufuddin, M.; Dias, H. V. *Chem. Commun.* **2011**, *47*, 4478.
- [201] Martínez-Salvador, S.; Forniés, J.; Martín, A.; Menjón, B. *Angew. Chem. Int. Ed.* **2011**, *50*, 6571.
- [202] Dias, H. V.; Dash, C.; Yousufuddin, M.; Celik, M. A.; Frenking, G. *Inorg. Chem.* **2011**, *50*, 4253.
- [203] Schaefer, J.; Kraft, A.; Reininger, S.; Santiso-Quinones, G.; Himmel, D.; Trapp, N.; Gellrich, U.; Breit, B.; Krossing, I. *Chem. Eur. J.* **2013**, *19*, 12468.
- [204] Celik, M. A.; Dash, C.; Adiraju, V. A.; Das, A.; Yousufuddin, M.; Frenking, G.; Dias, H. V. *Inorg. Chem.* **2013**, *52*, 729.
- [205] Zeineddine, A.; Estévez, L.; Mallet-Ladeira, S.; Miqueu, K.; Amgoune, A.; Bourissou, D. *Nat. Commun.* **2017**, *8*, 565.
- [206] Messina, M. S.; Stauber, J. M.; Waddington, M. A.; Rheingold, A. L.; Maynard, H. D.; Spokoyny, A. M. *J. Am. Chem. Soc.* **2018**, *140*, 7065.
- [207] Cinellu, M. A.; Zucca, A.; Stoccoro, S.; Minghetti, G.; Manassero, M.; Sansoni, M. *J. Chem. Soc., Dalt. Trans.* **1996**, 4217.
- [208] Cinellu, M. A.; Minghetti, G.; Pinna, V.; Stoccoro, S.; Zucca, A.; Manassero, M.; Sansoni, M. *J. Chem. Soc., Dalt. Trans.* **1998**, 1735.
- [209] Cinellu, M. A.; Minghetti, G.; Cocco, F.; Stoccoro, S.; Zucca, A.; Manassero, M.; Arca, M. *J. Chem. Soc. Dalt. Trans.* **2006**, 5703.
- [210] Hooper, T. N.; Butts, C. P.; Green, M.; Haddow, M. F.; McGrady, J. E.; Russell, C. A. *Chem. Eur. J.* **2009**, 12196.
- [211] Dias, H. V. R.; Fianchini, M.; Cundari, T. R.; Campana, C. F. *Angew. Chem. Int. Ed.* **2008**, *47*, 556.

- [212] Lee, K.; Lee, P. H. *Tetrahedron Lett.* **2008**, *49*, 4302.
- [213] Chadwick, N.; Kumar, D. K.; Ivaturi, A.; Grew, B. A.; Upadhyaya, H. M.; Yellowlees, L. J.; Robertson, N. *Eur. J. Inorg. Chem.* **2015**, 4878.
- [214] Hooper, T. N.; Green, M.; McGrady, J. E.; Patel, J. R.; Russell, C. A. *Chem. Commun.* **2009**, 3877.
- [215] Brown, T. J.; Dickens, M. G.; Widenhoefer, R. A. *J Am. Chem. Soc.* **2009**, *131*, 6350.
- [216] Fauvarque, J. F.; Pflüger, F.; Troupel, M. *J. Organomet. Chem.* **1981**, *208*, 419.
- [217] Li, Q. S.; Wan, C. Q.; Zou, R. Y.; Xu, F. B.; Song, H. B.; Wan, X. J.; Zhang, Z. Z. *Inorg. Chem.* **2006**, *45*, 1888.
- [218] Herrero-Gómez, E.; Nieto-Oberhuber, C.; López, S.; Benet-Buchholz, J.; Echavarren, A. M. *Angew. Chem. Int. Ed.* **2006**, *45*, 5455.
- [219] Lavallo, V.; Frey, G. D.; Kousar, S.; Donnadiou, B.; Bertrand, G. *Proc. Natl. Acad. Sci.* **2007**, *104*, 13569.
- [220] Pérez-Galán, P.; Delpont, N.; Herrero-Gómez, E.; Maseras, F.; Echavarren, A. M. *Chem. Eur. J.* **2010**, *16*, 5324.
- [221] Robinson, P. S.; Khairallah, G. N.; Da Silva, G.; Lioe, H.; O'Hair, R. A. *Angew. Chem. Int. Ed.* **2012**, *51*, 3812.
- [222] Lewis, A. K. D. K.; Caddick, S.; Cloke, F. G. N.; Billingham, N. C.; Hitchcock, P. B.; Leonard, J. J. *J. Am. Chem. Soc.* **2003**, *125*, 10066.
- [223] Senn, H. M.; Ziegler, T. *Organometallics* **2004**, *23*, 2980.
- [224] Amatore, C.; Pflüger, F. *Organometallics* **1990**, *9*, 2276.
- [225] Portnoy, M.; Milstein, D. *Organometallics* **1993**, *12*, 1665.
- [226] O'Brien, H. M.; Manzotti, M.; Abrams, R. D.; Elorriaga, D.; Sparkes, H. A.; Davis, S. A.; Bedford, R. B. *Nat. Catal.* **2018**, *1*, 429.
- [227] Shan, H.; Yang, Y.; James, A. J.; Sharp, P. R. *Science* **1997**, *275*, 1460.
- [228] Holland, P. L. *Dalton Trans.* **2010**, *39*, 5415.
- [229] Ung, G.; Bertrand, G. *Angew. Chem. Int. Ed.* **2013**, *52*, 11388.
- [230] Klatt, G.; Xu, R.; Pernpointner, M.; Molinari, L.; Quang Hung, T.; Rominger, F.; Hashmi, A. S. K.; Köppel, H. *Chem. Eur. J.* **2013**, *19*, 3954.
- [231] Rekhroukh, F.; Estevez, L.; Mallet-Ladeira, S.; Miqueu, K.; Amgoune, A.; Bourissou, D. *J. Am. Chem. Soc.* **2016**, *138*, 11920.

References

- [232] Miyaura, N.; Yanagi, T.; Suzuki, A. *Synth. Commun.* **1981**, *11*, 513.
- [233] Brown, D. G.; Boström, J. *J. Med. Chem.* **2016**, *59*, 4443.
- [234] Suzuki, A. *Angew. Chem. Int. Ed.* **2011**, *50*, 6723.
- [235] Miyaura, N.; Suzuki, A. *Chem. Rev.* **1995**, *95*, 2457.
- [236] Han, F. S. *Chem. Soc. Rev.* **2013**, *42*, 5270.
- [237] Asghar, S.; Tailor, S. B.; Elorriaga, D.; Bedford, R. B. *Angew. Chem. Int. Ed.* **2017**, *56*, 16367.
- [238] Neely, J. M.; Bezdek, M. J.; Chirik, P. J. *ACS Cent. Sci.* **2016**, *2*, 935.
- [239] González-Arellano, C.; Corma, A.; Iglesias, M.; Sánchez, F. *J. Catal.* **2006**, *238*, 497.
- [240] González-Arellano, C.; Abad, A.; Corma, A.; García, H.; Iglesias, M.; Sánchez, F. *Angew. Chem. Int. Ed.* **2007**, *46*, 1536.
- [241] Lauterbach, T.; Livendahl, M.; Rosellón, A.; Espinet, P.; Echavarren, A. M. *Org. Lett.* **2010**, *12*, 3006.
- [242] Corma, A.; Juárez, R.; Boronat, M.; Sánchez, F.; Iglesias, M.; García, H. *Chem. Commun.* **2011**, *47*, 1446.
- [243] Dwadnia, N.; Roger, J.; Pirio, N.; Cattey, H.; Ben Salem, R.; Hierso, J.-C. *Chem. Asian J.* **2017**, *12*, 459.
- [244] Arvela, R. K.; Leadbeater, N. E.; Sangi, M. S.; Williams, V. A.; Granados, P.; Singer, R. D. *J. Org. Chem.* **2005**, *70*, 161.
- [245] Märkl, G. *Angew. Chem. Int. Ed.* **1966**, *5*, 846.
- [246] Peruzzini, M.; Gonsalvi, L. *Catalysis by Metal Complexes, Volume 37: Phosphorus Compounds: Advanced Tools in Catalysis and Materials Science*; Springer Science+Business Media, 2011.
- [247] Müller, C.; Wasserberg, D.; Weemers, J. J.; Pidko, E. A.; Hoffmann, S.; Lutz, M.; Spek, A. L.; Meskers, S. C.; Janssen, R. A.; Van Santen, R. A.; Vogt, D. *Chem. Eur. J.* **2007**, *13*, 4548.
- [248] Zhang, L.; Peng, D.; Leng, X.; Huang, Z. *Angew. Chem. Int. Ed.* **2013**, *52*, 3676.
- [249] Balaraman, E.; Gnanaprakasam, B.; Shimon, L. J. W.; Milstein, D. *J. Am. Chem. Soc.* **2010**, *132*, 16756.
- [250] Pullmann, T.; Engendahl, B.; Zhang, Z.; Hölscher, M.; Zanotti-Gerosa, A.; Dyke, A.; Franciò, G.; Leitner, W. *Chem. Eur. J.* **2010**, *16*, 7517.

- [251] Sirbu, D.; Consiglio, G.; Gischig, S. *J. Organomet. Chem.* **2006**, *691*, 1143.
- [252] Childers, W. E.; Havran, L. M.; Asselin, M.; Bicksler, J. J.; Chong, D. C.; Grosu, G. T.; Shen, Z.; Abou-Gharbia, M. A.; Bach, A. C.; Harrison, B. L.; Kagan, N.; Kleintop, T.; Magolda, R.; Marathias, V.; Robichaud, A. J.; Sabb, A. L.; Zhang, M. Y.; Andree, T. H.; Aschmies, S. H.; Beyer, C.; Comery, T. A.; Day, M.; Grauer, S. M.; Hughes, Z. A.; Rosenzweig-Lipson, S.; Platt, B.; Pulicicchio, C.; Smith, D. E.; Sukoff-Rizzo, S. J.; Sullivan, K. M.; Adedoyin, A.; Huselton, C.; Hirst, W. D. *J. Med. Chem.* **2010**, *53*, 4066.
- [253] Li, A.-H.; Ahmed, E.; Chen, X.; Cox, M.; Crew, A. P.; Dong, H.-Q.; Jin, M.; Ma, L.; Panicker, B.; Siu, K. W.; Steinig, A. G.; Stolz, K. M.; Tavares, P. A. R.; Volk, B.; Weng, Q.; Werner, D.; Mulvihill, M. J. *Org. Biomol. Chem.* **2007**, *5*, 61.
- [254] Hashmi, A. S. K.; Bechem, D. B.; Loos, A. A.; Hamzic, M.; Rominger, A. F.; C, H. R. *Aust. J. Chem.* **2014**, *67*, 481.
- [255] Malberg, J.; Bodensteiner, M.; Paul, D.; Wiegand, T.; Eckert, H.; Wolf, R. *Angew. Chem. Int. Ed.* **2014**, *53*, 2771.
- [256] Zalesskiy, S. S.; Sedykh, A. E.; Kashin, A. S.; Ananikov, V. P. *J. Am. Chem. Soc.* **2013**, *135*, 3550.
- [257] Altaf, M.; Monim-ul Mehboob, M.; Isab, A. a.; Dhuna, V.; Bhatia, G.; Dhuna, K.; Altuwaijri, S. *New J. Chem.* **2015**, *39*, 377.
- [258] Brandys, M.-C.; Jennings, M. C.; Puddephatt, R. J. *J. Chem. Soc., Dalton Trans.* **2000**, 4601.
- [259] Cordón, J.; López-De-Luzuriaga, J. M.; Monge, M. *Organometallics* **2016**, *35*, 732.
- [260] Nonaka, S.; Sugimoto, K.; Ueda, H.; Tokuyama, H. *Adv. Synth. Catal.* **2016**, *358*, 380.
- [261] Tobisu, M.; Kita, Y.; Ano, Y.; Chatani, N. *J. Am. Chem. Soc.* **2008**, *130*, 15982.
- [262] Heiss, C.; Marzi, E.; Mongin, F.; Schlosser, M. *Eur. J. Org. Chem.* **2007**, 669.
- [263] Stuart, A. M.; Coe, P. L.; Moody, D. J. *J. Fluor. Chem.* **1998**, *88*, 179.
- [264] Lamba, J. J. S.; Tour, J. M. *J. Am. Chem. Soc.* **1994**, *116*, 11723.
- [265] Ye, B. H.; Naruta, Y. *Tetrahedron* **2003**, *59*, 3593.
- [266] Doszczak, L.; Kraft, P.; Weber, H. P.; Bertermann, R.; Triller, A.; Hatt, H.; Tacke, R. *Angew. Chem. Int. Ed.* **2007**, *46*, 3367.
- [267] Tsoi, Y. T.; Zhou, Z.; Yu, W. *Org. Lett.* **2011**, *13*, 5370.

References

- [268] Hevesi, L.; Dehon, M.; Crutzen, R.; Lazarescu-Grigore, A. *J. Org. Chem.* **1997**, *62*, 2011.
- [269] Das, M.; O'Shea, D. F. *Chem. Eur. J.* **2015**, *21*, 18717.
- [270] Nagaki, A.; Kim, H.; Usutani, H.; Matsuo, C.; Yoshida, J.-I. *Org. Biomol. Chem.* **2010**, *8*, 1212.
- [271] Kraszkiewicz, L. *Arkivoc* **2003**, *2003*, 881.
- [272] Frei, R.; Courant, T.; Wodrich, M. D.; Waser, J. *Chem. Eur. J.* **2015**, *21*, 2662.
- [273] Adamczyk-Woźniak, A.; Borys, K. M.; Czerwińska, K.; Gierczyk, B.; Jakubczyk, M.; Madura, I. D.; Sporzyński, A.; Tomecka, E. *Spectrochim. Acta. A. Mol. Biomol. Spectrosc.* **2013**, *116*, 616.
- [274] Vasdev, N.; Rotstein, B. H.; Stephenson, N. A.; Liang, H. Preparation of fluorinated aromatic compounds using iodine(III)-mediated radiofluorination reaction, U.S. Patent US 20150252007, 2015.
- [275] Guptill, D. M.; Davies, H. M. L. *J. Am. Chem. Soc.* **2014**, *136*, 17718.
- [276] Sakai, N.; Moriya, T.; Konakahara, T. *J. Org. Chem.* **2007**, *72*, 5920.
- [277] Li, G.; Leow, D.; Wan, L.; Yu, J.-Q. *Angew. Chem. Int. Ed.* **2013**, *52*, 1245.
- [278] Vechorkin, O.; Proust, V.; Hu, X. *J. Am. Chem. Soc.* **2009**, *131*, 9756.
- [279] Barontini, M.; Proietti Silvestri, I.; Nardi, V.; Bovicelli, P.; Pari, L.; Gallucci, F.; Spezia, R.; Righi, G. *Tetrahedron Lett.* **2013**, *54*, 5004.
- [280] Balti, M.; Lotfi, M.; Leadbeater, N. E. *Tetrahedron Lett.* **2016**, *57*, 1804.
- [281] Das, S.; Li, Y.; Junge, K.; Beller, M. *Chem. Commun.* **2012**, *48*, 10742.
- [282] Asao, N.; Aikawa, H.; Sakie, T.; Umetsu, K. *Org. Lett.* **2007**, *9*, 4299.
- [283] Colombel, V.; Rombouts, F.; Oehrich, D.; Molander, G. A. *J. Org. Chem.* **2012**, *77*, 2966.
- [284] Hellal, M.; Falk, F. C.; Wolf, E.; Dryzhakov, M.; Moran, J. *Org. Biomol. Chem.* **2014**, *12*, 5990.
- [285] Yang, C. T.; Zhang, Z. Q.; Liu, Y. C.; Liu, L. *Angew. Chem. Int. Ed.* **2011**, *50*, 3904.
- [286] Neumann, T.; Benajiba, L.; Göring, S.; Stegmaier, K.; Schmidt, B. *J. Med. Chem.* **2015**, *58*, 8907.
- [287] Niwa, T.; Ochiai, H.; Watanabe, Y.; Hosoya, T. *J. Am. Chem. Soc.* **2015**, *137*, 14313.

-
- [288] Blessley, G.; Holden, P.; Walker, M.; Brown, J. M.; Gouverneur, V.; John, M.; Gouverneur, V. *Org. Lett.* **2012**, *14*, 2754.
- [289] Liang, Y.; Fu, G. C. *J. Am. Chem. Soc.* **2015**, *137*, 9523.
- [290] Cave, G. W. V.; Raston, C. L. *J. Chem. Soc. Perkin Trans. 1* **2001**, 3258.
- [291] Huang, X.; Lu, Z.; Wang, Z.; Fan, C.; Fan, W.; Shi, X.; Zhang, H.; Pei, M. *Dye. Pigment.* **2016**, *128*, 33.
- [292] Louka, A.; Gryparis, C.; Stratakis, M. *Arkivoc* **2015**, *2015*, 38.
- [293] Bruker, SAINT+ Integration Engine, Data Reduction Software, Bruker Analytical X-ray Instruments Inc., Madison, WI, USA. 2007.
- [294] Bruker, SADABS, Bruker AXS area detector scaling and absorption correction, Bruker Analytical X-ray Instruments Inc., Madison, Wisconsin, USA, 2001.
- [295] Sheldrick, G. M. *Acta Cryst. A* **2007**, *64*, 112.
- [296] Sheldrick, G. M. *Acta Cryst. C* **2015**, *71*, 3.
- [297] Dolomanov, O. V.; Bourhis, L. J.; Gildea, R. J.; Howard, J. A. K.; Puschmann, H. *J. Appl. Crystallogr.* **2009**, *42*, 339.